Monitoring of human cellular immune responses in infectious diseases

Malaria vaccine associated responses and
immune status characterization of Buruli ulcer patients

INAUGURALDISSERTATION

zur

Erlangung der Würde einer Doktorin der Philosophie

vorgelegt der

Philosophisch-Naturwissenschaftlichen Fakultät

Der Universität Basel

von

Elisabetta Martina Peduzzi

aus

Isorno (Ticino)

Basel, 2006

Genehmigt von der Philosophisch-Naturwissenschaftlichen Fakultät der Universität Basel auf Antrag von

Prof. Dr. G. Holländer, Prof. Dr. G. Pluschke, Prof. Dr. N. Weiss

und PD Dr. C. Daubenberger, Prof. Dr. G. Spagnoli.

Basel, 29. November 2006

Prof. Dr. Hans-Peter Hauri

Dekan

Table of Content

Summary i
Zusammenfassung iii
Abbreviations v

Chapter 1 Introduction

1.1 Host-pathogen interactions in chronic infectious diseases 2
1.2 *Plasmodium falciparum* malaria 4
1.2.1 Natural immunity 5
1.2.2 Vaccine development 8
1.2.2.1 Hurdles 8
1.2.2.2 Strategies 9
1.2.2.3 Synthetic peptides 10
1.2.2.4 Virosomal antigen delivery technology 11
1.3 *Mycobacterium ulcerans* infection (Buruli ulcer) 13
1.3.1 *M. ulcerans* toxins and mycolactone 14
1.3.2 Clinical presentation and histopathology 15
1.3.3 Diagnosis and treatment 16
1.3.4 Immune response 17
1.4 References 19

Chapter 2 Objectives

2.1 *Plasmodium falciparum* malaria 30
2.2 *Mycobacterium ulcerans* infection (Buruli ulcer) 31

Chapter 3 *Plasmodium falciparum* malaria

3.1
Design of a virosomally formulated synthetic malaria peptide eliciting sporozoite inhibitory antibodies 36

3.2
Generation of malaria specific CD4 T cell responses with a virosomally formulated synthetic peptide 74

3.3
Structural and functional characterization of the TLR9 of *Aotus nancymaae,* a primate model for malaria vaccine 98

Chapter 4 *Mycobacterium ulcerans* infection (Buruli ulcer)

4.1
Systemic suppression of IFN-γ responses in Buruli ulcer patients 118

4.2
Local activation of the innate immune system in Buruli ulcer lesions 142

Chapter 5 Discussion

5.1 Monitoring cellular immune responses in clinical vaccine trials and characterization of host-pathogen interactions 164

5.2 *Plasmodium falciparum* malaria vaccine development 169

5.2.1 Virosome: novel antigen delivery system for synthetic peptides 169

5.2.2 Interaction of the virosome with the immune system 170

5.2.3 Induction of cellular immunity to anchored peptides 172

5.2.4 *Aotus* monkeys as malaria vaccine model 174

5.3 Host-pathogen interactions in Buruli ulcer and treatment implications 176

5.4 References 180

Chapter 6 Appendix

6.1
Raw data, supplementary figures and tables of the Phase Ia clinical trial (Chapter 3.2) 190

6.2
Preliminary *in vitro* immunological studies with a *M. ulcerans* CpG ODN 208

Acknowledgments
Curriculum vitae

Summary

Within the context of the establishment of a virosomal-based subunit malaria vaccine including synthetic peptides derived from *Plasmodium falciparum* antigens demonstrated that it is possible to improve immunogenic properties of synthetic peptides in a medicinal chemistry type optimization process. A close to natural conformation of peptides appears to be crucial for the induction of parasite-binding and inhibitory antibodies. In the case of a circumsporozoite protein (CSP) derived synthetic peptide we showed that this is achieved by conformational restriction of the peptide. In a phase Ia clinical trial of the virosomally formulated apical membrane antigen 1 (AMA-1) -derived 49 amino acid long phosphatidylethanolamin peptide conjugate AMA49-CPE, we measured both vaccine induced humoral and cellular responses. In 50% of the volunteers a peripheral blood mononuclear cells (PBMC) lymphoproliferative response specific for AMA49-CPE was elicited. Moreover, all volunteers who developed high titers of parasite cross-reactive IgG in immunofluorescence assay (IFA) and Western blot analysis, were positive in the anti-synthetic peptide lymphoproliferation. No interference was found between the magnitude of the pre-existing influenza specific T cell response and the vaccination-induced AMA49-CPE specific humoral and cellular immune response. We demonstrate that the virosomal antigen delivery platform combined with surface-anchored synthetic peptides is suitable to elicit specific human CD4 T cell responses.

Mycobacterium ulcerans infection (Buruli ulcer) is unique among mycobacteria in that much of the pathology and local immunosuppression appears to be mediated by the production of a cytopathic toxin called mycolactone. IFN-γ ELISpot was used to compare reactivity of PBMC of Buruli ulcer patients with complex antigens such as isopentenyl pyrophosphate (IPP), purified protein derivative (PPD) and influenza antigens prior to and after surgical treatment. The results demonstrated that *M. ulcerans* infection-associated systemic reduction in IFN-γ response is not confined to stimulation with mycobacterial antigens. Immunosuppression reversed after surgical treatment, indicating that this T cell anergy is not the consequence of a genetic defect but rather related to *M. ulcerans* infection. In the affected tissue we detected mRNA coding for innate immune system markers, even though the lack of inflammatory responses is a hallmark of Buruli ulcer disease. These were distributed within the

lesion in a very focal and heterogeneous way. IL-8, IL-6, and TNF-α mRNA was detectable by real time PCR in all lesions, whereas the expression of IFN-α, IL12p40, IL-10, and IFN-γ was only found in some lesions. Correlations of the distribution of mRNA encoding for the activation marker CD83 and the DC subset markers CD123 and CD11c indicate that both activated plasmacytoid and myeloid DC were present in the lesions. These results suggest that adaptive M. *ulcerans* specific immune responses may develop once therapeutic interventions have limited the production of mycolactone.

Zusammenfassung

Im Rahmen der Entwicklung eines auf der Virosomen-Technologie basierenden Malaria Subunit-Impfstoffes haben wir die immunogenen Eigenschaften von synthetisch hergestellten Peptiden in einem schrittweisen Optimierungsprozess systematisch verbessert. Dabei war es essentiell die 3-dimensionale Struktur der synthetischen Peptide der nativen Konformation des Zielantigens möglichst weitgehend anzunähern, um eine optimale Induktion von kreuzreaktiven und inhibitorischen Antikörpern zu erreichen. Im Falle der von *Plasmodium falciparum* Circumsporozoite Protein (CSP) abgeleiteten synthetischen Peptide UK39 und BP66, haben wir dies durch Restriktion der konformationellen Dynamik der Peptide erreicht. In einem klinische Phase Ia Versuch haben wir die zellulären Immunantwort virosomaler Formulierungen von UK39 und AMA49-CPE untersucht. Gegen das von Apical Membrane Antigen-1 (AMA-1) abgeleitete Peptid AMA49-CPE, nicht aber gegen UK39, zeigte die Hälfte der Probanden eine spezifische lymphoproliferative Antwort der peripheren mononukleären Zellen des Blutes (PBMC). Die Probanden, bei welchen hohe Titer von Parasiten-bindenden IgG-Antikörpern in Immunfluoreszenz-Anfärbung und Western Blotting gemessen wurden, wiesen auch eine positive zelluläre Immunantwort im Lymphoproliferations-Test auf. Die Intensität der bereits vorhandener Influenza-spezifischen T-Zell-Antworten hatte keinen Einfluss auf die Impfstoff-induzierten AMA49-CPE spezifischen humoralen und zelluläre Immunantworten. Mit unseren Ergebnissen haben wir aufzeigen können, dass die Virosomen-Technologie, kombiniert mit auf der Oberfläche verankerten synthetischen Peptid-Phospholipid Konjugaten, benutzt werden kann, um eine spezifische CD4 T-Zell Immunantwort auszulösen.

Der von *Mycobacterium ulcerans* hervorgerufene Buruli Ulkus ist einzigartig unter den mykobakteriellen Infektionen, in dem ein vom Bakterium produziertes Toxin namens Mycolakton entscheidend an der Pathogenese und lokalen Immunsuppression beteiligt ist. Die IFN-γ ELISpot Technik wurde verwendet, um die Immunantworten von PBMC verschiedener Buruli Ulkus Patienten zu vergleichen, welche mit Isopentenyl-pyrophosphate (IPP), 'Purified Protein Derivative' (PPD) oder Influenza-Antigenen stimuliert wurden. Unsere Ergebnisse mit PBMC, die vor oder nach chirurgischer Entfernung der Läsionen präpariert wurden, zeigten, dass eine mit der

Infektion einhergehende systemische Reduktion der IFN-γ Produktion nicht auf die Stimulation mit mycobakteriellen Antigenen beschränkt ist. Im erkrankten Gewebe haben wir mit real-time PCR mRNAs detektiert, welche für Marker des angeborenen Immunsystems kodieren, selbst wenn in Buruli Ulkus eine massive Entzündungsreaktion fehlt. Infiltrate scheinen in einer fokalen und heterogenen Weise innerhalb der Läsion verteilt zu sein. Während die mRNA von IL-8, IL-6, and TNF-α in allen untersuchten Läsionen detektierbar war, wurde IFN-α, IL12p40, IL-10 und IFN-γ nur in einigen Läsionen gefunden. Die positive Korrelation der Verteilung von mRNA des Aktivierungsmarkers CD83 und von Markern für verschiedene Untergruppen von dendritischen Zellen (CD123 und CD11c) weist auf die Anwesenheit von aktivierten plasmazytoiden und myeloiden dendritischen Zellen in den Läsionen hin. Unsere Ergebnisse lassen vermuten, dass eine Antwort des adaptiven Immunsystems in *M. ulcerans* Läsionen aufkommen kann, sobald therapeutische Interventionen die Produktion des Toxins Mykolakton beschränkt haben.

AA	Amino acid
Ab	Antibody
AFB	Acid fast bacilli
Ag	Antigen
APC	Antigen presenting cell/s
APL	Altered peptide ligand/s
BCG	Bacillus Calmette-Guérin
BU	Buruli ulcer
CCR	Chemokine (C-C motif) receptor
CD	Cluster of Differentiation
cDNA	Complementary Deoxyribonucleic acid
Ci	Curie
CpG	Cytosin phosphatidyl Guanosin
cpm	Counts per minute
CFSE	Carboxy-fluorescein diacetate, succinimidyl ester
CTL	Cytotoxic T lymphocyte
DC	Dendritic cell/s
DNA	Deoxyribonucleic acid
DNase	Deoxyribonuclease
dNTP	deoxyribonucleoside triphosphate
ELISA	Enzyme-linked immunosorbent assay
ELISpot	Enzyme-linked immune spot assay
FACS	Fluorescence activated cell scanning
FCS	Fetal calf serum
FITC	Fluorescin isothiocyanat
HA	Hemagglutinin
HAV	Hepatitis A virus/es
HBSS	Hanks balanced salt solution
HIV	Human immunodeficiency virus
HLA	Human leukocyte antigen
Ig	Immunoglobulin
IL	Interleukin
IFA	Immunofluorescence assay
IFN	Interferon
IPP	Isopentenyl pyrophosphate
IRIV	Immunopotentiated reconstituted influenza virosome
IS	Insertion Sequence
mAb	Monoclonal Antibody
M-DC	Myeloid dendritic cells

MHC	Mayor histocompatibility complex
mRNA	Messenger ribonucleic acid
MyD88	Myeloid differentiation primary response gene 88
NA	Neuraminidase
NF-κB	Nuclear factor kappa B
NMR	Nuclear magnetic resonance
NO	Nitric oxide
NPNA	Asparagine-Proline-Asparagine-Alanine
OD	Optical density
ODN	Oligodeoxynucleotides
PBC	Peripheral blood compartment
PBMC	Peripheral blood mononuclear cells
PBS	Phosphate buffered saline
PCR	Polymerase chain reaction
P-DC	Plasmacytoid dendritic cells
PE	Phosphatidylethanolamin
PHA	Phytohemagglutinin
PPD	Purified protein derivative
RBC	Red blood cell/s
SFU	Spot forming unit
SI	Stimulation index
spp.	Species
TCR	T cell receptor
Th	T helper cell
TLR	Toll-like receptor
TNF	Tumor necrosis factor
TT	Tetanus toxoid
WHO	World Health Organisation
ZN	Ziehl-Neelsen staining

Chapter 1

Introduction

1.1 Host-pathogen interactions in chronic infectious diseases

History shows that vaccines and successful treatments are most easily developed for those pathogens that induce natural, sterile immunity after a single infection [1]. Infectious agents can cause recurrent or persistent disease by avoiding normal host defense mechanisms or by subverting them to promote their own replication. Antigen variation, latency and suppression of immune effector mechanisms all contribute to persistent and medically important infections. Some pathogens use immune activation to spread the infection, and some others strongly activate the immune system which is in the end the actual cause of the disease. Each of these mechanisms has to be characterized and often requires a different medical approach to prevent or to treat the caused infection.

Malaria remains one of the world's greatest public health challenges. Although first visualized by Laveran more than 120 years ago, the parasite has resisted all efforts to control it. Today, an estimated 40% of the world's population remains at risk of malaria, with 500 million of cases estimated annually, resulting in 1-2 million deaths, mostly young children [2]. Partial immunity against malaria develops only after several years of endemic exposure and for its maintenance repeated infections over the lifetime of the individual is required [3,4]. Immunity seems to be lost (or becomes less effective) when a previously immune person moves away from an endemic area [4,5]. Antigenic variation, high polymorphism and life stage specific antigen-expression are considered important evasion mechanisms of *Plasmodium falciparum* parasite.

Buruli ulcer is a disease of skin and soft tissue caused by an environmental pathogen, *Mycobacterium ulcerans*. It has been first described by Sir Robert Cook in 1897 in northeast Congo [6] and definitively characterized by MacCallum in 1948 in Australia [7]. In the last decade, the incidence in West African countries increased dramatically. In Southern Benin, a recent study has reported detection rates of 21.5/100'000 per year, exceeding that of leprosy and tuberculosis [8]. Worldwide, it represents the third most common mycobacterial disease in immune-competent people, after tuberculosis and leprosy [9]. In Buruli ulcer affected people, spontaneous healing might occur in late stages after a chronic phase of variable length and relapse events can occur. The length of incubation time, the presence of dormant forms in

healthy people and the mechanisms by which the host may eventually overcomes immune suppression and develop a protective immune response are still open questions in Buruli ulcer infections. The toxin elaborated by *M. ulcerans* plays an important role in the development of Buruli ulcer disease, but other virulence factors may also contribute to the observed systemic immunosuppression in Buruli ulcer patients [10].

Understanding immune responses to chronic infectious diseases like malaria and Buruli ulcer is crucial for the effective design and implementation of urgently needed vaccines, drugs and treatments. The present thesis is focusing on monitoring specific immune responses to malaria antigens, within the context of clinical malaria vaccine Phase Ia trial, and on the characterization of systemic and local immune status of Buruli ulcer patients.

The objectives of this thesis are fully illustrated in Chapter 2.

1.2 *Plasmodium falciparum* malaria

Malaria tropica is caused by *P. falciparum* and is responsible for about 90% of the malaria morbidity and mortality worldwide [3]. The pre-erythrocytic stage (sporozoite/liver) represents the body's first encounter with the parasite and the erythrocytic stage is responsible for all symptoms and pathology of malaria. Exponential growth of parasites in the erythrocytes, modification of infected red cells in terms of parasite proteins expressed on the cell surface and the concomitant immune response to the parasite ultimately result in the disease manifestations of malaria. In recent years, the burden and mortality of the disease has increased substantially in malaria-endemic countries [11], and its transmission has spread to new areas [12]. The major causes are the development of resistance to drugs [13] and insecticides [14], the deterioration of national control programs, the increased human migration, and tourism [15-17].

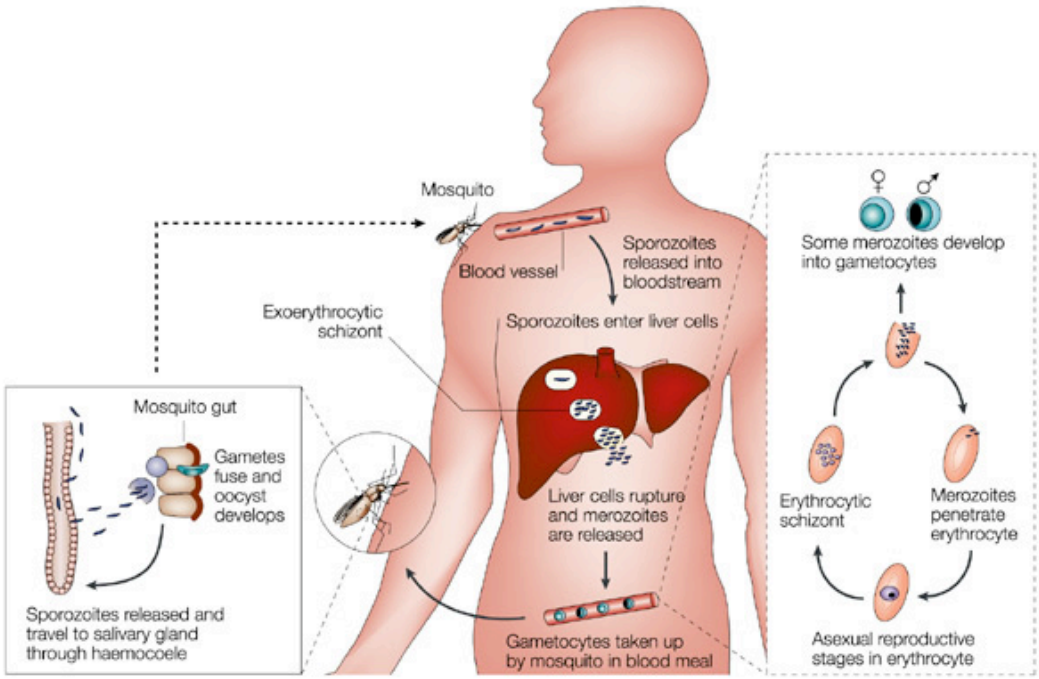

Figure 1 Life cycle of *Plasmodium falciparum*. Stevenson et al., *Nature Immunology*, 2004

1.2.1 Natural Immunity

Natural immunity to malaria is complex and varies with the levels of endemicity, genetic makeup, age of the host and parasite species. Generally in high endemic areas, maternal antibodies protect infants until 6 month of age. When this protection is lost infants become susceptible to severe forms of the disease with high mortality until about 3 years of age. The parasite is then controlled by the host, rather than eliminated or prevented: in clinically immune individuals asymptomatic re-infection, low-density parasitemia, and carriage of infective gametocytes continue [4,18]. The marked reduction in parasite density (10^4 to 10^6-fold lower than in naïve individuals [19]) and the decline in the prevalence and severity of symptoms are the indicators of valuable anti-parasitic and anti-disease effectors mechanisms by the human host. The natural immunity against malaria is still poorly understood but there is evidence that humoral as well as cellular mediated immunity are involved with a clear participation of the innate immunity. There is general agreement that antibodies, specific for the surface of parasitized erythrocytes and for the free merozoites (asexual blood-stages), are largely responsible for the semi-immune status providing direct protection against the pathological consequences of blood-stage re-infection [20-22]. Unfortunately the majority of the elicited antibodies do not recognize a common epitope found on all infected red blood cells, but mainly epitopes that are strain specific [23,24] requiring multiple infections to acquire immunity. The natural immunity against the sporozoites and liver stage (pre-erythrocytic stages) is comparatively more limited and does not appear to markedly hinder development of parasites in blood stages [5]. A lower prevalence of antibodies to liver stage antigen-1 (LSA-1) and circumsporozoite protein (CSP) than to blood-stage associated antigens (apical membrane antigen-1, AMA-1 and merozoite surface protein-2, MSP-2) has been reported [25,26]. The level of immunity to gametocytes and gamete antigens is variable and transmission-blocking antibodies are present in only a minority of sera from immune adults [27-29]. Hence, clinically immune adults provide a reservoir of infection for mosquitoes and consequently for transmission of malaria within the population. The investigation of immune mechanisms and pathogenesis of malaria is supported by the work with rodent Plasmodium species (spp.): *P. chabaudi, P. berghei, P. yoelii* and *P. vinckei* [30,31]. However, it has to be mentioned that no single rodent model replicates all of the features of human malaria infections [31]. Based on ongoing animal studies,

Figure 2 illustrates a possible regulation of adaptive immunity to blood-stage malaria by cytokines produced by the innate immune system.

In humans, low levels of plasma IL-12 [32-34] and IL-18 [35] are associated with severe malaria pathology. Prospective epidemiological studies suggest that IL-12 production is inversely associated with risk of infection and positively associated with hemoglobin concentration, IFN-γ and TNF-α production [36]. Recently studies propose possible mechanisms of dendritic cells (DC) regulation in malaria disease. Purified *P. falciparum* hemozoin, the insoluble residue of hemoglobin that accumulates in phagocytes, activate mice bone marrow DC through TLR9: $TLR9^{-/-}$ and $MyD88^{-/-}$ mice or DC, but not $TLR2\text{-}4^{-/-}$ or $TLR7^{-/-}$ showed an impaired production of cytokines and chemokines after hemozoin stimulation [37]. On the other hand, *in vitro* studies show that parasite infected erythrocytes bind to CD36 expressed on human DC activating the release IL-12 and IL-18 [38]. The exact relevance of these mechanisms for *P. falciparum* host immunomodulation is debated [38,39]. Summarizing, naturally acquired immunity to malaria is not sterile and appears largely due to the acquisition of mechanisms to control blood-stages, allowing co-existence of host and pathogen. Survival and immune-evasion mechanisms of the parasite, requirement of frequent parasite-exposure by the host to maintain a good semi-immune status (pre-munition) and lack of long lasting memory are sentinels of non-sterile immunity. In which extent these problems are malaria-specific rather than generic (i.e. result from inherent limitations of the vertebrate immune system) is not yet clear [4]. Previously immune adults revisiting endemic areas are at risk of developing symptomatic malaria. However, case fatality rates are significantly higher among non-immune travelers [40-42]. These observations suggest that a limited memory against malaria is present, but somehow incomplete. The development and maintenance of malaria specific memory are still open questions. Some experiments in mice models point out that malaria parasites can to some extent modulate memory T and B cells: newly *P. berghei* infected mice can selectively delete by apoptosis adoptive transferred CD4 T cells specific for the parasite [43]. Vaccines usually induce sterilizing or complete transmission-blocking immunity by means of antibody and T cell responses to one or a few antigens. For malaria, the absence of such immunity in the vast majority of exposed individuals suggest that for an effective vaccine the response should be of greater magnitude, duration and strain-

transcendence than in naturally acquired immunity. An alternative, ambitious, long-term approach is to use a cocktail of many antigens to elicit a better focused and more effective response [22,44].

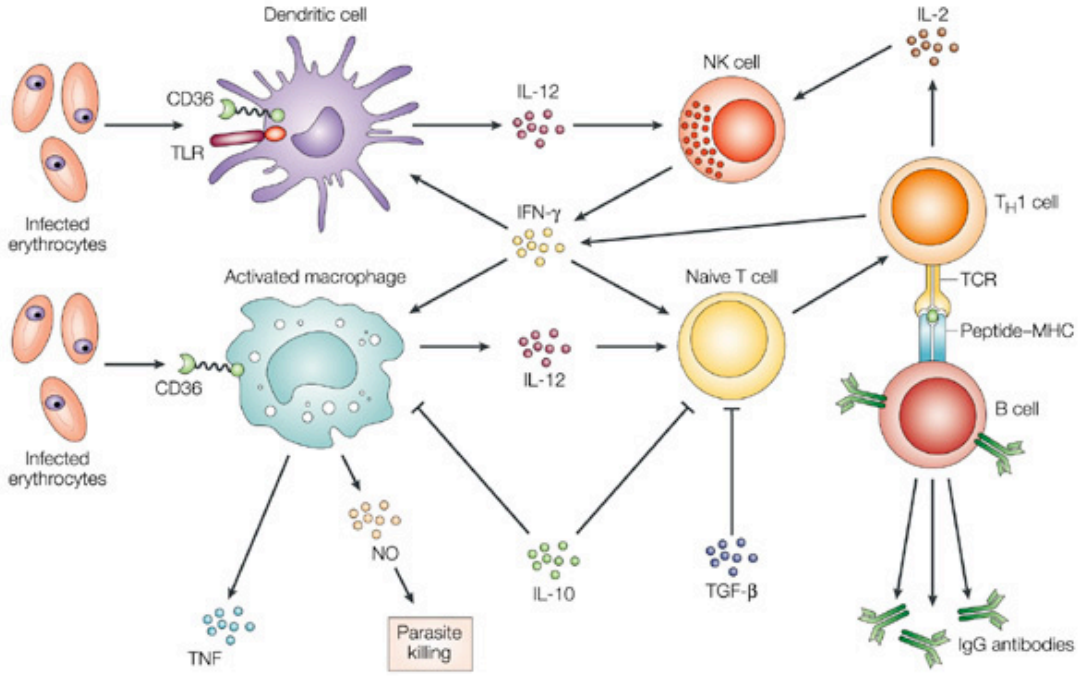

Figure 2 Link between innate and adaptive immunity to blood-stage malaria based on mice models. In response to parasite ligands, DC mature and migrate to the spleen. Released IL-12 activate the production of IFN-γ by natural killer cells (NK) and induce the differentiation of T helper (Th) 1 cells and further maturation of DC. These processes facilitate the clonal expansion of CD4 T cells and activation of macrophages, allowing the amplification of the adaptive immune response. [nitric oxide (NO)]. Stevenson et al., *Nature Immunology*, 2004

1.2.2 Vaccine development

The concept for the development of a malaria vaccine arose in 1967 from experimental immunization studies with irradiated sporozoites in mice [45]. In 1975, human volunteers immunized with irradiated attenuated *P. falciparum* sporozoites developed a short term protective immune response against subsequent malaria infections [46-48]. The cloning of the first Plasmodium spp. antigen in 1983 and the publication of the complete *P. falciparum* genome in 2002 further encouraged the malaria vaccine research [49]. However, the vaccine still appears to be a long way off, scientific community estimate that its development will take not less than 10 years [21,50]. Nowadays malaria drug development is the research priority and vaccine development is one aspect of efforts to control the disease. However, an effective vaccine still represents the most cost-effective way to protect humans against infectious diseases. There are three intermediate goals of malaria vaccine research: (i) induction of strong, strain transcending, durable immune responses; (ii) identification of protective antigens for stage specific immunity, and (iii) successful combination of immunogenic candidates [22]. Meanwhile, the WHO Roll Back Malaria program is coordinating other strategies to control the disease: improved case management; promote insecticide-treated bed-nets to reduce malaria mortality [51].

1.2.2.1 Hurdles

Many immunodominant malaria antigens contain highly polymorphic regions (AMA-1, MSP-1, MSP-2) [52-58]. Furthermore, some *P. falciparum* antigens present irrelevant but immunodominant epitopes, which induce non-protective immune response of the host. On the other hand, some potentially protective conserved target epitopes/antigens appear to be cryptic and are consequently not able to induce effective immunity following natural malaria exposure [21]. These mechanisms have to be considered by the design of good vaccine candidates [21,59]. Infants and very young children represent the principal target of a malaria vaccine, many of them will carry maternal antibodies specific for the parasite. These antibodies may be important in providing protection against malaria [60,61], but it is well documented that the presence of specific maternally derived antibodies at the time of immunization may interfere with the development of the infant's own active immune response by blocking access to critical B cell epitopes [62,63]. Delayed immunization, until levels

of maternally antibodies decrease, or the use of alternate epitopes for infant vaccines are proposed solutions [63]. On the other hand the adult population receiving the vaccine is already infected, therefore there may be a boost of preexisting memory T and B cells. In this respect the potential ability of the malaria parasite to modulate host memory immune responses has to be considered and further investigated. Some studies in mice show that new malaria infections can lead to anergy and deletion of parasite pre-existing memory CD4 T cells [43]. Anergy can be the consequence of the presentation of closely related peptide variants which provide altered activation signals to the T cell, resulting in the inactivation of some of its effector functions [64]. In malaria, down-regulation of T cell responses by epitope variants that vary in only one or few amino acid (AA), so called altered peptide ligands (APL), has been classically described for T cell clones expressing a specific T cell receptor structure [65-69]. In this respect, allelic polymorphism of *P. falciparum* antigens has probably evolutionary been maintained because of a parasite survival advantage of cohabiting allelic types [70]. Studies with the CSP, show that simultaneous stimulation with certain naturally occurring T cell epitope variants turns off effector T cell immunity, resulting in enhanced parasite survival [67]. Allelic MSP-1 epitopes with low T cell reactivity to dominant alleles have the capacity to turn off polyclonal T cell responses in both naïve and malaria exposed individuals [71]. The consequence of allelic interference with T cell priming is the induction of a state of partial activation of CD4 T cells independently described with both anergic and suppressor cell functions. The lack of priming of fully functional CD45RO memory T cells from naïve precursors is likely to lead to 'holes' in the effector T cell repertoire [70,72]. Depletion of CD4+CD25+ regulatory T cells has been shown to protect mice from death when infected with a lethal strain of *P. yoelii* [73].

1.2.2.2 Strategies

An anti malaria vaccine could act at different stages of the parasite life cycle and infectious mechanisms: (i) block sporozoites from invading or developing within hepatocytes (pre-erythrocytic anti-infection vaccine) [74-76]; (ii) prevent the merozoite invasion of red blood cells or inhibit development of schizonts (anti-disease vaccine) [77,78]; (iii) obstruct the pathology inducing effects of cytokines, parasite sequestration and parasite toxin release (disease-modifying vaccine) [79]; (iv) block human-mosquito transmission by immunization against the sexual stages of the

parasite (transmission-blocking vaccine) [80,81]. The design of a malaria-vaccine ranges from a subunit to a whole parasite approach. The traditional whole-organism approach was considered till now the most protective but also least achievable, due to cost and safety problems. However some recent works and projects awaked the interest for this approach. Hoffman has raised the ambitious project to produce a vaccine with irradiated sporozoites dissected out from infected mosquitoes by keeping the production costs as low as possible [82]. Furthermore, results obtained with mice immunized with genetically modified *P. berghei* sporozoites, that do not develop beyond the liver stage, showed good challenge protection [83]. Concerning the asexual blood stages experiments with naïve volunteers infected with an ultra-low dose of malaria parasites (thirty *P. falciparum*-infected red blood cells, RBC) showed a good humoral and cellular immune response [84]. Mice vaccinated with crude preparation of parasitized red blood cells combined with the adjuvant IL-12 or CpG were protected against *P. chabaudi* challenge [85].

Most malaria vaccine projects are focused on subunit vaccine technologies. The combination of conserved epitopes representing the different stages of the parasite life cycle [78], should diminish the impact of antigen polymorphism. An appropriate adjuvant as well as cost problems of producing a multi-component vaccine are important obstacles for this approach. In this respect the use of DNA vaccines [86-89], or more effective adjuvants, like the virosomal delivery systems and, the application of CpG and IL-12 as immunostimulators are approaches under assessment [85,90-93].

1.2.2.3 Synthetic peptides

The advantages of synthetic peptides over conventional protein-based vaccines include, ease of handling and storage due to their higher stability, ease of synthesis and avoidance of problems associated with materials produced in cells. A further appeal is that the ideal subunit vaccine will induce immune responses only against determinants relevant for protection, thus minimizing the possibility of deleterious responses. Within the context of a malaria multi-component, multi-stage vaccine the criteria for epitope selection include sequence conservation, known induction of parasite inhibitory antibodies and identified secondary structure motifs indicating surface exposition. Based on these criteria in our malaria vaccine project a series of peptides vaccine candidates were developed, including CSP, MSP-1 and AMA-1

derived peptides. Starting from a lead structure, the peptide sequences and/or conformations were optimized in cycles and only the peptides with satisfactory immunological properties were selected for final preclinical profiling and clinical testing. In the case of CSP and MSP-1 derived peptides conformational restriction of the peptide was crucial for the induction of parasite-binding antibodies in mice [91,93]. Only correctly folded MSP-1 peptides with all three disulfide bonds in place induced parasite-binding antibodies but not peptides with blocked cysteins [94]. For the development of conformationally restricted synthetic peptide, parallel 3D structural studies were crucial [93,95,96]. In contrast, the AMA-1 derived peptide AMA49-C1 (loop I of AMA-1 domain III) seemed to have enough internal driving force to adopt a conformation suitable to elicit parasite cross-reactive antibodies recognizing a discontinuous epitopes. Indeed, the cyclized and the linear forms of this peptide had comparable immunogenic properties [83]. AMA-1 is an example of an antigen, where induction of parasite inhibitory antibodies has been reported without a detailed characterization and localization of the epitope. In such cases peptide libraries covering the whole protein sequence can help selecting an epitope inducing inhibitory antibodies. These examples underline the importance of a detailed preclinical profiling and optimization of every candidate antigen for inclusion into a malaria vaccine. Synthetic peptide chemistry strongly facilitates a medicinal chemistry approach for vaccine design, allowing rational stepwise peptide optimization based on structure-activity observations.

1.2.2.4 Virosomal antigen delivery technology

Peptide-based vaccines require efficacious and safe vaccine adjuvants. The virosomal technology is one of the approaches currently under evaluation. Immunopotentiating reconstituted influenza virosomes (IRIVs) are prepared by the detergent removal of influenza glycoproteins, hemagglutinin (HA) and neuraminidase (NA), which are subsequently combined with natural and synthetic phospholipids. The resulting IRIVs are spherical, unilamellar vesicles with a mean diameter of approximately 150 nm [97-99]. The influenza HA plays a key role in the mode of action of the IRIVs. The HA globular head subunit (HA1) contain sialic acid site for HA and it is therefore assumed that the IRIVs bind to such receptors of antigen presenting cells (e.g. macrophages, DC, lymphocytes) initiating a successful immune response (adjuvant, immunepotentiator effect). The entry of influenza viruses into cells occurs through

receptor mediated endocytosis [100]. The HA2 subunit mediates the fusion of viral and endosomal membranes, which is required to initiate "infection" of cells. It is expected that this mediates the rapid release of the transported antigen into the membranes of the target cells [99,101]. There are currently two vaccines on the market exploiting, the IRIV delivery system: Hepatitis A (Epaxal) and Influenza (Inflexal V) vaccines. Epaxal was licensed for human use in 1996. It contains formalin-inactivated and highly purified hepatitis A viruses (HAV) coupled to IRIV vesicles. 10 days after immunization 100% of seroconversion was measured [102] and the adverse effect are less than for the conventional, alum adsorbed, forms of vaccination [103]. The superior immunogenic and protective abilities of IRIVs in terms of antibodies titers were evidenced also by comparing alum and IRIV formulation of diphteria and tetanus toxoids [104]. The suitability of virosomes for a multi-epitope malaria peptide vaccine approach was shown in mice, which developed antibodies cross-reactive with the parasite [83,90,91,93].

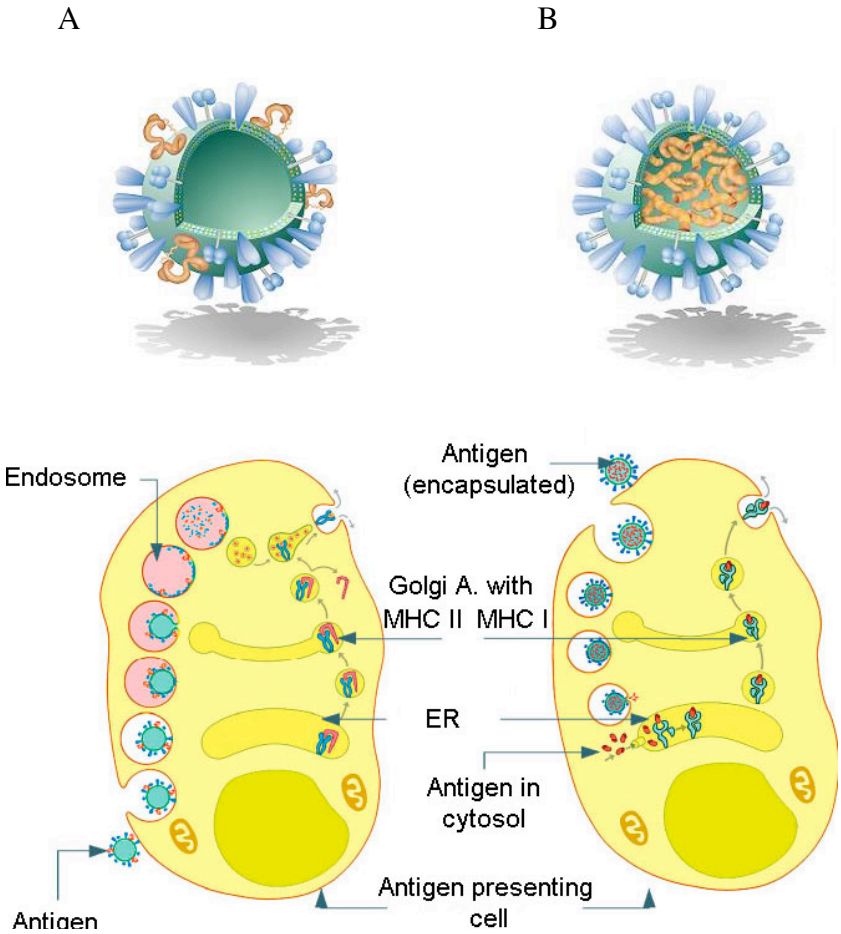

Figure 3 Representation of IRIV mode of action; **A** with antigen presented on surface, **B** with encapsuled antigen. Westerfeld and Zurbriggen, *Journal of Peptide Science*, 2005

1.3 *Mycobacterium ulcerans* infection (Buruli ulcer)

Buruli ulcer, caused by an environmental pathogen *M. ulcerans*, is a chronic ulcerative disease of skin and soft tissue with the potential to leave massive scarring and deformities. The main burden of disease falls on children living in Sub-Saharan Africa but healthy people of all ages, races and socioeconomic classes are susceptible. *M. ulcerans* is the third most important mycobacterial pathogen in immuno-competent people, after *M. tuberculosis* and *M. leprae* [9]. The slowly growing *M. ulcerans*, with an *in vitro* generation time of 20 hours [105] belongs to a group of mycobacteria that are potentially pathogenic for humans and animals. These are sometimes called "occasional pathogens" to distinguish them from strict pathogens. Most species belonging to this group are widespread in the environment and may become pathogenic under specific circumstances [106]. Changes in the environment, such as the construction of irrigation systems and dams, seem to have played a role in the resurgence of Buruli ulcer disease [107]. The exact mode of transmission to humans is still unclear, skin trauma or the bite of an infected water insect might be involved. Specific *M. ulcerans* DNA can be detected by PCR in some aquatic insects, as well as in aquatic snails, small fish, and the biofilm of aquatic plants [108,109]. *M. ulcerans* is found extracellularly in established Buruli ulcer lesions [110]. Recent studies showed that it proceeds through an initial phase where bacilli are internalized by phagocytic cells [111]. The transition to the extracellular phase occurs probably by the action of released toxins. *M. ulcerans* is unique among mycobacteria in that much of the pathology appears to be mediated by production of toxic macrolides that are required for virulence [110].

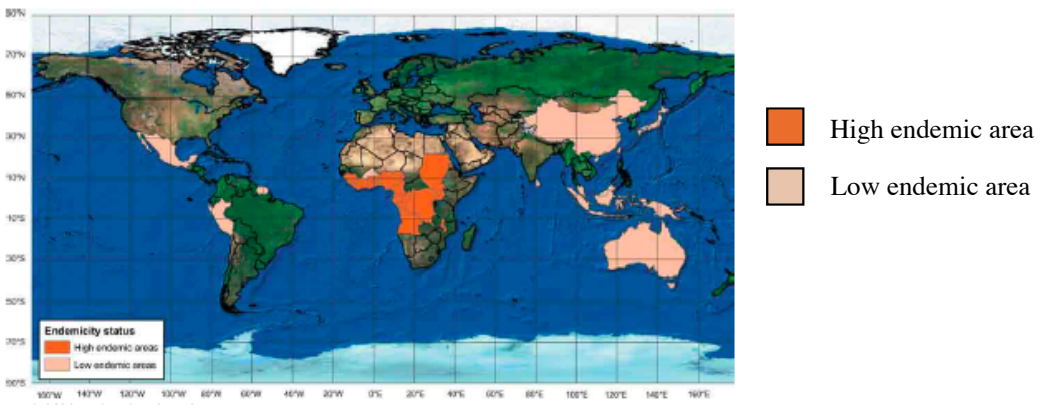

Figure 4 Countries reporting Buruli ulcer. Johnson et al., *PLoS Med.*, 2005

1.3.1 *M. ulcerans* toxins and mycolactone

The pathogenesis of *M. ulcerans* and its extra-cellular localization are closely associated with the expression of plasmid-encoded enzymes that are involved in the synthesis of mycolactones. In 1965 Connor hypothesized the presence of toxins in early Buruli ulcer lesions: histopathological results evidenced that the necroses were more extended than the bacterial burden [112]. In 1999 this hypothesis was confirmed by the isolation of a macrolide toxin from bacteria culture filtrates called mycolactone (Figure 5). The name combines its mycobacterial source and chemical structure. Possibly other toxins, e.g. phospholipase C also play a role in the pathology of *M. ulcerans* [113]. The culture-isolated mycolactone has immunosuppressive and cytotoxic effects *in vitro*, inhibition of cytokine production and NF-κB function has been observed in human monocytes cultures [114]. When injected into healthy guinea pigs, histopathological changes comparable to Buruli ulcer lesions were induced [115]. Comparison of animal models infected with mycolactone producing and mycolactone negative *M. ulcerans* strains suggests that inflammatory cells are rapidly killed by necrosis when they encounter high concentrations of the toxin. Inflammatory cells more distant from the necrotic centre are killed via apoptosis [114]. Until now, no cell receptor has been found to explain the cascade of effects induced by mycolactone [116]. In contrast, in animals experimentally infected with mycolactone-negative mutants, granulomatous lesions with strong self-healing tendencies are observed. Additionally, mycolactone negative mutants fail to colonize the salivary glands of water insects, suggesting that this molecule may also play a role in the ability of *M. ulcerans* to colonize potential reservoir species [110,117].

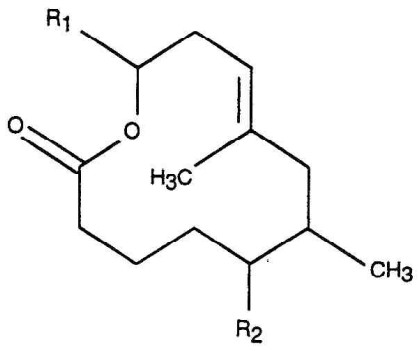

Figure 5 Mycolactone core structure: 12-membered ring to which two polyketide-derived side chains (R_1 and R_2) are attached. George et al., *Science*, 1999

1.3.2 Clinical presentation and histopathology

A painless papule or firm nodule indicates the first stage of Buruli ulcer (Figure 6a-b). A papule is defined as a painless, raised skin lesion surrounded by reddened skin (Figure 6b). The nodule is characterized as an extended lesion from the skin into the subcutaneous tissue. Occasionally, some patients develop extensive indurate lesions or plaques that present irregular edges (Figure 6c). These first stages of the disease are characterized by coagulative necrosis of the lower dermis and subcutaneous fat. The bacteria are present in clumps or in smaller microcolonies in the centre of the lesion and there is little or no evidence of an inflammatory response or the development of granuloma formation [118]. In the second stage, ulceration takes place at the base of the small origin ulcer, which displays a white cotton wool-like appearance in the necrotic slough (Figure 6d). Many acid fast bacilli (AFB) are present in the slough, and the necrosis can extent away from the site where *M. ulcerans* is located (Figure 6e). As the disease progresses all elements of the skin are affected including nerves and blood vessels. At this stage granulomas containing epithelioid macrophages and Langerhans giant cells may be seen [118]. The host may somehow overcome the immunosuppressive effects of the toxin, usually only after extended periods of progressing ulceration, and a healing process can start (Figure 6f). This process may delay or never take place with consequent heavy complications for the host, including affection of the bone (osteomyelitis), the loss of organs such as the eye and breast, the amputation of limbs or other permanent disabilities [119,120].

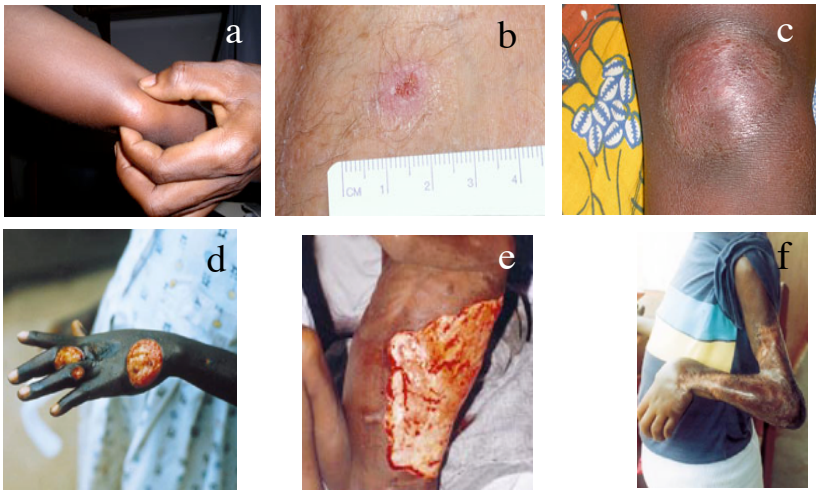

Figure 6 Clinical forms of Buruli ulcer. a: nodule, b: papule, c: plaque, d: early ulcer, e: late ulcer, f: crippling deformity after self healing. Asiedu et al., WHO 2000; Portaels et al., WHO 2001

1.3.3 Diagnosis and treatment

Early treatment of *M. ulcerans* disease provides a better outcome than extensive surgical treatment of the ulcerative forms. In a known endemic area, an experienced person can diagnose an advanced *M. ulcerans* infection on clinical grounds: painless ulcer with undermined edges and a necrotic slough, no clinically detectable lymphadenitis and no systemic symptoms such a fever or malaise suggesting staphylococcal or streptococcal infection. Since, in particular, early and healing lesions may be confused with other skin diseases, laboratory confirmation of clinically diagnosed cases is desirable. The commonly used diagnostic laboratory tests are: (i) detection of mycobacteria by Ziehl-Nielsen (ZN) staining, a technique that lacks sensitivity and specificity, (ii) culture of *M. ulcerans*, which may take several months, (iii) detection of characteristic histopathological changes in excised tissue and (iv) detection of *M. ulcerans* DNA by PCR. PCR represents a rapid and sensitive diagnostic method but requires advanced technical expertise and high laboratory standards that are not always available in developing countries. While swabs can be taken to test the undefined edges of ulcerative lesions, it is much more problematic to take punch biopsies from pre-ulcerative lesions, since this technique may promote the spread of the mycobacteria. The WHO global Buruli ulcer initiative has asked the research community to develop a simple rapid diagnostic test in order to improve the detection rate of Buruli ulcer patients and to implement preventive therapy and early treatments [121]. Traditionally, the mainstay of treatment has been surgical excision of early lesions. Unfortunately many patients do not present until there is extensive and disfiguring ulceration, when there is no alternative but wide excision followed by skin-grafting, and sometimes even amputation [122]. Currently it is not clear how extensive surgeries should be performed and it is largely left to the individual judgment of the surgeon to find the right balance between an oversized excision and an incomplete removal of pathogen, thus increasing the risk of recurrence [123]. Relapse after surgery may occur in 15-47% of the cases [8,124]. For a long time, treatment of *M. ulcerans* infections with antimycobacterial agents has generally been disappointing, probably partly due to the suboptimal penetration of drugs to the necrotic lesions. *In vitro,* the bacteria are susceptible to several antimycobacterial drugs. The most promising combination in the mouse footpad model is rifampicin with amikacin [125]. A human trial has recently shown that early nodular lesions may

be rendered culture negative after a minimum of 4 weeks therapy with rifampicin plus streptomycin [126]. These results have encouraged WHO to recommend the use of this antibiotic combination to support surgical treatment [127].

1.3.4 Immune response

The mechanism of immune protection in *M. ulcerans* remains unclear. The predominant pattern in the pathology of this bacterial disease is that in early, pre-ulcerative and ulcerative lesions, large numbers of extra-cellular mycobacteria are seen, with extensive necrosis and very little inflammatory response, and no granuloma formation. In surgical specimens of later stages during healing, bacilli are scanty or even absent usually accompanied by granuloma formation [7,128,129]. Several research groups, using different models, have observed that in early stages of the disease, specific immune protection seems to be lost. Almost 30 years ago, studies of the delayed hypersensitivity response in patients with Buruli ulcer after intradermal injection of a crude preparation of *M. ulcerans* sonicate (burulin) showed that patients with early *M. ulcerans* disease do not react, whereas a positive response is found in most patients with healing lesions, who were initially non-reactive, indicating a degree of T cell sensitization [130]. Burulin has not been prepared to the standard required for *in vivo* work with human beings since that time.

Evidence from genetic defects in the IFN-γ signaling pathway supports the role of IFN-γ in protection against a range of non-tuberculous mycobacterial disease, including *M. ulcerans* [131]. Many healthy individuals in Buruli ulcer-endemic areas show specific immune responses to *M. ulcerans* [132,133], suggesting that, in analogy with leprosy and tuberculosis, the disease develops only in a limited proportion of those infected [134]. Gooding et al. describe the case of an unaffected household contact, the mother of an infected child with Buruli ulcer disease, which during the study developed an ulcerative *M. ulcerans* disease. A resulting shift from Th1 to Th2 cytokines production was monitored by stimulating peripheral blood mononuclear cells (PBMC) with *M. ulcerans* [135,136]. Further evidence that a cellular immune response may protect individuals with Buruli ulcer is provided by a case reports that describes aggressive, disseminated *M. ulcerans* disease in patients co-infected with HIV [137]. However, unlike tuberculosis, the emergence of Buruli ulcer has not been linked with co-infection by the human immunodeficiency virus [138]. Host

susceptibility factors need to be explored to understand mechanisms explaining the development of BU once individuals have been infected with *M. ulcerans* [138-140]. *In vitro* immune analysis have confirmed the notion of a systemic T cell anergy in Buruli ulcer affected people: PBMC from patients showed significantly reduced lymphoproliferation and IFN-γ production in response to stimulation with *M. bovis,* Bacillus Calmette-Guérin (BCG) or *M. ulcerans*, and a Th2 type (IL-4, IL-5) cytokine mRNA pattern was present [135,141] suggesting Th2 mediated Th1 down-regulation. Prevot et al., tried to link systemic and local immune responses. By semi-quantitative PCR analysis he suggests that the systemic Th1 down modulation is mirrored by local, intralesional cytokine profiles. High IFN-γ with low IL-10 mRNA levels were present in early, nodular lesions and low IFN-γ mRNA levels were detected in late ulcerative lesions [142]. Hence, in active *M. ulcerans* disease, the Th1 response seems to be down-regulated both locally and systemically. A mouse model has been used to analyze the primary immune response against *M. ulcerans* [139]: histopathological analysis of the lesions induced by the infection showed comparable necrosis and changes in vasculature and collagen degeneration as in the patients. In the model an initial phase, where bacilli are internalized by macorphages was observed. This complies with most mycobacterial species. The transition to an extracellular phase is probably owing to the presence of mycolactone, which induces host cell death within days of infection *in vitro*. Several lines of evidence suggest that this transient intracellular step may contribute to the successful establishment of a chronic extracellular infection [111,143]. There is no specific vaccine against *M. ulcerans* infection, but *M. bovis* BCG offers some protection, albeit short lived [143,144]. Current prospects for better vaccines include improved BCG vaccination, development of a live vaccine based on an attenuated *M. ulcerans* isolate, and subunit vaccines aimed at immunodominant protein antigens or the toxin itself [145,146].

1.4 References

1. Wack A, Rappuoli R: Vaccinology at the beginning of the 21st century. *Curr Opin Immunol* 2005, 17:411-418.
2. WHO: World Malaria Report. 2005.
3. Marsh K: Malaria--a neglected disease? *Parasitology* 1992, 104 Suppl:S53-69.
4. Struik SS, Riley EM: Does malaria suffer from lack of memory? *Immunol Rev* 2004, 201:268-290.
5. Hoffman SL, Oster CN, Plowe CV, Woollett GR, Beier JC, Chulay JD, Wirtz RA, Hollingdale MR, Mugambi M: Naturally acquired antibodies to sporozoites do not prevent malaria: vaccine development implications. *Science* 1987, 237:639-642.
6. Historical overview of Buruli ulcer on World Wide Web URL: http://www.who.int/gtb-buruli/archives/yamoussoukro/abstracts/potaels.htm
7. MacCallum P, Tolhurst JC, Buckle G, Sisson HA: A new mycobacterial infection in man. *J. Pathol Bacteriol* 1948:93-122.
8. Debacker M, Aguiar J, Steunou C, Zinsou C, Meyers WM, Portaels F: Buruli ulcer recurrence, Benin. *Emerg Infect Dis* 2005, 11:584-589.
9. Asiedu K, Scherpbier R, Ravaglione M: Buruli ulcer, Mycobacterium ulcerans infection. Geneva. 2000.
10. Duker AA, Portaels F, Hale M: Pathways of Mycobacterium ulcerans infection: a review. *Environ Int* 2006, 32:567-573.
11. Shanks GD, Biomndo K, Hay SI, Snow RW: Changing patterns of clinical malaria since 1965 among a tea estate population located in the Kenyan highlands. *Trans R Soc Trop Med Hyg* 2000, 94:253-255.
12. le Sueur D, Sharp BL, Gouws E, Ngxongo S: Malaria in South Africa. *S Afr Med J* 1996, 86:936-939.
13. Greenwood B, Mutabingwa T: Malaria in 2002. *Nature* 2002, 415:670-672.
14. Hemingway J, Field L, Vontas J: An overview of insecticide resistance. *Science* 2002, 298:96-97.
15. Muentener P, Schlagenhauf P, Steffen R: Imported malaria (1985-95): trends and perspectives. *Bull World Health Organ* 1999, 77:560-566.
16. Martens P, Hall L: Malaria on the move: human population movement and malaria transmission. *Emerg Infect Dis* 2000, 6:103-109.
17. Guerin PJ, Olliaro P, Nosten F, Druilhe P, Laxminarayan R, Binka F, Kilama WL, Ford N, White NJ: Malaria: current status of control, diagnosis, treatment, and a proposed agenda for research and development. *Lancet Infect Dis* 2002, 2:564-573.
18. Bruce-Chwatt LJ: A Longitudinal Survey Of Natural Malaria Infection In A Group Of West African Adults. *West Afr Med J* 1963, 12:199-217.
19. Druilhe P, Perignon JL: A hypothesis about the chronicity of malaria infection. *Parasitol Today* 1997, 13:353-357.
20. O'Donnell RA, de Koning-Ward TF, Burt RA, Bockarie M, Reeder JC, Cowman AF, Crabb BS: Antibodies against merozoite surface protein (MSP)-1(19) are a major component of the invasion-inhibitory response in individuals immune to malaria. *J Exp Med* 2001, 193:1403-1412.
21. Good MF, Stanisic D, Xu H, Elliott S, Wykes M: The immunological challenge to developing a vaccine to the blood stages of malaria parasites. *Immunol Rev* 2004, 201:254-267.

22. Moorthy VS, Good MF, Hill AV: Malaria vaccine developments. *Lancet* 2004, 363:150-156.
23. Marsh K, Howard RJ: Antigens induced on erythrocytes by P. falciparum: expression of diverse and conserved determinants. *Science* 1986, 231:150-153.
24. Newbold CI, Pinches R, Roberts DJ, Marsh K: Plasmodium falciparum: the human agglutinating antibody response to the infected red cell surface is predominantly variant specific. *Exp Parasitol* 1992, 75:281-292.
25. Taylor RR, Smith DB, Robinson VJ, McBride JS, Riley EM: Human antibody response to Plasmodium falciparum merozoite surface protein 2 is serogroup specific and predominantly of the immunoglobulin G3 subclass. *Infect Immun* 1995, 63:4382-4388.
26. Taylor RR, Egan A, McGuinness D, Jepson A, Adair R, Drakely C, Riley E: Selective recognition of malaria antigens by human serum antibodies is not genetically determined but demonstrates some features of clonal imprinting. *Int Immunol* 1996, 8:905-915.
27. Carter R, Graves PM, Quakyi IA, Good MF: Restricted or absent immune responses in human populations to Plasmodium falciparum gamete antigens that are targets of malaria transmission-blocking antibodies. *J Exp Med* 1989, 169:135-147.
28. Drakeley CJ, Mulder L, Tchuinkam T, Gupta S, Sauerwein R, Targett GA: Transmission-blocking effects of sera from malaria-exposed individuals on Plasmodium falciparum isolates from gametocyte carriers. *Parasitology* 1998, 116 (Pt 5):417-423.
29. Healer J, McGuinness D, Carter R, Riley E: Transmission-blocking immunity to Plasmodium falciparum in malaria-immune individuals is associated with antibodies to the gamete surface protein Pfs230. *Parasitology* 1999, 119 (Pt 5):425-433.
30. Shear HL, Marino MW, Wanidworanun C, Berman JW, Nagel RL: Correlation of increased expression of intercellular adhesion molecule-1, but not high levels of tumor necrosis factor-alpha, with lethality of Plasmodium yoelii 17XL, a rodent model of cerebral malaria. *Am J Trop Med Hyg* 1998, 59:852-858.
31. Langhorne J, Quin SJ, Sanni LA: Mouse models of blood-stage malaria infections: immune responses and cytokines involved in protection and pathology. *Chem Immunol* 2002, 80:204-228.
32. Luty AJ, Perkins DJ, Lell B, Schmidt-Ott R, Lehman LG, Luckner D, Greve B, Matousek P, Herbich K, Schmid D, et al.: Low interleukin-12 activity in severe Plasmodium falciparum malaria. *Infect Immun* 2000, 68:3909-3915.
33. Perkins DJ, Weinberg JB, Kremsner PG: Reduced interleukin-12 and transforming growth factor-beta1 in severe childhood malaria: relationship of cytokine balance with disease severity. *J Infect Dis* 2000, 182:988-992.
34. Malaguarnera L, Imbesi RM, Pignatelli S, Simpore J, Malaguarnera M, Musumeci S: Increased levels of interleukin-12 in Plasmodium falciparum malaria: correlation with the severity of disease. *Parasite Immunol* 2002, 24:387-389.
35. Malaguarnera L, Pignatelli S, Musumeci M, Simpore J, Musumeci S: Plasma levels of interleukin-18 and interleukin-12 in Plasmodium falciparum malaria. *Parasite Immunol* 2002, 24:489-492.
36. Dodoo D, Omer FM, Todd J, Akanmori BD, Koram KA, Riley EM: Absolute levels and ratios of proinflammatory and anti-inflammatory cytokine production in vitro predict clinical immunity to Plasmodium falciparum malaria. *J Infect Dis* 2002, 185:971-979.

37. Coban C, Ishii KJ, Sullivan DJ, Kumar N: Purified malaria pigment (hemozoin) enhances dendritic cell maturation and modulates the isotype of antibodies induced by a DNA vaccine. *Infect Immun* 2002, 70:3939-3943.
38. Ndungu FM, Sanni L, Urban B, Stephens R, Newbold CI, Marsh K, Langhorne J: CD4 T cells from malaria-nonexposed individuals respond to the CD36-Binding Domain of Plasmodium falciparum erythrocyte membrane protein-1 via an MHC class II-TCR-independent pathway. *J Immunol* 2006, 176:5504-5512.
39. Millington OR, Di Lorenzo C, Phillips RS, Garside P, Brewer JM: Suppression of adaptive immunity to heterologous antigens during Plasmodium infection through hemozoin-induced failure of dendritic cell function. *J Biol* 2006, 5:5.
40. Castelli F, Matteelli A, Caligaris S, Gulletta M, el-Hamad I, Scolari C, Chatel G, Carosi G: Malaria in migrants. *Parassitologia* 1999, 41:261-265.
41. Matteelli A, Colombini P, Gulletta M, Castelli F, Carosi G: Epidemiological features and case management practices of imported malaria in northern Italy 1991-1995. *Trop Med Int Health* 1999, 4:653-657.
42. Jelinek T, Schulte C, Behrens R, Grobusch MP, Coulaud JP, Bisoffi Z, Matteelli A, Clerinx J, Corachan M, Puente S, et al.: Imported Falciparum malaria in Europe: sentinel surveillance data from the European network on surveillance of imported infectious diseases. *Clin Infect Dis* 2002, 34:572-576.
43. Hirunpetcharat C, Good MF: Deletion of Plasmodium berghei-specific CD4+ T cells adoptively transferred into recipient mice after challenge with homologous parasite. *Proc Natl Acad Sci U S A* 1998, 95:1715-1720.
44. Doolan DL, Hoffman SL: DNA-based vaccines against malaria: status and promise of the Multi-Stage Malaria DNA Vaccine Operation. *Int J Parasitol* 2001, 31:753-762.
45. Nussenzweig RS, Vanderberg J, Most H, Orton C: Protective immunity produced by the injection of x-irradiated sporozoites of plasmodium berghei. *Nature* 1967, 216:160-162.
46. Clyde DF: Immunization of man against falciparum and vivax malaria by use of attenuated sporozoites. *Am J Trop Med Hyg* 1975, 24:397-401.
47. Hafalla JC, Rai U, Morrot A, Bernal-Rubio D, Zavala F, Rodriguez A: Priming of CD8+ T cell responses following immunization with heat-killed Plasmodium sporozoites. *Eur J Immunol* 2006, 36:1179-1186.
48. Doolan DL, Martinez-Alier N: Immune response to pre-erythrocytic stages of malaria parasites. *Curr Mol Med* 2006, 6:169-185.
49. Gardner MJ, Hall N, Fung E, White O, Berriman M, Hyman RW, Carlton JM, Pain A, Nelson KE, Bowman S, et al.: Genome sequence of the human malaria parasite Plasmodium falciparum. *Nature* 2002, 419:498-511.
50. Targett GA: Malaria vaccines 1985-2005: a full circle? *Trends Parasitol* 2005, 21:499-503.
51. WHO: The Roll Back Malaria program. 2004.
52. Miller LH, Roberts T, Shahabuddin M, McCutchan TF: Analysis of sequence diversity in the Plasmodium falciparum merozoite surface protein-1 (MSP-1). *Mol Biochem Parasitol* 1993, 59:1-14.
53. Jongwutiwes S, Tanabe K, Kanbara H: Sequence conservation in the C-terminal part of the precursor to the major merozoite surface proteins (MSP1) of Plasmodium falciparum from field isolates. *Mol Biochem Parasitol* 1993, 59:95-100.

54. Marshall VM, Zhang L, Anders RF, Coppel RL: Diversity of the vaccine candidate AMA-1 of Plasmodium falciparum. *Mol Biochem Parasitol* 1996, 77:109-113.
55. Oliveira DA, Udhayakumar V, Bloland P, Shi YP, Nahlen BL, Oloo AJ, Hawley WE, Lal AA: Genetic conservation of the Plasmodium falciparum apical membrane antigen-1 (AMA-1). *Mol Biochem Parasitol* 1996, 76:333-336.
56. Escalante AA, Grebert HM, Chaiyaroj SC, Magris M, Biswas S, Nahlen BL, Lal AA: Polymorphism in the gene encoding the apical membrane antigen-1 (AMA-1) of Plasmodium falciparum. X. Asembo Bay Cohort Project. *Mol Biochem Parasitol* 2001, 113:279-287.
57. Cortes A, Mellombo M, Mueller I, Benet A, Reeder JC, Anders RF: Geographical structure of diversity and differences between symptomatic and asymptomatic infections for Plasmodium falciparum vaccine candidate AMA1. *Infect Immun* 2003, 71:1416-1426.
58. Ferreira MU, Ribeiro WL, Tonon AP, Kawamoto F, Rich SM: Sequence diversity and evolution of the malaria vaccine candidate merozoite surface protein-1 (MSP-1) of Plasmodium falciparum. *Gene* 2003, 304:65-75.
59. Good MF, Kumar S, Miller LH: The real difficulties for malaria sporozoite vaccine development: nonresponsiveness and antigenic variation. *Immunol Today* 1988, 9:351-355.
60. McGregor IA: The Passive Transfer Of Human Malarial Immunity. *Am J Trop Med Hyg* 1964, 13:SUPPL 237-239.
61. Riley EM, Wagner GE, Akanmori BD, Koram KA: Do maternally acquired antibodies protect infants from malaria infection? *Parasite Immunol* 2001, 23:51-59.
62. Harte PG, Playfair JH: Failure of malaria vaccination in mice born to immune mothers. II. Induction of specific suppressor cells by maternal IgG. *Clin Exp Immunol* 1983, 51:157-164.
63. Siegrist CA: Vaccination in the neonatal period and early infancy. *Int Rev Immunol* 2000, 19:195-219.
64. Jameson SC, Bevan MJ: T cell receptor antagonists and partial agonists. *Immunity* 1995, 2:1-11.
65. Evavold BD, Allen PM: Separation of IL-4 production from Th cell proliferation by an altered T cell receptor ligand. *Science* 1991, 252:1308-1310.
66. Sette A, Vitiello A, Reherman B, Fowler P, Nayersina R, Kast WM, Melief CJ, Oseroff C, Yuan L, Ruppert J, et al.: The relationship between class I binding affinity and immunogenicity of potential cytotoxic T cell epitopes. *J Immunol* 1994, 153:5586-5592.
67. Plebanski M, Lee EA, Hill AV: Immune evasion in malaria: altered peptide ligands of the circumsporozoite protein. *Parasitology* 1997, 115 Suppl:S55-66.
68. Daubenberger CA, Nickel B, Ciatto C, Grutter MG, Poltl-Frank F, Rossi L, Siegler U, Robinson J, Kashala O, Patarroyo ME, et al.: Amino acid dimorphism and parasite immune evasion: cellular immune responses to a promiscuous epitope of Plasmodium falciparum merozoite surface protein 1 displaying dimorphic amino acid polymorphism are highly constrained. *Eur J Immunol* 2002, 32:3667-3677.
69. Bastian M, Lozano JM, Patarroyo ME, Pluschke G, Daubenberger CA: Characterization of a reduced peptide bond analogue of a promiscuous CD4 T

cell epitope derived from the Plasmodium falciparum malaria vaccine candidate merozoite surface protein 1. *Mol Immunol* 2004, 41:775-784.
70. Plebanski M, Lee EA, Hannan CM, Flanagan KL, Gilbert SC, Gravenor MB, Hill AV: Altered peptide ligands narrow the repertoire of cellular immune responses by interfering with T-cell priming. *Nat Med* 1999, 5:565-571.
71. Lee EA, Flanagan KL, Minigo G, Reece WH, Bailey R, Pinder M, Hill AV, Plebanski M: Dimorphic Plasmodium falciparum merozoite surface protein-1 epitopes turn off memory T cells and interfere with T cell priming. *Eur J Immunol* 2006, 36:1168-1178.
72. Read S, Mauze S, Asseman C, Bean A, Coffman R, Powrie F: CD38+ CD45RB(low) CD4+ T cells: a population of T cells with immune regulatory activities in vitro. *Eur J Immunol* 1998, 28:3435-3447.
73. Hisaeda H, Maekawa Y, Iwakawa D, Okada H, Himeno K, Kishihara K, Tsukumo S, Yasutomo K: Escape of malaria parasites from host immunity requires CD4+ CD25+ regulatory T cells. *Nat Med* 2004, 10:29-30.
74. Alloueche A, Milligan P, Conway DJ, Pinder M, Bojang K, Doherty T, Tornieporth N, Cohen J, Greenwood BM: Protective efficacy of the RTS,S/AS02 Plasmodium falciparum malaria vaccine is not strain specific. *Am J Trop Med Hyg* 2003, 68:97-101.
75. Alonso PL, Sacarlal J, Aponte JJ, Leach A, Macete E, Aide P, Sigauque B, Milman J, Mandomando I, Bassat Q, et al.: Duration of protection with RTS,S/AS02A malaria vaccine in prevention of Plasmodium falciparum disease in Mozambican children: single-blind extended follow-up of a randomised controlled trial. *Lancet* 2005, 366:2012-2018.
76. Dunachie SJ, Walther M, Vuola JM, Webster DP, Keating SM, Berthoud T, Andrews L, Bejon P, Poulton I, Butcher G, et al.: A clinical trial of prime-boost immunisation with the candidate malaria vaccines RTS,S/AS02A and MVA-CS. *Vaccine* 2006, 24:2850-2859.
77. Good MF, Kaslow DC, Miller LH: Pathways and strategies for developing a malaria blood-stage vaccine. *Annu Rev Immunol* 1998, 16:57-87.
78. Genton B, Betuela I, Felger I, Al-Yaman F, Anders RF, Saul A, Rare L, Baisor M, Lorry K, Brown GV, et al.: A recombinant blood-stage malaria vaccine reduces Plasmodium falciparum density and exerts selective pressure on parasite populations in a phase 1-2b trial in Papua New Guinea. *J Infect Dis* 2002, 185:820-827.
79. Schofield L, Hewitt MC, Evans K, Siomos MA, Seeberger PH: Synthetic GPI as a candidate anti-toxic vaccine in a model of malaria. *Nature* 2002, 418:785-789.
80. Arevalo-Herrera M, Solarte Y, Yasnot MF, Castellanos A, Rincon A, Saul A, Mu J, Long C, Miller L, Herrera S: Induction of transmission-blocking immunity in Aotus monkeys by vaccination with a Plasmodium vivax clinical grade PVS25 recombinant protein. *Am J Trop Med Hyg* 2005, 73:32-37.
81. Collins WE, Barnwell JW, Sullivan JS, Nace D, Williams T, Bounngaseng A, Roberts J, Strobert E, McClure H, Saul A, et al.: Assessment of transmission-blocking activity of candidate Pvs25 vaccine using gametocytes from chimpanzees. *Am J Trop Med Hyg* 2006, 74:215-221.
82. Hoffman SL, Goh LM, Luke TC, Schneider I, Le TP, Doolan DL, Sacci J, de la Vega P, Dowler M, Paul C, et al.: Protection of humans against malaria by immunization with radiation-attenuated Plasmodium falciparum sporozoites. *J Infect Dis* 2002, 185:1155-1164.

83. Mueller MS, Renard A, Boato F, Vogel D, Naegeli M, Zurbriggen R, Robinson JA, Pluschke G: Induction of parasite growth-inhibitory antibodies by a virosomal formulation of a peptidomimetic of loop I from domain III of Plasmodium falciparum apical membrane antigen 1. *Infect Immun* 2003, 71:4749-4758.
84. Pombo DJ, Lawrence G, Hirunpetcharat C, Rzepczyk C, Bryden M, Cloonan N, Anderson K, Mahakunkijcharoen Y, Martin LB, Wilson D, et al.: Immunity to malaria after administration of ultra-low doses of red cells infected with Plasmodium falciparum. *Lancet* 2002, 360:610-617.
85. Su Z, Tam MF, Jankovic D, Stevenson MM: Vaccination with novel immunostimulatory adjuvants against blood-stage malaria in mice. *Infect Immun* 2003, 71:5178-5187.
86. Schneider J, Gilbert SC, Hannan CM, Degano P, Prieur E, Sheu EG, Plebanski M, Hill AV: Induction of CD8+ T cells using heterologous prime-boost immunisation strategies. *Immunol Rev* 1999, 170:29-38.
87. Parker SE, Monteith D, Horton H, Hof R, Hernandez P, Vilalta A, Hartikka J, Hobart P, Bentley CE, Chang A, et al.: Safety of a GM-CSF adjuvant-plasmid DNA malaria vaccine. *Gene Ther* 2001, 8:1011-1023.
88. Birkett A, Lyons K, Schmidt A, Boyd D, Oliveira GA, Siddique A, Nussenzweig R, Calvo-Calle JM, Nardin E: A modified hepatitis B virus core particle containing multiple epitopes of the Plasmodium falciparum circumsporozoite protein provides a highly immunogenic malaria vaccine in preclinical analyses in rodent and primate hosts. *Infect Immun* 2002, 70:6860-6870.
89. McConkey SJ, Reece WH, Moorthy VS, Webster D, Dunachie S, Butcher G, Vuola JM, Blanchard TJ, Gothard P, Watkins K, et al.: Enhanced T-cell immunogenicity of plasmid DNA vaccines boosted by recombinant modified vaccinia virus Ankara in humans. *Nat Med* 2003, 9:729-735.
90. Poltl-Frank F, Zurbriggen R, Helg A, Stuart F, Robinson J, Gluck R, Pluschke G: Use of reconstituted influenza virus virosomes as an immunopotentiating delivery system for a peptide-based vaccine. *Clin Exp Immunol* 1999, 117:496-503.
91. Moreno R, Jiang L, Moehle K, Zurbriggen R, Gluck R, Robinson JA, Pluschke G: Exploiting conformationally constrained peptidomimetics and an efficient human-compatible delivery system in synthetic vaccine design. *Chembiochem* 2001, 2:838-843.
92. Near KA, Stowers AW, Jankovic D, Kaslow DC: Improved immunogenicity and efficacy of the recombinant 19-kilodalton merozoite surface protein 1 by the addition of oligodeoxynucleotide and aluminum hydroxide gel in a murine malaria vaccine model. *Infect Immun* 2002, 70:692-701.
93. Pfeiffer B, Peduzzi E, Moehle K, Zurbriggen R, Gluck R, Pluschke G, Robinson JA: A virosome-mimotope approach to synthetic vaccine design and optimization: synthesis, conformation, and immune recognition of a potential malaria-vaccine candidate. *Angew Chem Int Ed Engl* 2003, 42:2368-2371.
94. James S, Moehle K, Renard A, Mueller MS, Vogel D, Zurbriggen R, Pluschke G, Robinson JA: Synthesis, Solution Structure and Immune Recognition of an Epidermal Growth Factor-Like Domain from Plasmodium falciparum Merozoite Surface Protein-1. *Chembiochem* 2006.
95. Pizarro JC, Chitarra V, Verger D, Holm I, Petres S, Dartevelle S, Nato F, Longacre S, Bentley GA: Crystal structure of a Fab complex formed with PfMSP1-19, the C-terminal fragment of merozoite surface protein 1 from

Plasmodium falciparum: a malaria vaccine candidate. *J Mol Biol* 2003, 328:1091-1103.
96. Ghasparian A, Moehle K, Linden A, Robinson JA: Crystal structure of an NPNA-repeat motif from the circumsporozoite protein of the malaria parasite Plasmodium falciparum. *Chem Commun (Camb)* 2006:174-176.
97. Gluck R, Metcalfe IC: New technology platforms in the development of vaccines for the future. *Vaccine* 2002, 20 Suppl 5:B10-16.
98. Zurbriggen R: Immunostimulating reconstituted influenza virosomes. *Vaccine* 2003, 21:921-924.
99. Huckriede A, Bungener L, Daemen T, Wilschut J: Influenza virosomes in vaccine development. *Methods Enzymol* 2003, 373:74-91.
100. Matlin KS, Reggio H, Helenius A, Simons K: Infectious entry pathway of influenza virus in a canine kidney cell line. *J Cell Biol* 1981, 91:601-613.
101. Gluck R: Liposomal presentation of antigens for human vaccines. *Pharm Biotechnol* 1995, 6:325-345.
102. Wiedermann G, Kundi M, Ambrosch F: Estimated persistence of anti-HAV antibodies after single dose and booster hepatitis A vaccination (0-6 schedule). *Acta Trop* 1998, 69:121-125.
103. Holzer BR, Hatz C, Schmidt-Sissolak D, Gluck R, Althaus B, Egger M: Immunogenicity and adverse effects of inactivated virosome versus alum-adsorbed hepatitis A vaccine: a randomized controlled trial. *Vaccine* 1996, 14:982-986.
104. Zurbriggen R, Gluck R: Immunogenicity of IRIV- versus alum-adjuvanted diphtheria and tetanus toxoid vaccines in influenza primed mice. *Vaccine* 1999, 17:1301-1305.
105. Josse R, Guedenon A, Darie H, Anagonou S, Portaels F, Meyers WM: [Mycobacterium ulcerans cutaneous infections: Buruli ulcers]. *Med Trop (Mars)* 1995, 55:363-373.
106. Portaels F: Epidemiology of mycobacterial diseases. *Clin. Dermatol.* 1995, 13:207-222.
107. Veitch MG, Johnson PD, Flood PE, Leslie DE, Street AC, Hayman JA: A large localized outbreak of Mycobacterium ulcerans infection on a temperate southern Australian island. *Epidemiol Infect* 1997, 119:313-318.
108. Johnson PD, Stinear T, Small PL, Pluschke G, Merritt RW, Portaels F, Huygen K, Hayman JA, Asiedu K: Buruli ulcer (M. ulcerans infection): new insights, new hope for disease control. *PLoS Med* 2005, 2:e108.
109. Marsollier L, Stinear T, Aubry J, Saint Andre JP, Robert R, Legras P, Manceau AL, Audrain C, Bourdon S, Kouakou H, et al.: Aquatic plants stimulate the growth of and biofilm formation by Mycobacterium ulcerans in axenic culture and harbor these bacteria in the environment. *Appl Environ Microbiol* 2004, 70:1097-1103.
110. George KM, Chatterjee D, Gunawardana G, Welty D, Hayman J, Lee R, Small PL: Mycolactone: a polyketide toxin from Mycobacterium ulcerans required for virulence. *Science* 1999, 283:854-857.
111. Coutanceau E, Marsollier L, Brosch R, Perret E, Goossens P, Tanguy M, Cole ST, Small PL, Demangel C: Modulation of the host immune response by a transient intracellular stage of Mycobacterium ulcerans: the contribution of endogenous mycolactone toxin. *Cell Microbiol* 2005, 7:1187-1196.
112. Connor DH, Lunn HF: Mycobacterium ulcerans infection (with comments on pathogenesis). *Int J Lepr* 1965, 33:Suppl:698-709.

113. Gomez A, Mve-Obiang A, Vray B, Rudnicka W, Shamputa IC, Portaels F, Meyers WM, Fonteyne PA, Realini L: Detection of phospholipase C in nontuberculous mycobacteria and its possible role in hemolytic activity. *J Clin Microbiol* 2001, 39:1396-1401.
114. Adusumilli S, Mve-Obiang A, Sparer T, Meyers W, Hayman J, Small PL: Mycobacterium ulcerans toxic macrolide, mycolactone modulates the host immune response and cellular location of M. ulcerans in vitro and in vivo. *Cell Microbiol* 2005, 7:1295-1304.
115. George KM, Pascopella L, Welty DM, Small PL: A Mycobacterium ulcerans toxin, mycolactone, causes apoptosis in guinea pig ulcers and tissue culture cells. *Infect Immun* 2000, 68:877-883.
116. Snyder DS, Small PL: Uptake and cellular actions of mycolactone, a virulence determinant for Mycobacterium ulcerans. *Microb Pathog* 2003, 34:91-101.
117. Marsollier L, Robert R, Aubry J, Saint Andre JP, Kouakou H, Legras P, Manceau AL, Mahaza C, Carbonnelle B: Aquatic insects as a vector for Mycobacterium ulcerans. *Appl Environ Microbiol* 2002, 68:4623-4628.
118. Hayman J: Out of Africa: observations on the histopathology of Mycobacterium ulcerans infection. *J Clin Pathol* 1993, 46:5-9.
119. van der Werf TS, van der Graaf WT, Tappero JW, Asiedu K: Mycobacterium ulcerans infection. *Lancet* 1999, 354:1013-1018.
120. disease DoMu: *World Health Organization* 2001.
121. Portaels F: Buruli ulcer, diagnosis of Mycobacterium ulcerans disease. Geneva 2001.
122. Buntine F, Crofts K: Buruli ulcer, Managment of Mycobacterium ulcerans disease. Geneva 2001.
123. (WHO) WHO: Managment of Mycobacterium ulcerans disease. 2001.
124. Teelken MA, Stienstra Y, Ellen DE, Quarshie E, Klutse E, van der Graaf WT, van der Werf TS: Buruli ulcer: differences in treatment outcome between two centres in Ghana. *Acta Trop* 2003, 88:51-56.
125. Dega H, Bentoucha A, Robert J, Jarlier V, Grosset J: Bactericidal activity of rifampin-amikacin against Mycobacterium ulcerans in mice. *Antimicrob Agents Chemother* 2002, 46:3193-3196.
126. Etuaful S, Carbonnelle B, Grosset J, Lucas S, Horsfield C, Phillips R, Evans M, Ofori-Adjei D, Klustse E, Owusu-Boateng J, et al.: Efficacy of the combination rifampin-streptomycin in preventing growth of Mycobacterium ulcerans in early lesions of Buruli ulcer in humans. *Antimicrob Agents Chemother* 2005, 49:3182-3186.
127. (WHO) WHO: Provisorial guidance on the role of specific antibiotics in the managment of Mycobacterium ulcerans disease (Buruli ulcer). 2006.
128. Hayman J, McQueen A: The pathology of Mycobacterium ulcerans infection. *Pathology* 1985, 17:594-600.
129. Guarner J, Bartlett J, Whitney EA, Raghunathan PL, Stienstra Y, Asamoa K, Etuaful S, Klutse E, Quarshie E, van der Werf TS, et al.: Histopathologic features of Mycobacterium ulcerans infection. *Emerg Infect Dis* 2003, 9:651-656.
130. Stanford JL, Revill WD, Gunthorpe WJ, Grange JM: The production and preliminary investigation of Burulin, a new skin test reagent for Mycobacterium ulcerans infection. *J Hyg (Lond)* 1975, 74:7-16.
131. Ottenhoff TH, Verreck FA, Hoeve MA, van de Vosse E: Control of human host immunity to mycobacteria. *Tuberculosis (Edinb)* 2005, 85:53-64.

132. Okenu DM, Ofielu LO, Easley KA, Guarner J, Spotts Whitney EA, Raghunathan PL, Stienstra Y, Asamoa K, van der Werf TS, van der Graaf WT, et al.: Immunoglobulin M antibody responses to Mycobacterium ulcerans allow discrimination between cases of active Buruli ulcer disease and matched family controls in areas where the disease is endemic. *Clin Diagn Lab Immunol* 2004, 11:387-391.
133. Diaz D, Dobeli H, Yeboah-Manu D, Mensah-Quainoo DE, Friedlein A, Soder N, Rondini S, Bodmer T, Pluschke PG: Use of the immunodominant 18 kDa small heat shock protein as serological marker for exposure to M. ulcerans. *Clin Vaccine Immunol* 2006.
134. Meyers WM, Connor DH, McCullough B, Bourland J, Moris R, Proos L: Distribution of Mycobacterium ulcerans infections in Zaire, including the report of new foci. *Ann Soc Belg Med Trop* 1974, 54:147-157.
135. Gooding TM, Johnson PD, Smith M, Kemp AS, Robins-Browne RM: Cytokine profiles of patients infected with Mycobacterium ulcerans and unaffected household contacts. *Infect Immun* 2002, 70:5562-5567.
136. Gooding TM, Kemp AS, Robins-Browne RM, Smith M, Johnson PD: Acquired T-helper 1 lymphocyte anergy following infection with Mycobacterium ulcerans. *Clin Infect Dis* 2003, 36:1076-1077.
137. Toll A, Gallardo F, Ferran M, Gilaberte M, Iglesias M, Gimeno JL, Rondini S, Pujol RM: Aggressive multifocal Buruli ulcer with associated osteomyelitis in an HIV-positive patient. *Clin Exp Dermatol* 2005, 30:649-651.
138. Stienstra Y, van der Graaf WT, te Meerman GJ, The TH, de Leij LF, van der Werf TS: Susceptibility to development of Mycobacterium ulcerans disease: review of possible risk factors. *Trop Med Int Health* 2001, 6:554-562.
139. Casanova JL, Abel L: Genetic dissection of immunity to mycobacteria: the human model. *Annu Rev Immunol* 2002, 20:581-620.
140. Stienstra Y, van der Werf TS, Oosterom E, Nolte IM, van der Graaf WT, Etuaful S, Raghunathan PL, Whitney EA, Ampadu EO, Asamoa K, et al.: Susceptibility to Buruli ulcer is associated with the SLC11A1 (NRAMP1) D543N polymorphism. *Genes Immun* 2006, 7:185-189.
141. Gooding TM, Johnson PD, Campbell DE, Hayman JA, Hartland EL, Kemp AS, Robins-Browne RM: Immune response to infection with Mycobacterium ulcerans. *Infect Immun* 2001, 69:1704-1707.
142. Prevot G, Bourreau E, Pascalis H, Pradinaud R, Tanghe A, Huygen K, Launois P: Differential production of systemic and intralesional gamma interferon and interleukin-10 in nodular and ulcerative forms of Buruli disease. *Infect Immun* 2004, 72:958-965.
143. Portaels F, Aguiar J, Debacker M, Guedenon A, Steunou C, Zinsou C, Meyers WM: Mycobacterium bovis BCG vaccination as prophylaxis against Mycobacterium ulcerans osteomyelitis in Buruli ulcer disease. *Infect Immun* 2004, 72:62-65.
144. Smith PG, Revill WD, Lukwago E, Rykushin YP: The protective effect of BCG against Mycobacterium ulcerans disease: a controlled trial in an endemic area of Uganda. *Trans R Soc Trop Med Hyg* 1977, 70:449-457.
145. Huygen K: Prospects for vaccine development against Buruli disease. *Expert Rev Vaccines* 2003, 2:561-569.
146. Coutanceau E, Legras P, Marsollier L, Reysset G, Cole ST, Demangel C: Immunogenicity of Mycobacterium ulcerans Hsp65 and protective efficacy of

a Mycobacterium leprae Hsp65-based DNA vaccine against Buruli ulcer. *Microbes Infect* 2006.

Chapter 2

Objectives

Goals of the thesis

2.1 *Plasmodium falciparum* malaria

The underlying challenge of developing an effective malaria vaccine is that natural immunity to malaria is slow to develop, unstable and not complete even after years of endemic parasite exposure. Today, vaccine development against *P. falciparum* and other infectious diseases is focusing largely on subunit vaccines technology. A delivery system highly suitable for subunit vaccines is based on immuno-potentiating reconstituted influenza virosomes (IRIVs). The aim of the project was to prove that IRIVs are an appropriate delivery system for synthetic peptides hooked to the virosomal surface via a phospholipid anchor. In particular we wanted to demonstrate that peptide-specific T cell responses can be induced by virosomal formulations.

Specific objectives

1. To optimize the structure of an IRIV-anchored synthetic peptide eliciting *P. falciparum* sporozoite inhibitory antibodies

2. To demonstrate that malaria peptide specific CD4 T cell responses can be generated by virosomally-anchored synthetic peptides

3. To evaluate whether the magnitude of a pre-existing influenza specific T cell response affects the immune response elicites by virosomally formulated malaria peptides

4. To characterize TLR9 of *Aotus nancymaae* as a potential model to evaluate TLR9 ligands as immunostimulator components for a malaria subunit vaccine formulation

2.2 *Mycobacterium ulcerans* infection (Buruli ulcer)

A better understanding of the immunopathology of *M. ulcerans* disease in the human and of the immunomodulatory mechanisms of the bacterium may help to improve treatment modalities and to support the development of a vaccine and of new laboratory diagnostic methods.

Specific objectives

5. To study the extent of systemic immunosuppression in Buruli ulcer and to monitor recovery of the immunoresponsiveness after surgical treatment

6. To analyze whether elements of the adaptive and non-adaptive immune system are locally present in active Buruli ulcer lesions

Chapter 3

Plasmodium falciparum malaria

Chapter 3.1

Structure-Activity Based Design of a Synthetic Malaria Peptide Eliciting Sporozoite Inhibitory Antibodies in a Virosomal Formulation

Shinji L. Okitsu[1], Ursula Kienzl[2], Kerstin Moehle[2], Olivier Silvie[3], Elisabetta Peduzzi[1], Markus S. Mueller[1], Robert W. Sauerwein[4], Hugues Matile[5], Rinaldo Zurbriggen[6], Dominique Mazier[3], John A. Robinson[2], and Gerd Pluschke[1]

[1]Molecular Immunology, Swiss Tropical Institute, CH-4002 Basel, Switzerland,
[2]Institute of Organic Chemistry, University of Zurich, CH-8057 Zurich, Switzerland,
[3]Inserm U511, Immunobiologie Cellulaire et Moléculaire des Infections Parasitaires, Centre Hospitalo-Universitaire Pitié-Salpêtrière, Université Pierre et Marie Curie, 75013 Paris[3], France,
[4]University Medical Centre St Radboud, Department of Medical Microbiology, 6500HB Nijmegen[4], The Netherlands,
[5]F. Hoffmann La Roche Ltd., Basel, Switzerland and
[6]Pevion Biotech Ltd., CH-3018 Bern, Switzerland

This article has been submitted in:
Chemistry & Biology

Summary

The circumsporozoite protein (CSP) of *Plasmodium falciparum* is a leading candidate antigen for inclusion in a malaria subunit vaccine. We describe here the design of a conformationally constrained synthetic peptide, designated UK39, which has structural and antigenic similarity to the NPNA-repeat region of native CSP. NMR studies on the antigen support the presence of helical turn-like structures within consecutive NPNA motifs in aqueous solution. Intramuscular delivery of UK39 to mice and rabbits on the surface of immunopotentiating reconstituted influenza virus-like particles (IRIV) elicited high titers of sporozoite cross-reactive antibodies. Influenza virus proteins were crucially important for the immunostimulatory activity of the IRIV-based antigen delivery system, since a liposomal formulation of UK39 was not immunogenic. IgG antibodies elicited by UK39 loaded virosomes inhibited invasion of hepatocytes by *P. falciparum* sporozoites, but not by antigenically distinct *P. yoelii* sporozoites. This approach to optimized IRIV-formulated synthetic peptide vaccines should be generally applicable and amenable for other infectious and non-infectious diseases.

Introduction

Malaria is the most important parasitic disease in people and may cause as many as 2.5 million deaths per annum [1]. Vaccine development against both *Plasmodium falciparum* and *P. vivax* is ongoing [2] and one candidate vaccine, RTS,S/AS02A demonstrated 30% protection against the first episode of malaria and 58% protection against severe malaria in a clinical trial in Mozambican children [3]. Nevertheless, it is assumed that it will take at least another decade until a malaria vaccine will be available that is more effective and more cost effective than current malaria control tools, such as insecticide treated bed nets and intermittent preventive treatment in infants [4-6].

Apart from plans to develop a radiation-attenuated sporozoite vaccine [7], vaccine development against malaria is focusing largely on subunit vaccine technologies [8]. It is thought that an effective malaria subunit vaccine will have to incorporate antigens against several developmental stages of the parasite. A combination of actions against sporozoites, infected liver cells, merozoites and infected red blood cells may be required to achieve substantial protective activity [8]. The fact that most vaccines currently available are based on attenuated or inactivated whole pathogens or material derived directly from them demonstrates that the technological problems associated with peptide and protein subunit vaccine design are still incompletely solved. Major obstacles include difficulties to retain the native conformation of key antibody epitopes and the need for an effective but safe human-compatible exogenous adjuvant in order to achieve efficient immune responses [9].

We are addressing the problem of protein subunit vaccine design by developing synthetic peptide structures that elicit antibodies against surface epitopes of native malaria antigens [10-12], and coupling them to the surface of immunopotentiating reconstituted influenza virosomes (IRIVs) as a liposomal carrier system [12, 13]. IRIVs are spherical, unilammelar vesicles, prepared by detergent removal from a mixture of natural and synthetic phospholipids and influenza surface glycoproteins. The hemagglutinin membrane glycoprotein of the influenza virus is a fusion-inducing component, which facilitates antigen delivery to immunocompetent cells. IRIVs represent a universal antigen-delivery system for multi-component subunit vaccines, since antigens can be either attached to their surface to elicit antibody responses or

encapsulated in their lumen to elicit CD8 T cell responses. They have an excellent safety profile and are already registered for human use [14].

Sequential rounds of optimization of synthetic peptide structures, as typically applied in drug research, may ideally lead to vaccine candidate antigens, which elicit primarily or exclusively antibodies that contribute to immune protection. In the case of the central repeat region $(NPNA)_{\approx 37}$ of the circumsporozoite protein (CSP) of *P. falciparum* sporozoites, results of clinical trials with a linear $(NANP)_3$ peptide conjugated to tetanus toxin in alum [15, 16] were disappointing. We have previously described the synthesis and immunological properties of template-bound NPNA peptides, which were superior to their linear counterparts in eliciting sporozoite-binding antibodies [10-12]. Building on NMR and modeling studies we designed and synthesized an improved cyclic NPNA-repeat region peptide (designated BP65), which has been shown to efficiently elicit anti-sporozoite antibody responses in mice [11]. Here we describe functional properties of monoclonal antibodies (mAbs) elicited by BP65, and the properties and preclinical profiling of a synthetically more accessible derivative (UK39). An IRIV-based formulation of this peptide, designated PEV302, is currently being tested in human clinical trials.

Results

Sporozoite-inhibitory activity of anti-BP65 mAbs

Two mAbs (designated EP3 and EP9) specific for the synthetic compound BP65 (Figure 1) were generated from spleen cells of mice immunized with BP65-loaded IRIVs. Both mAbs bind to sporozoites in IFA, and functional inhibitory activity was assessed by performing *in vitro* invasion inhibition assays with *P. falciparum* sporozoites and primary human hepatocytes. At a concentration of 200 μg/ml mAb EP3 caused 82% and mAb EP9 100% invasion inhibition (Figure 2A). The inhibitory activity decreased in a dose dependent manner, when increasing concentrations of BP66 were added to the antibody-parasite mixture (Figure 2B) confirming the specificity of the inhibitory activity of the mAbs.

Design of UK40 and its phosphatidylethanolamine (PE)-conjugate UK39

In an attempt to minimize the size of the synthetic vaccine antigen, a derivative of BP65, called BP-125, without the C-terminal PNA and N-terminal NPNA portions was produced and tested for reactivity with the sporozoite-inhibitory anti-BP65 mAbs EP3 and EP9. Only a strongly diminished reactivity was observed (Figure S1), indicating that BP65 represents the minimal essential structure.

In BP65 the folded conformation of the peptide is stabilized by cross-linking an amino group at the ß-position of Pro^{6} to a spatially adjacent side chain carboxyl of Glu as a replacement for Ala^{16} [11]. Since limited availability of orthogonally protected (2S,3R)-3-aminoproline required for the synthesis of BP65 represented an obstacle for up-scaling of the synthesis for clinical grade material, we synthesized derivatives of BP65 designated UK40 and UK39 (PE- conjugate of UK40), in which this building block is replaced by (2S,4S)-4-aminoproline (Figure 1). The required orthogonally protected N(□)-Fmoc(2S,4S)-4-(Boc)aminoproline ((2S,4S)-Boc-4-amino-1-Fmoc-pyrrolidine-2-carboxylic acid) is commercially available.

NMR studies of UK40

The solution structure of UK40 was investigated in water (90% H_2O, 10% D_2O, pH 5.0, 293 K) by ^{1}H NMR spectroscopy. The ^{1}H NMR spectrum of UK40 indicated the existence of a major and two minor forms in a ratio of 14:3:1, which interconvert slowly on the NMR timescale, caused by *cis-trans* isomerism at Asn-Pro peptide

bonds. Similar *cis-trans* rotamers were found in BP66 in earlier work [11], and in linear peptides containing multiple NPNA-repeats [17]**.** The major form can be assigned the all *trans* conformation on the basis of observed NOE connectivities. Resonance overlap prevented an assignment of the minor forms to specific peptide bond rotamers. Chemical shift assignments for the major rotamer (Table S1) were made using standard 2D NMR methods [18]. Side chain proton frequencies in UK40 exhibited major spectral overlap, although this problem was not as severe as seen in linear peptides containing multiple tandem NPNA-repeats. This is illustrated in Figure S2, where HN-C(□)H cross peaks from 2D DQF-COSY spectra are shown for UK40 and the peptide Ac-$(NPNA)_3$-NH_2. Notable in the spectrum of UK40 are the significantly upfield shifted amide HN resonances of Asn^9 and Ala^{12}. The amide proton chemical shift temperature coefficients were measured and are given in Figure S3. Notable are the low values for both Ala^8 and Asn^9, suggesting that both these amide NHs are involved in intramolecular hydrogen bonding. A low value is also seen for Ala^{12}, but not for Asn^{13}.

2D NOESY spectra of UK40 showed d_{NN} (i, i+1) NOE connectivities between amide protons of Asn_{i+3}, Ala_{i+4} and Asn_{i+5} within each NAN motif, as shown in Figure S3 and Figure S4. The same pattern of NOE interactions was also found earlier in BP66 [11]. Furthermore, characteristic medium range $d_{□N}$ (i, i+2) NOEs were found between Asn^7 and Asn^9, Asn^9 and Asn^{11}, Pro^{10} and Ala^{12}, Pro^{14} and Glu^{16} in UK40. Weak NOE contacts between side chains of the first Asn and the Ala of each NPNA motif are also seen, as predicted in the structure model of an NPNA motif in a helical turn conformation (vide infra) (Figure 3A). No other medium/long range NOEs were observed in NOESY spectra.

Using the available short and medium range NOE connectivities, average solution structures for UK40 were calculated using DYANA. The final ensemble of 20 structures (see Table S2) is shown in Figure 3B. The backbone atoms of residues 6-16 enclosed within the macrocyclic ring can be superimposed with an rmsd of 1.6 Å, whereas the remaining residues at the N- and C-termini show much greater conformational diversity. When each tetrapeptide motif within the macrocycle is considered, the highest structural similarity both to the ANPNA crystal structure and to a model helical turn conformation is seen in the first (N^5-A^8) and in particular the central (N^9-A^{12}) tetrapeptide motifs (Figure 4), suggesting that helical turns are

significantly populated in this portion of the molecule. Within the third unit N^{13}-E^{16}, however, the helical turn conformations are adopted much less frequently, or not at all, in the 20 lowest energy DYANA structures, suggesting either that the turn is not significantly populated or, as seems more likely, that the average NMR structures do not represent accurately these regions of the macrocycle due to the presence of multiple rapidly interconverting helical and extended conformations. The low number and weak intensity of many NOEs are indicative of significant backbone flexibility. Moreover, the occurrence of significant restraint violations, such as from the Glu^{16} C(□)H to Asn^{17} HN NOE, indicate also the presence of extended (ß) chain forms.

Antigenic properties

The antigenic properties of virosomally formulated UK39 were compared to those of BP65 and two previously described [12] template-bound peptides (JL934 and JL1036) (see Figure 1). Panels of CSP repeat region specific sporozoite-binding mAbs obtained after immunization of mice with either NPNA peptides or with *P. falciparum* sporozoites were tested in ELISA for cross-reactivity with the first to fourth generation compounds (Table 1). The results demonstrate that antibodies with a range of different fine-specificities can bind to native CSP on the sporozoite surface. Thus mAb 1.26 the only sporozoite cross-reactive mAb elicited by the antigen JL934 [12] did not bind to the other peptide antigens and only three of the four sporozoite-binding mAbs elicited by the peptide antigen JL1036 [12] cross-reacted with the antigens BP65 and UK39. The two mAbs elicited by virosomal formulations of BP65 both recognized sporozoites and UK39, while only one mAb (EP9) recognized JL1036 and none JL934. Cross-reactivity analysis with a set of twelve CSP repeat region specific mAbs raised against *P. falciparum* sporozoites demonstrated that only two of these mAbs cross-reacted with JL934, five with JL1036 and all 12 with BP65 and UK39. While cross-reactivity of mAbs Sp4-7H1 and Sp4-1B4 with the antigen BP65 was only weak, all twelve anti-sporozoite mAbs cross-reacted strongly with UK39, indicating that this compound better reflects the native structure of the CSP repeat region.

Immunogenicity of virosomally formulated UK39

Already one immunization of BALB/c mice with UK39-loaded IRIVs elicited detectable titers of anti-UK39 IgG in ELISA (Figure 5A) and sporozoite cross-reactive IgG in IFA (Figure 5B). While a second immunization led to a strong titer increase, a third immunization had only a moderate further booster effect. In Western blots with a lysate of *P. falciparum* salivary gland sporozoites, anti-UK39 IgG stained a characteristic CSP double-band of 50-55 kDa (not shown).

Comparison of immune responses elicited by a liposomal and an IRIV-based formulation of UK39 demonstrated the importance of influenza virus proteins for the immunopotentiating activity of IRIVs (Figure 5C). The strong immunogenicity of virosomally formulated UK39 is virtually abolished when the peptide is presented on liposomes, lacking influenza derived hemagglutinin and neuraminidase. Also, no parasite cross-reactive IgG was detected in IFA (not shown). Already one dose of IRIV formulated UK39 elicited high ELISA and IFA IgG titers in rabbits (Figure S5). Additional immunizations had only a minor booster effect. IgG from immunized animals stained the CSP double-band in Western blots (not shown).

Generation of sporozoite inhibitory antibodies by UK39

Total IgG (final concentration 1mg/ml) purified from UK39-immunized rabbits showed inhibitory activity in sporozoite *in vitro* invasion inhibition assays (Figure 6A). Inhibition decreased in a dose dependent manner. Control IgG preparations from rabbits immunized with empty IRIVs had no inhibitory activity. Sera inhibiting invasion of *P. falciparum* sporozoites did not inhibit invasion of *P. yoelii* into murine hepatocytes (not shown), demonstrating specificity of the inhibitory activity.

Purified IgG from rabbits immunized with UK39 inhibited parasite gliding motility, as demonstrated by immunofluorescence analysis of the trails of CSP shed by *P. falciparum* sporozoites gliding on glass slides [19]. At a concentration of 1 mg/ml of total IgG, traces were reduced (Figure 6B). Furthermore, CSP was precipitated at the apical ends of the sporozoites as described [20] and sporozoites were agglutinated. Serum of rabbits immunized with empty IRIVs had no effect on gliding motility or on parasite morphology.

Discussion

An important goal here was the design of a conformationally constrained peptidomimetic of the immunodominant NPNA repeat region of CSP, which could be delivered to the immune system on the surface of immunopotentiating reconstituted influenza virosomes (IRIVs). Linear peptides are generally unsuitable as immunogens, due to their inherent conformational flexibility. As a result, there are many different ways that linear peptides can be recognized (by B-cell receptors), correlating with the number of accessible conformational states available to the peptide chain. Only a small subset of these will be relevant for cross-recognition of the cognate folded protein. A peptide chain restrained into the biologically relevant backbone conformation, on the other hand, should be a more effective immunogen, since it should be recognized preferentially in a conformation that promotes cross-reaction with the folded protein. There is the further advantage that linear peptides are usually degraded by proteolysis within minutes in biological fluids, which limits the window of accessibility to B-cell receptors.

Our strategy for the design of a multi-stage multi-component subunit malaria vaccine is to focus immune responses onto protection-relevant structural elements of key parasite proteins. Moreover, synthetic peptides and proteins with native-like folds can be presented to the immune system on IRIVs, thereby bypassing many of the problems associated with the production of stable recombinant protein-based vaccine formulations. A key parameter used for selecting vaccine candidates was the cross-reactivity of elicited antibodies with the native target antigen on the cell surface of the parasite. IRIV formulations of the peptide antigens evaluated here were immunogenic in mice and rabbits. The optimized structure, UK39, has remarkable structural and antigenic similarity with the native repeat region of the key sporozoite vaccine antigen CSP and is suitable for large scale GMP production.

Key structural information used to guide the design of UK39 came from earlier NMR and modeling studies [11]. Already NMR studies on linear peptides containing one or several tandemly linked NPNA motifs suggested the presence of turn-like structures based on the NPNA cadence, stabilized by hydrogen bonding, but in rapid dynamic equilibrium with extended chain forms [17]. Recently, an X-ray crystal structure was reported of the pentapeptide Ac-ANPNA-NH_2, which confirmed that the NPNA unit adopts a type-I ß-turn conformation in aqueous solution [21]**.** Nevertheless, a key

question remains how individual ß-turns in a longer $(NPNA)_n$ oligomer might be interconnected to form a repeat structure. In earlier work, we were strongly influenced by the observation in NOESY spectra of various $(NPNA)_n$-containing cyclic and linear peptides, of strong sequential backbone NH-NH NOEs between both Asn^{i+2} and Ala^{i+3} as well as Ala^{i+3} and Asn^{i+4}. This led us to consider backbone conformations of extended $(NPNA)_n$ oligomeric peptides, in which Pro^{i+1}, Asn^{i+2} and Ala^{i+3} are in the □-helical region, leaving only Asn^{i} in the ß-region of □□□ space; a combination called here a helical-turn. A computer model of such a turn is shown in Figure 3A, where the close approach of the backbone amide NHs of Asn^{i+2} and Ala^{i+3} as well as Ala^{i+3} and Asn^{i+4} can be seen. With these □□□ angles for each NPNA motif, and assuming *trans* peptide bonds, a cross-linked peptidomimetic was designed using a computer model of an extended $(NPNA)_n$-oligomer, as described earlier [11]. In our first effort, (2S,3R)-3-aminoproline was used to synthesize the mimetic BP66, and its phospholipid conjugate BP65. Here, we have investigated the related peptidomimetics UK39 and UK40 (Figure 1), which use instead the synthetically more accessible (2S,4S)-4-aminoproline.

NMR studies on UK40 in aqueous solution provide insights into the preferred backbone conformations of this mimetic, and confirm a close similarity to those deduced earlier for BP66 [11]. As expected, the residues contained within the macrocyclic ring of UK40 are more restrained in their conformation than the NPNA units outside the macrocycle at the N- and C-termini (Figure 3B). The Asn^{5}-Ala^{8} and Asn^{9}-Ala^{12} motifs, in particular, appear to populate helical turns, as seen in the average solution structures calculated using NOE-derived distance restraints (Figure 4). However, especially the Asn^{13}-Glu^{16} motif within the macrocycle appears to be more disordered and to exist in dynamic equilibrium with extended forms. It is less clear what role (if any) the observed minor *cis*-(Asn-Pro) peptide bond conformers might play in eliciting antibodies cross-reactive with the CSP.

As far as the antigenic properties are concerned, UK39 was recognized by all tested CSP repeat region specific mAbs elicited by sporozoite-immunization of mice, and by the majority of sera from human donors living in malaria endemic regions (data not shown). One major limitation in using peptide antigens as vaccine components is their poor immunogenicity. We demonstrate here that presentation of UK39 on the surface of virus-like particles elicited a strong parasite cross-reactive antibody response both

in mice and in rabbits. Lack of immunogenicity of a liposomal formulation demonstrated the importance of influenza protein antigens for the immunopotentiating activity of IRIVs. We have observed better immune responses with liposomal formulations of PE-conjugates of larger peptides, but also in these cases IRIV formulations were far superior (unpublished results). While two immunizations were needed to reach high IgG titers in mice, one immunization was sufficient in rabbits. Seroconversion was not only observed in all inbred mice, but also in all rabbits with diverse immunogenetic backgrounds. Genetic restriction of the response in humans may therefore not represent a serious limitation for IRIV-based peptide vaccines. As previously observed for other antigens [13, 22], pre-immunization of animals with an influenza vaccine improved the titers of antibodies elicited by the IRIV formulation (data not shown). Possible explanations for this phenomenon are (i) opsonization of IRIVs with pre-existing anti-influenza antibodies, leading to enhanced uptake by antigen presenting cells and (ii) activation of influenza-specific memory T cells, providing T cell help to UK39-specific B cells. The presence of antibodies against influenza are not a prerequisite for the induction of a good immune response but optimize the adjuvant effect of virosomes [13]. Widespread outbreaks of influenza have been reported for Africa [23], making the virosomal antigen delivery system applicable in malaria endemic areas of Africa. Results of the animal immunogenicity studies described here suggested that two immunizations with a 10 μg dose of UK39 will elicit a potent antibody response in influenza pre-exposed humans, irrespective of their immunogenetic background. Preliminary immunogenicity data of clinical trials with two IRIV-based malaria vaccine components, UK39 and a peptide loop derived from the *P. falciparum* Apical Membrane Antigen-1 [10, 22] support this assumption and the general concept of delivering peptides as IRIV-bound phosphatidylethanolamine (PE)-conjugates to the human immune system.

Antibodies against BP65 and its easier to synthesize derivative UK39 inhibited sporozoite invasion into hepatocytes *in vitro*. Inhibition with mAbs against BP65 was up to 100% whereas only lower levels of inhibition were observed with purified IgG from UK39-immunized rabbits. This reduced effect can be explained by the fact that we used total IgG from immunized animals. Thus, despite using high concentrations of IgG (1 mg/ml), only a minor fraction of the antibodies is specific for the NPNA

repeats. Additionally, physiological serum IgG concentrations of rabbits are higher than 1 mg/ml, pointing towards an increased inhibitory effect *in vivo*.

The mechanism of this inhibition is not clearly understood. The observed inhibition of gliding motility suggests interference with parasite motility, which is necessary to invade the target cell, as described before [24]. Whether gliding inhibition is based on a specific block of the mechanism promoting movement or just the result of steric hindrance remains to be elucidated as the involvement of CSP in the process of gliding motility is still controversial [25]. The protective potential of anti-CSP repeat antibodies has been shown *in vivo* by passive transfer of anti-CSP repeat antibodies, which can protect mice from experimental sporozoite challenge [26]. The mechanism of this protection is at least in part due to antibody-mediated immobilization of sporozoites in the skin after injection by the mosquito [27].

It is not likely that antibodies against UK39 alone would result in complete protection against malaria. However, in the context of a multi-stage vaccine, they may reduce the number of sporozoites entering liver cells and thus support immune protection elicited by components directed against the liver and blood stages of the malaria parasite. Moreover it is thought that reduction of the number of merozoites released from the liver by anti-pre-erythrocytic vaccination [3] or reduction of the sporozoite inoculum by the use of insecticide treated bed-nets [28] can reduce the incidence of severe malaria.

The universal IRIV-based antigen delivery platform described in this report is highly suitable for combining antigens specific for the different development stages of the parasite into a multi-component malaria subunit vaccine.

Significance

With increasing global prevalence of malaria and emerging resistance of *P. falciparum* to drug treatment, the need for an efficient malaria vaccine is greater than ever. Although it was shown more than 30 years ago that man can be protected against malaria by vaccination [29], a safe, effective and affordable vaccine is still many years away [4]. Especially the lack of safe and potent adjuvant/delivery systems and the technical and regulatory problems associated with recombinant protein production has hampered vaccine development. We have developed a technology platform based on the design of conformationally constrained synthetic peptides and the IRIV delivery system, which allows for the rational development of a malaria vaccine. The parasite-binding capacity of antibodies elicited by immunization of mice with virosomally-formulated peptides was used as a key indicator for the optimization of peptide antigens. The universal IRIV-based antigen delivery platform is highly suitable for combining antigens specific for the different development stages of the parasite into a multi-component malaria subunit vaccine. As the IRIV system is already registered for use in humans, this platform can contribute to the rapid development of a safe, efficient and cost-effective malaria vaccine.

Acknowledgements

We thank G.J. van Gemert, J.F. Franetich, T. Houpert and L. Hannoun for their contribution to this study. This project was co-financed by the Commission for Technology and Innovation (BBT, Switzerland).

Experimental procedures

Synthesis of peptides

Synthesis of JL934, JL1036 and BP65 has been described previously [11, 12, 30]. For UK40, a linear peptide was first assembled on Rink Amide MBHA resin (0.73 mM/g) (*Novabiochem)* using an *Applied Biosystems ABI433A* peptide synthesizer, and Fmoc-protected amino acids (Fmoc-Asn(Mtt)-OH, Fmoc-Pro-OH, Fmoc-Ala-OH, Fmoc-Glu(*t*Bu)-OH and Fmoc-(4S,2S)-4-aminoproline(Boc)-OH) and HBTU/HOBt (4 eq.) for activation. After cleavage of the linear peptide from the resin with 95% TFA, 2.5% TIS and 2.5% water over 3 h, the peptide was precipitated using iPr_2O and dried. The linear peptide was then stirred overnight with HATU (4eq.) and HOAt (4 eq.) in DMF with 1 % v/v iPr_2EtN (2 mg/ml peptide). After drying in vacuo the peptide was stirred in 20 % piperidine in DMF for 15 min. The solvent was evaporated and peptide was precipitated using iPr_2O, dried in vacuo, and then purified by reverse phase HPLC (C18 column using a gradient of MeCN/H_2O (+0.1% TFA; 5 to 95% MeCN ; t_R = 11 min). ES-MS m/z: 2276 $(M+H)^+$.

The cyclic peptide (40 mg) was coupled to PE-CO-$(CH_2)_2$-COOH (PE-succinate; 4 eq.) in DMF (5 ml), CH_2Cl_2 (5 ml) and 1% iPr_2EtN using HATU and HOAt with stirring overnight at rt. The solvent was then removed and the product purified by reverse phase HPLC (C4 column *Vydac 214 TP 1010, 25cmx10mm)* using a gradient of 50 % ethanol in water to 100 % ethanol (+0.1% TFA) over 15 min. UK39 appears as a broad peak at about 90 % ethanol. ES-MS m/z: 1427 $(M+2H)^{2+}$. Alternatively, the cyclic peptide was acetylated with acetic anhydride in MeOH and NH_4HCO_3 buffer and UK40 was purified by reverse phase HPLC (C18 column *Vydac*) using a gradient of 0 to 100% MeCN in water. ES-MS m/z: 1049 $(M+2H)^{2+}$.

NMR studies

For NMR studies, UK40 was dissolved in 90%H_2O/10%D_2O, pH 5.0, at a concentration of ca. 10 mg/ml. 1D and 2D ^1H NMR spectra were recorded at 600 MHz (Bruker AV-600 spectrometer). Water suppression was by presaturation. The sequential resonance assignments were based on DQF-COSY, TOCSY and NOESY spectra. Distance restraints were obtained from NOESY spectra with mixing times of 80 and 250 ms. Spectra were collected with 1024 x 256 complex data points zero-filled prior to Fourier transformation to 2048 x 1024, and transformed with a cosine-

bell weighting function. Data processing was carried out with XWINNMR (Bruker) and XEASY. [31]

The structure calculations were performed by restrained molecular dynamics in torsion angle space by applying the simulated annealing protocol implemented in the program DYANA. [32] Starting from 100 randomized conformations a bundle of 20 conformations were selected with the lowest DYANA target energy function. The program MOLMOL [33] was used for structure analysis and visualization of the molecular models.

Preparation of peptide-loaded virosomes

For the preparation of IRIVs loaded with phosphatidylethanolamine (PE)-peptide conjugates, a solution of purified Influenza A/Singapore hemagglutinin (4 mg) in phosphate buffered saline (PBS) was centrifuged for 30 min at 100,000 g and the pellet was dissolved in PBS (1.33 ml) containing 100 mM octaethyleneglycolmonodecylether (PBS-OEG). Peptide-PE conjugates (4 mg), phosphatidylcholine (32 mg; Lipoid, Ludwigshafen, Germany) and PE (6 mg) were dissolved in a total volume of 2.66 ml of PBS-OEG. The phospholipid and the hemagglutinin solutions were mixed and sonicated for 1 min. This solution was then centrifuged for 1 hour at 100,000 g and the supernatant was filtered (0.22 μm) under sterile conditions. Virosomes were then formed by detergent removal using BioRad SM BioBeads (BioRad, Glattbrugg, Switzerland).

Mouse immunogenicity studies

BALB/c mice were pre-immunized intramuscularly with 1 □g of purified Influenza A/Singapore hemagglutinin in 0.1 ml PBS. . At least three weeks later they were immunized with PE-peptide conjugate-loaded IRIVs (containing 10 □g PE-peptide) in intervals of at least two weeks. Blood was collected before each immunization and two weeks after the final injection.

Generation of hybridomas and production of mAbs

Hybridomas were generated from spleen cells of mice three days after a booster immunization with BP65 loaded IRIVs using PAI mouse myeloma cells as a fusion partner. Hybrids were selected in HAT medium and cells that secreted anti-BP65

mAbs were identified by ELISA. For large-scale mAb production, hybridoma cell lines were cultured in 175 cm^2 flasks and mAbs were purified by protein A or G affinity chromatography (Protein A Sepharose™ CL4B or HiTrap™ Protein G HP, Piscataway, NJ). Purified mAbs were dialyzed against PBS, aliquoted and stored at -80°C. Generation of anti-*P. falciparum* sporozoite mAbs has been described previously [34].

Rabbit immunogenicity studies

Rabbits were pre-immunized intramuscularly 5 □g of purified Influenza A/Singapore hemagglutinin in 0.1 ml PBS. . At least three weeks later they were immunized with peptide-loaded IRIVs (containing 10 □g PE-peptide) in intervals of at least two weeks. Blood was collected before each immunization and two weeks after the final injection. Rabbit IgG was purified from immune sera by protein A affinity chromatography.

ELISA

ELISA analyses with peptide-PE conjugates were performed essentially as described before [10]. Briefly, Polysorp™ plates (Nunc, Fisher Scientific, Wohlen, Switzerland) were coated overnight at 4°C with 100 μl of a 10 μg/ml solution of UK39 in PBS (pH 7.2). After three washings with PBS containing 0.05% Tween-20 wells were blocked with 5% milk powder in PBS for 30 min at 37°C and washed three times again. Plates were then incubated with serial dilutions of anti-peptide mouse or rabbit sera or anti-peptide mAbs in PBS containing 0.05% Tween-20 and 0.5% milk powder for 2 h at 37°C. After washing, plates were incubated with alkaline phosphatase-conjugated goat anti-mouse IgG (Fc-specific) antibodies (Sigma, St. Louis, Mo) for 1 h at 37°C. After washing again, phosphatase substrate solution (1 mg/ml p-nitrophenyl phosphate (Sigma, St. Louis, Mo) in a pH 9.8 buffer solution containing 10% [vol/vol] diethanolamine and 0.02% $MgCl_2$) was added and the plates were incubated in the dark at room temperature until the colorimetric reaction had progressed sufficiently. The optical density was measured at 405 nm on a Titertek Multiscan MCC/340 reader (Labsystems, Helsinki, Finland). For experiments with rabbit sera, horseradish peroxidase-conjugated goat anti-rabbit IgG heavy and light chain antibodies (Bio-Rad Laboratories, Hercules, CA) were used as secondary antibody.

The TMB microwell peroxidase substrate system (KPL, Gaithersburg, MD) was used according to the manufacturer and optical density was measured at 650 nm. After stopping the reaction by addition of 50 µl 1N HCl per well OD was measured at 450nm.

Indirect immunofluorescence assay (IFA)

Air-dried unfixed *P. falciparum* (strain NF54) salivary gland sporozoites attached to microscope glass slides were incubated for 15 min at room temperature with 25 µl blocking solution containing 1% fatty acid-free bovine serum albumin (BSA) in PBS. Immunostaining was performed by incubating the wells with 25 µl of an appropriate serum dilution in blocking solution in a humid chamber for 1 h at room temperature. After five washes with blocking solution 25 µl of 5 µg/ml cyanine dye (Cy3)-conjugated affinity-pure $F(ab')_2$ fragment goat anti-mouse IgG (Fc-specific) antibodies (Jackson Immuno Research Laboratories, West Grove, Pa.) or Cy3-conjugated donkey anti-rabbit IgG heavy and light chain antibody (Jackson Immuno Research Laboratories, West Grove, PA), diluted in blocking solution containing 0.01 mg/ml Hoechst dye no. 33256 (Sigma, St. Louis, Mo) were added to the wells and incubated for 1 h at room temperature. Finally, wells were washed five times with PBS, mounted with mounting solution (90% [vol/vol] glycerol containing 0.1 M Tris-Cl, pH 8.0 and 2 mg/ml *o*-phenylenediamine) and covered with a coverslip. Antibody binding and DNA staining were assessed by fluorescence microscopy on a Leitz Dialux 20 fluorescence microscope and documented with a Leica DC200 digital camera system.

SDS-PAGE and immunoblotting

100 µl of an *Anopheles stephensi* salivary gland lysate containing about 100'000 *P. falciparum* sporozoites were diluted with an equal volume of 2x loading buffer (1.7ml, 0.5M Tris-HCl pH 6.8, 2 ml glycerol, 4.5 ml 10% SDS, 1 ml β-mercaptoethanol, 0.8 ml 0.3% w/v bromophenol blue) and heated to 95°C for 10 minutes. Proteins were separated on a 10% SDS PAGE mini-gel. Separated proteins were electrophoretically transferred to a nitrocellulose filter (Protran® Nitrocellulose, BA85, Schleicher & Schuell) by semi-dry blotting. Blots were blocked with PBS containing 5% milk powder and 0.1% Tween-20 over night at 4°C. The filter was cut

into strips and incubated with appropriate dilutions of immune sera in blocking buffer for 2 h at room temperature. Filter strips were then washed three times for 10 minutes in blocking buffer and incubated at room temperature for 1 h with alkaline peroxidase-conjugated goat anti-mouse IgG (Fc-specific) antibodies (Sigma, St. Louis, Mo) diluted 1:30'000 in blocking buffer or horseradish peroxidase-conjugated goat anti-rabbit IgG heavy and light chain antibodies (Bio-Rad Laboratories, Hercules, CA) diluted 1:6'000 in blocking buffer. After washing again, blots were finally developed using ECL™ Western blotting detection (Amersham Biosciences, Buckinghamshire, England) reagents to visualize bands.

P. falciparum and P. yoelii in vitro invasion inhibition assay

Inhibition assays were performed as described before [35, 36]. Briefly, primary human or mouse hepatocytes were isolated as described [37, 38], and inoculated with *P. falciparum* (NF54 strain) or *P. yoelii* (265BY strain) sporozoites (1 x 105/Labtek well) obtained from salivary glands of infected *Anopheles stephensi* mosquitoes. After 3 h at 37°C, the cultures were washed, further incubated in fresh medium for 3 days (P. falciparum) or 2 days (P. yoelii) before fixation in methanol. Quantification of exoerythrocytic forms was done by immunofluorescence. To determine the effects of anti-CSP antibodies on sporozoite infectivity, sporozoites were incubated with hepatocytes in the presence of increasing concentrations of mAbs or purified polyclonal rabbit IgG from immunized animals. The percentage of inhibition was determined in comparison to PBS control.

Gliding inhibition

To analyze sporozoite motility, 30,000 sporozoites were deposited on multispot glass slide wells precoated with anti-*P. falciparum* CSP (*Pf*CSP) mAb E9 (100 μg/ml 1 h at 37 °C) and incubated at 37 °C for 1 h. The slides were then washed, and the deposited CSP trails were fixed with 4% paraformaldehyde for 15 min. The trails were then labeled using the anti-*Pf*CSP mAb E9 conjugated to Alexa Fluor® 488 and visualized under a fluorescence microscope.

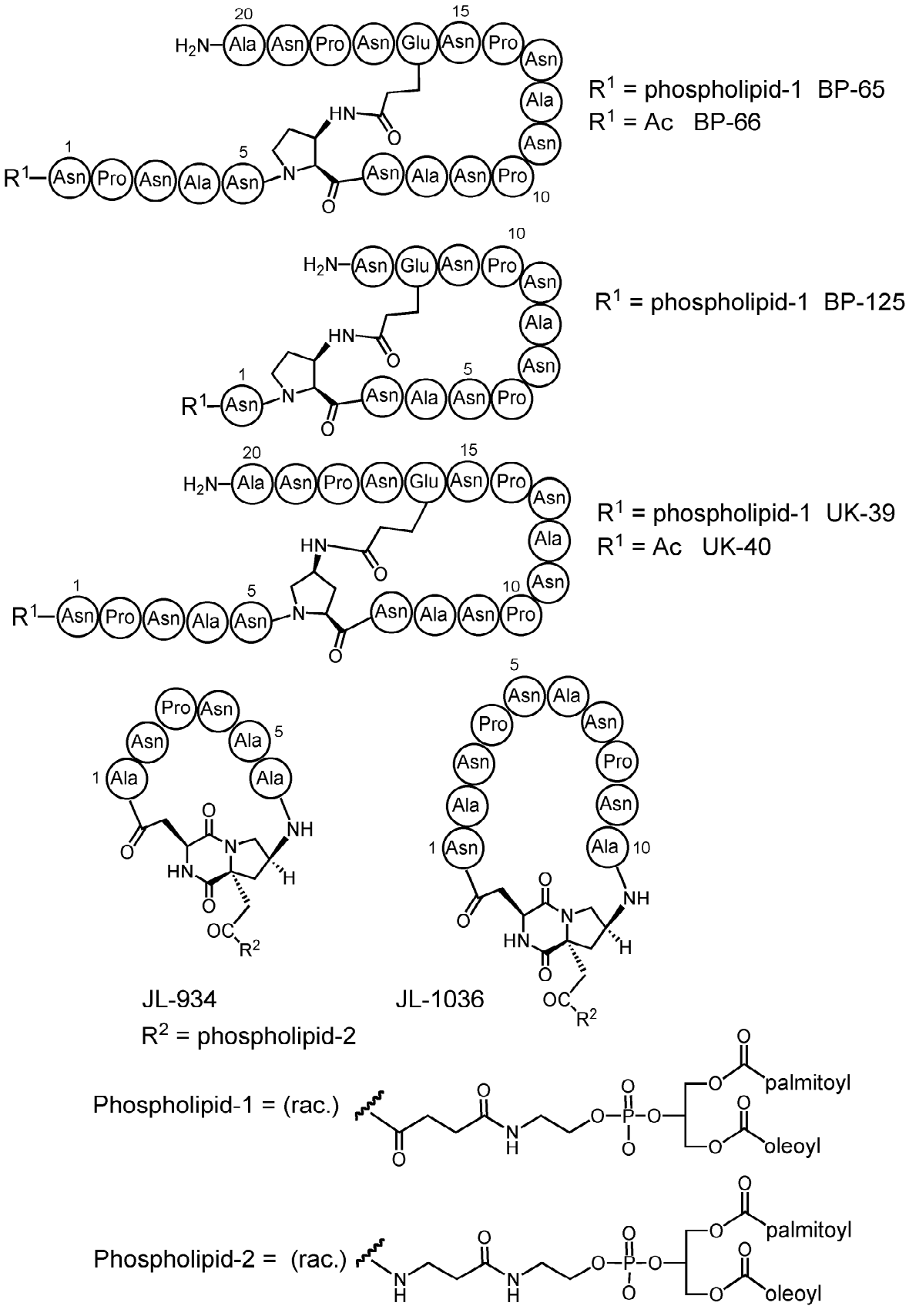

Figure 1. Structures of peptidomimetics discussed in the text.

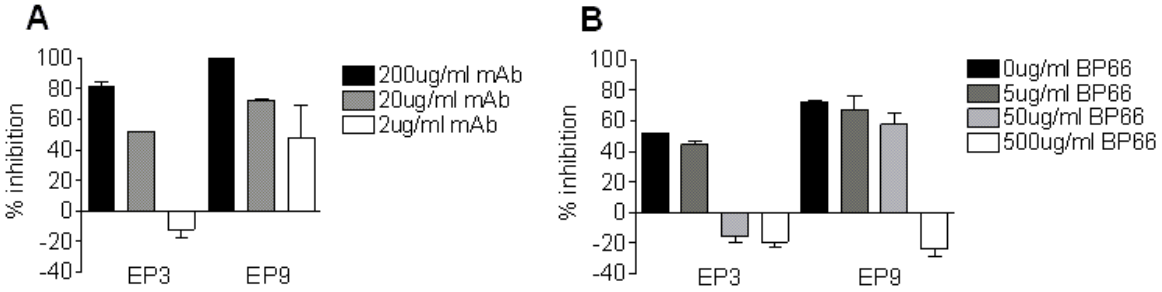

Figure 2. Hepatocyte invasion inhibition by anti-BP65 mAbs. A: Inhibition of parasite invasion into primary human hepatocytes by mAb EP3 and mAb EP9. Shown is the mean percentage of inhibition compared to PBS control ± SD deviation for duplicates. B: Competition of invasion inhibition by increasing concentrations of BP66 peptide (BP65 without PE). Inhibitory mAbs were used at a constant concentration of 20 □g/ml.

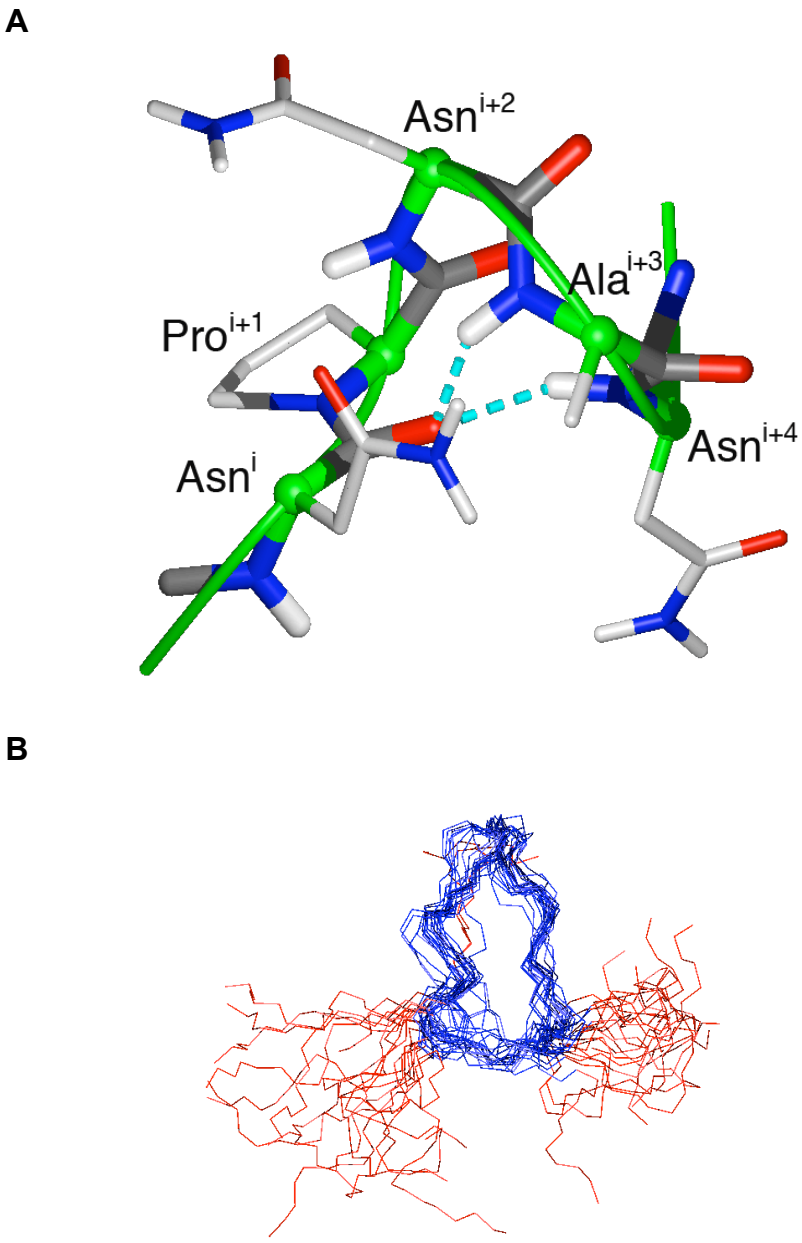

Figure 3. A: An NPNA motif is depicted in a helical turn conformation (see text). N-atoms dark blue, O-atoms red, C-atoms grey, amide H-atoms light white, H-bonds pale blue broken line. Here the first Asn has □□□ angles in the ß-region, and the following Pro, Asn and Ala in the □-region. A green ribbon traces the backbone. B: Superimposition of the final 20 DYANA structures for UK40. The backbone only is represented, superimposed using all heavy atoms from Apro6 to Glu16 (region in blue).

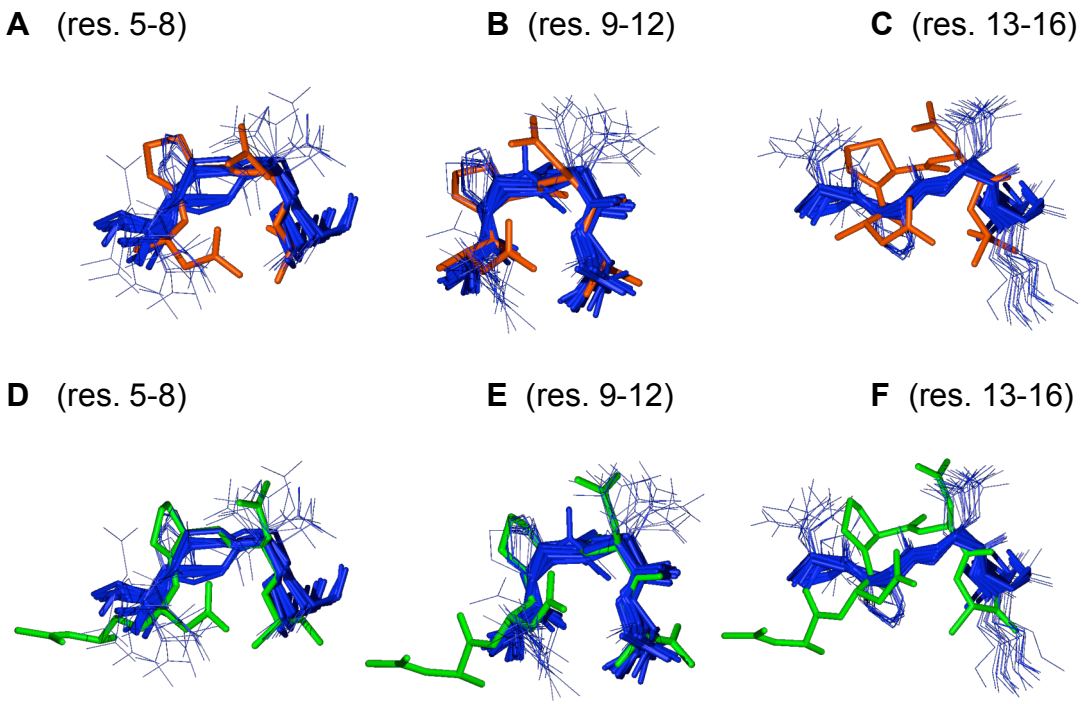

Figure 4. Backbone superimposition of the 20 DYANA structures of UK40 with a helical turn conformation (red, A - C), and with the ANPNA crystal structure (green, D - F). In A and D only residues 5-8 in UK40 were used for the superimposition, for B and E only residues 9-12, and for C and F only residues 13-16.

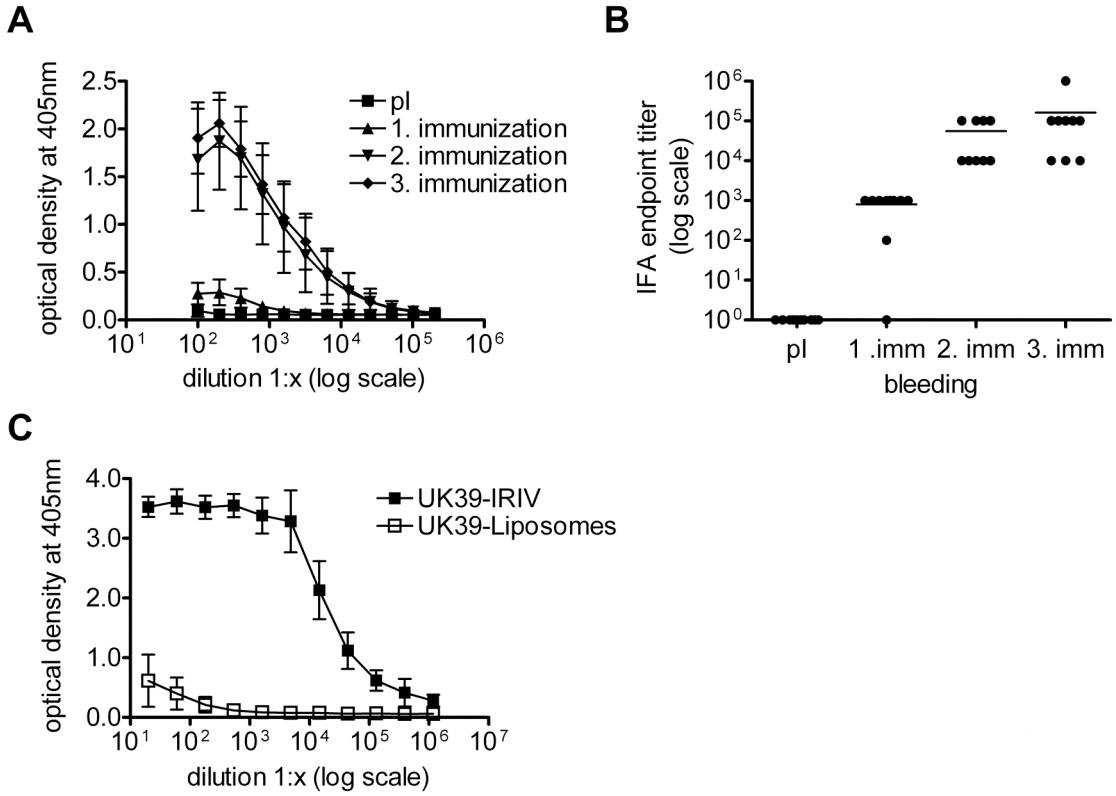

Figure 5. Immunogenicity of virosomal and liposomal formulations of UK39 in mice. A: Anti-UK39 IgG response in ELISA after immunization with IRIV-formulated UK39. Shown are mean ELISA readouts ± SD obtained with serial dilutions of mouse sera taken pre-immune and two weeks after the first, second and third immunization. Sera from 10 animals were analyzed at every time point. B: Induction of *P. falciparum* sporozoite cross-reactive IgG upon immunization with UK39. Shown are IFA endpoint titers of 10 individual mice. Sera have been taken pre-immune and two weeks after first, second and third immunization. C: Anti-UK39 IgG response in ELISA of mice immunized with UK39 presented either on liposomes or on virosomes. Shown are the means ± SD of 5 animals per group. Sera have been taken 2 weeks after the third immunization.

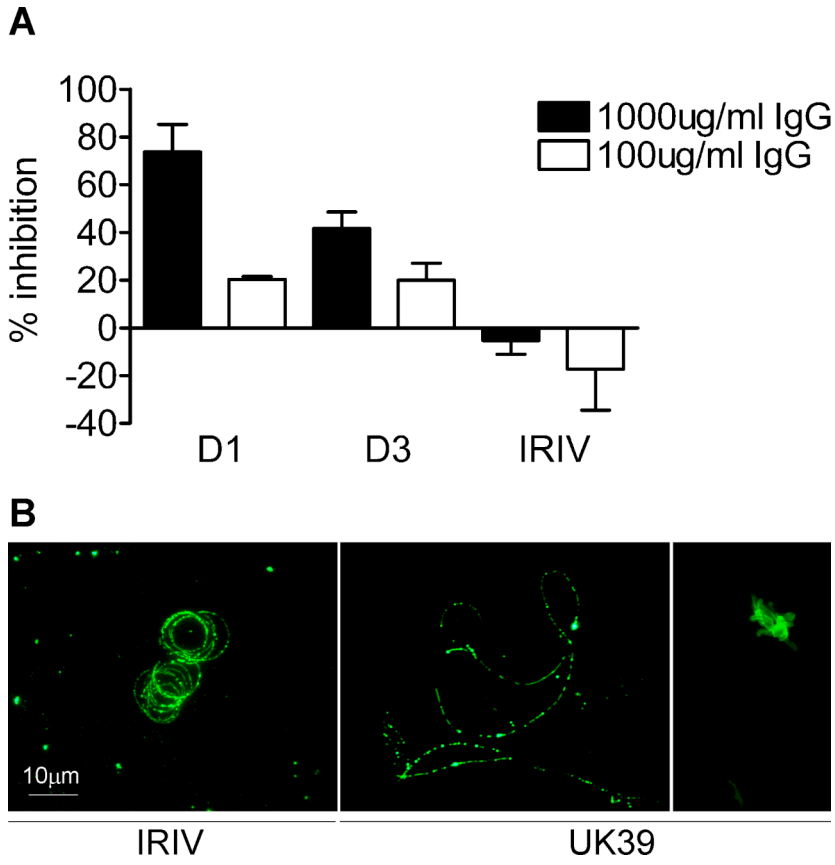

Figure 6. Inhibitory capacity of anti-UK39 antibodies. Sporozoite invasion inhibition by purified IgG from rabbits immunized with UK39. A: *P. falciparum* sporozoites have been cultured with primary human hepatocytes in the presence of purified polyclonal rabbit IgG at different concentrations. Shown is the mean percentage of inhibition compared to PBS control ± SD of 3 experiments for two animals immunized with IRIV-formulated UK39 (D1 and D3) and one control animal immunized with empty IRIVs (IRIV). B: Fluorescence microscopy of CSP trails deposited by *P. falciparum* sporozoites upon gliding on a glass slide. Left panel: Trails of sporozoites incubated with purified IgG from a rabbit immunized with empty IRIVs. Middle panel: Reduced trails of sporozoites incubated with purified IgG from an UK39-immunized animal. Right panel: Agglutination of sporozoites incubated with purified IgG from a rabbit immunized with UK39.

mab	Immunogen	Cross-reactivity with				
		JL934[c]	**JL1036**[c]	**BP-65**[c]	**UK-39**[c]	**Sporozoites**[d]
1.26[e]	JL934[a]	+	-	-	ND	+
1.7[e]		+	-	ND	ND	-
1.15[e]		+	-	ND	ND	-
2.1[e]	JL1036[a]	-	+	+	+	+
3.1[e]		-	+	+	+	+
3.2[e]		-	+	-	-	+
3.3[e]		-	+	+	+	+
3.4[e]		-	+	ND	ND	-
3.5[e]		-	+	ND	ND	-
EP3	BP-65[a]	-	-	+	+	+
EP9		-	+	+	+	+
Sp4-5F2	*Pf* sporozoites[b]	(+)	+	+	+	+
Sp4-2H1		(+)	+	+	+	+
Sp3-E6		-	+	+	+	+
Sp3-C6		-	(+)	+	+	+
Sp3-E9		-	(+)	+	+	+
Sp4-4B6		-	-	+	+	+
Sp4-7C2		-	-	+	+	+
Sp4-7E4		-	-	+	+	+
Sp4-7H1		-	-	(+)	+	+
Sp4-4D7		-	-	+	+	+
Sp3-B4-C12		-	-	+	+	+
Sp4-1B4		-	-	(+)	+	+

Table 1. Cross-reactivity of anti-NPNA mAbs.

[a]mice were immunized with IRIVs loaded with the respective peptide
[b]mice were immunized with *P. falciparum* sporozoites from *A. stephensi* salivary glands in Freund's adjuvant
[c]ELISA reactivity to the peptides
[d]IFA reactivity to *P. falciparum* sporozoites
[e]Described by Moreno et al. 2001

Supplementary material

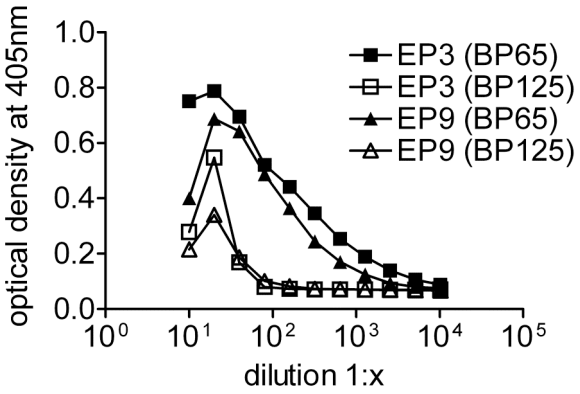

Figure S1. BP-125 a shortened version of BP65. ELISA with anti-BP65 mAbs EP3 and EP9 on CSP mimetics BP65 and the shortened version BP-125. Shown are serial dilutions of the mAbs on constant concentrations of the two peptides.

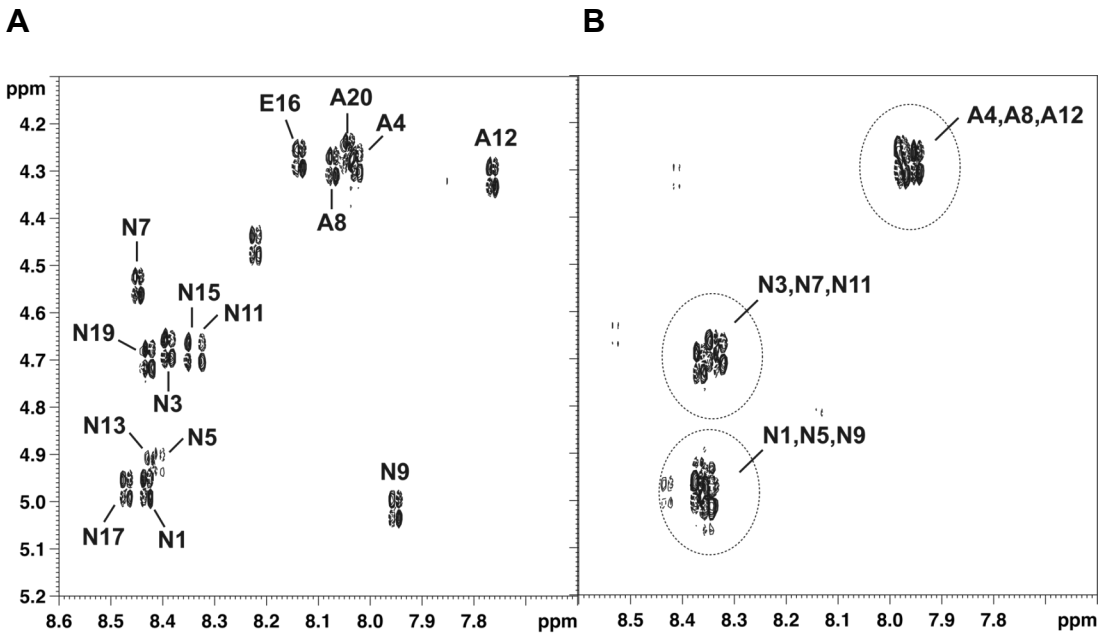

Figure S2. Sections from 2D DQF-COSY spectra in aqueous solution for: A, UK40; and B, the linear peptide Ac-$(NPNA)_3$-NH_2. Cross-peaks for HN-C(□)H ^3J couplings are indicated.

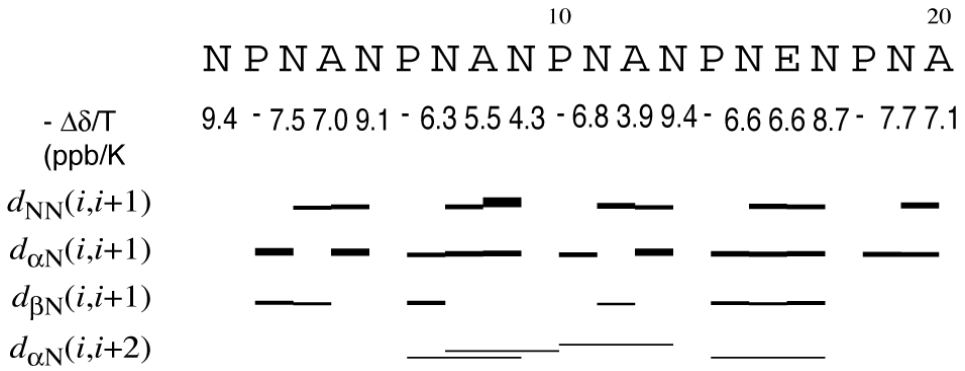

Figure S3. Results from 2D COESY spectra of UK40. NOE connectivities from NOESY spectra, and temperature coefficients (□□□□/□T ppb/K) of peptide amide NH resonances from 2D TOCSY spectra of UK40 measured in the range 279 -314 K. The thickness of the lines for the sequential distances d_{NN} (*i,i+1*), $d_{\square N}$ (*i,i+1*) and $d_{\square N}$ (*i,i+1*) is inversely proportional to the squared upper distance restraint.

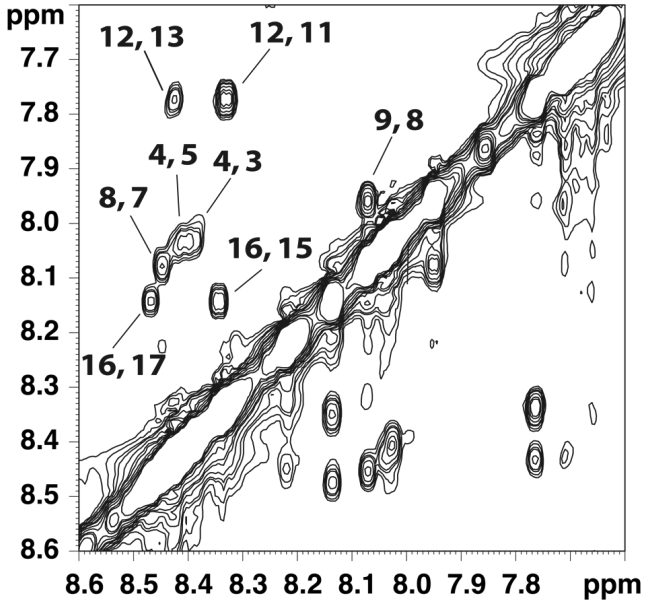

Figure S4. Backbone amide HN-HN cross peaks in a NOESY spectrum of UK40 in aqueous solution. The residue assignments are shown for each cross peak.

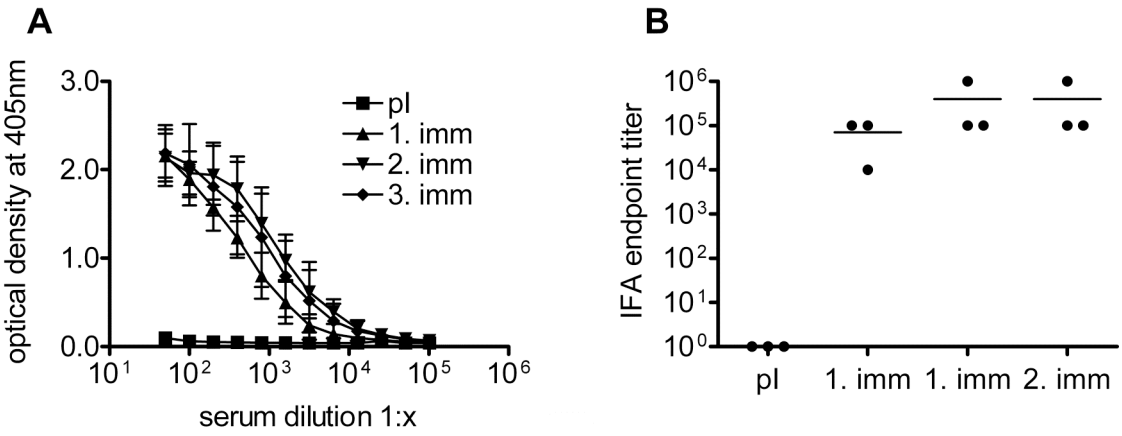

Figure S5. Immunogenicity of UK39 in rabbits. A: Anti-UK39 IgG levels measured in ELISA. Shown are the means ± SD of 3 rabbits. Sera have been taken pre-immune and two weeks after first, second and third immunization. B: Cross-reactivity of UK39 induced IgG with *P. falciparum* sporozoites. Shown are IFA endpoint titers of 3 individual animals pre-immune and two weeks after first, second and third immunization. Arrows indicate immunizations with IRIV-formulated UK39.

Residue	NH	H-C(a)	H-C(b)	Others
UK-40				
Asn[1]	8.43	4.97	2.86, 2.71	NH(d)[a]
Pro[2]	-	4.43	2.31, 1.98	CH(g) 2.04 – 1.98; CH_2(d) 3.81, 3.81
Asn[3]	8.38	4.67	2.85, 2.74	NH(d)a[a]
Ala[4]	8.02	4.28	1.39	
Asn[5]	8.41	4.91	2.87, 2.74	NH(d)[a]
Apro[6]	8.21[b]	4.51	2.66, 2.00	CH(g) 4.45; CH_2(d) 4.24, 3.62
Asn[7]	8.44	4.54	2.80, 2.80	NH(d) 7.63, 6.95
Ala[8]	8.07	4.29	1.40	
Asn[9]	7.95	5.009	2.92, 2.74	NH(d) 7.71, 7.08
Pro[10]	-	4.40	2.33, 1.96	CH_2(g) 2.04 – 1.98; CH_2(d) 3.81, 3.81
Asn[11]	8.33	4.68	2.88, 2.76	NH(d)[a]
Ala[12]	7.76	4.31	1.40	
Asn[13]	8.42	4.92	2.87, 2.76	NH(d)[a]
Pro[14]	-	4.43	2.31, 1.99	CH_2(g) 2.04 – 1.98; CH_2(d) 3.80, 3.80
Asn[15]	8.34	4.68	2.84, 2.74	NH(d) 7.66, 6.98
Glu[16]	8.13	4.27	2.12, 1.99	CH_2(g) 2.34, 2.34
Asn[17]	8.47	4.97	2.88, 2.74	a(d)[a]
Pro[18]	-	4.43	2.30, 1.99	CH_2(g) 2.04 – 1.98; CH_2(d) 3.80, 3.80
Asn[19]	8.42	4.69	2.87, 2.75	NH(d)[a]
Ala[20]	8.04	4.25	1.41	

[a] Overlapping resonances. Range H(d) (Z) 7.75-7.65 and H(d)E 7.11-6.96
[b] The C(g)-NH proton, Apro[6] = (2S,4S)-4-aminoproline

Table S1. ^{1}H Chemical shift assignments for UK40 in 90% H_2O/10% D_2O, pH 5, 293 K.

	UK-40
	99
NOE upper-distance limits	27
Intraresidue	60
Sequential	12
Medium- and longe-range	
Residual target function value ($Å^2$)	0.16 ± 0.05
Mean rmsd values (Å)	
All backbone atoms	3.74 ± 1.02
Backbone atoms of residue 6-16	1.59 ± 0.54
Residual NOE violation	
Number > 0.2 Å	13
Maximum (Å)	0.34

Table S2. Experimental distance restraints and statistics for the final 20 NMR structures calculated for UK40.

References

1. Snow, R.W., Guerra, C.A., Noor, A.M., Myint, H.Y., and Hay, S.I. (2005). The global distribution of clinical episodes of Plasmodium falciparum malaria. Nature *434*, 214-217.
2. Targett, G.A. (2005). Malaria vaccines 1985-2005: a full circle? Trends Parasitol *21*, 499-503.
3. Alonso, P.L., Sacarlal, J., Aponte, J.J., Leach, A., Macete, E., Milman, J., Mandomando, I., Spiessens, B., Guinovart, C., Espasa, M., Bassat, Q., Aide, P., Ofori-Anyinam, O., Navia, M.M., Corachan, S., Ceuppens, M., Dubois, M.C., Demoitie, M.A., Dubovsky, F., Menendez, C., Tornieporth, N., Ballou, W.R., Thompson, R., and Cohen, J. (2004). Efficacy of the RTS,S/AS02A vaccine against Plasmodium falciparum infection and disease in young African children: randomised controlled trial. Lancet *364*, 1411.
4. Greenwood, B. (2005). Malaria vaccines. Evaluation and implementation. Acta Trop *95*, 298-304.
5. Greenwood, B.M., Bojang, K., Whitty, C.J., and Targett, G.A. (2005). Malaria. Lancet *365*, 1487-1498.
6. Waters, A. (2006). Malaria: new vaccines for old? Cell *124*, 689-693.
7. Luke, T.C., and Hoffman, S.L. (2003). Rationale and plans for developing a non-replicating, metabolically active, radiation-attenuated Plasmodium falciparum sporozoite vaccine. J.Exp.Biol. *206*, 3803.
8. Good, M.F. (2005). Vaccine-induced immunity to malaria parasites and the need for novel strategies. Trends Parasitol *21*, 29-34.
9. Tongren, J.E., Zavala, F., Roos, D.S., and Riley, E.M. (2004). Malaria vaccines: if at first you don't succeed. Trends Parasitol. *20*, 604.
10. Mueller, M.S., Renard, A., Boato, F., Vogel, D., Naegeli, M., Zurbriggen, R., Robinson, J.A., and Pluschke, G. (2003). Induction of parasite growth-inhibitory antibodies by a virosomal formulation of a peptidomimetic of loop I from domain III of Plasmodium falciparum apical membrane antigen 1. Infect.Immun. *71*, 4749.
11. Pfeiffer, B., Peduzzi, E., Moehle, K., Zurbriggen, R., Gluck, R., Pluschke, G., and Robinson, J.A. (2003). A Virosome-Mimotope Approach to Synthetic Vaccine Design and Optimization: Synthesis, Conformation, and Immune

Recognition of a Potential Malaria-Vaccine Candidate. Angew.Chem.Int.Ed Engl. *42*, 2368.

12. Moreno, R., Jiang, L., Moehle, K., Zurbriggen, R., Gluck, R., Robinson, J.A., and Pluschke, G. (2001). Exploiting conformationally constrained peptidomimetics and an efficient human-compatible delivery system in synthetic vaccine design. Chembiochem. *2*, 838.
13. Poltl-Frank, F., Zurbriggen, R., Helg, A., Stuart, F., Robinson, J., Gluck, R., and Pluschke, G. (1999). Use of reconstituted influenza virus virosomes as an immunopotentiating delivery system for a peptide-based vaccine. Clin.Exp.Immunol. *117*, 496.
14. Zurbriggen, R. (2003). Immunostimulating reconstituted influenza virosomes. Vaccine *21*, 921.
15. Ballou, W.R., Hoffman, S.L., Sherwood, J.A., Hollingdale, M.R., Neva, F.A., Hockmeyer, W.T., Gordon, D.M., Schneider, I., Wirtz, R.A., Young, J.F., and et al. (1987). Safety and efficacy of a recombinant DNA Plasmodium falciparum sporozoite vaccine. Lancet *1*, 1277-1281.
16. Herrington, D.A., Clyde, D.F., Losonsky, G., Cortesia, M., Murphy, J.R., Davis, J., Baqar, S., Felix, A.M., Heimer, E.P., Gillessen, D., and et al. (1987). Safety and immunogenicity in man of a synthetic peptide malaria vaccine against Plasmodium falciparum sporozoites. Nature *328*, 257-259.
17. Dyson, H.J., Satterthwait, A.C., Lerner, R.A., and Wright, P.E. (1990). Conformational preferences of synthetic peptides derived from the immunodominant site of the circumsporozoite protein of Plasmodium falciparum by 1H NMR. Biochemistry *29*, 7828-7837.
18. Wüthrich, K. (1986). NMR of Proteins and Nucleic acids (New York: J. Wiley & Sons).
19. Stewart, M.J., and Vanderberg, J.P. (1988). Malaria sporozoites leave behind trails of circumsporozoite protein during gliding motility. J Protozool *35*, 389-393.
20. Vanderberg, J.P. (1974). Studies on the motility of Plasmodium sporozoites. J.Protozool. *21*, 527.

21. Ghasparian, A., Moehle, K., Linden, A., and Robinson, J.A. (2006). Crystal structure of an NPNA-repeat motif from the circumsporozoite protein of the malaria parasite Plasmodium falciparum. Chem Commun (Camb), 174-176.
22. Zurbriggen, R., and Gluck, R. (1999). Immunogenicity of IRIV- versus alum-adjuvanted diphtheria and tetanus toxoid vaccines in influenza primed mice. Vaccine *17*, 1301.
23. Montefiore, D., Drozdov, S.G., Kafuko, G.W., Fayinka, O.A., and Soneji, A. (1970). Influenza in East Africa, 1969-70. Bull.World Health Organ *43*, 269.
24. Stewart, M.J., Nawrot, R.J., Schulman, S., and Vanderberg, J.P. (1986). Plasmodium berghei sporozoite invasion is blocked in vitro by sporozoite-immobilizing antibodies. Infect.Immun. *51*, 859.
25. Kappe, S.H., Buscaglia, C.A., and Nussenzweig, V. (2004). Plasmodium sporozoite molecular cell biology. Annu.Rev.Cell Dev.Biol. *20*, 29.
26. Yoshida, N., Nussenzweig, R.S., Potocnjak, P., Nussenzweig, V., and Aikawa, M. (1980). Hybridoma produces protective antibodies directed against the sporozoite stage of malaria parasite. Science *207*, 71.
27. Vanderberg, J.P., and Frevert, U. (2004). Intravital microscopy demonstrating antibody-mediated immobilisation of Plasmodium berghei sporozoites injected into skin by mosquitoes. Int.J.Parasitol. *34*, 991.
28. Nevill, C.G., Some, E.S., Mung'ala, V.O., Mutemi, W., New, L., Marsh, K., Lengeler, C., and Snow, R.W. (1996). Insecticide-treated bednets reduce mortality and severe morbidity from malaria among children on the Kenyan coast. Trop Med Int Health *1*, 139-146.
29. Clyde, D.F., Most, H., McCarthy, V.C., and Vanderberg, J.P. (1973). Immunization of man against sporozite-induced falciparum malaria. Am J Med Sci *266*, 169-177.
30. Bisang, C., Jiang, L., Freund, E., Emery, F., Bauch, C., Matile, H., Pluschke, G., and Robinson, J.A. (1998). Synthesis, Conformational Properties, and Immunogenicity of a Cyclic Template-Bound Peptide Mimetic Containing an NPNA Motif from the Circumsporozoite Protein of Plasmodium falciparum. J. Am. Chem. Soc. *120*, 7439-7449.
31. Bartels, C., Xia,Tai-he, Billeter,Martin, Güntert,Peter, Wüthrich,Kurt (1995). The program XEASY for computer-supported NMR spectral analysis of

biological macromolecules, Journal of Biomolecular NMR. Journal of Biomolecular NMR *6*, 1-10.

32. Guntert, P., Mumenthaler, C., and Wuthrich, K. (1997). Torsion angle dynamics for NMR structure calculation with the new program DYANA. J Mol Biol *273*, 283-298.
33. Koradi, R., Billeter, M., and Wuthrich, K. (1996). MOLMOL: a program for display and analysis of macromolecular structures. J Mol Graph *14*, 51-55, 29-32.
34. Stuber, D., Bannwarth, W., Pink, J.R., Meloen, R.H., and Matile, H. (1990). New B cell epitopes in the Plasmodium falciparum malaria circumsporozoite protein. Eur.J.Immunol. *20*, 819.
35. Mazier, D., Mellouk, S., Beaudoin, R.L., Texier, B., Druilhe, P., Hockmeyer, W., Trosper, J., Paul, C., Charoenvit, Y., Young, J., and et al. (1986). Effect of antibodies to recombinant and synthetic peptides on P. falciparum sporozoites in vitro. Science *231*, 156-159.
36. Silvie, O., Franetich, J.F., Charrin, S., Mueller, M.S., Siau, A., Bodescot, M., Rubinstein, E., Hannoun, L., Charoenvit, Y., Kocken, C.H., Thomas, A.W., van Gemert, G.J., Sauerwein, R.W., Blackman, M.J., Anders, R.F., Pluschke, G., and Mazier, D. (2004). A Role for Apical Membrane Antigen 1 during Invasion of Hepatocytes by Plasmodium falciparum Sporozoites. Journal of Biological Chemistry *279*, 9490.
37. Mazier, D., Beaudoin, R.L., Mellouk, S., Druilhe, P., Texier, B., Trosper, J., Miltgen, F., Landau, I., Paul, C., Brandicourt, O., and et al. (1985). Complete development of hepatic stages of Plasmodium falciparum in vitro. Science *227*, 440-442.
38. Renia, L., Mattei, D., Goma, J., Pied, S., Dubois, P., Miltgen, F., Nussler, A., Matile, H., Menegaux, F., Gentilini, M., and et al. (1990). A malaria heat-shock-like determinant expressed on the infected hepatocyte surface is the target of antibody-dependent cell-mediated cytotoxic mechanisms by nonparenchymal liver cells. Eur J Immunol *20*, 1445-1449.

Chapter 3.2

Generation of malaria specific CD4 T cell responses with a virosomally formulated synthetic peptide

Elisabetta Peduzzi*, Rinaldo Zurbriggen†, Gerd Pluschke*, Claudia A. Daubenberger*

* Swiss Tropical Institute, Molecular Immunology, CH 4002 Basel, Switzerland

† Pevion Biotech Ltd., CH-3018 Bern, Switzerland

This article will be submitted in:

Journal of Immunology

Abstract

Peptide vaccines containing surface loops of protective antigens provide the advantages of low cost, safety, and stability while focusing host responses on relevant targets of protective immunity. However, the limited diversity of the elicited immune response raises questions regarding their equivalence to immune responses elicited by recombinant protein vaccines or whole inactivated parasite vaccines. Here we have addressed the question whether a virosomally formulated peptide, optimized for generating parasite-binding antibodies can also elicit CD4 T cells specific for the malaria antigen apical membrane antigen-1 (AMA-1) derived sequence stretch used for vaccination. In a phase Ia clinical trial of the virosomally formulated 49 amino acid long phosphatidylethanolamin peptide conjugate AMA49-CPE, we measured both vaccine induced humoral and cellular responses. In 50% of the volunteers (8/16) peripheral blood mononuclear cells lymphoproliferative response specific for the AMA49-CPE was elicited. Moreover, all four volunteers who developed high titers (>1000) of parasite cross-reactive IgG in immunofluorescence assay and Western blot analysis, were positive in the anti-synthetic peptide lymphoproliferation assay. No interference was found between the magnitude of the pre-existing influenza specific T cell response and the vaccination-induced AMA49-CPE specific humoral and cellular immune response. These studies demonstrate that the virosomal antigen delivery platform combined with surface-anchored synthetic peptides is suitable to elicit specific human CD4 T cell responses. These responses are not essential for eliciting target peptide specific IgG, but may improve the quality of the humoral immune response.

Introduction

The use of synthetic peptide for the design of subunit vaccines represents an alternative approach to recombinant proteins and pathogen-purified components, which bypasses many of the problems related to antigen production and handling. However, the poor immunogenicity of the synthetic peptides, principally due to their small size (1), is hampering their use as vaccines. An optimal presentation of the synthetic peptides to the immune system is therefore essential. The suitability of immnopotentiating reconstituted influenza virosomes (IRIVs) as peptide carrier and immunopotentiator system has already been proven in preclinical studies (2-6). The repetitive arrangement of the antigen on the virosomal surface enables a good crosslinking of the B cell receptors and therefore, an optimal B cell stimulation (7). On the other side, the influenza hemagglutinin (HA) binds to sialic acid on antigen presenting cells (APC), e.g. macrophages, dendritic cells (DC) or B lymphocytes, enabling a receptor-mediated endocytosis of the virosomes. The HA2 subunit mediates the fusion of viral and endosomal membranes. Subsequently, virosomal surface particles and synthetic peptides can be degraded within the endosomal/lysosomal compartment (8) and the generated peptides might associate with MHC class II molecules giving access to the T helper pathway. There are two commercially available virosome-based vaccines licensed for human use: Inflexal® to prevent the influenza-infection itself and Epaxal® against Hepatitis A virus (HAV)-infections. For the later one intact virions of inactivated HAV were associated to the surface of IRIV, and a vaccine induced seroconversion in 100% of the vaccinated people with long lasting antibody-mediated immunity was obtained (9). At present, our research on IRIVs is focused on their use for the design of synthetic peptide based vaccines, containing either encapsulated peptides or surface exposed peptide-phospholipid conjugates. A first phase Ia clinical trial combining the virosomal technology with synthetic peptides anchored on the virosome surfaces was conducted in 2003-2005 within the context of a multi-stage malaria subunit vaccine project. The two peptide-phosphatidylethanolamin (PE) conjugate included in the vaccine formulations represented optimized B cell antigens derived from the leading malaria vaccine candidates circumsporozoite protein (CSP) and apical membrane antigen-1 (AMA-1) (Genton et al. submitted, Okitsu et al. submitted) (5). The specific objectives of the trial have been completely fulfilled: the three immunizations of all

vaccine formulations were safe, well tolerated and at appropriate antigen doses seroconversion rates of 100% were achieved, attesting the concept that virosomal technology is suitable to elicit high titers of antibodies also against small synthetic peptides (Genton et al. submitted). Here we addressed the question whether such formulation can also be used to elicit peptide specific CD4 T cells. It is assumed that influenza antigen specific CD4 T cells provide T cell help for the malaria peptide specific B cells, assure the antibody class switching and development of memory B cells (8, 10). But an extra priming of CD4 T cells against the synthetic peptides may further enhance humoral immunity to the malaria peptide. To investigate the cellular immune responses against the AMA-1 derived synthetic was monitored in 30 vaccinated volunteers by lymphoproliferation analysis and *ex vivo* IFN-γ ELISpot.

Materials and Methods:

Subjects and study design

The prospective phase Ia, single blind, randomized, placebo controlled, dose-escalating study was conducted in 46 healthy adult volunteers (Genton et al., submitted). 30 male and female volunteers, aged 18-45 years randomized into four groups were selected for cellular analysis: PEV301 50 μg (n = 8; Group 3), PEV302 50 μg (n = 8; Group 4), PEV301 50 μg + PEV302 50 μg (n = 8; Group 5) or unmodified virosomes (IRIVs) serving as controls (n = 6; Group 6) (Table I, Figure 1).

Vaccine

Two virosome-formulated *Plasmodium falciparum* malaria vaccines PEV301 (incorporating the AMA-1 derived PE-peptide conjugate AMA49-CPE) and PEV302 (incorporating the CSP derived PE-peptide conjugate UK39) were produced according to the rules of good manufacturing practice (GMP). Tests for sterility, pyrogenicity, immunogenicity in animals, stability and chemical composition were performed on the vaccine lots used in this trial. Each dose was composed of 50 μg AMA49-CPE or UK39, 10 μg influenza HA, 100 μg phospholipids and 0.5 ml PBS.

Immunological analyses

Volunteers were immunized with the different vaccine combinations on days 0, 30 and 180. Blood samples for cellular analysis were taken during the screening visit, 21 days after each vaccination. 25 ml of venous blood were obtained in BD vacutainer covered with EDTA and peripheral blood mononuclear cells (PBMC) were isolated by Ficoll-Paque gradient centrifugation. Cells were analyzed the same day by *ex vivo* IFN-γ ELISpot analysis and lymphoproliferation assay. PBMC were resuspended in cell culture medium consisting of RPMI 1640 supplemented with 10 % heat-inactivated non-immune pooled human AB serum (Milan Analytica AG, La Roche, Switzerland), 2 mM glutamine and antibiotics (100 U/ml penicillin, 100 □g/ml streptomycin).

Ex vivo IFN-γ ELISpot

PBMC were adjusted to 2 x 10^6 cells/ml and incubated for 24 h in 5 ml polypropylene round-bottom tube (Falcon BD) at 37 °C, 5 % CO_2 humidified atmosphere with

medium alone, influenza antigens (H1N1 A/Singapore/6/86) (40 μg/ml), UK40 (40 μg/ml) or AMA-C1 (40 μg/ml). *Ex vivo* INF-γ ELISpot assays were performed to detect antigen-specific effector T cells from freshly isolated PBMC. The anti-IFN-γ monoclonal antibody (mAb, 1-D1K) and the biotinylated anti-IFN-γ monoclonal antibody (mAb, 7-B6-1) (Mabtech, Stockholm, Sweden) were used according to the manufacturer's instructions. Nitrocellulose-backed 96-well plates MultiScreenIP plates (Millipore AG, Volketswil, Switzerland) were coated with 10 μg/ml of capture antibody (1-DIK) overnight at 4 °C. The plates were then washed five times with PBS and blocked with cell culture medium for 1 h. Medium was decanted and cells were distributed in triplicate wells at a concentration of 1 x 10^5 cells/well for influenza antigens stimulation and at 2 x 10^5 cells/well for the AMA-C1 and UK40 stimulation for a further 20 h incubation period. After six times washing with PBS, secondary mAb 7-B6-1 was applied at 1 μg/ml concentration for 2 h at room temperature. Plates were washed six times with PBS before application of streptavidine-alkaline phosphatase (1:1000 dilution in PBS, 0,5 % FCS, 100 ml/well) for 1 h at room temperature. Wells were washed seven times with PBS and spots were revealed by incubation for 4 to 10 min until distinct spots emerged with developing buffer (BCIP/NBT, diluted 1:100). Development was stopped by washing the plates with tap water. Plates were evaluated using the automated ELISpot Reader system (AID, Germany) using the same settings throughout the whole study for better comparability of the results. Results are expressed as numbers of spot forming units (SFU) per 10^6 PBMC.

Lymphoproliferation assays

Fresh PBMC were distributed in triplicates (4 x 10^5 cells/well) in 96 well round bottomed plates in 200 ml final volume and incubated for 5 days at 37 °C in a humified atmosphere containing 5 % CO_2. During the last 16 h of incubation, 1 μCi/well of [^{3}H]-Thymidine (Moravek Biochemicals, CA) was present. Antigens tested included the AMA49-C1 (40 μg/ml), UK40 (40 μg/ml) and influenza antigens (40 μg/ml). Data were expressed as stimulation index (SI), calculated as: SI = arithmetic mean experimental count per minutes (cpm) with antigen / arithmetic mean control cpm without antigen. A SI > 2 was regarded as positive response.

Immunogenetic analysis

The HLA-DRB gene expression of the volunteers vaccinated with AMA49-CPE (group 3 and group 5) were analyzed by IMGM Laboratories GmbH (Martinsried, Germany, http://www.imgm.de/hla_typing.php).

In silico analysis

AMA49-C1 peptide sequence was analyzed with the software TEPITOPE that predict promiscuous HLA class II ligands on the basis of virtual matrices (threshold used: 3%) (www.imtech.res.in/raghava/propred/) (11)

Statistical analysis

Linear regression was applied for *ex vivo* IFN-γ ELISpot assay on the SFU/10^6 PBMC and for lymphoproliferation assay on SI values to compare the follow up times (1^{st}, 2^{nd} and 3^{rd} immunizations) with the pre-immunization time for each vaccination group. Random effect was taken into account at individual level in order to consider correlations due to the repeated measurement on the same individual.

Immunofluorescence analysis (IFA), Western blot and ELISA

The procedures have been described elsewhere (Gentom et al. submitted, Mueller at al. submitted)

Results

Cellular immune response to the virosomally formulated peptide-PE conjugate AMA49-CPE

Freshly isolated PBMC of volunteers vaccinated with 50 μg of a virosomal formulation of the peptide-PE conjugate AMA49-CPE either alone (vaccination group 3) or in combination with the CSP-derived peptide-PE conjugate UK39 (group 5) were analyzed three weeks after each of the three immunizations by *ex vivo* IFN-γ ELISpot assay and lymphoproliferation analysis. In both test systems cells were stimulated with the 49-mer peptide, AMA49-C1 (AMA49-CPE without lipid anchor; Table I, Figure 1) or influenza antigens.

In the *ex vivo* IFN-γ ELISpot analysis, the reference baseline in all tested vaccination groups (1-6), i.e. PBMC incubated without any stimulus, was oscillating between 0 and 140 SFU/10^6 with an average of 10 SFU/10^6 PBMC per well. The cut-off frequency was set at 100 SFU/10^6 PBMC with a minimal difference of 75 SFU/10^6 PBMC from the baseline. Based on these criteria, none of the PBMC preparations tested contained a significant number of AMA49-C1 SFU (0 to 75 SFU/10^6 PBMC, Figure 2A). The validity of the ELISpot assay was proven by parallel PBMC stimulation with influenza antigens, where a high frequency of SFUs was observed with all PBMC preparations (ranging from 110 to 1080). The geometric mean frequency of influenza SFUs was already considerably high prior to the first vaccination (>400 SFU/10^6 PBMC) and did not further increase significantly in the course of the vaccinations (Figure 2B).

While none of the 16 PBMC samples taken prior to the first immunization with AMA49-CPE (groups 3 and 5) had a SI > 2 in the lymphoproliferation assay with AMA49-C1, altogether 13 of the 46 post-immunization samples tested yielded a value above this threshold (Table 2). In contrast, only one post-immunization PBMC sample from the 14 volunteers receiving empty virosomes (group 6) or a virosomal formulation of the unrelated peptide-PE conjugate UK39 alone (group 4) showed a AMA49-C1 SI slightly above the threshold (SI = 2.1). While the response rate after the first and after the second AMA49-CPE immunization was comparable (37.5% [6/16] and 40% [6/15], respectively) it had dropped considerably after the third immunization (6.7% [1/15]). Only one volunteers (#41) responded after all three

immunizations, but altogether 50% (8/16) of the volunteers had a positive readout with at least one of the three post-immunization samples (Table 2). These eight volunteers were associated with a diverse spectrum of HLA-DR haplotypes (Table 3).

In the lymphoproliferation assay with influenza antigens the mean SI of PBMC preparations taken prior to the first immunization was 24, with a wide range between 3 and 118. After the first, second and third vaccination no significantly increase of the anti-influenza geometric means (SI = 19, 34 and 33, respectively) was found.

Correlation between the generation of parasite-binding antibodies, AMA49-C1 specific lymphoproliferative response and HLA-DRB1

While all volunteers vaccinated with 50 μg of AMA49-CPE (vaccination groups 3 and 5) developed an anti-AMA49-CPE IgG-response in peptide ELISA (Genton et al. submitted), only some of them (Table 2) developed titers of parasite cross-reactive IgG that were above the detection limit of *P. falciparum* blood stage parasite IFA and Western blotting assays (Müller et al. submitted). Only borderline correlations ($r = 0.34$, $p = 0.059$) between the elicited anti-peptide IgG ELISA titers and the SI values in the AMA49-C1 lymphoproliferation assay after the first and second immunization was observed (Figure 3). However, the four volunteers (#27, #30, #39, #46) who had developed both high (>1000) IFA and Western blotting titers with blood stage parasites were all positive in the AMA49-C1-lymphoproliferation assay (Table 2). Three of them (#30, #39 and #46) had positive values both after the first and after the second immunization, one (#27) only after the second.

Using the TEPITOPE software (http://www.imtech.res.in/raghava/propred)(11), we searched for predicted HLA class-II ligands within the AMA49-C1 peptide sequence. The thirteen best scoring epitope/HLA-DR allele combinations are listed in Table 4. The only volunteers expressing one of these predicted high affinity binding HLA-DRB1 alleles were volunteers #27, #30 and #46. Strikingly, all three belonged to the group of four volunteers which were both positive in the AMA49-C1 lymphoproliferation assay and in the IFA and Western blotting assays for parasite cross-reactive IgG (Table 2). All three expressed HLA-DRB1*0301 which yielded a high score with the predicted AMA49-C1 derived epitope FISDDKDSL. Of the HLA-DR alleles expressed by the fourth volunteer (#39) of the lymphoproliferation and IFA/Western blotting double positive group, the HLA-DRB5*0101/peptide

IERESKRIK combination yielded the best score, when the TEPITOPE analysis was performed at lower stringency.

General lack of correlation between the pre-existing influenza specific T cell response and the vaccination-induced AMA49-C1 specific humoral and cellular immune responses

No correlation between the magnitude of the pre-existing anti-influenza lymphoproliferative response and the elicited AMA49-C1 specific lymphoproliferative responses induced by the first or second immunization was observed (Table 5). Similarly the pre-existing anti-influenza *ex vivo* frequency given in SFU/10^6 PBMC did not show any association with the AMA49-C1 specific lymphoproliferative responses after the second immunization. On the contrary, a negative correlation with the anti-AMA49-C1 SI values after the 1st immunization might indicate some interference of high pre-existing anti-influenza CD4$^+$ T cell frequency (Table 5). A general lack of correlation was observed also between the magnitude of the ELISA anti-peptide (AMA49-CPE) IgG titers after each immunization and the two measured pre-existing anti-influenza cellular compartments (SI, SFU). The only exception was the negative correlation between the anti-influenza pre-existing lymphoproliferation and the anti-AMA49-CPE IgG titers after the second immunization (Table 5). To this concern it has to be mentioned that volunteers #27 and #28 presented extremely high IgG titers after the second immunization (1:102'400) which 'regularized' again after the third immunization (data not shown, Genton et al.).

Discussion

This is the first analysis of the cellular immune response against a synthetic peptides anchored to the surface of IRIVs. The results obtained here with the AMA-1 derived synthetic peptide AMA49-C1 prove the feasibility to elicit a proliferative CD4 T cell response against the synthetic peptide. Generally, the issue of T-cell monitoring during a clinical trial is complex and always requires a multifaceted decision which type of assays to use. Both standardization and validation of the various monitoring tools for cellular responses is insufficient and difficult (12). Enormous limitations are specimen availability since responding specific T-cell subsets may not always be present in peripheral blood compartment (PBC) (13, 14). Only few studies monitored T cell responses in vaccine site draining lymph node (13). In this trial we analyzed fresh isolated human PBMC using lymphoproliferation and *ex vivo* IFN-γ ELISpot assays. The first assay measures the T helper function at the level of the entire cell population, thus requiring prior *in vitro* expansion, the second one measures *ex vivo* T cell IFN-γ functionality at a single cell level. No significant increase in SFU beyond the pre-immune background has been detected for AMA49-C1 *ex vivo* ELISpot, whereas 50% of the volunteers were positive in AMA49-C1 lymphoproliferation after at least one of the three immunizations. The discrepancy between the two assays may be explained by various factors. (i) The two assays measure different T cell subpopulations as suggested by natural immunity analyses in adults from malaria endemic regions. PBMC stimulation with different CSP T cell epitopes gave for all donors different reactivity patterns according to the assay employed (lymphoproliferation, *ex vivo* ELISpot and 14-days cultured ELISpot, respectively). Thus, depending on the assay different protein regions emerged as immunodominant and the peptide reactivity pattern for each donor was unique (15). (ii) Detection limits of *ex vivo* ELISpot technology have been observed with tumor-specific T cells. ELISpot was less sensitive than IFN-γ intracellular flow cytometry in detecting T cells producing low amount of IFN-γ (16, 17). (iii) On the other side, in malaria exposed adults, T cell responses with different liver-stage antigen 1 (LSA-1) and thrombospondin-related adhesive protein (TRAP) peptides were detected with 5-days cultured IFN-γ ELISpot but not with *ex vivo* ELISpot (18). Moreover, the 5-days cultured ELISpot was less sensitive compared to ELISA proposing, in naturally exposed population, low frequency of high IFN-γ producing T cells specific for

malaria epitopes (18). The data we present here suggest that the *in vitro* expansion step of the lymphoproliferation assay increased the frequency of AMA49-C1 specific T cells sufficiently to yield SI ranging from 2 to 4.5 after the 1st and 2nd immunization. A decrease of response after the third inoculation (lymphoproliferative and *ex vivo* ELISpot values) has also been reported after immunization with the recombinant *P. falciparum* $MSP1_{42}$ delivered with AS02A adjuvant (19). This decrease is probably mainly attributable to the limitations of the peripheral blood-sampling compartment. The low frequency of AMA49-C1 specific T cells may be explained by paucity of promiscuous immnuodominant T cell eptitopes. The thirteen predicted best scoring AMA49-C1-epitope/HLA-DR allele combinations comprise only one (DRB1*0301) of the twelve HLA-DR molecules most prevalent throughout the world (11, 20). All three volunteers expressing DRB1*0301 were positive both for AMA49-C1 lymphoproliferation and for parasite cross-reactive IgG in IFA and Western blotting assays. Inclusion of promiscuous CD4 T cell epitopes thus may represent an option to extend the T cell immunogenicity of virosomally formulated peptide vaccines.

In children living in regions endemic for malaria, a malaria vaccine may boost pre-existing anti-malaria T cell responses. More importantly, malaria antigen specific T cells elicited by natural exposure are expected to provide T cell help for vaccine induced B cells upon reinfection. Several lines of evidence indicate that influenza antigen specific immune responses enhance immunogenicity of IRIV-associated peptides. In mice a substantial increase in antibodies responses against IRIV-coupled antigens (diphtheria toxoid, tetanus toxoid, malaria peptides) was observed when pre-immunized with influenza vaccine (2, 21) Furtheremore, influenza antigen CD4 specific T cells enhanced the induction of melanoma peptide specific cytotoxic T lymphocytes (CTLs) *in vitro*. The spike protein hemagglutinin (HA), comprised in the virosomal formulation is described as good CD4 T cell activator (22). Our lymphoproliferation and *ex vivo* ELISpot data reconfirm that healthy adult Caucasian have usually developed a solid anti-influenza T cell response (23-25). When using IRIV for antigen delivery, the influence of pre-existing immunity to the viral components is an important issue, because of possible interference and impairment problems among the different responses. HA-specific CD4+CD25+ T regulatory cells capable of nonspecific bystander suppression have been described *in vitro* (26). A general lack of correlation between the magnitude of the pre-existing influenza

specific T cell response and the vaccination-induced AMA49-C1 specific humoral and cellular immune responses was found indicating that the different responses are not interfering among each other.

Furthermore, we have shown that the combination of influenza virosomes carrying two different malaria-antigen-peptides did not negatively influence the immune response directed against AMA49-C1 peptide, because AMA-C1 lymphoproliferative responders are equally represented in the two considered vaccine formulation groups. Thus, IRIV appear to be a platform for the inclusion of several malaria-antigens in one vaccine-application targeting either the humoral immune response as well as CD4 T cells. The inclusion of CD8 T cell epitopes is possible as well, as IRIV have demonstrated to induce CTLs if the peptide to be loaded onto MHC class I was encapsulated in the lumen of the virosomal particle (27, 28).

vaccine formualtion group	synthetic peptide	synthetic peptide dose	total IRIV amount	vaccine formulation name
group 3	AMA49-CPE	50 µg	10 µg influenza HA 100 µg phospholipids	PEV301
group 4	UK40	50 µg	10 µg influenza HA 100 µg phospholipids	PEV302
group 5	AMA49-CPE & UK40	50 µg	20 µg influenza HA 200 µg phospholipids	PEV301&302
group 6	none	-	10 µg influenza HA 100 µg phospholipids	IRIV

Table 1. *Vaccine formulation groups analysed with IFN-γ ex vivo ELISpot and lymphoproliferation assay*

Vaccine formulation	Volunteers	Lymphoproliferation/SI				Abs specificity/titers	
		0-Pre	1-st	2-nd	3-rd	IFA/3-rd	Western blot/ 3-rd
group 3	21	0.8	0.4	0.3	0.4	-	-
PEV301	24	0.9	0.3	0.1	0.6	-	-
AMA49-CPE 50	26	0.4	0.4	0.4	0.6	-	-
	27	0.1	1.2	**2.4**	0.3	**++**	**++**
	28	0.3	0.4	1.6	1.4	-	**++**
	29	0.3	0.9	**3.6**	0.1	-	-
	30	0.6	**2.0**	**4.0**	0.6	**++**	**++**
	32	0.3	0.2	0.7	0.7	-	**++**
group 5	37	0.4	**4.0**	0.9	0.9	-	-
PEV301&PEV302	38	1.2	0.7	1.6	0.9	-	**++**
AMA49-CPE 50	39	1.2	**4.4**	**2.8**	1.9	**++**	**++**
UK39 50 μg	41	1.5	**4.1**	**2.7**	**2.5**	-	**++**
	43	1.0	**3.6**	*drop out*			
	44	0.9	0.9	1.1	1.3	**+**	-
	45	1.1	0.7	1.7	1.6	**+**	-
	46	0.5	**2.4**	**4.5**	1.3	**++**	**++**

Table 2. *Comparison of AMA49-C1 lymphoproliferative response with anti-parasite antibodies.*

Bold indicates a positive response: for lymphoroliferation assay a stimulation index (SI) > 2; for IFA or Western blot analysis a titer > 100, + 100-1000, ++ >1000. Frame indicates a positive response in all three assays. 0-Pre: pre-immunization blood sample, 1-st: 1st immunization blood sample, 2-nd: 2nd immunization blood sample, 3-rd: 3rd immunization blood sample.

Lymphoproliferation assay were run in triplicate; SI = arithmetic mean cpm of AMA49-C1 stimulated PBMC / arithmetic mean cpm of unstimulated PBMC

Vaccine formulation	Volunteers	HLA-DRB locus			
		HLA-DRB1	HLA-DRB3	HLA-DRB4	HLA-DRB5
group 3	21	*0101/*1301*	*0101	-	-
PEV301	24	*0103/*0701	*0101	-	-
AMA49-CPE	26	*0801/*1101	*0202	-	-
	27	*0101/*0301*	*0101		-
	28	*0701/*1104	*0202	*0103	-
	29	*0801/*1501	*0101	-	-
	30	*0301/*1201	*0101/*0202	-	-
	32	*0101/*1001	-	-	-
group 5	**37**	**0405*/*1101	*0202	*0103	-
PEV301&PEV302	38	*1104/*1501	*0202	*0101	-
AMA49-CPE	**39**	*1302/*1501	*0301	-	**0101*
UK39	**41**	*0404/*1401	*0202	*0103	-
	43	*drop out*	-	-	-
	44	*0701/*1501	*0103	*0101	-
	45	*1501	*0101	-	-
	46	*0301/*1502	*0101	-	*0102

Table 3. *Overview of HLA-DRB typing results of AMA49-CPE vaccinated volunteers*

Dash indicates a negative result. Bold indicates volunteers with a SI > 2 in lymphoproliferation assay. Frame indicates a positive response in the three assays (lymphoproliferation, IFA and Western blot analysis). Underlined indicates the best scoring HLADRB/AMA49-C1 epitopes. Italic indicates the next best scoring HLADRB/AMA49-C1 epitopes obtained with TEPITOPE software
(www.imtech.res.in/raghava/propred/)

HLA DRB1-locus	AMA49-C1 peptide
DRB1_0301	GGCYKDEIKKEIERESKRIKLNDNDDEGNKKIIAPRIFISDDKDSLKCG
DRB1_0305	GGCYKDEIKKEIERESKRIKLNDNDDEGNKKIIAPRIFISDDKDSLKCG
DRB1_0306	GGCYKDEIKKEIERESKRIKLNDNDDEGNKKIIAPRIFISDDKDSLKCG
DRB1_0307	GGCYKDEIKKEIERESKRIKLNDNDDEGNKKIIAPRIFISDDKDSLKCG
DRB1_0308	GGCYKDEIKKEIERESKRIKLNDNDDEGNKKIIAPRIFISDDKDSLKCG
DRB1_0309	GGCYKDEIKKEIERESKRIKLNDNDDEGNKKIIAPRIFISDDKDSLKCG
DRB1_0311	GGCYKDEIKKEIERESKRIKLNDNDDEGNKKIIAPRIFISDDKDSLKCG
DRB1_0410	GGCYKDEIKKEIERESKRIKLNDNDDEGNKKIIAPRIFISDDKDSLKCG
DRB1_0421	GGCYKDEIKKEIERESKRIKLNDNDDEGNKKIIAPRIFISDDKDSLKCG
DRB1_1102	GGCYKDEIKKEIERESKRIKLNDNDDEGNKKIIAPRIFISDDKDSLKCG
DRB1_1107	GGCYKDEIKKEIERESKRIKLNDNDDEGNKKIIAPRIFISDDKDSLKCG

Table 4. In silico results of the AMA49-C1 peptide with the software TEPITOPE using a threshold of 3% (www.imtech.res.in/raghava/propred/). Underlined indicates the predicted T cell epitope nonamers.

pre-existing anti-influenza responses	anti-AMA49 peptide responses	Immunization (anti-peptide responses)	Spearman correlation
Lymphoproliferation/SI	Lymphoproliferation/SI	1-st	r = 0.22 p = 0.40
	(AMA49-C1)	2-nd	r = -0.22 p = 0.44
IFN-γ ex-vivo Elispot/ SFU/10^6 PBMC	Lymphoproliferation/SI	1-st	r = -0.64 p = 0.007
	(AMA49-C1)	2-nd	r = -0.41 p = 0.13
Lymphoproliferation/SI	ELISA/titers	1-st	r = -0.04 p = 0.9
	(AMA49-CPE)	2-nd	r = -0.59 p = 0.02
		3-rd	r = -0.49 p = 0.07
IFN-γ ex-vivo Elispot/ SFU/10^6 PBMC	ELISA/titers	1-st	r = 0.33 p = 0.21
	(AMA49-CPE)	2-nd	r = 0.23 p = 0.4
		3-rd	r = 0.18 p = 0.53

Table 5. *Sperman's correlation between the pre-existing anti-influenza T cell responses and the vaccine induced AMA49-CPE peptide specific immune responses*. Spearman's correlations with an r ranging from 0.3 to 0.6 and a $p < 0.05$ are low to moderate positive; with an $r > 0.6$ and a $p < 0.05$ are positive to strong positive. On the other side, Sperman's correlations with an r ranging from - 0.3 to – 0.6 and a $p < 0.05$ are low to moderate negative; with an $r < - 0.6$ and a $p < 0.05$ are negative to strong negative. Other results than the one just described indicate lack of correlation.

AMA49-CPE

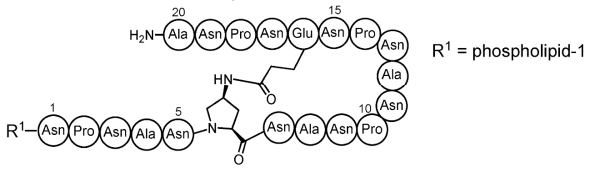

UK39

FIGURE 1. Structures of synthetic peptides discussed in the text.

Synthetic peptides without R1 conjugate (phosphatidylethanolamin, PE): **AMA49-C1 and UK40**

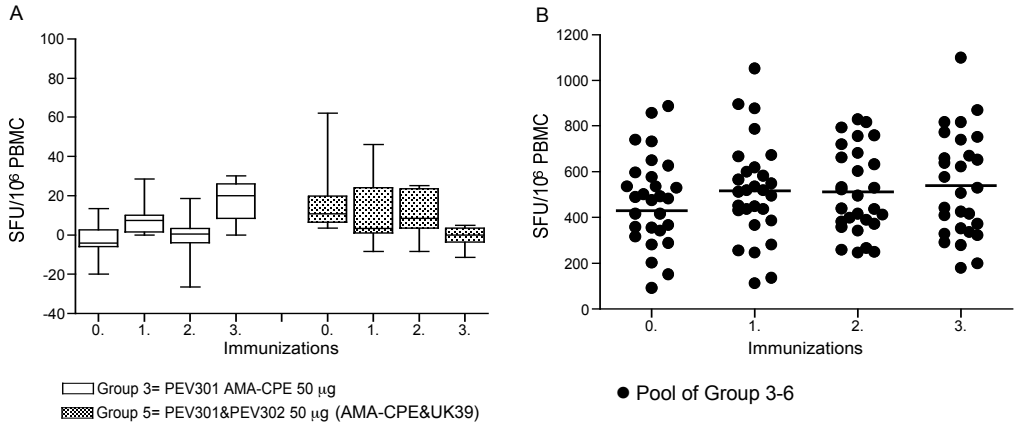

FIGURE 2. Summary of *ex vivo* IFN-γ ELISpot results. All the assays were run in triplicates. A) fresh isolated PBMC of group 3 and group 5 were stimulated for 24 h with AMA49-C1. B) fresh isolated PBMC of group 3-6 were stimulated for 24 h with influenza antigens.
Spot forming unit (SFU) = arithmetic mean of spots of stimulated PBMC – arithmetic mean of spots of unstimulated PBMC. The obtained results were multiplied (x 5) for AMA49-C1 stimulated PBMC (A) and (x 10) for influenza antigen stimulated cells (B) in order to get SFU/10^6 PBMC. The cut-off frequency was set at 100 SFU/10^6 PBMC with a minimal difference of 75 SFU/10^6 from the baseline.

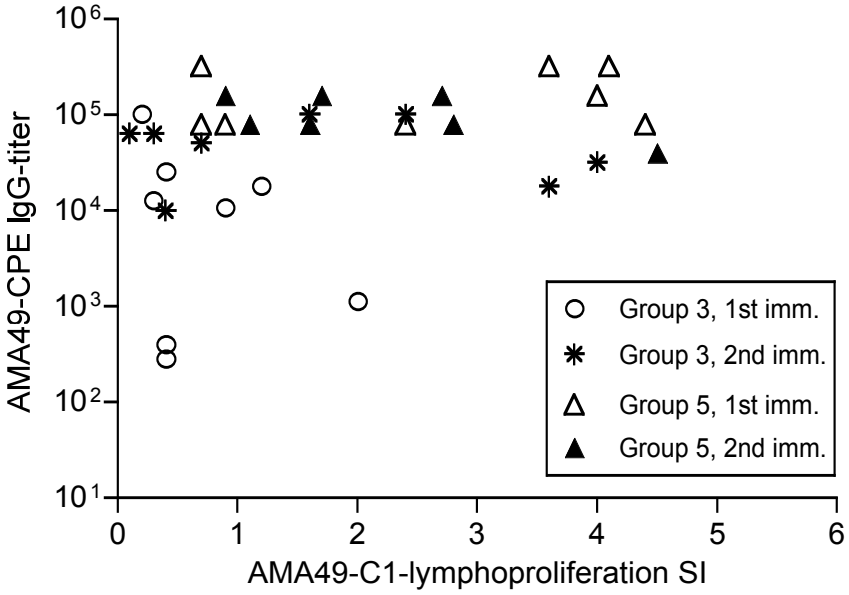

FIGURE 3. Sperman's correlation between AMA-C1 lymphoproliferation SI and AMA-CPE specific antibody titers (r = 0.34, p = 0.059). SI: Stimulation index. Spearman's correlations with an r ranging from 0.3 to 0.6 and a p value of < 0.05 are low to moderate positive; with an r > 0.6 and a p < 0.05 are positive to strong positive

References

1. Aichele, P., K. Brduscha-Riem, R. M. Zinkernagel, H. Hengartner, and H. Pircher. 1995. T cell priming versus T cell tolerance induced by synthetic peptides. *J Exp Med 182:261.*
2. Poltl-Frank, F., R. Zurbriggen, A. Helg, F. Stuart, J. Robinson, R. Gluck, and G. Pluschke. 1999. Use of reconstituted influenza virus virosomes as an immunopotentiating delivery system for a peptide-based vaccine. *Clin Exp Immunol 117:496.*
3. Moreno, R., L. Jiang, K. Moehle, R. Zurbriggen, R. Gluck, J. A. Robinson, and G. Pluschke. 2001. Exploiting conformationally constrained peptidomimetics and an efficient human-compatible delivery system in synthetic vaccine design. *Chembiochem 2:838.*
4. Pfeiffer, B., E. Peduzzi, K. Moehle, R. Zurbriggen, R. Gluck, G. Pluschke, and J. A. Robinson. 2003. A virosome-mimotope approach to synthetic vaccine design and optimization: synthesis, conformation, and immune recognition of a potential malaria-vaccine candidate. *Angew Chem Int Ed Engl 42:2368.*
5. Mueller, M. S., A. Renard, F. Boato, D. Vogel, M. Naegeli, R. Zurbriggen, J. A. Robinson, and G. Pluschke. 2003. Induction of parasite growth-inhibitory antibodies by a virosomal formulation of a peptidomimetic of loop I from domain III of Plasmodium falciparum apical membrane antigen 1. *Infect Immun 71:4749.*
6. Westerfeld, N., and R. Zurbriggen. 2005. Peptides delivered by immunostimulating reconstituted influenza virosomes. *J Pept Sci 11:707.*
7. Bachmann, M. F., R. M. Zinkernagel, and A. Oxenius. 1998. Immune responses in the absence of costimulation: viruses know the trick. *J Immunol 161:5791.*
8. Huckriede, A., L. Bungener, T. Stegmann, T. Daemen, J. Medema, A. M. Palache, and J. Wilschut. 2005. The virosome concept for influenza vaccines. *Vaccine 23 Suppl 1:S26.*
9. Gluck, R., and E. Walti. 2000. Biophysical validation of Epaxal Berna, a hepatitis A vaccine adjuvanted with immunopotentiating reconstituted influenza virosomes (IRIV). *Dev Biol (Basel) 103:189.*
10. Schumacher, R., M. Adamina, R. Zurbriggen, M. Bolli, E. Padovan, P. Zajac, M. Heberer, and G. C. Spagnoli. 2004. Influenza virosomes enhance class I restricted CTL induction through CD4+ T cell activation. *Vaccine 22:714.*
11. Sturniolo, T., E. Bono, J. Ding, L. Raddrizzani, O. Tuereci, U. Sahin, M. Braxenthaler, F. Gallazzi, M. P. Protti, F. Sinigaglia, and J. Hammer. 1999. Generation of tissue-specific and promiscuous HLA ligand databases using DNA microarrays and virtual HLA class II matrices. *Nat Biotechnol 17:555.*
12. Keilholz, U., J. Weber, J. H. Finke, D. I. Gabrilovich, W. M. Kast, M. L. Disis, J. M. Kirkwood, C. Scheibenbogen, J. Schlom, V. C. Maino, H. K. Lyerly, P. P. Lee, W. Storkus, F. Marincola, A. Worobec, and M. B. Atkins. 2002. Immunologic monitoring of cancer vaccine therapy: results of a workshop sponsored by the Society for Biological Therapy. *J Immunother 25:97.*
13. Scheibenbogen, C., A. Letsch, A. Schmittel, A. M. Asemissen, E. Thiel, and U. Keilholz. 2003. Rational peptide-based tumour vaccine development and T cell monitoring. *Semin Cancer Biol 13:423.*

14. Sun, P., R. Schwenk, K. White, J. A. Stoute, J. Cohen, W. R. Ballou, G. Voss, K. E. Kester, D. G. Heppner, and U. Krzych. 2003. Protective immunity induced with malaria vaccine, RTS,S, is linked to Plasmodium falciparum circumsporozoite protein-specific CD4+ and CD8+ T cells producing IFN-gamma. *J Immunol 171:6961.*
15. Flanagan, K. L., E. A. Lee, M. B. Gravenor, W. H. Reece, B. C. Urban, T. Doherty, K. A. Bojang, M. Pinder, A. V. Hill, and M. Plebanski. 2001. Unique T cell effector functions elicited by Plasmodium falciparum epitopes in malaria-exposed Africans tested by three T cell assays. *J Immunol 167:4729.*
16. Kaech, S. M., E. J. Wherry, and R. Ahmed. 2002. Effector and memory T-cell differentiation: implications for vaccine development. *Nat Rev Immunol 2:251.*
17. Scheibenbogen, C., A. Letsch, E. Thiel, A. Schmittel, V. Mailaender, S. Baerwolf, D. Nagorsen, and U. Keilholz. 2002. CD8 T-cell responses to Wilms tumor gene product WT1 and proteinase 3 in patients with acute myeloid leukemia. *Blood 100:2132.*
18. John, C. C., A. M. Moormann, P. O. Sumba, A. V. Ofulla, D. C. Pregibon, and J. W. Kazura. 2004. Gamma interferon responses to Plasmodium falciparum liver-stage antigen 1 and thrombospondin-related adhesive protein and their relationship to age, transmission intensity, and protection against malaria. *Infect Immun 72:5135.*
19. Ockenhouse, C. F., E. Angov, K. E. Kester, C. Diggs, L. Soisson, J. F. Cummings, A. V. Stewart, D. R. Palmer, B. Mahajan, U. Krzych, N. Tornieporth, M. Delchambre, M. Vanhandenhove, O. Ofori-Anyinam, J. Cohen, J. A. Lyon, and D. G. Heppner. 2006. Phase I safety and immunogenicity trial of FMP1/AS02A, a Plasmodium falciparum MSP-1 asexual blood stage vaccine. *Vaccine 24:3009.*
20. Doolan, D. L., S. Southwood, R. Chesnut, E. Appella, E. Gomez, A. Richards, Y. I. Higashimoto, A. Maewal, J. Sidney, R. A. Gramzinski, C. Mason, D. Koech, S. L. Hoffman, and A. Sette. 2000. HLA-DR-promiscuous T cell epitopes from Plasmodium falciparum pre-erythrocytic-stage antigens restricted by multiple HLA class II alleles. *J Immunol 165:1123.*
21. Zurbriggen, R., and R. Gluck. 1999. Immunogenicity of IRIV- versus alum-adjuvanted diphtheria and tetanus toxoid vaccines in influenza primed mice. *Vaccine 17:1301.*
22. Huckriede, A., L. Bungener, T. Daemen, and J. Wilschut. 2003. Influenza virosomes in vaccine development. *Methods Enzymol 373:74.*
23. Dercamp, C., V. Sanchez, J. Barrier, E. Trannoy, and B. Guy. 2002. Depletion of human NK and CD8 cells prior to in vitro H1N1 flu vaccine stimulation increases the number of gamma interferon-secreting cells compared to the initial undepleted population in an ELISPOT assay. *Clin Diagn Lab Immunol 9:230.*
24. Lucas, M., C. L. Day, J. R. Wyer, S. L. Cunliffe, A. Loughry, A. J. McMichael, and P. Klenerman. 2004. Ex vivo phenotype and frequency of influenza virus-specific CD4 memory T cells. *J Virol 78:7284.*
25. Roman, E., E. Miller, A. Harmsen, J. Wiley, U. H. Von Andrian, G. Huston, and S. L. Swain. 2002. CD4 effector T cell subsets in the response to influenza: heterogeneity, migration, and function. *J Exp Med 196:957.*

26. Walker, M. R., B. D. Carson, G. T. Nepom, S. F. Ziegler, and J. H. Buckner. 2005. De novo generation of antigen-specific CD4+CD25+ regulatory T cells from human CD4+CD25- cells. *Proc Natl Acad Sci U S A 102:4103*.
27. Schumacher, R., M. Amacker, D. Neuhaus, R. Rosenthal, C. Groeper, M. Heberer, G. C. Spagnoli, R. Zurbriggen, and M. Adamina. 2005. Efficient induction of tumoricidal cytotoxic T lymphocytes by HLA-A0201 restricted, melanoma associated, L(27)Melan-A/MART-1(26-35) peptide encapsulated into virosomes in vitro. *Vaccine 23:5572*.
28. Amacker, M., O. Engler, A. R. Kammer, S. Vadrucci, D. Oberholzer, A. Cerny, and R. Zurbriggen. 2005. Peptide-loaded chimeric influenza virosomes for efficient in vivo induction of cytotoxic T cells. *Int Immunol 17:695*.

Chapter 3.3

Structural and functional characterization of the Toll like receptor 9 of *Aotus nancymaae*, a non-human primate model for malaria vaccine development

Rolf Spirig[†], Elisabetta Peduzzi[†], Manuel E. Patarroyo*, Gerd Pluschke[†], Claudia A. Daubenberger[†]

[†] Swiss Tropical Institute, Molecular Immunology, CH 4002 Basel, Switzerland
* Fundaciòn Instituto de Immunologia de Colombia, FIDIC, Calle 26 No 50-00, Santa Fe de Bogotà, Bogota, Colombia

This article has been published in:
***Immunogenetics* 2005 Apr; 57: 283-288**

Abstract

In the absence of suitable rodent animal models for *P. falciparum* malaria, efficacy testing of asexual blood-stage vaccine candidates in *Aotus nancymaae* represents a tool to select between different formulations before conducting expensive human clinical trials. CpG oligo-nucleotides (ODN) specifically promote the production of pro-inflammatory and Th1-type cytokines and they enhance immunogenicity of co-administered antigens. Toll like receptor 9 (TLR-9) binds directly and sequence-specifically to single-stranded un-methylated CpG-DNA mediating the biological effects of CpG ODN. We cloned and characterized functionally the TLR-9 cDNA of *A. nancymaae*. The cDNA encompassed 3099 base pairs predicted to code for 1032 amino acid residues. Results of homology searches to human TLR-9 suggested that the receptor is 93 and 94 % identical at the nucleotide and amino acid sequence level, respectively. Stimulation of splenocytes of *A. nancymaae* with CpG ODN resulted in proliferative responses in all animals analyzed. The B cell marker CD20 was up-regulated after incubation of cultures with CpG ODN as assessed in FACS analysis consistent with B cell activation by CpG ODN. The high level of sequence conservation of Aona-TLR-9 reinforces the suitability of *A. nancymaae* as animal model for malaria sub-unit vaccine development.

The development of a safe and effective malaria vaccine remains an urgent medical need for human populations living in malaria-endemic regions (Malaney et al. 2004; Richie and Saul 2002). *A. nancymaae* is one of the few permissive hosts for asexual forms of two major human malaria parasites, *Plasmodium falciparum* and *P. vivax* (Gysin 1998). Immunisation and parasite challenge studies in *A. nancymaae* can rationally support decisions concerning further development of sub-unit malaria vaccines based on distinct antigens, antigen-combinations and antigen delivery systems (Chang et al. 1996). We have carried out immuno-genetic studies to characterize the adaptive immune system of this species in order to define at the molecular level its suitability as an experimental model in asexual blood-stage malaria vaccine development (Daubenberger et al. 2001; Diaz et al. 2000; Diaz et al. 2002; Diaz et al. 2000; Favre et al. 1998; Nino-Vasquez et al. 2000; Vecino et al. 1999).

The vertebrate innate immune system recognizes conserved, pathogen-associated molecular patterns not present in the host, and responds through secretion and activation of a number of effector molecules (Klinman 2004). Recognition of un-methylated CpG di-nucleotides within specific flanking bases has evolved as a pattern recognition mechanism used by the innate immune system to detect DNA of pathogens (Klinman 2004). The central involvement of the Toll like receptor 9 (TLR-9) in responses to un-methylated CpG dinucleotides has been demonstrated using TLR-9-deficient mice (Hemmi et al. 2000) and CpG DNA is bound directly by the TLR-9 in the lysosomal compartment after cellular uptake (Cornelie et al. 2004; Latz et al. 2004). B cells and plasmacytoid dendritic cells are the main human cell types that express TLR-9 and respond directly to CpG ODN stimulation. Human memory B cells constitutively express high levels of TLR-9 and memory B cells proliferate and differentiate to immunoglobulin-secreting cells in response to CpG (Bernasconi et al. 2003). At least three structurally distinct classes of CpG ODNs have been described in primates. K-type CpG ODN induce strong B- and NK-cell activation, D-type ODN provoke high levels of IFN-α secretion by plasmacytoid dendritic cells while C-type ODN combine properties of K- and D-type ODN (Vollmer el. 2004). Examples of K-type include ODN 2006, an ODN with four “TCGT” motifs separated by polyT (Hartmann et al. 2000). K-type ODN rapidly activate CD19+ B cells in the peripheral blood to proliferate and secrete large amounts of IgM, IL-6 and IL-10 (Klinman et al. 2004).

Addition of K-type ODN to vaccines against influenza virus, measles virus, hepatitis B virus surface antigen or tetanus toxoid increased antigen-specific antibody titres in mice by up to three orders of magnitude (Klinman 2004). Optimal immuno-stimulatory CpG DNA motifs differ between mouse and human based on amino acid sequence variations between the extra-cellular regions of human and mouse TLR-9 (Bauer et al. 2001). Therefore, experiments to determine whether a particular CpG ODN may be of therapeutic benefit in humans are initiated in rodents, followed by evaluations in non-human primates finally leading to phase I clinical trials (Cooper et al. 2004; Krieg et al. 2004).

In the current study we analyzed at the molecular and functional level the TLR-9 of *A. nancymaae* (Aona-TLR-9). This study was motivated by the hypothesis that CpG ODN might have suitable adjuvant activity for induction of Th1-mediated immune responses in malaria vaccine development (Jones et al. 1999a). Additionally, a recent report demonstrated that schizont extracts of *P. falciparum* may contain a novel non-CpG ODN ligand binding to human TLR-9 leading to possible novel insights into early events in host-parasite interactions in malaria (Pichyangkul et al. 2004).

The animals analyzed were captured in the Colombian Amazon area close to Leticia and kept at the experimental primate station of the Fundacion Instituto de Immunologia de Colombia (FIDIC). The animals were kept in accordance with recommendations of the Committee on Care and Use of Laboratory Animals, US and the Colombian National Institute of Health guidelines for use of laboratory animals and supervised by the Colombian Wildlife Corporation (CORPOAMAZONIA). Mononuclear cells from three healthy monkeys numbered as 23964, 23967 and 23968 were obtained by splenectomy followed by density gradient separation. Total RNA was isolated from spleen cells of monkey 23968 as described (Daubenberger et al. 2001) using RNAeasy Mini Kit (Qiagen, Germany) according to the manufacturer's protocol. After reverse transcription using Superscript and random hexamer primers, the complete cDNA of TLR9 was amplified in overlapping fragments. The primer sequences used were designed according to human TLR-9 sequence (GenBank accession number NM017442) and are summarized in Table 1. The following temperature profile was employed: 3 min 94 C, and 30 cycles with a profile of 30 sec each at 94 °C, 58 °C and 72 °C. Amplicons were purified using a PCR product purification kit (Roche Molecular Biochemicals) according to manufacturer's protocol

and cloned into the pGEM5 T-vector (Promega, Catalys AG). After isolation of plasmids using the NucleoSpin kit (Macherey-Nagel AG), double stranded plasmid DNA was sequenced and analyzed employing an ABI PRISM 310 genetic analyzer (Perkin Elmer) on both strands. To exclude possible PCR errors, all products were amplified from two independently obtained cDNA and several independent plasmids of each amplification reaction were sequenced.

Phylogenetic analysis

Phylogenetic analysis was performed employing the PHYLIP 3.572 software package available under http://bioweb.pasteur.fr. The phylogenetic tree was constructed according to the neighbour-joining method based on Kimura two-parameter distances estimates (Saitou and Nei 1987).

Oligodeoxynucleotides

The CpG ODN used were designed with a phosphoro-thioate backbone, which confers nuclease resistance on the DNA protecting them from rapid degradation within the cells. The CpG sequences were chosen on the basis of the studies of Hartmann et al (Hartmann et al. 2000a) demonstrating that ODN 2006 (5´-TCGTCGTTTTGTCGTTTTGTCGTT -3´) is an optimal sequence for stimulation of human B cells. Control ODN IMT022 (5´-TGCTGCAAAAGAGCAAAAGAGCAA-3´) has been described (Elias et al. 2003). Desalted phosphoro-thioate oligonucleotides (ODN), HPLC purified, were purchased from Metabion GmbH (Germany). Purity was assessed by HPLC assays. ODN were suspended in HBSS buffer (Sigma) and kept at -20 °C until used.

Lymphocyte proliferation assay

Spleen cells derived from *A. nancymaae* were isolated by Ficoll-Hypaque (Amersham Pharmacia Biotech, Switzerland) density gradient centrifugation and were used after preservation in liquid nitrogen. Cells were cultured in cell culture medium composed of RPMI 1640 supplemented with 10 % heat-inactivated human AB serum (Milan AG, Switzerland), 2mM L-glutamine, 100 U/ml penicillin and 100 mg/ml streptomycin (Sigma). *A. nancymaee* spleen cells (1 x 10^5 cells/well) were stimulated for 72 h with phosphoro-thioate ODN 2006 and control ODN IMT022 at 6 µg/ml in 96-well round bottomed plates (Nunc) or with medium alone. 16 h before harvest,

[^{3}H]thymidine was added (1 μCi/well), the cultures harvested onto glass-fibre filters and the incorporated radioactivity measured by scintillation counting.

FACS analysis of in vitro B cell stimulation

Briefly, spleen cells of *A. nancymaae* were cultivated at 3 x 10^5 cells/ml in cell culture medium in 48-well plates (Nunc) for 96 hours in the presence of medium alone or the ODN 2006 and IMT022. Cells were recovered, resuspended in HBSS buffer containing 1% human serum albumin and 0.01 % NaN_3 (FACS buffer), transferred to FACS tubes and stained for flow cytometry with the B cell specific anti-CD20 mAb B-Ly1 (Daubenberger et al. 2001c). Cells were gated using forward and side scatter parameters for dead cell exclusion. In each sample, 10 000 events were measured and data analyzed using the CellQuest software (BD Biosciences) to determine mean fluorescence intensities.

Results

Using primer pairs designed according to the human TLR-9 sequence (GenBank accession number NM017442), a set of RT-PCR products were obtained which comprised the entire coding sequence of *A. nancymaae* TLR-9 cDNA (Aona-TLR-9). The total length of the Aona-TLR-9 open reading frame (ORF) was 3099 bp coding for a protein of 1032 amino acids. The nucleotide sequences and the amino acid sequences displayed 93 % and 94% identity, respectively, to the human TLR-9 (Figure 1A). A comparison of structural features using the SMART architecture research program (http://www.smart.embl-heidelberg.de) demonstrated that the structure of Aona-TLR-9 is highly conserved to human TLR-9. Eighteen leucine-rich repeats (LRR) were identified by the program, followed by one leucine rich repeat C-terminal domain and the toll - interleukin 1 – resistance domain (TIR) encompassing residues 869 to 1016 (Figure 1A). A single-nucleotide polymorphism of TLR-9 in human populations has been described (Lazarus et al. 2003). One of the allelic variants in humans carried at amino acid position 5 cysteine instead of arginine (R5C). Alignment of human and Aotus TLR-9 amino acid sequences demonstrated the same sequence polymorphism (R5C) between these two species. Phylogenetic analysis confirmed that the amino acid sequences of human and Aona-TLR-9 are closely related clustering together on a separate branch, separated from rodent and carnivora TLR-9 sequences (Figure 1B).

Next we wanted to demonstrate that Aona-TLR9 bind to CpG ODN leading to cell activation. It is well established that K-type CpG ODN induce proliferative responses via TLR-9 binding in B cells (Krieg et al. 1995). Therefore, we measured proliferative responses of splenocytes upon incubation with ODN 2006 and control ODN IMT022. In splenocytes of all three Aotus animals tested, ODN 2006 induced significant proliferative responses. The [^{3}H]thymidine uptake in cultures incubated with control ODN IMT022 was comparable to un-stimulated cultures demonstrating that the effect of ODN 2006 was dependent on a distinct ODN sequence (Figure 2).

In order to confirm that Aotus B cells were activated by CpG ODN 2006, we analyzed changes in CD20 expression level. As demonstrated in Figure 3, incubation of spleen cells with ODN 2006 resulted in increase of mean fluorescence intensity. In cultures incubated with medium or control ODN IMT022, the values ranged between 180 and

141, respectively, while in ODN 2006 treated cultures the mean fluorescence intensity reached 202.

Discussion

Aluminium compounds, the only adjuvant used widely in humans, do not support the development of Th1-type cell-mediated immune responses. Since this arm of the cellular immune response seems to play a central role in protection in a number of infectious diseases including malaria (Gupta 1998) novel approaches to develop vaccine formulations that induce Th1-type and cytotoxic T cell responses are needed.

CpG ODN have potential to be developed as components in novel vaccine formulations (Klinman 2004e). CpG ODN trigger the production of chemokines, Th1-type and pro-inflammatory cytokines (including IFN-γ, IL-6, IL-12, IL-18 and TNF-α) and promote antigen-specific humoral immune responses by acting with B cells (Krieg et al., 1995). TLR-9 molecules expressed by different species have diverged over evolutionary periods and the precise sequence motif optimal for stimulating immune cells from one species frequently differs from those in other species (Bauer et al. 2001a). PBMC from humans, rhesus macaques, chimpanzees and orang utans respond to the same broad classes of CpG ODN while rodents respond poorly to some but not all CpG ODN that are highly active in primates. Thus efforts to determine whether CpG ODN may be of therapeutic benefit are typically initiated in mice and then followed by studies involving non-human primates (Klinman et al. 2004a).

Introduction of double alanine mutations (D535A and Y537A) strongly diminished the CpG-sequence specific DNA binding supporting that the region containing D535 and Y537 is involved in DNA binding (Rutz et al. 2004). These two amino acid residues of functional importance are conserved between all full length TLR-9 sequences available in the GeneBank and also in Aona-TLR-9. The CD20 molecule, also known as Bp35, is expressed from the pre-B to mature B cell stages and while its precise functional role remains unknown, a role in B cell activation, proliferation and differentiation is suggested (Clark et al. 1985). We report here to our knowledge the first time that CD20 is up-regulated upon incubation of B-cells with CpG ODN 2006. Furthermore, the first TLR-9 cDNA sequence of a non-human primate is described here.

Aotus monkeys immunized with a synthetic malaria peptide formulated in CpG ODN 2006 responded with significantly higher antibody levels compared to animals treated with control ODN (Jones et al. 1999b). In summary, these results support the

suitability of Aotus monkeys to analyze CpG ODN as adjuvant compound for subunit based vaccines against *P. falciparum* and *P. vivax*.

```
H. sapiens          MGFCRSALHPLSLLVQAIMLAMTLALGTLPAFLPCELQPHGLVNCNWLFLKSVPHFSMAA
60
A. nancymaae     MGFCCSALHPLSLLVQAMMLAMTLALGTLPAFLPCELQPHGLVNCNWLFLKSVPHFSVAA 60
                 **** ************:****************************************:**
H. sapiens          PRGNVTSLSLSSNRIHHLHDSDFAHLPSLRHLNLKWNCPPVGLSPMHFPCHMTIEPSTFL
120
A. nancymaae        PRGNVTSLSLSSNRIHHLHDSDFAHLPSLRHLDLKWNCPPVGLSPMHFPCHMTIEPNTFL
120
                 *******************************:**********************.***
H. sapiens          AVPTLEELNLSYNNIMTVPALPKSLISLSLSHTNILMLDSASLAGLHALRFLFMDGNCYY
180
A. nancymaae        AVPTLEELNLSYNSITAVPALPKSLVSLTLSRTNILVLDSASLAGLHALRFLFMDGNCYY
180
                 *************.*  :********:**:**:****:***********************
H. sapiens          KNPCRQALEVAPGALLGLGNLTHLSLKYNNLTVVPRNLPSSLEYLLLSYNRIVKLAPEDL
240
A. nancymaae        KNPCRRALEVAPGALLGLGNLTHLSLKYNNLTVVPRNLPSSLEYLLLSYNHIIKLAPGDL
240
                 *****:*********************************************:*:**** **
H. sapiens          ANLTALRVLDVGGNCRRCDHAPNPCMECPRHFPQLHPDTFSHLSRLEGLVLKDSSLSWLN
300
A. nancymaae        ANLTALRVLDVGGNCRRCDHAPNPCMECPRHFPQLHPNTFSHLSRLEGLVLKDSSLSWLN
300
                 ************************************:**********************
H. sapiens          ASWFRGLGNLRVLDLSENFLYKCITKTKAFQGLTQLRKLNLSFNYQKRVSFAHLSLAPSF
360
A. nancymaae        ASWFHGLGNLRVLDLSENFLYECITKTKAFQGLTQLRKLNLSFNYQKRVSFAHLSLAPSF
360
                 ****:****************:************************************
H. sapiens          GSLVALKELDMHGIFFRSLDETTLRPLARLPMLQTLRLQMNFINQAQLGIFRAFPGLRYV
420
A. nancymaae        GSLFSLEELDMHGIFFRSLDETTLRPLARLSRLQTLHLQMNFINQAQLGIFGAFPGLRHV
420
                 **.:*:************************. ****:************** ******:*
H. sapiens          DLSDNRISGASELTATMGEADGGEKVWLQPGDLAPAPVDTPSSEDFRPNCSTLNFTLDLS
480
A. nancymaae        DLSDNRISGASELAATTGEADGGGRVWLQPGDLAPAPVDAPSSEDFTANCSTLNFTLDLS
480
                 *************:** ****** :***************:****** .************
H. sapiens          RNNLVTVQPEMFAQLSHLQCLRLSHNCISQAVNGSQFLPLTGLQVLDLSHNKLDLYHEHS
540
A. nancymaae        RNNLVTVRPEMFARLSHLQCLRLSHNCIMQAVNGSQFLPLTDLRVLDLSHNKLDLYHEHS
540
                 *******:*****:************** ************.*:*****************
H. sapiens          FTELPRLEALDLSYNSQPFGMQGVGHNFSFVAHLRTLRHLSLAHNNIHSQVSQQLCSTSL
600
A. nancymaae        FTELPRLEALDLSYNSQPFGMQGVGHNFSFVAHLRTLRYLSLAHNNIHSRVSPQLRSTSL
600
                 ************************************:**********:** ** ****
```

Fig. 1 a Amino acid sequence comparison of TLR-9 of *A. nancymaae* and *H. sapiens* using the ClustalW program available under http://www.ebi.ac.uk/clustalw/.

Symbols "*","**:**" and "**.**" indicate identical, conserved and semi-conserved amino acid residues, respectively. Both sequences were analyzed for its domain structure using the SMART program available under http://smart.embl-heidelberg.de/. The predicted signal sequence is given in italics, the leucine-rich repeat region (LRR) is underlined and the boxed sequences indicate the Toll – IL-1 - resistance domain (TIR).

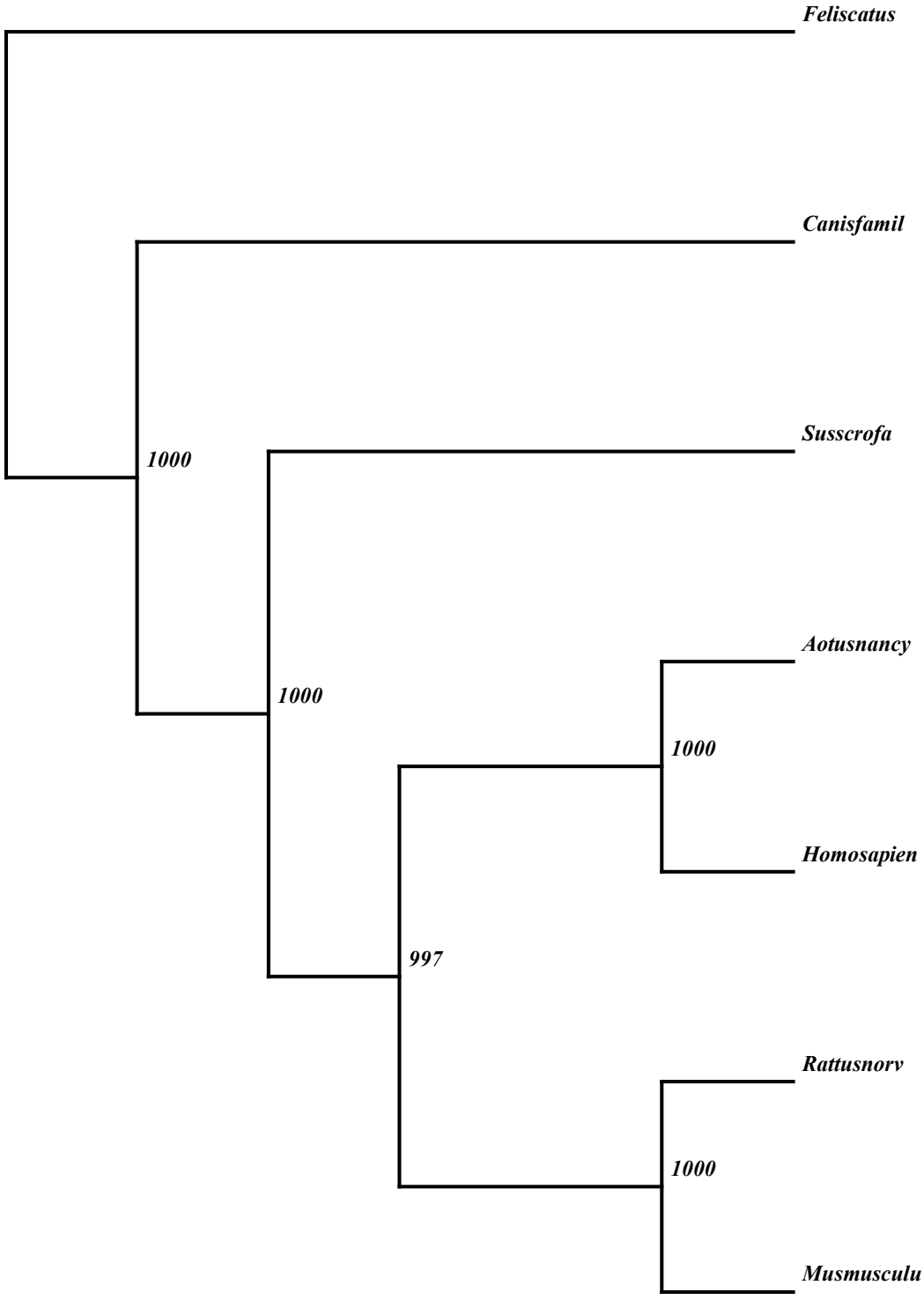

Fig. 1 b Unrooted phylogenetic tree established from deduced TLR-9 amino acid sequences of *Canis familiaris* (NP_001002998), *Sus scrofa* (NP_999123), *Rattus norvegicus* (NP_937764), *Homo sapiens* (NP_059138), *Felis catus* (AAN15751), *Mus musculus* (NP_112455) and *A. nancymaae* AY788894 using the neighbor-joining algorithm of the PHYLIP 3.572 program package available at http://bioweb.pasteur.fr. The numbers at the nodes indicate the percentage of recovery of that node in 1,000 bootstrap replications.

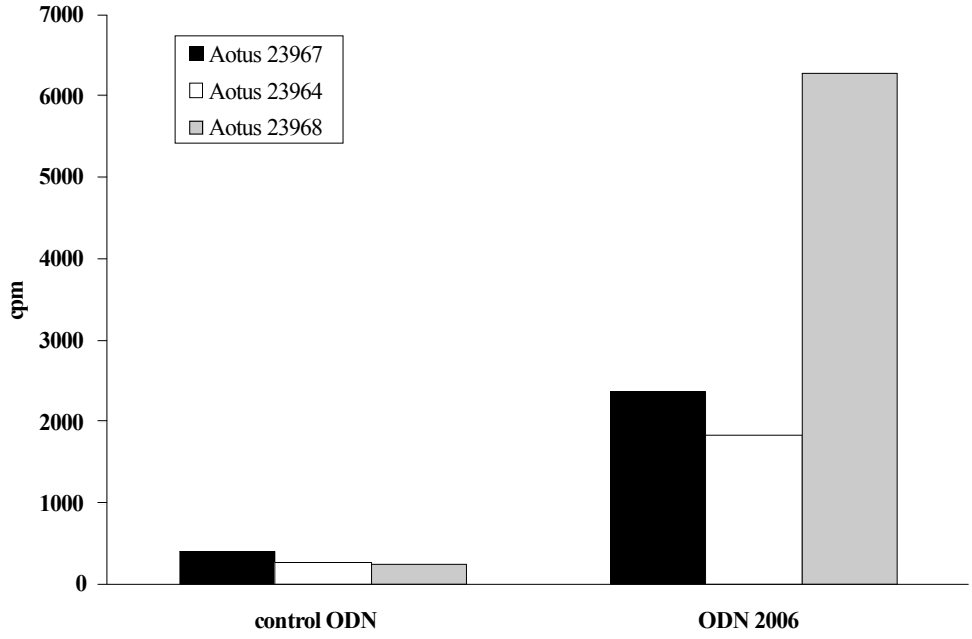

Fig. 2 Stimulation of spleen cells of *A. nancymaae* by ODN. *A. nancymaae* spleen cells were cultured in the presence of 6 μg/ml ODN for 72 h, pulsed during the last 16 h with [^{3}H]-thymidine and incorporated radioactivity was measured. Data represent mean cpm of triplicate cultures of three different animals.

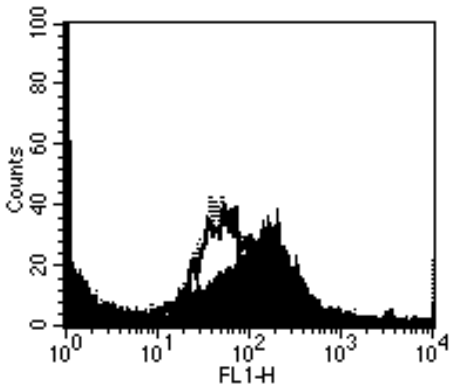

Fig. 3 The B cell marker CD20 is up-regulated upon incubation with CpG ODN 2006. Spleen cells were incubated for 96 h with medium alone (dotted line), CpG ODN IMT022 (black line) and 2006 (filled graph) at 6 μg/ml. Then cells were removed from culture and stained with anti-CD20 mAb and analyzed by FACS analysis.

References

Bauer S, Kirschning CJ, Hacker H, Redecke V, Hausmann S, Akira S, Wagner H, Lipford GB (2001) Human TLR9 confers responsiveness to bacterial DNA via species-specific CpG motif recognition. Proc. Natl. Acad. Sci. U. S. A 98:9237-9242

Bernasconi NL, Onai N, Lanzavecchia A (2003) A role for Toll-like receptors in acquired immunity: up-regulation of TLR9 by BCR triggering in naive B cells and constitutive expression in memory B cells. Blood 101:4500-4504

Chang SP, Case SE, Gosnell WL, Hashimoto A, Kramer KJ, Tam LQ, Hashiro CQ, Nikaido CM, Gibson HL, Lee-Ng CT, Barr PJ, Yokota BT, Hut GS (1996) A recombinant baculovirus 42-kilodalton C-terminal fragment of *Plasmodium falciparum* merozoite surface protein 1 protects Aotus monkeys against malaria. Infect Immun 64:253-261

Clark EA, Shu G, Ledbetter JA (1985) Role of the Bp35 cell surface polypeptide in human B-cell activation. Proc. Natl. Acad. Sci. U. S. A 82:1766-1770

Cooper CL, Davis HL, Morris ML, Efler SM, Krieg AM, Li Y, Laframboise C, Al Adhami MJ, Khaliq Y, Seguin I, Cameron DW (2004) Safety and immunogenicity of CPG 7909 injection as an adjuvant to Fluarix influenza vaccine. Vaccine 22: 3136-3143

Cornelie S, Hoebeke J, Schacht AM, Bertin B, Vicogne J, Capron M, Riveau G (2004) Direct evidence that toll-like receptor 9 (TLR9) functionally binds plasmid DNA by specific cytosine-phosphate-guanine motif recognition. J Biol Chem 279:15124-15129

Daubenberger CA, Salomon M, Vecino W, Hubner B, Troll H, Rodriques R, Patarroyo ME, Pluschke G (2001) Functional and structural similarity of V gamma 9V delta 2 T cells in humans and Aotus monkeys, a primate infection model for *Plasmodium falciparum* malaria. J Immunol. 167:6421-6430

Diaz D, Daubenberger CA, Zalac T, Rodriguez R, Patarroyo ME (2002) Sequence and expression of MHC-DPB1 molecules of the New World monkey *Aotus nancymaae*, a primate model for *Plasmodium falciparum*. Immunogenetics 54:251-259

Diaz D, Naegeli M, Rodriguez R, Nino-Vasquez JJ, Moreno A, Patarroyo ME, Pluschke G, Daubenberger CA (2000) Sequence and diversity of MHC DQA and DQB genes of the owl monkey *Aotus nancymaae*. Immunogenetics 51:528-537

Diaz OL, Daubenberger CA, Rodriguez R, Naegeli M, Moreno A, Patarroyo ME, Pluschke G (2000) Immunoglobulin kappa light-chain V, J, and C gene sequences of the owl monkey *Aotus nancymaae*. Immunogenetics 51:212-218

Elias F, Flo J, Lopez RA, Zorzopulos J, Montaner A, Rodriguez JM (2003) Strong cytosine-guanosine-independent immunostimulation in humans and other primates by synthetic oligodeoxynucleotides with PyNTTTTGT motifs. J Immunol. 171:3697-3704

Favre N, Daubenberger C, Marfurt J, Moreno A, Patarroyo M, Pluschke G (1998) Sequence and diversity of T-cell receptor alpha V, J, and C genes of the owl monkey Aotus nancymaae. Immunogenetics 48:253-259

Gupta RK (1998) Aluminum compounds as vaccine adjuvants. Adv. Drug Deliv. Rev. 32:155-172

Gysin J (1998) Animal models: primates. In: Sherman IW (ed) ASM Press, Washington DC, pp 419-439

Hartmann G, Weeratna RD, Ballas ZK, Payette P, Blackwell S, Suparto I, Rasmussen WL, Waldschmidt M, Sajuthi D, Purcell RH, Davis HL, Krieg AM (2000) Delineation of a CpG phosphorothioate oligodeoxynucleotide for activating primate immune responses in vitro and in vivo. J Immunol. 164:1617-1624

Hemmi H, Takeuchi O, Kawai T, Kaisho T, Sato S, Sanjo H, Matsumoto M, Hoshino K, Wagner H, Takeda K, Akira S (2000) A Toll-like receptor recognizes bacterial DNA. Nature 408:740-745

Jones TR, Obaldia N, III, Gramzinski RA, Charoenvit Y, Kolodny N, Kitov S, Davis HL, Krieg AM, Hoffman SL (1999) Synthetic oligodeoxynucleotides containing CpG motifs enhance immunogenicity of a peptide malaria vaccine in Aotus monkeys. Vaccine 17:3065-3071

Klinman DM (2004) Immunotherapeutic uses of CpG oligodeoxynucleotides. Nat. Rev. Immunol. 4:249-258

Krieg AM, Yi AK, Matson S, Waldschmidt TJ, Bishop GA, Teasdale R, Koretzky GA, Klinman DM (1995) CpG motifs in bacterial DNA trigger direct B-cell activation. Nature 374:546-549

Krieg AM, Efler SM, Wittpoth M, Al Adhami MJ, Davis HL (2004) Induction of systemic TH1-like immunity in normal volunteers following subcutaneous but not intravenous administration of CPG 7909, a synthetic B-class CpG oligonucleotide TLR9 agonist. J. Immunother. 27:460-471.

Latz E, Schoenemeyer A, Visintin A, Fitzgerald KA, Monks BG, Knetter CF, Lien E, Nilsen NJ, Espevik T, Golenbock DT (2004) TLR9 signals after translocating from the ER to CpG DNA in the lysosome. Nat. Immunol. 5:190-8

Lazarus R, Klimecki WT, Raby BA, Vercelli D, Palmer LJ, Kwiatkowski DJ, Silverman EK, Martinez F, Weiss ST (2003) Single-nucleotide polymorphisms in the Toll-like receptor 9 gene (TLR9): frequencies, pairwise linkage disequilibrium, and haplotypes in three U.S. ethnic groups and exploratory case-control disease association studies. Genomics 81:85-91

Malaney P, Spielman A, Sachs J (2004) The malaria gap. Am. J Trop. Med. Hyg. 71:141-146

Nino-Vasquez JJ, Vogel D, Rodriguez R, Moreno A, Patarroyo ME, Pluschke G, Daubenberger CA (2000) Sequence and diversity of DRB genes of *Aotus nancymaae*, a primate model for human malaria parasites. Immunogenetics 51:219-230

Pichyangkul S, Yongvanitchit K, Kum-arb U, Hemmi H, Akira S, Krieg AM, Heppner DG, Stewart VA, Hasegawa H, Looareesuwan S, Shanks GD, Miller RS (2004) Malaria blood stage parasites activate human plasmacytoid dendritic cells and murine dendritic cells through a Toll-like receptor 9-dependent pathway. J Immunol. 172:4926-4933

Richie TL, Saul A (2002) Progress and challenges for malaria vaccines. Nature 415:694-701

Rutz M, Metzger J, Gellert T, Luppa P, Lipford GB, Wagner H, Bauer S (2004) Toll-like receptor 9 binds single-stranded CpG-DNA in a sequence- and pH-dependent manner. Eur. J Immunol. 34:2541-50

Saitou N, Nei M (1987) The neighbor-joining method: a new method for reconstructing phylogenetic trees. Mol. Biol Evol. 4:406-425

Vecino W, Daubenberger C, Rodriguez R, Moreno A, Patarroyo M, Pluschke G (1999) Sequence and diversity of T-cell receptor beta-chain V and J genes of the owl monkey *Aotus nancymaae*. Immunogenetics 49:792-799

Chapter 4

Mycobacterium ulcerans infection (Buruli ulcer)

Chapter 4.1

Systemic suppression of interferon-gamma responses in Buruli ulcer patients resolves after surgical excision of the lesions caused by the extracellular pathogen *Mycobacterium ulcerans*

Dorothy Yeboah-Manu *,†, Elisabetta Peduzzi †, Ernestina Mensah-Quainoo ‡, Gerd Pluschke †, Claudia A. Daubenberger †

* Noguchi Memorial Institute for Medical Research, University of Ghana, Legon

† Swiss Tropical Institute, Molecular Immunology, CH 4002 Basel, Switzerland

‡ Ghana Health Service, Amasaman, Ga District, Ghana

This article has been published in:

Journal of Leukocyte biology **2006 Jun; 79(6): 1150-6**

Abstract

Buruli ulcer (BU), caused by *Mycobacterium ulcerans*, is the third most common mycobacterial infection in immuno-competent humans besides tuberculosis and leprosy. We have compared by *ex vivo* ELISpot analysis interferon-gamma (IFN-γ) responses in peripheral blood mononuclear cells (PBMC) from BU patients, household contacts and individuals living in an adjacent *M. ulcerans* non-endemic region. PBMC were stimulated with PPD and non-mycobacterial antigens like reconstituted influenza virus particles and isopentenyl-pyrophosphate. With all three antigens the number of IFN-γ spot forming units was significantly reduced in BU patients compared to the controls from a non-endemic area. This demonstrates for the first time that *M. ulcerans* infection-associated systemic reduction in IFN-γ responses is not confined to stimulation with live or dead mycobacteria and their products, but extends to other antigens. IL-12 secretion by PPD stimulated PBMC was not reduced in BU patients, indicating that reduction in IFN-γ responses was not caused by diminished IL-12 production. Several months after surgical excision of BU lesions, IFN-γ responses of BU patients against all antigens used for stimulation recovered significantly, indicating that the measured systemic immuno-suppression was not the consequence of a genetic defect in T cell function predisposing for BU but is rather related to the presence of *M. ulcerans* bacteria.

Introduction

BU caused by *M. ulcerans* is an infectious disease characterized by chronic, necrotizing ulceration of subcutaneous tissues and the overlying skin. The disease starts as a subcutaneous nodule, papule or plaque that eventually ulcerates and progresses over weeks to months until surgical excision or spontaneous healing occurs [1]. After tuberculosis and leprosy BU is the third most common mycobacterial infection in immuno-competent humans [2]. The main burden of disease falls on children living in sub-Saharan Africa but healthy people of all ages, races and socio-economic class are susceptible [3]. The effectiveness of anti-mycobacterial drug therapy has not been proven [3]. Consequently, surgery is presently the recommended treatment option [4]. In BU lesions clumps of extra-cellular acid-fast organisms surrounded by areas of necrosis are found particularly in subcutaneous fat tissue [5]. *M. ulcerans* produces a family of macrolide toxin molecules, the mycolactones, which are associated with tissue destruction and local immunosuppression [6]. In cell culture experiments mycolactones produce apoptosis and necrosis in many human cell types [7;8]. The toxin appears to play a role in inhibiting the recruitment of inflammatory cells to the site of infection, which explains at least in part why inflammatory responses are poor in BU lesions [5]. However, intra-lesional influx of leukocytes and granulomatous responses in the dermis and panniculus has been reported in late stages of the disease [9;10]. Spontaneous healing can occur and is often accompanied by a conversion of the Burulin (*M. ulcerans* sonicate) skin test from negative to positive. However, the immune mechanisms involved in protection against BU are largely unknown.

The importance of IFN-γ for immunity against mycobacterial infections in humans is demonstrated by the increased susceptibility of children carrying complete IFN-γR1 chain deficiency to environmental mycobacterial infection [11]. Apart from $CD4^+$ T cells, γδ T cells, natural killer cells and $CD8^+$ T cells are potent sources of IFN-γ. CD4 T cells can be differentiated into Th1 and Th2, distinguished by their patterns of cytokine production after antigen activation. Apart from other cytokines, Th1 cells preferentially secrete IFN-γ, while Th2 cells preferentially secrete IL-4 and IL-5. Th1 or Th2 development is determined by the cytokine environment during T cell activation in the primary response to antigen with IL-12 and IFN-γ implicated in the decision to adopt a Th1 phenotype [12]. IFN-γ binds to the IFN-γR1/IFN-γR2 receptor

complex and stimulates innate cell-mediated immunity through NK cells and activation of bactericidal mechanisms in macrophages. The central role of IFN-γ in MHC class I and class II restricted antigen processing and presentation is well documented [13]. At present, the contribution of IFN-γ in immunity to extra-cellular *M. ulcerans* remains to be established.

Peripheral blood mononuclear cells (PBMC) of BU patients with active disease showed significantly reduced lympho-proliferation and IFN-γ secretion in response to stimulation with live or killed preparations of *M. bovis*, *M. ulcerans*, *M. tuberculosis* and the recombinant protein Ag85 of *M. tuberculosis* [14-18]. Here we have determined in a cross-sectional study the frequency of IFN-γ secreting cells in PBMC from BU patients, their household contacts and controls from BU non-endemic areas by *ex vivo* ELISpot analysis. The antigens used for stimulation included isopentenyl-pyrophosphate (IPP), reconstituted influenza virus particles (virosomes) and tuberculin purified protein derivative (PPD) of *M. tuberculosis*, which stimulate distinct T cell subsets, like Vγ2Vδ2 T cells [19], CD4 T cells [20], CD4 and Vγ2Vδ2 T cells [21], respectively. Results demonstrate that BU associated reductions in IFN-γ responses are not confined to stimulation with live or dead mycobacteria and mycobacterial antigens. Furthermore, it is shown for the first time that in individual BU patients this suppression in IFN-γ secretion improved in a time interval of 5 to 10 months.

Materials and Methods

Study population

Thirteen BU patients, 19 clinically healthy household contacts that never had clinical BU and 18 healthy persons living in a *M. ulcerans* non-endemic districts in the Greater Accra region of Ghana were enrolled for the study (Table I). All BU patients enrolled were residents of the BU-endemic Ga District and presented with pre-ulcerative or ulcerative lesions at the Amasaman Health Centre. Informed consent was obtained from study participants or their parents or guardians before enrollment. For ethical reasons, the age range of the non-exposed controls that were included into the analysis was higher than that of the BU patients. Ethical approval for the study was obtained from the local ethical review board of the Noguchi Memorial Institute for Medical Research, University of Ghana, Legon. Clinical diagnosis of BU was reconfirmed as described [22;23] by one or more laboratory verification tests (Table II) including culture of *M. ulcerans*, microscopic detection of Acid Fast Bacilli (AFB) or IS*2404* PCR. The clinical pictures of the patients ranged from nodules or plaques to severe ulcerative forms (Table II). In the BU group nine persons and in the other two groups each 10 persons with a BCG scar were recruited (Table I). PBMC were isolated from venous peripheral blood using Ficoll-Hypaque gradient centrifugation following standard procedures and cryo-preserved prior to the analysis.

Antigens

After thawing PBMC were directly stimulated with 50 μM isopentenyl pyrophosphate (IPP; Sigma), 10 μg/ml tuberculin purified protein derivative of *M. tuberculosis* (PPD; Statens Seruminstitut, Denmark), 10 μg/ml PHA (Sigma) or 20 μg/ml reconstituted influenza virus particles (IRIV, Berna Biotech). These influenza virosomes are spherical uni-lamellar vesicles prepared by detergent removal from influenza surface glycoproteins and mixtures of natural and synthetic phospholipids containing H1N1 from influenza virus strain A/Singapore/6/86 [24]. Cell culture medium consisted of RPMI 1640, 10 % heat inactivated human AB serum, 2 mM glutamine, 100 U/ml penicillin, 100 □g/ml streptomycin (Gibco-BRL).

Ex vivo IFN-γ ELISpot analysis

PBMC were thawed, washed and suspended at a concentration of 2 x 10^6 cells/ml in complete cell culture medium. The cells were then stimulated with the different antigens at the final concentrations indicated above and incubated for 24 h at 37°C, 5 % CO_2 humidified atmosphere. A 96-well nitrocellulose-bottomed plate (Millipore) was coated overnight at 4°C with 10 µg/ml anti-human-IFN-γ primary antibody (clone1-D1K; Mabtech, Sweden). The plates were then washed five times with PBS and blocked with cell culture medium for 1 h at room temperature. The medium was decanted and pre-incubated cells (2 x 10^5 or 1 x 10^5) were added to each well in triplicate and incubated at 37 °C for another 20 h. Assays were terminated by washing plates three times with PBS-Tween 80 (0.05 %) followed by PBS another three times. Secondary antibody (biotin-labeled anti-human-IFN-γ; clone 7-B6-1) was added to each well at 1 µg/ml and the plate incubated for 2 h at RT. Plates were washed again six times with PBS before application of streptavidine-alkaline phosphatase (1 : 1000 dilution in PBS, 0,5 % FCS, 100 □l/well) for 1 h at RT. After washing wells seven times with PBS, distinct spots were developed by the incubation of plates at RT for 4 to 10 min following the addition of the developing buffer (BCIP/NBT, diluted 1 : 100, Bio-Rad). Spot development was stopped by washing the plates extensively with water and left to dry. Plates were later evaluated using the ELISpot Reader system (AID, Germany) to determine the number of spot forming units (SFU).

ELISA quantification of IL-12 in cell culture supernatants

Levels of total IL-12 in culture supernatant of PBMC incubated with PHA (10 µg/ml) and PPD (10 µg/ml) for 96 h were determined by ELISA employing a commercial kit (Mabtech, Sweden). Samples were analyzed in triplicates and results expressed as the average of the three readings in an ELISA reader at 450 nm with reference to curves generated using serially diluted recombinant human IL-12. The sensitivity of the assay was 30 pg/ml for total IL-12.

Statistical analysis

Data were analyzed using the STATA program (Stata Corporation). Comparisons among the paired samples were performed using the Wilcoxon signed-rank test whilst the Wilcoxon rank-sum test was used to analyze the significance of observed difference in IL-12 secretion between patients and un-exposed controls. For comparing the frequencies of antigen specific IFN-γ secreting cells, the data was transformed to normality using Box-Cox transformation before analyzed by linear regression. Data were considered statistically significant when $P< 0.05$.

Results

Frequency reduction of IFN-γ secreting spot forming units in PBMC from BU patients

Thirteen patients with laboratory-reconfirmed *M. ulcerans* infection, nineteen clinically healthy household contacts and eighteen individuals from a neighboring BU non-endemic area were enrolled for this study (Table I and Table II). The frequency of immediate IFN-γ secreting cells in PBMC upon stimulation with IPP, IRIV and PPD was analyzed using an *ex vivo* ELISpot assay. Fig. 1 shows that the mean of SFU upon stimulation with PPD, IPP and IRIV was significantly lower ($p=0.0086$, $p=0.001$ and $p=0.0002$, respectively) in BU patients compared to non-exposed controls. In household contacts, the mean of SFU after IPP and IRIV stimulation was significantly higher compared to BU patients ($p=0.005$ and $p=0.001$, respectively) while in PPD stimulated cultures no significant difference was observed ($p=0.82$).

Recovery from systemic immuno-suppression after surgical treatment

All patients enrolled for the study were treated by wide surgical excision of the BU lesions. Blood samples were collected several months after the first sampling (Table 2) and PBMC from both time points were analyzed in parallel using the same IFN-γ ELISpot assay as above. A 3.9, 3.7 and 3.6 fold median increase in cellular responses against IPP, IRIV and PPD stimulation, respectively, was observed when PBMC taken at the two time points were compared (Fig. 2A). Statistical analysis confirmed this increase of responses as highly significant with p-values of 0.021 and 0.003, respectively, after IPP and IRIV stimulation. PHA stimulated control wells showed only a slight (1.7 fold) median increase between the two different time points analyzed ($p=0.17$) and in PPD stimulated cultures the boost was not significant ($p=0.09$). One representative example of an ELISpot analysis is shown in Fig. 2B with the numbers of SFU detectable after IPP, IRIV and PPD stimulation rising between 1st and 2nd sampling. In contrast, medium and PHA control wells remained at a comparable level between the two analyses.

IL-12 production in PPD stimulated PBMC is not affected in BU patients

Next we wanted to determine whether the systemic suppression of IFN-γ responses in BU patients is related to a diminished capacity to secrete IL-12. PBMC of nine patients and ten persons from BU non-endemic areas were stimulated with PHA or PPD and the total IL-12 concentration in cell culture supernatants was measured by ELISA (Fig. 3). Interestingly, the IL-12 concentrations in PPD stimulated PBMC of individuals living in *M. ulcerans* non-endemic regions were statistically lower compared to BU patients ($p=0.011$) while in PHA stimulated cultures no significant difference was observed ($p=0.57$) (Fig. 3). The mean IL-12 concentrations in supernatants of PPD and PHA stimulated cultures of PBMC obtained before or after surgical treatment showed no difference (Fig. 3).

Discussion

An *ex vivo* ELISpot assay for detection of IFN-γ secretion permitting the direct detection of individual antigen-specific T cells at low frequencies was employed in the current study [25]. The 48 h antigen challenge of PBMC suffices to engage cytokine production in the memory/effector T lymphocyte but not in naïve T cells and allows determination of frequencies and cytokine signatures of re-circulating antigen-specific T cells [25]. The frequencies of systemic IFN-γ producing SFU after stimulation with IPP, IRIV or PPD was significantly reduced in BU patients compared to individuals living in a neighboring BU non-endemic area. This result is consistent with other reports demonstrating that PBMC from subjects with past or current *M. ulcerans* disease had reduced IFN-γ production in response to PPD of *M. tuberculosis* and *M. bovis* or whole killed *M. bovis* BCG or *M. ulcerans* [14-18]. However, our data strongly indicate that reduced IFN-γ production is not confined to immune responses specific for mycobacterial antigens or whole mycobacteria but extends to CD4 T cell responses specific for influenza virus [20] and Vγ2Vδ2 T cells [19].

Reduced IFN-γ production in BU patients could be the consequence of a genetic abnormality in T cell function predisposing for mycobacterial infections [11]. Therefore, we analyzed PBMC of BU patients sampled at two consecutive time points. When the paired PBMC samples were analyzed in parallel by ELISpot analysis, the numbers of IFN-γ secreting cells after IPP, IRIV and PPD stimulation increased significantly after surgical treatment. Comparable numbers of SFU in PHA stimulated PBMC in paired samples excluded a general suppression of cellular immune responses in BU and variations in quality of PBMC sample cryo-preservation. To our knowledge, this is the first report demonstrating that antigen-specific IFN-γ production in BU patients is coming back to normal levels after surgical treatment. Hence, confounding genetic defects do not seem to be responsible for the observed immuno-suppression. The question if IFN-γ production in patients undergoing spontaneous healing of BU will also improve over time is not addressed here.

IL-12 induces T and NK cells to produce several cytokines, including IFN-γ [26]. Total IL-12 concentrations in culture supernatants of PPD stimulated PBMC were statistically higher in BU patients (treated and untreated) than in the controls. This

may reflect a compensatory mechanism of the immune system to restore IFN-γ production and indicates that the observed reduction in systemic IFN-γ responses is not caused by diminished IL-12 production. Different cytokine expression profiles in both PBMC and skin lesions were described in patients suffering from the nodular and ulcerative forms of BU. Nodules were associated with higher IFN-γ and lower IL-10 production and BU with lower IFN-γ and higher IL-10 production [17]. Within the limited number of BU patients enrolled in our study, a relationship between different stages of BU disease and reduction of IFN-γ secretion was not observed.

Vγ2Vδ2 T cells compose the majority of human γδ T cells in circulation and among their defined ligands is IPP, a metabolite found in prokaryotic and eukaryotic cells including mycobacteria [27]. Studies in rhesus monkeys provided evidence that Vγ2Vδ2 T cells contribute to adaptive immune responses in mycobacterial infections [28]. A correlation between the absence or loss of Vγ2Vδ2 T cells and the extent of *M. tuberculosis* disease has been described [29]. An impaired ability of Vγ2Vδ2 T cells to produce cytokines or proliferate in response to phosphorylated microbial metabolites was observed in active *M. tuberculosis* pulmonary disease [30-32]. Interestingly, in 10 out of 13 BU patients analyzed here, the *ex vivo* IFN-γ secretion of IPP-reactive Vγ2Vδ2 T cells increased significantly after surgical treatment.

The diffusible macrolide toxins produced by *M. ulcerans* are considered as virulence factors responsible for pathogenicity of *M. ulcerans* and it has been hypothesized that lack of inflammatory responses in BU lesions are related to local immuno-suppressive activities of the mycolactones [6;33;34]. The treatment-associated reversal of immune suppression may indicate that mycolactones exert apart from local also systemic effects. Alternatively, additional other immune-suppressive mechanisms may be operative in chronic *M. ulcerans* disease. PBMC from healthy contacts of TB patients and TB patients with limited disease produce large quantities of IFN-γ in response to whole mycobacteria, PPD of *M. tuberculosis*, ESAT-6, 16-kDa and 38 kDa proteins [35-39]. In contrast, PBMC of active TB patients with advanced disease produce low quantities of IFN-γ after similar stimulation and following effective drug treatment the IFN-γ secretion improved [39;40]. Possible candidate structures mediating immune suppression in *M. tuberculosis* isolates like phenolic glycolipids have been described [41;42]. In leprosy induction of regulatory or suppressor T cells mediating immune suppression in affected hosts has been proposed [43;44]. Our findings, within their

limits due to the small number of BU patients analyzed and the timing of the blood samples drawn, may indicate that mycolactone-independent immunosuppressive mechanisms common to chronic mycobacterial infections contribute to the reduction of systemic IFN-γ responses in BU patients.

Acknowledgments

We thank Samuel Owusu, Dr. Kwasi Addo, John Tetteh, and Charles Atiogbe from Noguchi Memorial Institute for Medical Research Legon, Ghana; the Buruli ulcer Team nurses at Amasaman Health Centre, Ghana for technical and field support; and all the participants involved in the study for their time. This study was supported in part by the Stanley Thomas Johnson Foundation, the Ghana Government and a stipend from the Amt für Ausbildungsbeiträge of the county Basel-Stadt for D. Yeboah-Manu. We are grateful to Dr. Penelope Vounatsou for support in statistical analysis.

Characteristic	Buruli ulcer patient (n = 13)	Household contacts (n =19)	Controls from non-endemic area (n = 18)
Sex			
Male	5 (39%)	6 (32%)	8 (44%)
Female	8 (61%)	13 (68%)	10 (56%)
Median age (years)	15	15	29.5
Age range (years)	6 - 45	6 - 56	24 - 65
BCG scar present (%) [a]	69	52	55

TABLE 1. Characteristics of BU patients, household contacts and controls from a BU non-endemic area enrolled in the study.

[a] % values calculated for 13 patients, 14 household contacts and 14 controls, respectively. Five household contacts and four non-exposed controls remained with uncertain scar status.

patient	age	gender	clinical form[a]	BCG status[b]	AFB[c]	culture[d]	PCR[e]	1st blood sample [f]	2nd blood sample [f]
P03	45	f	ulcerative	-	+	+	+	3 mo	11 mo
P04	9	f	plaque	+	-	+	+	0	8 mo
P05	10	m	nodule	+	+	+	+	0	8 mo
P08	16	m	ulcerative	-	+	+	+	4 mo	14 mo
P09	5	f	ulcerative	+	+	-	+	3 mo	12 mo
P11	20	f	ulcerative	+	+	+	+	7 d	7 mo
P12	16	m	ulcerative	+	-	-	+	3 mo	12 mo
P13	11	f	ulcerative	-	+	+	+	7 d	7 mo
P14	15	m	plaque	-	-	-	+	7 d	8 mo
P15	7	f	ulcerative	+	+	+	+	0	9 mo
P19	6	m	nodule	+	+	+	+	0	6 mo
P21	17	f	nodule	+	+	-	+	0	5 mo
P22	17	f	nodule	+	+	+	-	0	5 mo

TABLE 2. Clinical data of patients presenting with lesions due to confirmed *M. ulcerans* infection.

[a] clinical forms of BU disease were graded according to the WHO case definition [1].

[b] BCG status was determined by confirmation of the presence of a BCG scar by two persons.

[c] Acid fast bacilli detection was performed by direct smearing of tissue exudates followed by Ziehl-Neelsen staining [1].

[d] Culture of *M. ulcerans* according to [22].

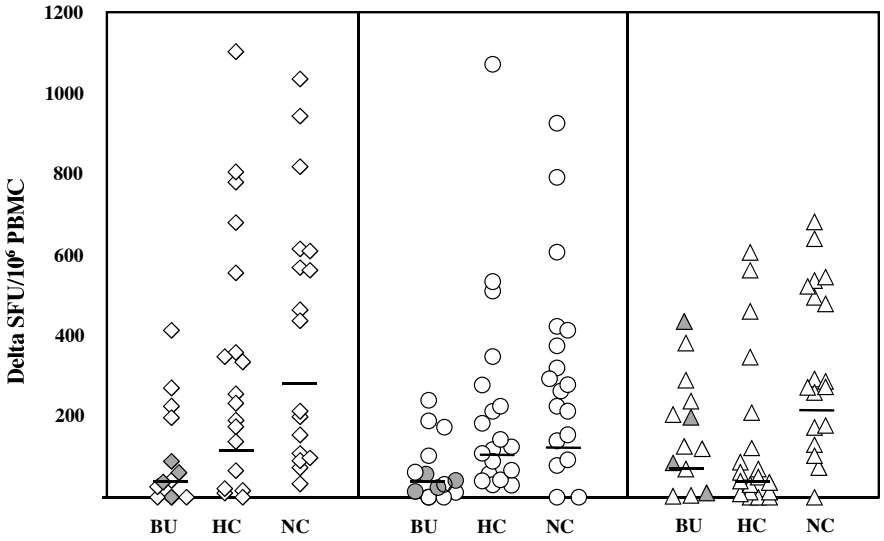

Fig. 1. Quantification of e*x vivo* IFN-γ secreting cells by ELISpot analysis after stimulation of PBMC with IPP (◊), IRIV (○) and PPD (△). PBMC derived from BU patients (BU), household contacts (HC) and controls from a BU non-endemic area (NC) were thawed into cell culture medium and kept overnight in the presence or absence of the different stimuli. For the detection of IFN-γ□ producing cells, 2 x10^5 PBMC/well were plated in triplicate wells and spots were developed after 24 h. Delta SFU = mean of SFU of stimulated triplicate cultures – mean SFU of un-stimulated triplicate cultures. Data from each individual analyzed are shown separately. Mean SFU/10^6 PBMC were 26 (6 – 102), 137 (57 – 327) and 262 (157 – 436) after stimulation with IPP in BU patients, HC and NC, respectively. In IRIV-stimulated cells, the mean SFU/10^6 cells were 22 (7 – 70), 135 (83 – 221), 149 (56 – 394) in BU patients, HC and NC, respectively. After PPD stimulation, 88 (35 – 223), 39 (14 – 106) and 212 (100 – 445) SFU/10^6 PBMC were recorded in BU patients, HC and NC, respectively. The values given in brackets are the 95 % confidence intervals of the geometric means of SFU. Data of patients P03, P08, P09 and P12 are shaded in grey.

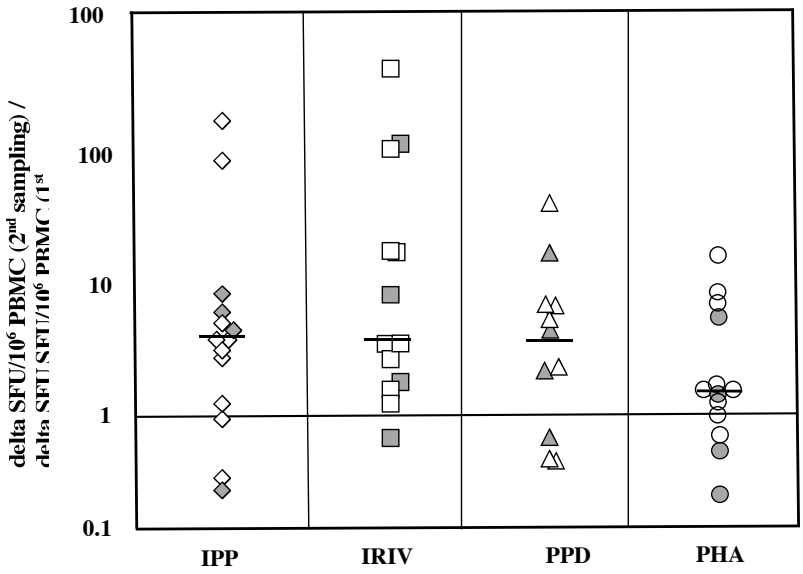

Fig. 2. (A) Frequency increase of antigen-specific *ex vivo* IFN-γ secreting cells in BU patients. PBMC of thirteen BU patients sampled at two time points (Table II) were thawed into cell culture medium and kept overnight in the presence or absence of IPP (◊), IRIV (□), PPD (△) and PHA (○). For the detection of IFN-γ producing cells, 2 x10^5 PBMC/well were plated in triplicate wells and spots were developed after 24 h. Delta SFU were calculated as described in Fig. 1. Given is the ratio of SFU obtained after 2nd sampling / 1st sampling. Data of patients P03, P08, P09 and P12 are shaded in grey.

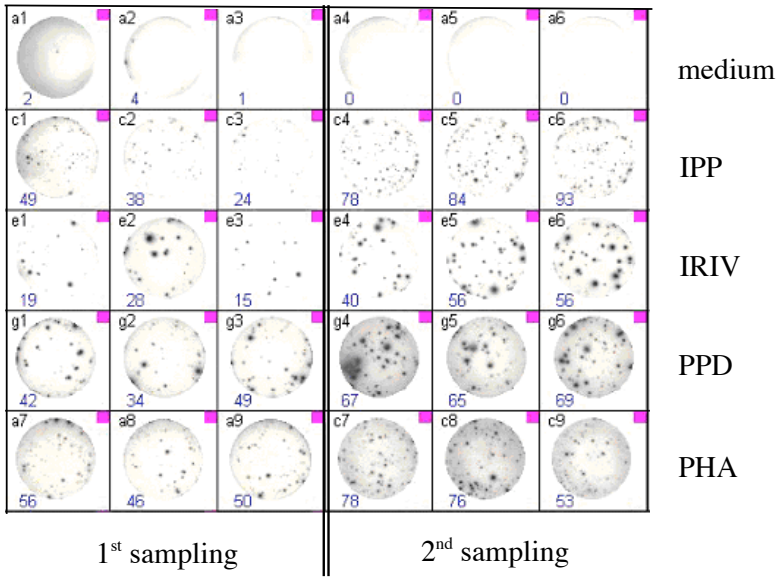

Fig. 2. (B) Representative IFN-γ ELISpot patterns of BU patient P21. PBMC of BU patient P21 were obtained immediately before surgical excision of the BU lesion (1st sampling) and 5 months later (2nd sampling). Parallel analysis of both samples was conducted in triplicates arranged horizontally with 2 x 10^5 cells/well plated. The different stimulators used are given on the right and the numbers of SFU/well are shown on the lower left corner.

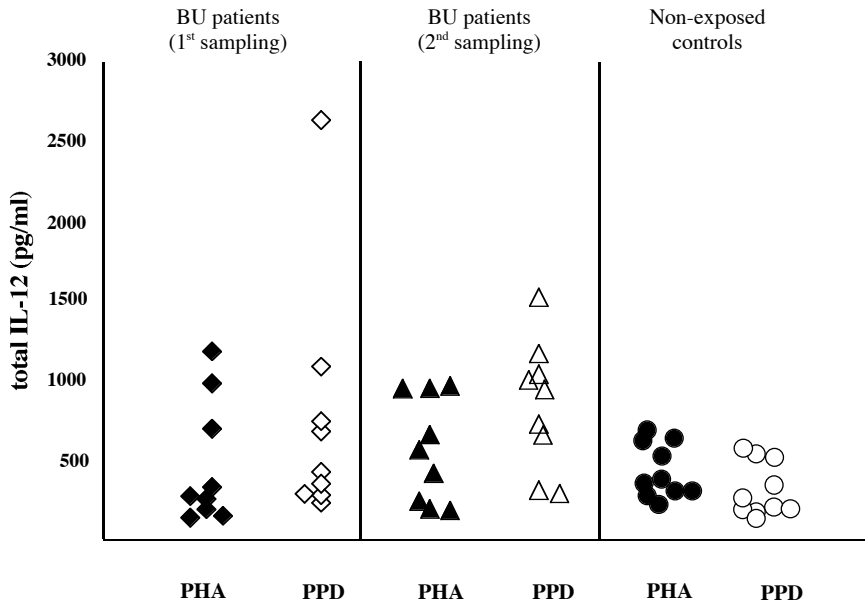

Fig. 3. Total IL-12 concentrations in cell culture supernatants of PHA and PPD stimulated PBMC of nine BU patients obtained at the two different sampling time points (TABLE 2). Mean of total IL-12 concentration (given in pg/ml) in PPD stimulated cultures was 543 and 750 after 1st and 2nd sampling, respectively, and in PHA stimulated cultures 348 and 472, respectively. PBMC of ten individuals living in a neighbouring *M. ulcerans* non-endemic region were treated similarly and the mean total IL-12 concentrations after PPD and PHA stimulation were 276 and 402, respectively.

References

1. Portaels,F., Johnson,P.D., Meyers,W.M. (2001) Buruli ulcer: Diagnosis of *Mycobacterium ulcerans* disease. World Health Organization.
2. Asiedu,K., Scherpbier,R., Raviglione,M. (2000). Buruli ulcer: *Mycobacterium ulcerans* infection. World Health Organisation.
3. Johnson,P.D., Stinear,T., Small,P.L., Pluschke,G., Merrit,R.W., Portaels,F., Huygen,K., Hayman,J.A., Asiedu,K. (2005) Buruli ulcer (*Mycobacterium ulcerans* infection): new insights, new hope for disease control. *PLOSMedicine* **2**, 0282-0286.
4. Buntine,J., Crofts,K. (2001) Buruli ulcer: Management of *Mycobacterium ulcerans* disease. World Health Organization.
5. Hayman,J., McQueen,A. (1985) The pathology of Mycobacterium ulcerans infection. *Pathology* **17**, 594-600.
6. George,K.M., Chatterjee,D., Gunawardana,G., Welty,D., Hayman,J., Lee,R., Small,P.L. (1999) Mycolactone: a polyketide toxin from Mycobacterium ulcerans required for virulence. *Science* **283**, 854-857.
7. George,K.M., Pascopella,L., Welty,D.M., Small,P.L. (2000) A *Mycobacterium ulcerans* toxin, mycolactone, causes apoptosis in guinea pig ulcers and tissue culture cells. *Infect. Immun.* **68**, 877-883.
8. Dobos,K.M., Small,P.L., Deslauriers,M., Quinn,F.D., King,C.H. (2001) *Mycobacterium ulcerans* cytotoxicity in an adipose cell model. Infect. Immun. **69**, 7182-7186.
9. Dodge,O.G. (1964) Mycobacterial skin ulcers in uganda: histopathological and experimental aspects. *J. Pathol. Bacteriol.* **88**, 169-174.
10. Hayman,J. (1993) Out of Africa: observations on the histopathology of *Mycobacterium ulcerans* infection. *J. Clin.Pathol.* **46**, 5-9.
11. van de Vosse,E., Hoeve,M.A., Ottenhoff,T.H. (2004) Human genetics of intracellular infectious diseases: molecular and cellular immunity against mycobacteria and salmonellae. *Lancet Infect. Dis.* **4**, 739-749.
12. Carmen,I. (1999) Th1/Th2 balance in infection. *Springer Seminars in Immunopathology* **21**, 317-338.
13. Boehm,U., Klamp,T., Groot,M., Howard,J.C. (1997) Cellular responses to interferon-gamma. Annu.Rev.Immunol. **15**, 749-795.

14. Gooding,T.M., Johnson,P.D., Smith,M., Kemp,A.S., Robins-Browne,R.M. (2002) Cytokine profiles of patients infected with *Mycobacterium ulcerans* and unaffected household contacts. *Infect. Immun.* **70**, 5562-5567.
15. Gooding,T.M., Johnson,P.D., Campbell,D.E., Hayman,J.A., Hartland,E.L., Kemp,A.S., Robins-Browne,R.M. (2001) Immune response to infection with *Mycobacterium ulcerans*. *Infect. Immun.* **69**, 1704-1707.
16. Gooding,T.M., Kemp,A.S., Robins-Browne,R.M., Smith,M., Johnson,P.D. (2003) Acquired T-helper 1 lymphocyte anergy following infection with *Mycobacterium ulcerans*. *Clin.Infect. Dis.* **36**, 1076-1077.
17. Prevot,G., Bourreau,E., Pascalis,H., Pradinaud,R., Tanghe,A., Huygen,K., Launois,P. (2004) Differential production of systemic and intra-lesional gamma interferon and interleukin-10 in nodular and ulcerative forms of Buruli disease. *Infect. Immun.* **72**, 958-965.
18. Westenbrink,B.D., Stienstra,Y., Huitema,M.G., Thompson,W.A., Klutse,E.O., Ampadu,E.O., Boezen,H.M., Limburg,P.C., Van Der Werf,T.S. (2005) Cytokine responses to stimulation of whole blood from patients with buruli ulcer disease in Ghana. *Clin.Diagn.Lab. Immunol.* **12**, 125-129.
19. Wesch,D., Marx,S., Kabelitz,D. (1997) Comparative analysis of alpha beta and gamma delta T cell activation by *Mycobacterium tuberculosis* and isopentenyl pyrophosphate. *Eur.J. Immunol.* **27**, 952-956.
20. Schumacher,R., Adamina,M., Zurbriggen,R., Bolli,M., Padovan,E., Zajac,P., Heberer,M., Spagnoli,G.C. (2004) Influenza virosomes enhance class I restricted CTL induction through CD4+ T cell activation. *Vaccine* **22**, 714-723.
21. Green,A.E., Lissina,A., Hutchinson,S.L., Hewitt,R.E., Temple,B., James,D., Boulter,J.M., Price,D.A., Sewell,A.K. (2004) Recognition of non-peptide antigens by human V gamma 9V delta 2 T cells requires contact with cells of human origin. *Clin.Exp.Immunol.* **136**, 472-482.
22. Yeboah-Manu,D., Bodmer,T., Mensah-Quainoo,E., Owusu,S., Ofori-Adjei,D., Pluschke,G. (2004) Evaluation of decontamination methods and growth media for primary isolation of *Mycobacterium ulcerans* from surgical specimens. *J. Clin.Microbiol.* **42**, 5875-5876.

23. Noeske,J., Kuaban,C., Rondini,S., Sorlin,P., Ciaffi,L., Mbuagbaw,J., Portaels,F., Pluschke,G. (2004) Buruli ulcer disease in Cameroon rediscovered. *Am.J Trop.Med.Hyg.* **70**, 520-526.
24. Zurbriggen,R., (2003) Immunostimulating reconstituted influenza virosomes. *Vaccine* **21**, 921-924.
25. Letsch,A., Scheibenbogen,C. (2003) Quantification and characterization of specific T-cells by antigen-specific cytokine production using ELISPOT assay or intracellular cytokine staining. *Methods* **31**, 143-149.
26. Trinchieri,G. (2003) Interleukin-12 and the regulation of innate resistance and adaptive immunity. *Nat.Rev.Immunol.* **3**, 133-146.
27. Bonneville,M., Fournie,J.J. (2005) Sensing cell stress and transformation through Vgamma9/Vdelta2 T cell-mediated recognition of the isoprenoid pathway metabolites. *Microbes.Infect.* **7**, 503-509.
28. Shen,Y., Zhou,D., Qiu,L., Lai,X., Simon,M., Shen,L., Kou,Z., Wang,Q., Jiang,L., Estep,J., Hunt,R., Clagett,M., Sehgal,P.K., Li,Y., Zeng,X., Morita,C.T., Brenner,M.B., Letvin,N.L., Chen,Z.W. (2002) Adaptive immune response of Vgamma2Vdelta2+ T cells during mycobacterial infections. *Science* **295**, 2255-2258.
29. Li,B., Rossman,M.D., Imir,T., Oner-Eyuboglu,A.F., Lee,C.W., Biancaniello,R., Carding,S.R. (1996). Disease-specific changes in gamma/delta T cell repertoire and function in patients with pulmonary tuberculosis. *J. Immunol.* **157**, 4222-4229.
30. Gioia,C., Agrati,C., Casetti,R., Cairo,C., Borsellino,G., Battistini,L., Mancino,G., Goletti,D., Colizzi,V., Pucillo,L.P., Poccia,F. (2002) Lack of CD27-CD45RA-V gamma 9V delta 2+ T cell effectors in immuno-compromised hosts and during active pulmonary tuberculosis. *J. Immunol.* **168**, 1484-1489.
31. Boom,W.H., Canaday,D.H., Fulton,S.A., Gehring,A.J., Rojas,R.E., Torres,M. (2003) Human immunity to *Mycobacterium tuberculosis*: T cell subsets and antigen processing. *Tuberculosis* **83**, 98-106.
32. Dieli,F., Sireci,G., Caccamo,N., Di Sano,C., Titone,L., Romano,A., Di Carlo,P., Barera,A., Accardo-Palumbo,A., Krensky,A.M., Salerno,A. (2002) Selective depression of interferon-gamma and granulysin production with increase of

proliferative response by Vgamma9/Vdelta2 T cells in children with tuberculosis. *J. Infect. Dis.* **186**, 1835-1839.

33. Pahlevan,A.A., Wright,D.J., Andrews,C., George,K.M., Small,P.L., Foxwell,B.M.(1999) The inhibitory action of *Mycobacterium ulcerans* soluble factor on monocyte/T cell cytokine production and NF-kappa B function. *J. Immunol.* **163**, 3928-3935.
34. Pimsler,M., Sponsler,T.A., Meyers,W.M. (1988) Immunosuppressive properties of the soluble toxin from *Mycobacterium ulcerans*. *J. Infect. Dis.* **157**, 577-580.
35. Al Attiyah,R., Mustafa,A.S., Abal,A.T., Madi,N.M., Andersen,P. (2003) Restoration of mycobacterial antigen-induced proliferation and interferon-gamma responses in peripheral blood mononuclear cells of tuberculosis patients upon effective chemotherapy. *FEMS Immunol.Med.Microbiol.* **38**, 249-256.
36. Dlugovitzky,D., Bay,M.L., Rateni,L., Urizar,L., Rondelli,C.F., Largacha,C., Farroni,M.A., Molteni,O., Bottasso,O.A. (1999) *In vitro* synthesis of interferon-gamma, interleukin-4, transforming growth factor-beta and interleukin-1 beta by peripheral blood mononuclear cells from tuberculosis patients: relationship with the severity of pulmonary involvement. *Scand.J. Immunol.* **49**, 210-217.
37. Dlugovitzky,D., Bay,M.L., Rateni,L., Fiorenza,G., Vietti,L., Farroni,M.A., Bottasso,O.A. (2000) Influence of disease severity on nitrite and cytokine production by peripheral blood mononuclear cells (PBMC) from patients with pulmonary tuberculosis (TB). *Clin.Exp.Immunol.* **122**, 343-349.
38. Lee,J.S., Song,C.H., Kim,C.H., Kong,S.J., Shon,M.H., Kim,H.J., Park,J.K., Paik,T.H., Jo,E.K. (2002) Profiles of IFN-gamma and its regulatory cytokines (IL-12, IL-18 and IL-10) in peripheral blood mononuclear cells from patients with multidrug-resistant tuberculosis. *Clin.Exp.Immunol.* **128**, 516-524.
39. Jo,E.K., Park,J.K., Dockrell,H.M. (2003) Dynamics of cytokine generation in patients with active pulmonary tuberculosis. *Curr.Opin.Infect Dis.* **16**, 205-210.
40. Dieli,F., Friscia,G., Di Sano,C., Ivanyi,J., Singh,M., Spallek,R., Sireci,G., Titone,L., Salerno,A. (1999) Sequestration of T lymphocytes to body fluids in tuberculosis: reversal of anergy following chemotherapy. *J. Infect. Dis.* **180**, 225-228.

41. Reed,M.B., Domenech,P., Manca,C., Su,H., Barczak,A.K., Kreiswirth,B.N., Kaplan,G., Barry,C.E., III, (2004) A glycolipid of hyper-virulent tuberculosis strains that inhibits the innate immune response. *Nature* **431**, 84-87.
42. Manca,C., Reed,M.B., Freeman,S., Mathema,B., Kreiswirth,B., Barry,C.E., III, Kaplan,G. (2004) Differential monocyte activation underlies strain-specific Mycobacterium tuberculosis pathogenesis. *Infect. Immun.* **72**, 5511-5514.
43. Mutis,T., Cornelisse,Y.E., Datema,G., van den Elsen,P.J., Ottenhoff,T.H., de Vries,R.R. (1994) Definition of a human suppressor T-cell epitope. *Proc.Natl.Acad.Sci.U.S.A* **91**, 9456-9460.
44. Belkaid,Y., Rouse,B.T. (2005) Natural regulatory T cells in infectious disease. *Nat.Immunol.* **6**, 353-360.

Chapter 4.2

Local activation of the innate immune system in Buruli ulcer lesions

Elisabetta Peduzzi [1]*, Célia Groeper [2]*, Daniela Schütte [1], Paul Zajac [2], Simona Rondini [1], Ernestina Mensah-Quainoo [3], Giulio Cesare Spagnoli [2], Gerd Pluschke [1], Claudia Andrea Daubenberger [1]

[1] Swiss Tropical Institute, Department of Medical Parasitology and Molecular Infection Biology, Basel, Switzerland

[2] Institut für Chirurgische Forschung und Spitalmanagement, Basel University Hospital, Basel, Switzerland

[3] Ghana Health Service, Ministry of Health, Ghana

*these two authors contributed equally

This article has been published in:

Journal of Investigative Dermatology

(2006 Oct, Epub ahead of print)

Abstract

Buruli ulcer caused by *Mycobacterium ulcerans* is a chronic necrotising disease of the skin and the underlying soft tissue. Fat tissue necrosis accompanied by minimal inflammation is considered the most reliable histopathologic feature of Buruli ulcer. There may be a constant influx of inflammatory cells to the sites of active infection but these are thought to be killed by mycolactone, a polyketide toxin produced by *M. ulcerans*, through apoptosis and necrosis. Here we describe the spatial correlations between mycobacterial load and the expression of dendritic cell surface markers (CD83, CD11c, CD123), the Toll-like receptor (TLR) 9 and pro-inflammatory and anti-inflammatory cytokines (IL-8, IL-6, TNF-α, IFN-α, IL-12p40, IL-10 and IFN-γ) within Buruli ulcer lesions. While IL-8, IL-6, and TNF-α mRNA was detectable by real-time PCR in all lesions, the expression of the other cytokines was only found as small foci in some lesions. Correlations of the distribution of mRNA encoding the activation marker CD83 and the dendritic cell subset markers CD123 and CD11c indicate that both activated plasmacytoid and myeloid dendritic cells were present in the lesions. Results suggest that M. ulcerans specific immune responses may develop once therapeutic interventions have limited the production of mycolactone.

Introduction

Buruli ulcer (BU) caused by *Mycobacterium ulcerans* is a chronic necrotizing disease of skin and soft tissue. Generally it manifests initially as firm, non-tender, subcutaneous nodules, probably at the sites of penetrating skin trauma (pre-ulcerative stage). Subsequently, these areas become fluctuant, followed by the formation of an ulceration with undermined edges (ulcerative stage). Ulcers can be extensive, involving more than 10% of the patient's skin surface (Johnson et al., 2005). Subcutaneous fat is particularly affected, but underlying bone may also become involved in advanced cases. In BU lesions clumps of extra-cellular acid fast bacilli surrounded by areas of necrosis are found. Fat tissue necrosis accompanied by minimal inflammation is considered the most reliable histopathologic feature of BU (Guarner et al., 2003; Hayman, 1993; Hayman and McQueen, 1985). In late stages of the disease, intra-lesional influx of leukocytes and granulomatous responses in the dermis and panniculus has been described. If left untreated, spontaneous healing of BU lesions can occur after extended periods of progressive ulceration (Asiedu et al., 2000). Traditionally, BU is treated by wide surgical excision, drug therapy has been considered ineffective, but recent data suggest that combinations of anti-mycobacterial antibiotics can support or replace surgical treatment (Etuaful et al., 2005). Provisional WHO guidelines now recommend the use of rifampicin and streptomycin for the treatment of BU (WHO, 2006). *M. ulcerans* is unique among mycobacterial pathogens in that it is mainly extra-cellular and produces a plasmid-encoded toxin with a polyketide derived macrolide structure, named mycolactone (Stinear et al., 2004). Mycolactone is believed to play a central role in determining the extra-cellular localisation of the bacteria and modulation of immunological responses to *M. ulcerans* (Adusumilli et al., 2005). Observations in rodents experimentally infected with mycolactone producing and mycolactone negative *M. ulcerans* strains suggested that inflammatory cells are rapidly killed by necrosis when encountering high toxin concentrations. Inflammatory cells more distant from the necrotic centre are thought to be killed via apoptosis resulting in extra-cellular bacteria surrounded by an area of coagulation necrosis. In contrast, granulomatous lesions with strong self-healing tendencies were observed with mycolactone-negative mutants (Oliveira et al., 2005).

Intrigued by the described lack of inflammatory responses in BU lesions, we have analysed the impact of *M. ulcerans* infection on the activation of the skin innate immune system, including dendritic cells (DC). Here we describe the spatial correlations between bacterial load and the expression of DC surface markers (CD83, CD11c, CD123), the intracellular receptor TLR9 and pro-inflammatory and anti-inflammatory cytokines (IL-8, IL-6, TNF-□, IFN-α, IL-12p40, IL-10 and IFN-γ) within BU lesions.

Results

Quantitative real-time PCR was used to determine the spatial distribution of mRNA encoding cytokines and cell-surface markers of the innate immune system within surgically excised early ulcerative BU lesions of three selected patients. Histopathological changes and M. ulcerans DNA levels in the same tissue samples have been described previously (Rondini et al., 2006). A summary of these data is provided in Figures 1 and 2 for direct comparison with the distribution of cytokine and DC marker mRNA.

Distribution of DC marker mRNA

Figure 1 shows the spatial pattern of mRNA encoding the cell surface marker CD83, CD11c, CD123 and the intracellular receptor TLR9. Percent values normalised to β-actin mRNA are provided. In all three patients CD83 (Figure 1, d–f) and CD123 mRNA (Figure 1, j–l) was detectable along the entire lesions. Relative levels ranged from 0 to 4.2% (as compared to 0.2 ± 0.1% in normal skin) and from 0 to 7.4% (0.2 ± 0.2% in normal skin), respectively. CD11c (Figure 1, g-i) and TLR9 mRNA (Figure 1, m-o) showed a more focal distribution with relative levels ranging from 0 to 92% (0.4 ± 0.2% in normal skin) and 0 to 1.2% (< 0.01% in normal skin), respectively. For all four markers peak values were thus much higher than in normal skin. In many cases peaks were located close to foci of M. ulcerans DNA (sample G in patient A, samples D and F in patient B and samples D and E in patient C).

Distribution of cytokine mRNA

Expression of cytokines with pro-inflammatory or anti-inflammatory activity was analyzed (Figure 2). IL-8, IL-6 and TNF-α mRNA was detectable in all three BU lesions, albeit in different amounts and in markedly different spatial patterns. Peaks of the relative levels of IL-8 mRNA were associated with the ulcerations and the histological detection of neutrophils (Figure 2, a-c). In contrast, location of the relative peaks of IL-6 mRNA with respect to the location of ulcerations and peaks of M. ulcerans DNA varied markedly between lesions. In patient A, the relative IL-6 mRNA levels were highest at the less affected borders of the excised tissue, in patient B it was peaking at the nodular pre-ulcerative lesion and in patient C at and around the ulceration (Figure 2, d-f). TNF-α mRNA was broadly distributed over the lesion.

Relative peak levels of IL-8, IL-6, and TNF-α mRNA (13'395%, 10% and 2.3%, respectively) were dramatically higher than the levels found in normal skin (4.7 ± 5.1%, 0.1 ± 0.1% and 0.1 ± 0.1%, respectively).

Like in normal skin, IL-12p40 mRNA levels were below the detection limit in all three BU lesions analysed (< 0.03%) (data not shown). In contrast, IFN-α, IFN-γ and IL-10 mRNA, also undetectable in normal skin, was found at least in one of the three analysed lesions in spatially highly restricted foci. IL-10 and IFN-γ mRNA was detected only in patient B (Figure 2 n). While a peak of IL-10 mRNA was associated with the secondary non-ulcerated nodule (peak value 1.2%), IFN-γ mRNA was found in one sample close to the small ulceration and the associated granulomas (peak value 0.2%) (Figure 2 n). Significant levels of IFN-α mRNA were primarily found in patient C (Figure 2, j-l), peaking towards the right margin of the excised tissue (Figure 2 l, peak value in sample I, 246%).

Correlations of the spatial distribution of mRNA species

The spatial mRNA distributions of the two DC subset markers CD11c and CD123 were positively correlated with that of the cellular maturation marker CD83 (CD83 vs. CD123: $r = 0.63$, $p < 0.0001$; CD83 vs. CD11c: $r = 0.54$, $p = 0.001$; Figure 3 a, b). Also strong positive correlations of the distribution of CD83 with IL-6 and TNF-α were observed ($r = 0.67$, $p < 0.0001$ and $r = 0.80$, $p < 0.0001$, respectively; Figure 3 c, d). Correlation of IL-6 expression with CD123 was tighter ($r = 0.66$, $p < 0.001$; Figure 3 e) compared with CD11c ($r = 0.41$, $p = 0.02$; Figure 3 f). The correlation of both DC subset markers with TNF-α expression was moderate (CD11c vs. TNF-α: $r = 0.50$, $p = 0.002$; CD123 vs. TNF-α: $r = 0.48$, $p = 0.004$; data not shown). There was no indication of a correlation between IFN-α and CD123, CD83 or CD11c (data not shown).

Immunohistochemical detection of CD123 positive DCs

Results of quantitative real-time PCR and immunohistochemistry were highly associated, i.e. the relative numbers of CD123 and TLR9 positive cells were consistent with the mRNA levels detected by real-time PCR (Figure 4). In the thin sections of lesions positive for CD123 and TLR9 mRNA, CD123 and TLR9 antibodies stained cells with plasmacytoid features (inset, Figure 4 b, d).

Discussion

Under homeostatic conditions, cutaneous dendritic cells include epidermal Langerhans cells and interstitial/dermal dendritic cells that are of myeloid origin (M-DC) (Kupper and Fuhlbrigge, 2004). Our real time PCR and immunostaining data indicate that in addition to the CD11c positive CD123 negative M-DC (Colonna et al., 2004), CD123 positive plasmacytoid dendritic cells (P-DC), are present in early ulcerative lesions. P-DC are of lymphoid origin (Colonna et al., 2004), CD11c negative and known to be recruited to diseased skin in conditions such as systemic lupus erythematosus, atopic dermatitis, psoriasis vulgaris and contact dermatitis (Bangert et al., 2003; Nestle et al., 2005; Wollenberg et al., 2002).

One of the surface molecules up-regulated upon DC activation and maturation is CD83 (Lechmann et al., 2002). Although CD83 is also expressed on activated human B and T cells and a subpopulation of activated monocytes (Lechmann et al., 2002), the observed correlations of mRNA expression between CD83 and CD123 or CD11c indicated, that both P-DC and M-DC were activated in the BU lesions. The distribution of mRNA encoding the highly expressed pro-inflammatory cytokines IL-6 and TNF-α was also strongly correlated with the activation marker CD83. Expression of IL-6 was additionally strongly correlated with that of CD123, indicating that activated P-DC may represent the major source of IL-6 expression in the BU lesions. In contrast to M-DC, P-DC express TLR7 and TLR9 but lack TLR2, TLR3, TLR4 and TLR5. In the majority of patient samples analyzed, expression of TLR9 and CD123 mRNA was consistent, supporting the presence of P-DC in BU lesions (Figure 1). Signalling through TLR7 and TLR9 results in P-DC activation to secrete large amounts of type I IFN and moderate amounts of TNF-□ and IL-6 (Colonna et al., 2004). In contrast to IL-6, no correlation between CD123 and IFN-α mRNA was observed. IFN-α expression by P-DC seems to be variable; while P-DC activation by TLR9 in response to viruses results in secretion of large amounts of IFN-α (Colonna et al., 2004), during the development of psoriatic phenotype IFN-α expression by P-DC seems to be only an early and transient event (Nestle et al., 2005). Consistent with published data (Kiszewski et al., 2006; Phillips et al., 2006; Prevot et al., 2004), TNF-α and IL-8 mRNA levels were, like those of IL-6 and IFN-α RNA, much higher in the BU lesions than in normal skin. Since moderate

correlation between DC markers and TNF-α mRNA was observed, TNF-α mRNA expression may be in part associated with other cell types, like monocytes, activated T cells or NK cells.

The mechanism of immune protection in M. ulcerans remains unclear. Evidence from genetic defects in the IFN-γ signalling pathway supports the role of IFN-γ in protection against a range of non-tuberculous mycobacterial disease, including M. ulcerans (Ottenhoff et al., 2005). PBMC from BU patients with active disease showed significantly reduced lympho-proliferation and IFN-γ production in response to stimulation with live or dead *M. bovis* BCG, *M. ulcerans*, PPD of *M. tuberculosis*, isopentenyl pyrophosphate and non-mycobacterial antigens like reconstituted influenza virosomes (Gooding et al., 2001; Gooding et al., 2002; Gooding et al., 2003; Prevot et al., 2004; Yeboah-Manu et al., 2006). Prévot et al. showed with semi-quantitative PCR analyses that the systemic Th1 down modulation was mirrored by local, intra-lesional cytokine profiles. High IFN-γ with low IL-10 mRNA levels were present in early, nodular lesions and low IFN-γ mRNA levels were detected in late ulcerative lesions (Prevot et al., 2004). Hence, in active *M. ulcerans* disease, the Th1 response seemed to be down-regulated both locally and systemically. The presence of IL-6 during T cell priming may promote Th2 differentiation and simultaneously inhibit Th1 polarization (Diehl and Rincon, 2002). Therefore the close association of CD123 (P-DC) with IL-6 in conjunction with the lack of INF-α production may favour Th2 development and result in the observed Th1 down-modulation in BU. IL-6 is a pleiotropic cytokine involved in the growth and differentiation of numerous cell types, including those of dermal and epidermal origin (Paquet and Pierard, 1996). In the skin, it is induced in a broad range of dermatotoxic reactions and may be involved in wound healing (Hernandez-Quintero et al., 2006). The presence of high numbers of P-DC in the lesions in the absence of IFN-α gene expression raises also the issue of a tolerogenic role of these cells, as suggested in primary cutaneous melanomas (Vermi et al., 2003).

IL-10 and IFN-γ mRNA was detected in one of the three analysed BU lesions, where it was present only in highly focal areas. Phillips et al. showed wide variations in IL-10 and IFN-γ mRNA expression among individual skin punch biopsies (Phillips et al., 2006). Generally, our results demonstrate that expression of cytokines and cell surface

markers can vary considerably within a BU lesion. Therefore, results obtained with biopsies of BU lesions do not necessarily reflect the overall profile of a lesion. Our comparison of the spatial relationship between bacterial load, DC marker and pro-inflammatory cytokine mRNA suggests that the presence of clusters of *M. ulcerans* does not exclude innate immune system recruitment to the site of infection. This conclusion is consistent with the hypothesis of Oliveira et al., suggesting a constant influx of neutrophils, monocytes/macrophages and lymphocytes to active *M. ulcerans* lesions (Oliveira et al., 2005). Potentially, *M. ulcerans* specific immune responses may therefore develop, once a therapeutic intervention, such as a successful antibiotic treatment, is limiting the production of mycolactone.

Materials and Methods

Clinical specimens

Three BU patients with ulcerative lesions, who received standard treatment at the Amasaman Health Centre in the Ga district in Ghana, were enrolled in this study. The standard treatment comprised wide surgical excision including margins of macroscopically healthy tissue followed by skin grafting. BU clinical diagnosis was reconfirmed by IS2404 PCR, microscopic detection of acid fast bacilli and observation of characteristic histopathological changes. The distribution of M. ulcerans DNA and histopathological examination within the excised tissue samples analyzed here, have been described elsewhere (Rondini et al., 2006). Patient A presented with an ulcerated plaque (ulcer size 4 x 5 cm) on the dorsal aspect of the left upper arm. The central necrotic slough was associated with typical inflammatory cells while no granulomas were seen in any zone of the excision. The highest mycobacterial DNA burden was present at the base of the ulcer and decreased towards the margins of the excision (Figure 1 a). Patient B presented with a small ulcerated lesion (∅ 1 cm) and a larger non-ulcerated nodule located about 3 cm apart on the dorsal aspect of the right elbow. The *M. ulcerans* DNA was present with high load within the non-ulcerated nodule and, with lower load, in the ulcerated region. Between these two lesions no bacterial DNA was detected. Granulomas were present across the tissue from nodule to ulcer till the right margin of the excision (Figure 1 b). Patient C presented with a small ulcer 5 cm away from a larger ulcer, which was surrounded by scar tissue and showed evidence of previous treatment. *M. ulcerans* DNA was only present at the base of the small ulcer and no granulomas were detected in the whole excision (Figure 1 c). Ethical approval for analysing patient specimens was obtained from the local ethical review board of the Noguchi Memorial Institute for Medical Research and participants gave their written informed consent. The study was conducted according to the Declaration of Helsinki Principles.

RNA extraction, removal of genomic DNA and reverse transcription

RNA was extracted from several samples of equal size, each comprising skin and fat tissue, which were obtained from BU patients' excised lesions: patient A, 14 samples (A-N); patient B, 11 samples (A-K); patient C, 9 samples (A-I). Samples were disrupted by sonication for 2 min (Sonifer® Branson 250, Branson Ultrasonics

Corporation, Danbury, CT) and centrifuged for 3 min at 10'000 x g. RNA was extracted from the tissue lysate using the RNeasy Mini Kit (Qiagen AG, Basel, CH) and treated with DNase I (Invitrogen, Paisley, UK) to remove genomic DNA.
To synthesize complementary DNA (cDNA), total RNA was incubated with oligo d(T) for 10 min at 65°C, and put on ice. A reaction mixture containing dNTP mix (125 nM), DTT (10 mM) and reverse transcriptase M-MLV (200U) with corresponding first strand buffer was added (Invitrogen, Paisley, UK). The reaction mix was incubated for 60 min at 37°C before enzyme inactivation for 5 min at 94°C.

Quantitative real time polymerase chain reaction

Gene transcription was evaluated using the ABI Prism 7700 Sequence Detection System (Applied Biosystems, Foster City, CA). Primers and probes for 6 human cytokines (IL-6, IL-8, IL-10, IL-12p40, TNF-α, IFN-α, IFN-γ), cell surface proteins (CD11c, CD83, CD123, TLR9) were used to amplify specific cDNA in duplicate, according to the manufacturers instructions (Applied Biosystems, Foster City, CA). The β-actin gene was used as an internal house keeping gene reference. Primers and probes for β-actin, IL-8, IL-12p40, IFN-α, CD11c, CD83, CD123 and TLR9 were obtained from Applied Biosystems. Primer and probes for IL-6 (Hartwig et al., 2002), IL-10 (Giulietti et al., 2001), TNF-α (Razeghi et al., 2001) and IFN-γ (Kammula et al., 1999) were synthesised by Mycrosynth (Balgach, CH). Having verified that the amplification dynamic remains proportional at all tested dilutions, RNA expression of each surface marker and cytokine was presented as percentage relative to β-actin gene expression. The assays were run in duplicates and the results with a standard deviation > 2% were excluded. Correlation analyses were performed in Prism using the Spearman rank correlation coefficient. Mean values of surface markers and regulatory cytokines in six samples of healthy skin tissue are as follow: CD11c (0.4 ± 0.2%), CD123 (0.2 ± 0.2%), CD83 (0.2 ± 0.1%), TLR9 (< 0.01%), TNF-α (0.1 ± 0.1%), IL-6 (0.1 ± 0.1%) and IL-8 (4.7 ± 5.1%). IFN-α, IFN-γ, IL-10 and IL-12p40 mRNA were undetectable.

Immunohistochemistry

Tissue samples were fixed overnight in neutral buffered 4% paraformaldehyde, embedded in paraffin according to standard protocol and cut into 5 μm sections using a microtome. After de-paraffinization, sections were re-hydrated through graded

alcohols and washed in distilled water. Antigen retrieval was performed by microwave unmasking technique in 10 mM EDTA pH 8.0. Subsequently, endogenous peroxidase was blocked with 0.3% H_2O_2 for 30 min and unspecific binding prevented by incubating with blocking serum for 20 min at room temperature. CD123 monoclonal antibody (Biosciences, San Diego, CA) was diluted 1:100 in PBS plus 0.1% Tween-20 and slides incubated in a humid chamber for 1 h at room temperature. Sections were than incubated for 30 min at room temperature with the secondary antibody biotin labelled (Vector Laboratories; 1:200 in PBS). Slides were then labelled with streptavidin horseradish peroxidase conjugate (Vector Laboratories, Vectastain Elite ABC kit) for 30 min at room temperature and staining was performed by using Vector NovaRed and Hematoxylin (counter stain).

Acknowledgments

We are grateful to Laura Gosoniu for support in statistical analysis. This work was supported in part by the Stanley Thomas Johnson Foundation and in part by the Swiss National Science Foundation to GCS (3200B0-104060-1).

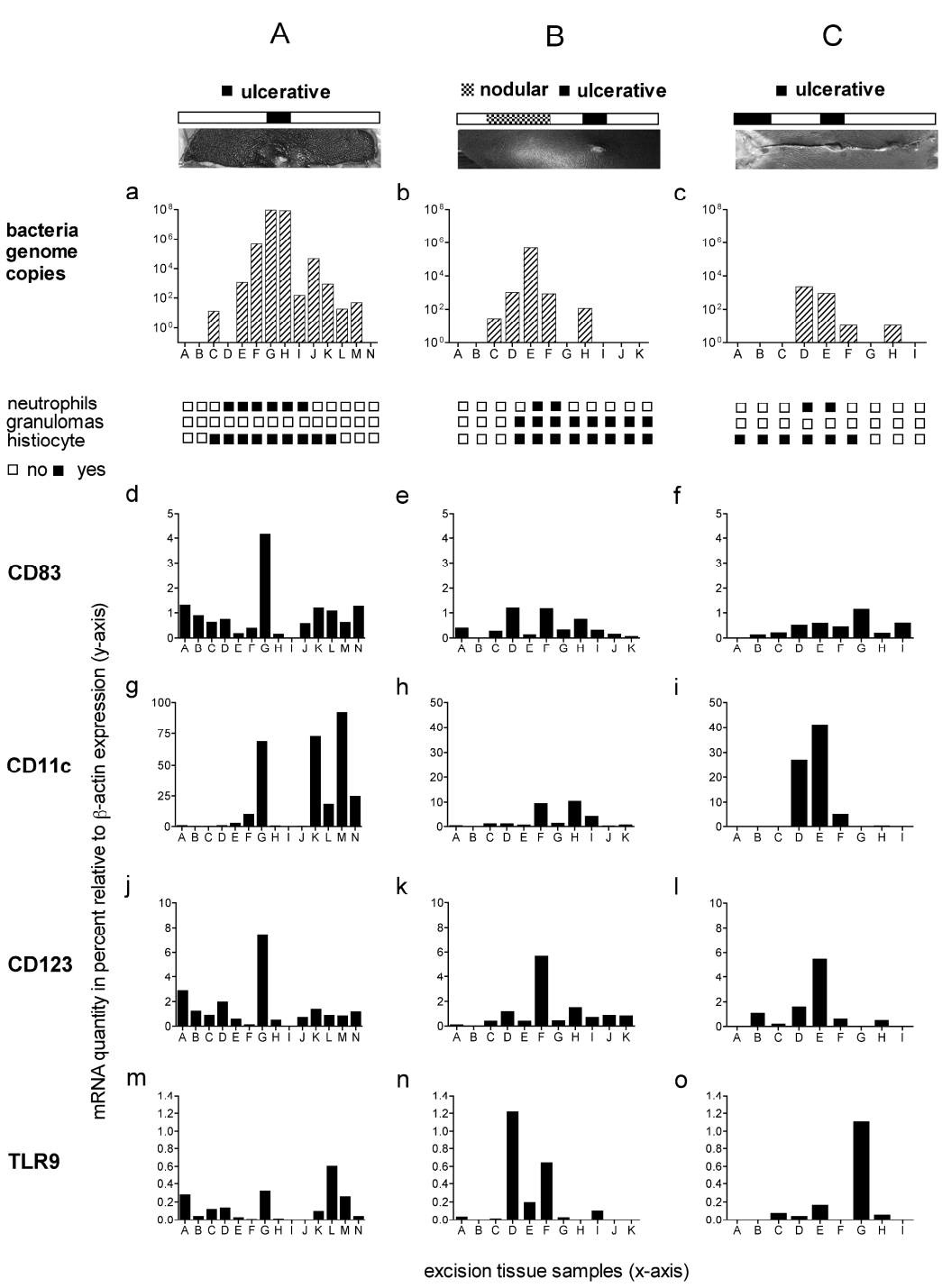

Figure 1. Spatial localisation of bacterial load and dendritic cell markers in BU lesions. Patients A, B and C excisions with tissue samples: A-N, A-K, A-I; respectively. Relative quantity of mRNA for the surface markers CD83 **(d-f)**, CD11c **(g-i)**, CD123 **(j-l)** and intracellular receptor TLR9 **(m-o)** expressed in percent relative to β-actin gene expression. M. ulcerans DNA load and histo-pathological changes of the excisions (a-c) (Rondini et al., 2006).

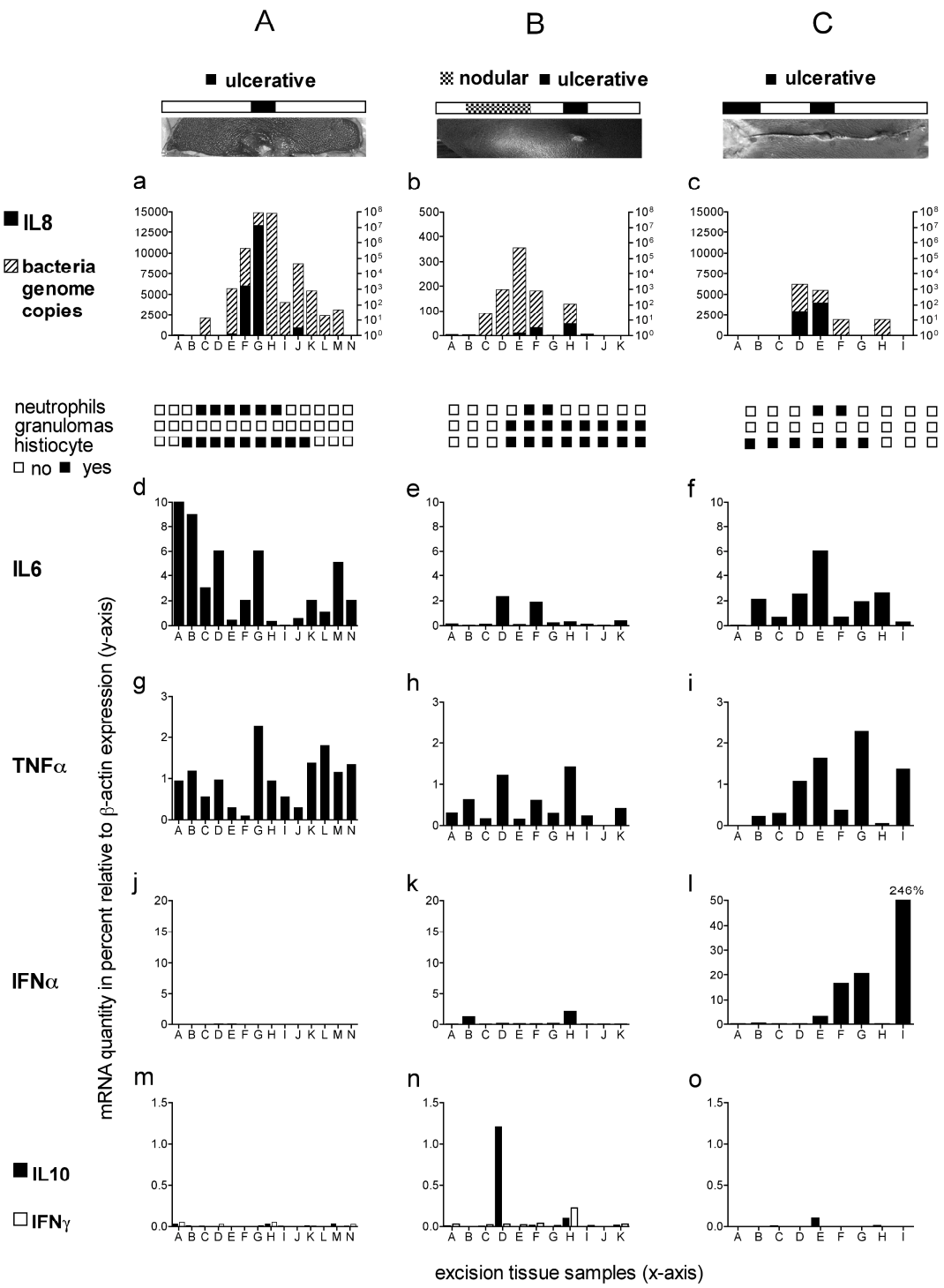

Figure 2. Distribution of bacterial load and regulatory cytokine mRNA in Buruli ulcer excisions. Patient A, B and C excisions with tissue samples: A-N, A-K, A-I; respectively. Relative quantity of mRNA for the cytokines IL-8 **(a-c)**, IL-6 **(d-f)**, TNF-α **(g-i)**, IFN-α **(j-l)**, IL-10 and IFN-γ **(m-o)** expressed in percent relative to β-actin gene expression. M. ulcerans DNA load and histo-pathological changes of the excisions (a-c) (Rondini et al., 2006).

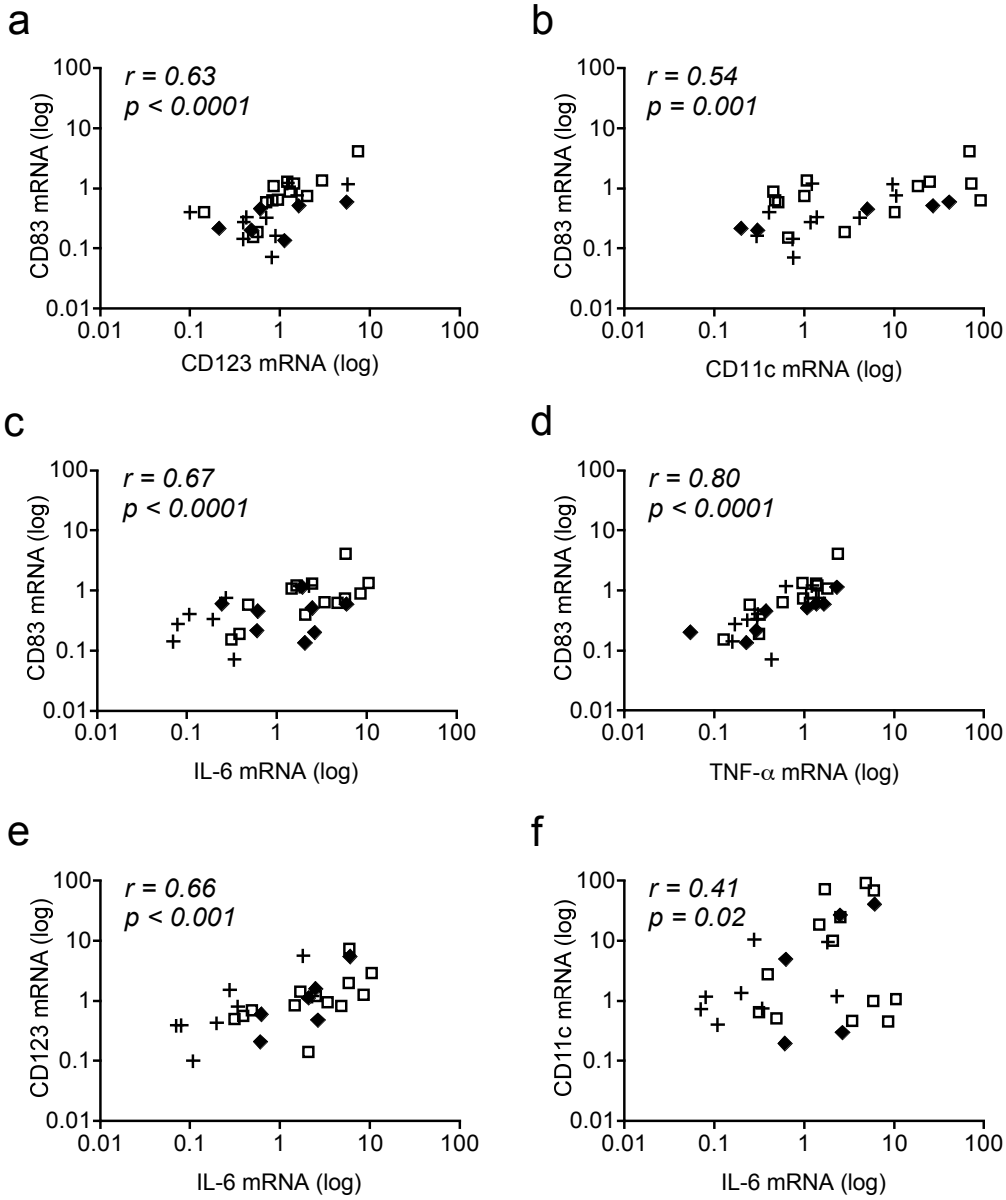

Figure 3. Correlations of dendritic cell markers and cytokine expression.

Patient A (□), B (♦), C (+). Spearman's correlations of the mRNA spatial distribution in the excisions are given. CD123 vs. CD83 (a); CD11c vs. CD83 (b); IL-6 vs. CD83 (c); TNF-α vs. CD83 (d); IL-6 vs. CD123 (e); IL-6 vs. CD11c (f). Spearman's correlations with an r ranging from 0.4 to 0.6 and p value of < 0.05 are moderate positive; with $r > 0.6$ and $p < 0.05$ are positive to strong positive. Each point represents the value of one tissue sample.

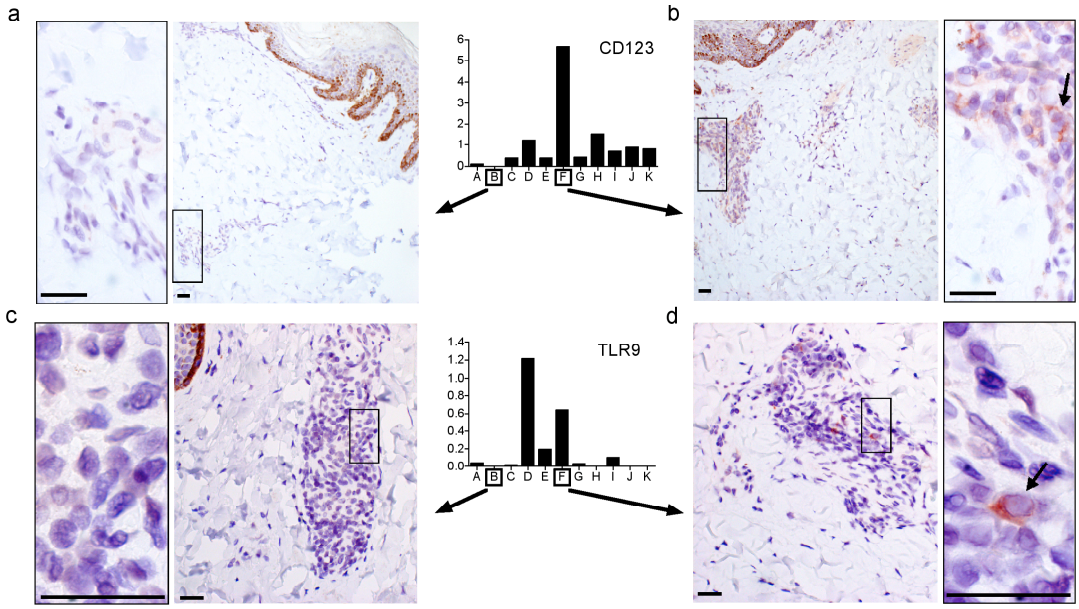

Figure 4. Immunohistochemical analysis of P-DC recruitment to BU excisions.

Immunohistochemical stainings in thin sections of tissues samples B and F of patient B. **(a, b)** CD123 staining (original magnification x100, inset original magnification x400) and **(c, d)** TLR9 staining (original magnification x200, inset original magnification x1'000), bars = 40 μm.

References

Adusumilli S, Mve-Obiang A, Sparer T, Meyers W, Hayman J, Small PL (2005) Mycobacterium ulcerans toxic macrolide, mycolactone modulates the host immune response and cellular location of M. ulcerans in vitro and in vivo. Cell Microbiol 7: 1295-04.

Asiedu K, Scherpbier R, Raviglione M (2000) Buruli ulcer: Mycobacterium ulcerans infection. World Health Organisation. http://whqlibdoc.who.int/hq/2000/WHO_CDS_CPE_GBUI_2000.1.pdf

Bangert C, Friedl J, Stary G, Stingl G, Kopp T (2003) Immunopathologic features of allergic contact dermatitis in humans: participation of plasmacytoid dendritic cells in the pathogenesis of the disease? J Invest Dermatol 121: 1409-18.

Colonna M, Trinchieri G, Liu YJ (2004) Plasmacytoid dendritic cells in immunity. Nat Immunol 5: 1219-26.

Diehl S, Rincon M (2002) The two faces of IL-6 on Th1/Th2 differentiation. Mol Immunol 39: 531-6.

Etuaful S, Carbonnelle B, Grosset J, Lucas S, Horsfield C, Phillips R et al. (2005) Efficacy of the combination rifampin-streptomycin in preventing growth of Mycobacterium ulcerans in early lesions of Buruli ulcer in humans. Antimicrob Agents Chemother 49: 3182-86.

Giulietti A, Overbergh L, Valckx D, Decallonne B, Bouillon R, Mathieu C (2001) An overview of real-time quantitative PCR: applications to quantify cytokine gene expression. Methods 25: 386-01.

Gooding TM, Johnson PD, Campbell DE, Hayman JA, Hartland EL, Kemp AS et al. (2001) Immune response to infection with Mycobacterium ulcerans. Infect Immun 69: 1704-07.

Gooding TM, Johnson PD, Smith M, Kemp AS, Robins-Browne RM (2002) Cytokine profiles of patients infected with Mycobacterium ulcerans and unaffected household contacts. Infect Immun 70: 5562-67.

Gooding TM, Kemp AS, Robins-Browne RM, Smith M, Johnson PD (2003) Acquired T-helper 1 lymphocyte anergy following infection with Mycobacterium ulcerans. Clin Infect Dis 36: 1076-77.

Guarner J, Bartlett J, Whitney EA, Raghunathan PL, Stienstra Y, Asamoa K et al. (2003) Histopathologic features of Mycobacterium ulcerans infection. Emerg Infect Dis 9: 651-56.

Hartwig D, Hartel C, Hennig H, Muller-Steinhardt M, Schlenke P, Kluter H (2002) Evidence for de novo synthesis of cytokines and chemokines in platelet concentrates. Vox Sang 82: 182-90.

Hayman J (1993) Out of Africa: observations on the histopathology of Mycobacterium ulcerans infection. J Clin Pathol 46: 5-9.

Hayman J, McQueen A (1985) The pathology of Mycobacterium ulcerans infection. Pathology 17: 594-600.

Hernandez-Quintero M, Kuri-Harcuch W, Gonzalez RA, Castro-Munozledo F (2006) Interleukin-6 promotes human epidermal keratinocyte proliferation and keratin cytoskeleton reorganization in culture. Cell Tissue Res. 325: 77-90.

Johnson PD, Stinear T, Small PL, Pluschke G, Merrit RW, Portaels F et al. (2005) Buruli ulcer (M. ulcerans infection): new insights, new hope for disease control. PLOS Medicine 2: 282-86.

Kammula US, Lee KH, Riker AI, Wang E, Ohnmacht GA, Rosenberg SA et al. (1999) Functional analysis of antigen-specific T lymphocytes by serial measurement of gene expression in peripheral blood mononuclear cells and tumor specimens. J Immunol 163: 6867-75.

Kiszewski AE, Becerril E, Aguilar LD, Kader IT, Myers W, Portaels F et al. (2006) The local immune response in ulcerative lesions of Buruli disease. Clin Exp Immunol 143: 445-51.

Kupper TS, Fuhlbrigge RC (2004) Immune surveillance in the skin: mechanisms and clinical consequences. Nat Rev Immunol 4: 211-22.

Lechmann M, Berchtold S, Hauber J, Steinkasserer A (2002) CD83 on dendritic cells: more than just a marker for maturation. Trends Immunol 23: 273-75.

Nestle FO, Conrad C, Tun-Kyi A, Homey B, Gombert M, Boyman O et al. (2005) Plasmacytoid pre-dendritic cells initiate psoriasis through interferon-alpha production. J Exp Med 202: 135-43.

Oliveira MS, Fraga AG, Torrado E, Castro AG, Pereira JP, Filho AL et al. (2005) Infection with Mycobacterium ulcerans induces persistent inflammatory responses in mice. Infect Immun 73: 6299-310.

Ottenhoff TH, Verreck FA, Hoeve MA (2005) Control of human host immunity to mycobacteria. Tuberculosis (Edinb) 85: 53-64.

Paquet P, Pierard GE (1996) Interleukin-6 and the skin. Int Arch Allergy Immunol 109: 308-17.

Phillips R, Horsfield C, Mangan J, Laing K, Etuaful S, Awuah P et al. (2006) Cytokine mRNA expression in Mycobacterium ulcerans-infected human skin and correlation with local inflammatory response. Infect Immun 74: 2917-24.

Prevot G, Bourreau E, Pascalis H, Pradinaud R, Tanghe A, Huygen K et al. (2004) Differential production of systemic and intra-lesional gamma interferon and interleukin-10 in nodular and ulcerative forms of Buruli disease. Infect Immun 72: 958-65.

Razeghi P, Mukhopadhyay M, Myers TJ, Williams JN, Moravec CS, Frazier OH et al. (2001) Myocardial tumor necrosis factor-alpha expression does not correlate with clinical indices of heart failure in patients on left ventricular assist device support. Ann Thorac Surg 72: 2044-50.

Rondini S, Horsfield C, Mensah-Quainoo E, Junghanss T, Lucas S, Pluschke G (2006) Contiguous spread of Mycobacterium ulcerans in Buruli ulcer lesions analysed by histopathology and real-time PCR quantification of mycobacterial DNA. J Pathol 208: 119-128.

Stinear TP, Mve-Obiang A, Small PL, Frigui W, Pryor MJ, Brosch R et al. (2004) Giant plasmid-encoded polyketide synthases produce the macrolide toxin of Mycobacterium ulcerans. Proc Natl Acad Sci U S A 101: 1345-49.

Vermi W, Bonecchi R, Facchetti F, Bianchi D, Sozzani S, Festa S et al. (2003) Recruitment of immature plasmacytoid dendritic cells (plasmacytoid monocytes) and myeloid dendritic cells in primary cutaneous melanomas. J Pathol 200: 255-68.

WHO (2006) Provisional guidance on the role of specific antibiotics in the management of Mycobacterium ulcerans disease (Buruli ulcer). http://www.who.int/buruli/information/antibiotics/en/index1.html

Wollenberg A, Wagner M, Gunther S, Towarowski A, Tuma E, Moderer M, et al. (2002) Plasmacytoid dendritic cells: a new cutaneous dendritic cell subset with distinct role in inflammatory skin diseases. J Invest Dermatol 119: 1096-102.

Yeboah-Manu D, Peduzzi E, Mensah-Quainoo E, Asante-Poku A, Ofori-Adjei D, Pluschke G et al. (2006) Systemic suppression of interferon-{gamma} responses in Buruli ulcer patients resolves after surgical excision of the lesions caused by the extracellular pathogen Mycobacterium ulcerans. J Leukoc Biol. 79: 1150-56.

Chapter 5

Discussion

5.1 Monitoring cellular immune responses in clinical vaccine trials and characterization of host-pathogen interactions

Based on current knowledge immune protection against malaria and Buruli ulcer is not a single variable or single compartment end point, but it is more likely to be a mosaic of immune responses comprising innate, adaptive, cellular and humoral effector mechanisms. In principle, there is general agreement that immune monitoring should guide the development of new vaccines and treatment modalities against infectious diseases and cancer [1,2]. Assessment of vaccine potency has become quite standard for humoral immune responses. Antibodies can reliably be detected in peripheral blood and saliva and, for some pathogens, protective titers have been well established [1]. On the other hand, specific parameters of cell mediated immunity are more and more needed to evaluate new vaccines: antibody titers are unlikely to remain the sole reliable measure of vaccine immunogenicity and protective efficacy [3]. However, up to date, the evaluation and standardization of cell-mediated immunity is the subject of long debates focusing on the relative merits and appropriate use of the various immune cellular monitoring tools [4]. One inherent limitation to cellular monitoring is that in the clinical setting, only the peripheral blood compartment (PBC) is generally accessible for serial analyses. Additionally, in contrast to antibody responses, specific T cell responses may not always be present in PBC and their presence in the blood is of undefined relevance for clinical efficacy. In humans, only few studies have also monitored T cell responses in the draining lymph node at the vaccine site [5]. This complicates the choice of the optimal blood sampling time points. Moreover, the consistent amount of blood required for T cell analysis limit the allowed blood sampling frequency. Often this decision is the results of a compromise. During the described malaria vaccine Phase Ia clinical trial with malaria synthetic peptides including optimized B cell epitopes (Chapter 3.2), the key readouts were anti-peptide antibody titers (ELISA) and anti-parasite titers (IFA, Western blot analysis) (Genton et al. submitted, Okitsu et al. submitted). The priority was therefore given to blood sampling for serum analysis. The cellular analysis was an additional readout to extent the understanding of virosomal technology for future applications. We received the blood samples prior to the first vaccination and 20 days after each immunization (in total 3 immunizations and four blood samplings). Most of the positive CD4 T cell responders were detected after the first and second

immunization (Chapter 3.2), therefore a unique post immunization sampling after the third immunization would have been detrimental for our T cell study.
A standardization of cellular monitoring is hampered also by the fact that suitable animal models are lacking, considering that most preclinical vaccine development is assessed in small rodents, which are not appropriate for serial monitoring of cellular immune responses in peripheral blood. Protection experiments in mice typically evaluate cellular responses in spleen or lymph nodes. Furthermore, different vaccine formulations may induce distinctive T cell subsets with diversities in cytotoxic and proliferative capacity or long-term memory. This can result in selective accumulation of the specific T cells in lymph nodes, PBC or tissues [6].

Different types of tests have been developed so far with the aim to address and overcome the limitations of cellular monitoring. They can be divided into three different generations, according to their properties:
The first generation was developed several decades ago and it includes three different assays based on measuring: (i) the overall T-cell proliferation after exposure to the target antigen, where the readout is in terms of ^{3}H-thymidine uptake; (ii) the lysis induced by cytotoxic cells (readout: ^{53}Cr release from target cells into the supernatant) and (iii) the cytokine release in the supernatant (sandwich ELISA). This category of assays assesses the T cell response at the whole cell population level, thus requiring prior *in vitro* expansion. The ability to detect T cell responses is based on the proliferative potential of the cells, and the results might be influenced by *in vitro* stimulation procedures.

In the last 10 years, the use of a second generation of assays based on single cell level analysis of the T cell properties is increasingly applied. Cytokine production after exposure to antigen is measured using either a plate- (*ex vivo* ELISpot assay) or a flow cytometry- readout, which includes intracellular cytokine staining or the capture of secreted cytokines by antibodies bound to the cell surface. On the other hand, the affinity of the T cell receptor (TCR) to a given epitope is measured by MHC peptide tetramers that allow the visualization and quantification of antigen-specific T cells. Limitations of the multimer analysis include, required knowledge of a defined epitope and availability of suitable tetramers for the respective epitope/HLA allele combination.

ELISpot and cytokine flow cytometry analyses provide, at the same time, *ex vivo* frequency and functional results. However, only the T cell subset producing the respective cytokine is detected. Usually, it is recommended to perform monitoring preferentially with two of these second generation assays. ELISpot is highly sensitive (detection limit 1/50'000 cells [7,8]) giving therefore the possibility to detect *ex vivo* specific cells [9]. However, *ex vivo* frequencies of antigen specific T cells in the PBC might be below this detection limit due to a complete lack of prior *in vitro* expansion of the specific population [10]. Longer cell-incubation times can increase the detection of specific responses, like in the described 5-days or 14-days cultured ELISpot [10,11]. Clearly, the mentioned cultured ELISpot assays do not give anymore an *ex vivo* quantification of the specific primed T cell population.

In both human and mouse the proliferative, IL-2 producing central memory is opposed to less proliferative, high IFN-γ producing effector memory [12]. It is therefore tempting to speculate that by detecting T cell IFN-γ responses with *ex vivo*-, 5-days cultured- and 14-days cultured- ELISpot there is a progressive shift in central memory cells [10,11]. Only detailed phenotype studies for the specific diseases and analyzed vaccination systems can elucidate these suppositions. We have also to consider that a prolonged cell culture time and extensive *in vitro* manipulations can lead to misleading artifacts [13]. During long cultivation periods, beside antigen-specific T cell stimulation, bystander T cell activation or apoptosis of specific T cells can more easily occur. Moreover, the use of different cell culture lengths is highlighting cell populations with diverse potential for *in vitro* growth [13].

We monitored, in the framework of a Phase Ia clinical trial, AMA-1 derived synthetic peptide specific immune responses both by ELISpot and lymphoproliferation analysis. Results revealed the detection limits of *ex vivo* ELISpot and discrepancies between assays with short and longer *in vitro* cultivation (ELISpot vs. lymphoproliferation). This underlines the importance of using at least two cellular monitoring methods in parallel (Chapter 3.2). On the other side, *ex vivo* IFN-γ ELISpot was appropriate to compare PBMC of Buruli ulcer patients prior to and after surgical excisions stimulated with complex antigens and immunostimulators such as IPP, PPD, PHA and influenza antigens (Chapter 4.1).

Although the development of computer-based image-analysis systems has increased the accuracy and speed of scoring ELISpot assays [14], there is still a certain degree

of subjectivity in the interpretation of the results, as the threshold for the size, intensity, and gradient of the spots are user-defined. Moreover, functional tests are much more sensitive to variation in assay conditions because the production of nonspecific background cytokines may limit the sensitivity of the assays [15]. In this respect, the settings for IFN-γ spots analysis (AID-reader system) were defined at the beginning of this thesis on the basis of results obtained with PBMC of Caucasian and African healthy volunteers stimulated with common antigens (tetanus toxoid, influenza antigens). These settings were then used to monitor vaccine related immune responses in the Phase Ia clinical trial (Chapter 3.2) and the reactivity recovery of systemic cellular immune responses in Buruli ulcer patients after surgery (Chapter 4.1). To reduce the variation in assay conditions, fresh PBMC were used throughout the vaccine trial. Only cryopreserved PBMC were available for the Buruli ulcer study.

For better comparability of results among different research groups, standardization of parameters that define a positive spot across laboratories and readers would be very helpful.

The third-generation of T cell assays is based on a two-step principle: the detection of specific T cells based on tetramers or cytokine flow cytometry is associated with a phenotypic or functional quantitative characterization. The additional markers employed for this purpose can define the cytokine production repertoire, the memory/effector phenotype, the cytotoxic capacity, the proliferative capacity, a migratory phenotype, a regulatory T cells subtype, the functional TCR affinity or avidity and the level of cell maturation. Since it can yield information on many facets of the nature of T cell responses, this type of analysis has a great potential for monitoring cellular immune responses in clinical vaccine trials and in characterizing host-pathogen interactions [16]. But, the specific role of these T cell characteristics for clinical vaccine efficacy has not yet been established.

In conclusion, there are four important levels in cellular immunological monitoring, the sampling compartment, the sampling time point, the measured cell features and the translation of the obtained results in terms of protective efficacy (clinical trials) or in terms of immonopathogenic relevance (characterization of host-pathogen interactions).

Within the framework of the present thesis, proliferation assays but not *ex vivo* IFN-γ ELISpot turned out to be suitable to monitor the cellular immune response to one peptide-based vaccine component (AMA-1 derived synthetic peptide). Attempts to characterize the peptide reactive T cells by generating a panel of T cell clones using established methods [17,18] failed. Reasons for this may be the low frequency of synthetic peptide positive cells (SI ranging from 2 to 4.5) found in the PBC, which is probably attributable to a paucity of promiscuous T cell epitopes in the short malaria synthetic peptide and/or limited specific T cell recirculation in the PBC. However, detailed monitoring of immune responses in trials with at least partially effective vaccines may help to develop surrogate markers of protection. In the case of malaria, experimental challenge Phase II trials represent a suitable setting for such analysis.

5.2 *Plasmodium falciparum* malaria vaccine development

The focus of the current research is the development of a multi-component, multi-stage subunit vaccine against malaria in order to overcome high antigenic variation, extensive polymorphism and life stage specific antigen-expression characteristic for *P. falciparum* parasite [19-21]. The goal is to reach greater magnitude, duration, and strain-transcendence than naturally acquired immunity and the endpoint in efficacy trials is now rather prevention of severe disease than infection (anti-disease vaccine).

5.2.1 Virosome: novel antigen delivery system for synthetic peptides

The physico-chemical nature and the spatial organization of antigens influence the vaccine immunogenicity. The attenuated or inactivated whole pathogens, the paradigms of vaccines, are particulate and immunogenic by definition. The rigid, repetitive organization of the antigens strongly promotes B cell receptor cross-linking required for optimal B cell activation [22,23]. However, small synthetic components (of sugar, protein or lipid origin) are very attractive for vaccine design because they overcome many safety problems related to inactivated or attenuated pathogens. But, these components do not have an auspicious physico-chemical nature. They are soluble, monovalent antigens that are poorly immunogenic, and may even induce tolerance [24]. Several attempts have been made to present small defined, purified antigens to the immune system in particulate form such as preparation of protein aggregates (by denaturation or crystallization), precipitation of the molecules with alum, generation of virus-like particles, and incorporation of antigens in liposomes, proteosomes, microparticles of immunostimulating complexes (ISCOMs). Still, only 25% of the vaccines currently in use are subunit-based and none is synthetic peptide-based. In this thesis we show that the virosomal technology represents an important step in this direction (Chapter 3.1-3.2). The CSP and AMA-1 malaria peptide candidates (UK39 and AMA49-CPE, respectively) were hooked to virosomes via a PE-anchor for non-covalent linking to the virosomal membrane. In the conducted Phase Ia clinical trial two immunizations with a 10 μg dose of UK39 and with a 50 μg dose of AMA49-CPE were enough to induce high anti-peptide antibody titers (Genton et al. submitted, Okitsu et al. submitted). Furthermore a boost of viral HA specific antibody-titers were observed after the first immunization. These results are indicative

for a suitable spatial arrangement of the malaria synthetic peptides on the virosomal surface. Furthermore, in the case of the CSP derived peptide we have shown that optimal conformational restriction of the peptide is decisive for the induction of parasite binding antibodies in mice. The first generation of peptides with single or double loops of NPNA repeats hooked to a rigid template were highly immunogenic but only low titer of parasite cross-reactive IgG were induced [25]. Only the internally cyclized and more flexible NPNA peptides BP65 [26] and UK39 were good at eliciting parasite-binding antibodies (Chapter 3.1). This more flexible type of conformation is close to the natural conformation found in CSP on the surface of sporozoites, as indicated by NMR and crystallization studies. In this respect a very crucial issue was to exclude conformational disturbance caused by the delivery system. Alum-adjuvanted formulation of NPNA first generation peptide elicited higher anti-peptide but only low parasite cross-reactive antibody titers compared to the IRIV formulation [25]. This indicates that the IRIV antigen delivery system does not disturb the spatial conformation of the coupled peptides.

5.2.2 Interaction of the virosome with the immune system

Further important parameters that can influence vaccine immunogenicity are the ability to induce T helper cells and to activate DC [23,27].

The information about DC activation by the virosome delivery system are still limited [28,29]. This is definitively an important issue to be further analyzed because antigens and delivery systems that lack the capacity to induce DC maturation may also be internalized by DC. However, in the absence of costimulatory molecules expression the activation of T helper cells is prevented and may induce antigen-specific tolerance by promoting differentiation of the T cells to regulatory/suppressor cells [27,30,31].

Due to the fusion-mediated activity of HA, the virosomal technology also has the potential to mediate efficient CTL induction against foreign encapsuled molecules [32-35]. Other delivery systems that do not give to the antigens direct access to the cytosol might gain the MHC class I route only through the so-called cross-presentation process [36].

The CD4 T cell response against influenza spike proteins (HA, NA) anchored on virosomal surface is the result of restimulation of a previously primed response, either due to former exposure to natural infection or prior vaccination. The peptide

sequences of HA and NA constantly change as a result of the well-described antigenic drift and shift [37]. In general, T cell epitopes of influenza proteins, particularly of matrix and nucleocapsid proteins, are more conserved across the different influenza strains and less influenced by antigenic drift [38]. T cell memory against influenza antigens remains therefore a very important issue. In old people presenting impaired T cell functions, the influenza vaccination programs are only 40-60% effective [3]. Moreover, the growing threat of the development of a new pandemic strain of influenza from the circulating avian influenza strains (antigen shift) reinforces the importance to promote, by vaccination, cross-species protection [38]. In both humans and mice two broad memory T cell subsets have been delineated according to their homing capacity and effector function [39-41]. CD4 central memory T cells home to the lymph nodes and have a limited effector function, but proliferate and become effector cells upon secondary stimulation ($CD62L^{high}CCR7+$). By contrast CD4 effector memory T cells home to peripheral tissues and can rapidly produce effector cytokines such as IFN-γ upon antigenic stimulation, but have limited proliferative capacity ($CD62L^{low}CCR7-$) [12]. The maintenance of memory T cells is dependent on the expression of anti-apoptotic molecules, such as BclXL [42], and their capacity to respond to homeostatic cytokines (IL-2, IL-7 and IL-15) [43]. Age-related IL-7 decline corresponds to a failure in optimal maintaining the influenza memory T helper cells [44] combined with IL-2 synthesis reduction and a shift toward Th2 cytokines [3].

For most infectious diseases, precise mechanisms for the generation of memory CD4 T cells their maintenance and delineation into diverse subsets, remain largely unknown. Studies in mice suggest that influenza specific CD4 T cells generated in secondary organs appear as multiple subsets in terms of numbers of cell division, phenotype and function. Thus, progressive stages of differentiation IL-2 and IFN-γ production are represented. The effector cells migrating to the lung were found to be the most differentiated population acquiring a phenotype of high and stable CD44 and CD49d expression, loss of CD62L, down-regulation of CCR7 and markedly reduced levels of IL-2 [45]. The memory cells detected in the lung were small resting cells expressing low levels of CD62L and CCR7 [46]. The model proposed for effectors and memory influenza specific CD4 T cells development, suggest quantitative and qualitative regulation affected by factors such as (i) the antigen-dose during the initial

T cell interaction with APC (ii) the duration of repeated antigen-interactions and (iii) the milieu of inflammatory and growth cytokines; which explains the heterogeneous spectrum of influenza CD 4 T cell responses [38].

In humans, small scale PBMC analysis with DR1-$HA_{306-318}$ tetramer detected *ex vivo* memory CD4 T cells frequencies ranging from 0.00012 to 0.0061%, characterized by a CD62L+ and CCR7+ phenotype, IFN-γ and IL-2 production [47]. Another study determined influenza *ex vivo* frequencies 60 days post-influenza vaccination with DR1-$HA_{306-318}$ tetramers, $CFSE^{low}$tetramer-positive T cells and *ex vivo* IFN-γ ELISpot and showed comparable frequencies with all assays (0.0033-0.17%) and an heterogenous CD62L and CCR7 expression [48]. The CD4 T cell influenza specific responses (Chapter 6.1, [49]) that we monitored on a large scale during the described Phase Ia clinical trial were indicative for cells with IL-2 and IFN-γ release abilities (lymphoproliferation and *ex vivo* IFN-γ ELISpot assays), which were detected in all thirty tested volunteers and all along the trial (Chapter 3.2). The *ex vivo* frequencies were ranging from 0.0093 to 0.11% and oscillation IFN-γ and lymphoproliferative abilities were observed during the trial (Chapter 3.2, Chapter 6.1). These data confirm a solid anti influenza CD4 T cell memory response in Caucasian healthy adults.

When using the virosome for antigen delivery, the influence of pre-existing immunity to the viral components is an important issue. A general lack of correlation between the magnitude of the pre-existing influenza specific T cell response and the vaccination-induced AMA49-C1 specific humoral and cellular immune responses was found. Thus, these results indicate that between pre-existing influenza immunity and the priming of synthetic peptide specific responses there is no interference (Figure 1). However, in the perspective of the development of a multi-component vaccine exploiting the virosomal technology, dose-combination studies of virosomes and the coupled synthetic peptides are recommended to find out which kind of population is favored by which dose of synthetic peptide and viral antigens (HA, NA) [50-52].

5.2.3 Induction of cellular immunity to anchored peptides

During this thesis, for the first time, the feasibility to elicit a CD4 T cell response against a synthetic peptide anchored on the virosomal surface was proven (Chapter 3.2, Figure 1). Moreover, all volunteers who developed high titers of parasite cross-reactive IgG in IFA and Western blot analysis, were positive in the anti-synthetic

peptide lymphoproliferation assay. These studies demonstrate that the virosomal antigen delivery platform combined with surface-anchored synthetic peptides is suitable to elicit specific human CD4 T cell responses. These responses are not essential for eliciting target IgG, but may improve the quality of the humoral immune response (Chapter 3.2). In children living in regions endemic for malaria, a malaria vaccine may boost pre-existing anti-malaria T cell responses. More importantly, malaria antigen specific T cells elicited by natural exposure are expected to provide T cell help for vaccine induced B cell upon reinfection.

For an application of the virosomal technology against infections where the elicited CD4 T cell response play a crucial role further optimization has to be considered such as the detection of an optimal synthetic peptide length, the incorporation of multiple promiscuous T cell epitopes, the issue of HLA restriction and the definition of markers of protection. An effective CD4 T cell response against synthetic peptides might be particularly helpful for vaccinating immunologically naïve adults or target population presenting an impaired T cell activity, e.g. old people. Other possible applications of this technology are post-infection immunizations during acute diseases. For example, the lack of specific Th1 effector cell response within the first months of acute hepatitis C virus infection represents an efficacious predictor of viral persistence and chronic course of the disease [53,54]. A post-infection vaccination during early acute disease might be successful in shifting the balance toward a Th1 specific response.

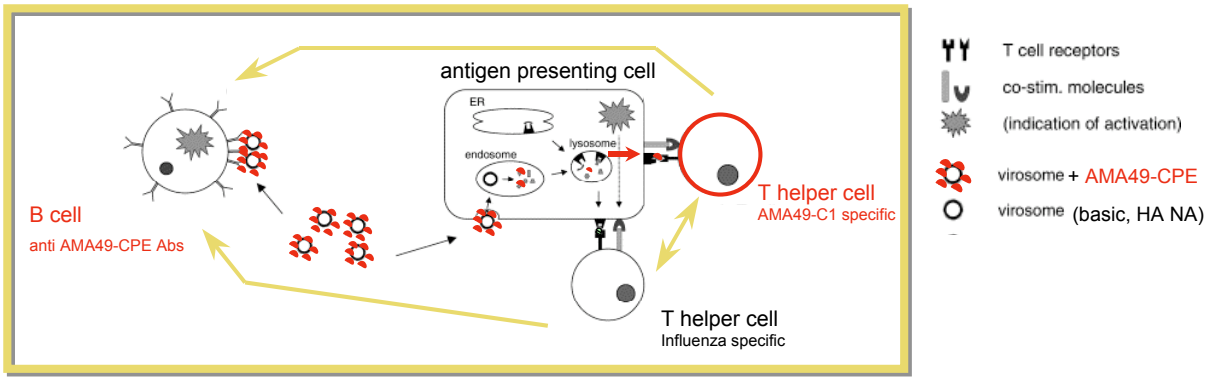

Figure 1 Virosome as delivery system for the synthetic peptide AMA49-CPE. The detection of specific AMA49-C1 T helper cells proved the feasibility to use the virosomal technology to elicit T helper cells specific for the anchored synthetic peptide. Yellow arrows indicate a non-interference relationship in the magnitude between the different immune response compartments.

5.2.4 Aotus monkeys as malaria vaccine model

Most investigations of malaria infection are conducted with rodent Plasmodium spp. in inbred mouse strains. However, no single rodent model replicates all the features of human malaria in terms of either pathology or immune responses [55]. The New World primate Aotus is one of the few non-human primate genus that is susceptible to infections with the human malaria parasites *P. falciparum* and *P. vivax*. Structural molecular similarities between the Aotus monkey and the human immune system have been analyzed in a series of studies which demonstrated a high degree of gene sequence conservation for αβ TCR, Ig κ-light chain, MHC class II molecules, and CD1b [56-61]. In our research group the similarities in function and structure of γδ T cells were studied [62] and a new panel of cross-reactive mAbs specific for immune surface molecules were detected by flow cytometry analysis [63]. Moreover, within this thesis the anti-INFγ mAb for ELISpot coating (GZ-4, Mabtech, Sweeden), cross-reactive for human, rhesus and cynomologous macaques IFN-γ, was found cross-reactive for *A. nancymaae* IFN-γ. However, there is still a general shortage of reagents tested for Aotus spp. cross-reactivity and a lack of exhaustive information at the immunogenetic level. The idea is to bridge this gap to further extent the use of this animal model for malaria research as recommended by the WHO [64]. In Chapter 3.3 the TLR9 Aotus-human homology was analyzed. Our results showed that *A. nancymaae* TLR9 has a 92% identity to human TLR9, whereas rodent TLR9 displayed only 73% of similarity at the amino acid sequence level. The high level of identity of a TLR9 to human could be very helpful within the context of a malaria vaccine using TLR9 ligands as adjuvants. In general, TLR ligands are proposed to have a great potential as vaccine-adjuvants due to their capacities to activate the immune system in very different ways according to their sequence [65]. Furthermore, the virosome technology has been already described as a platform for incorporation of additional adjuvant [23,66]. Mice vaccinated with influenza virosomes with an incorporated lipopeptide binding to TLR2 showed a 150-fold increase in IgG response compared to virosomes without the adjuvant [66]. For a virosomally formulated malaria vaccine the use of CpG ODN as immunomodulators may represent an option to stimulate the immune system of malaria endemic population, which is under constant complex interactions with *P. falciparum* parasites, in the most suitable way.

It is known that TLR ligands are recognized in species-specific manner [67], e.g. unmethylated CpG ODN highly active in rodents often showed no effects in primates [68,69]. In this respect the high homology we found between human and *A. nancymaae* TLR9 might also be very precious in helping to elucidate the stimulation of the innate immune system by *P. falciparum* in a more suitable animal model. Indeed, Coban et al. recently demonstrated an interaction of hemozoin with TLR9 on mice DC, by showing impaired TNF-α, IL12p40 and IL-6 release in $TLR9^{-/-}$ and $MyD88^{-/-}$ mice DC [70]. Hemozoin is the digestion product of hemoglobin metabolized by *P. falciparum*, which is released into the blood stream. *In vitro*, human RBC infected with *P. falciparum* schizont-stage lead to upregulation of CD86 and IFN-α release in P-DC [71,72]. Controversially, recent studies identified hemozoin as possible key player in malaria immunosuppression: hemozoin was not inducing mice DC maturation, since the levels of MHC class II, CD40 and CD86 were the same as the levels expressed by unstimulated control DC [73,74]. Evidence of immunosuppression in malaria infected patients are given by their higher susceptibility to secondary infection and reduced MHC class II levels on DC [75-78]. In this respect, the high homology between human and Aotus TLR9 might help elucidating the exact role of hemozoin and be the start point to better understand immunomodulatory mechanisms of *P. falciparum* parasite.

5.3 Host-pathogen interactions in Buruli ulcer and treatment implications

M. ulcerans bacteria proliferate freely in subcutaneous fatty tissue, where they find an optimal temperature for growth and secretion of mycolactone, causing death of lipocytes and fibroblasts by apoptosis and immunosuppression in the vicinity. The effect of the toxin in causing tissue necrosis and preventing inflammation may be confined to the immediate vicinity. In the adjacent tissue, to which mycolactone has not diffused, an anti-mycobacterial immune response may develop (Figure 2) [79]. Although intact *M. ulcerans* are rarely seen within cells, macrophages can process antigens released by *M. ulcerans* together with fragments of dead bacteria, initiating an inflammatory response where mycolactone has not yet diffused. Individuals infected with *M. ulcerans* may therefore develop a Th1 immune response, but the rate at which it develops varies from person to person [79].

A direct proof for the presence and the diffusion-pattern of mycolactone in infected human tissue does not exist, principally due to difficulties to develop immunological reagents suitable for reliable immunostaining against this macrolide toxin. Consequently, it is not known if and how mycolactone secretion is terminated in lesions that heal spontaneously. Various lines of research including histopathological data, cytokine expression profile analyses of punch biopsies, and mycolactone immunosuppressive studies both *in vitro* and *in vivo* (in mice and guinea pig) are indicative for the theory illustrated above [80-83].

In this study, we took advantage of the exceptional opportunity to investigate, within the same lesions, how immune system infiltrates relates with *M. ulcerans* distribution and the tissue damage caused by its presence. This provided a broad picture of the host-pathogen interaction in active Buruli ulcer lesions. The mRNA expression data obtained with a broad spectrum of innate immune system markers (Chapter 4.2, [84]) clearly demonstrated that the presence of immune system components can vary considerably both between lesions and within different areas of the same Buruli ulcer lesion. TLR9 and CD123 immunohistochemical analysis were indicative for an extremely focal localization of the infiltrates even within a single small tissue sample. High expression of innate immunity markers and granulocyte infiltrates were sometimes found in areas with high bacterial DNA content (Chapter 4.2,[84]). The employed IS2404 real-time PCR quantified the entire load of *M. ulcerans* DNA in a

tissue block including live and dead bacteria. Therefore DNA concentrations did not necessarily correlate with the presence of mycolactone. These results reinforce the assumption of a patchy intercalating picture of Buruli ulcer lesions composed by different levels of tissue damage, immunosuppression and inflammatory infiltrates, probably determined by the diffusion pattern of mycolactone in the affected tissue.

Buruli ulcer patients and many healthy household contacts show a specific humoral immune response to *M. ulcerans* antigens [85,86]. These data suggest that, in analogy to leprosy and tuberculosis [87], Buruli ulcer disease develops only in a limited proportion of the infected people. On the other hand, a lack of swollen lymph nodes and a reduced PBMC IFN-γ production in response to stimulation with live or dead *M. bovis* BCG and *M. ulcerans* has been repeatedly observed in Buruli ulcer affected people [80,88-90]. In this thesis, we extended the observation of a T cell anergy condition in Buruli ulcer patients to non-mycobacterial antigens (Chapter 4.1).

The reasons for this systemic immunosuppression are largely unknown and could be of different origin (Figure 2). There might be a local constant influx of neutrophils, monocytes/macrophages [91] and DC initiated, maintained and exacerbated by the presence of necrotic tissue and potential bacteria fragments in the mycolactone free spots that can lead to an intralesional chronic condition possibly affecting the systemic immune system. Indicative for such an assumption are the presence of high IL-8, IL-6 and TNF-α expression, activated P-DC and M-DC, neutrophils and TLR9 expression in all the analyzed lesions, which often exhibit coexpression profiles (Chapter 4.2). All three inflammatory cytokines have been already described as potential products released by TLR9 expressing cells after CpG ODN stimulation [92]. For example large amount of IL-8 and moderate IL-6 and TNF-α secretion were measured in human neutrophil granulocytes after bacterial CpG DNA stimulation [93]. IL-8 is one of the key regulators of leukocyte trafficking in inflammation. On the other side the Th2-polarizing properties [94] and inhibitory activities of IL-6 towards an adaptive IFN-γ response have been suggested in *M. tuberculosis* [95]. The presence of high P-DC marker and IL-6 expression in the analyzed Buruli ulcer lesions in the absence of IFN-α gene expression raises therefore the issue of induced inhibitory responses in the lesions (Chapter 4.2). CpG ODN embodying immunosuppressive motifs have been already described [96,97]. Therefore we do not exclude the possibility of a further inhibitory effect exerted by DNA or other TLR

ligands of *M. ulcerans* bacteria fragments that may be present in mycolactone free spots of the lesions. A direct comparison of immune system activation in antibiotics-untreated versus antibiotics-treated Buruli ulcer lesions would be very interesting and helpful to better evidence possible *M. ulcerans* key immunomodulators. Recently the combination of rifampicin (oral administration) with streptomycin (intramuscular administration) prior to surgical treatment has been shown to be useful in containing and diminishing the size of Buruli ulcer lesions and in reducing the recurrence rate [98]. Some preliminary immunohistochemical data indicate a better organized immune response in the treated lesions (Schütte personal communication). Therefore, *M. ulcerans* successful adaptive immune response may develop once an effective therapeutic intervention limits the production of mycolactone.

The reversal of systemic immune suppression after surgical treatment-associated (Chapter 4.1) indicates that a local removal or elimination of the *M. ulcerans* bacteria may be sufficient to eradicate the disease. In this respect, topical treatments could be a solution that obviates the surgical and post-surgical treatments comprising skin grafting and rehabilitation of the affected limb. Creams generating topical nitrogen oxides promoted healing in one small controlled trial [99]. Nitric oxide was also shown to kill *M. ulcerans in vitro* [100]. Phenytoin powder probably does not kill the organism, but it appeared to promote healing, perhaps through acceleration of fibrogenesis [101]. Taking advantage of the temperature sensitivity of *M. ulcerans*, localized application of heat to lesions has been reported to help healing [102]. An optimized topical treatment using effective antibiotics or other anti-mycobacterial agents [103] could be a solution to avoid the orally administration of antibiotics.

Disease prevention with an effective vaccine would be the most effective solution. From the above arguments, it appears that an effective vaccine for Buruli ulcer should prime an individual to mount a strong specific Th1 response to enhance his ability to control initial bacilli inoculation. On the other hand, the induction of a neutralizing antibody against mycolactone, which is essential for virulence, should in essence disarm the pathogen and prevent it from causing disease. Such a strategy will only be effective if the toxin can be neutralized by specific antibody responses. Mycolactone, which has a polyketide structure, is not ideal for the generation of highly affine mAbs, unless chemically modified. Therefore there is still the need to identify highly immunogenic *M. ulcerans* antigens for both vaccine development and serodiagnosis.

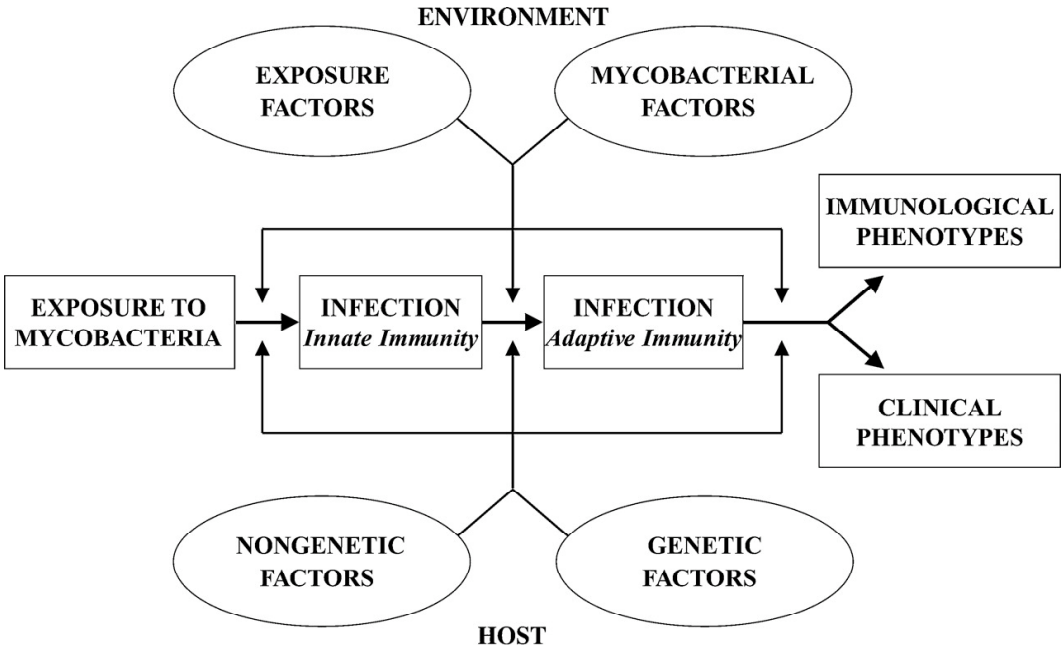

Figure 2 Various steps in the interaction between humans and mycobacteria. Exposure to mycobacteria does not always result in infection. Whether or not an established infection develops depends on innate immunity, alone or in conjunction with adaptive immunity. Immunological and clinical phenotypes may be detectable once mycobacterial infection is established and adaptive immunity to mycobacteria is involved. Each of the three steps in this process is under host and environmental control. Host factors may be genetic (e.g., mutation in a gene involved in immunity to mycobacteria) or nongenetic (e.g., skin lesion) and may have an impact at each stage of the interaction. Environmental factors may be mycobacterial (e.g., virulence factors) or related to the mode of exposure (e.g., direct inoculation) and may have an impact at each stage of the interaction.

Casanova and Abel *Annu. Rev. Immunol.* 2002

5.4 References

1. Keilholz U, Martus P, Scheibenbogen C: Immune monitoring of T-cell responses in cancer vaccine development. *Clin Cancer Res* 2006, 12:2346s-2352s.
2. Kanto T, Hayashi N: Measuring immunity in viral hepatitis. *J Gastroenterol* 2004, 39:709-716.
3. McElhaney JE: The unmet need in the elderly: designing new influenza vaccines for older adults. *Vaccine* 2005, 23 Suppl 1:S10-25.
4. Keilholz U, Weber J, Finke JH, Gabrilovich DI, Kast WM, Disis ML, Kirkwood JM, Scheibenbogen C, Schlom J, Maino VC, et al.: Immunologic monitoring of cancer vaccine therapy: results of a workshop sponsored by the Society for Biological Therapy. *J Immunother* 2002, 25:97-138.
5. Scheibenbogen C, Letsch A, Schmittel A, Asemissen AM, Thiel E, Keilholz U: Rational peptide-based tumour vaccine development and T cell monitoring. *Semin Cancer Biol* 2003, 13:423-429.
6. Letsch A, Keilholz U, Kern F, Asemissen AM, Thiel E, Scheibenbogen C: Specific central memory T cells in the bone marrow of patients immunized against tyrosinase peptides. *J Immunother* 2006, 29:201-207.
7. Mwau M, McMichael AJ, Hanke T: Design and validation of an enzyme-linked immunospot assay for use in clinical trials of candidate HIV vaccines. *AIDS Res Hum Retroviruses* 2002, 18:611-618.
8. McCutcheon M, Wehner N, Wensky A, Kushner M, Doan S, Hsiao L, Calabresi P, Ha T, Tran TV, Tate KM, et al.: A sensitive ELISPOT assay to detect low-frequency human T lymphocytes. *J Immunol Methods* 1997, 210:149-166.
9. Kalyuzhny AE: Chemistry and biology of the ELISPOT assay. *Methods Mol Biol* 2005, 302:15-31.
10. John CC, Moormann AM, Sumba PO, Ofulla AV, Pregibon DC, Kazura JW: Gamma interferon responses to Plasmodium falciparum liver-stage antigen 1 and thrombospondin-related adhesive protein and their relationship to age, transmission intensity, and protection against malaria. *Infect Immun* 2004, 72:5135-5142.
11. Keating SM, Bejon P, Berthoud T, Vuola JM, Todryk S, Webster DP, Dunachie SJ, Moorthy VS, McConkey SJ, Gilbert SC, et al.: Durable human memory T cells quantifiable by cultured enzyme-linked immunospot assays are induced by heterologous prime boost immunization and correlate with protection against malaria. *J Immunol* 2005, 175:5675-5680.
12. Lanzavecchia A, Sallusto F: Understanding the generation and function of memory T cell subsets. *Curr Opin Immunol* 2005, 17:326-332.
13. Hickling JK: Measuring human T-lymphocyte function. *Expert Rev Mol Med* 1998, 1998:1-20.
14. Herr W, Linn B, Leister N, Wandel E, Meyer zum Buschenfelde KH, Wolfel T: The use of computer-assisted video image analysis for the quantification of CD8+ T lymphocytes producing tumor necrosis factor alpha spots in response to peptide antigens. *J Immunol Methods* 1997, 203:141-152.
15. Hernandez-Fuentes MP, Warrens AN, Lechler RI: Immunologic monitoring. *Immunol Rev* 2003, 196:247-264.
16. Ghanekar SA, Maecker HT: Cytokine flow cytometry: multiparametric approach to immune function analysis. *Cytotherapy* 2003, 5:1-6.
17. Daubenberger CA, Nickel B, Ciatto C, Grutter MG, Poltl-Frank F, Rossi L, Siegler U, Robinson J, Kashala O, Patarroyo ME, et al.: Amino acid

dimorphism and parasite immune evasion: cellular immune responses to a promiscuous epitope of Plasmodium falciparum merozoite surface protein 1 displaying dimorphic amino acid polymorphism are highly constrained. *Eur J Immunol* 2002, 32:3667-3677.
18. Bastian M, Lozano JM, Patarroyo ME, Pluschke G, Daubenberger CA: Characterization of a reduced peptide bond analogue of a promiscuous CD4 T cell epitope derived from the Plasmodium falciparum malaria vaccine candidate merozoite surface protein 1. *Mol Immunol* 2004, 41:775-784.
19. Good MF: Vaccine-induced immunity to malaria parasites and the need for novel strategies. *Trends Parasitol* 2005, 21:29-34.
20. Moorthy VS, Good MF, Hill AV: Malaria vaccine developments. *Lancet* 2004, 363:150-156.
21. Good MF, Stanisic D, Xu H, Elliott S, Wykes M: The immunological challenge to developing a vaccine to the blood stages of malaria parasites. *Immunol Rev* 2004, 201:254-267.
22. Bachmann MF, Zinkernagel RM, Oxenius A: Immune responses in the absence of costimulation: viruses know the trick. *J Immunol* 1998, 161:5791-5794.
23. Huckriede A, Bungener L, Daemen T, Wilschut J: Influenza virosomes in vaccine development. *Methods Enzymol* 2003, 373:74-91.
24. Aichele P, Brduscha-Riem K, Zinkernagel RM, Hengartner H, Pircher H: T cell priming versus T cell tolerance induced by synthetic peptides. *J Exp Med* 1995, 182:261-266.
25. Moreno R, Jiang L, Moehle K, Zurbriggen R, Gluck R, Robinson JA, Pluschke G: Exploiting conformationally constrained peptidomimetics and an efficient human-compatible delivery system in synthetic vaccine design. *Chembiochem* 2001, 2:838-843.
26. Pfeiffer B, Peduzzi E, Moehle K, Zurbriggen R, Gluck R, Pluschke G, Robinson JA: A virosome-mimotope approach to synthetic vaccine design and optimization: synthesis, conformation, and immune recognition of a potential malaria-vaccine candidate. *Angew Chem Int Ed Engl* 2003, 42:2368-2371.
27. Mellman I, Steinman RM: Dendritic cells: specialized and regulated antigen processing machines. *Cell* 2001, 106:255-258.
28. Huckriede A, Bungener L, ter Veer W, Holtrop M, Daemen T, Palache AM, Wilschut J: Influenza virosomes: combining optimal presentation of hemagglutinin with immunopotentiating activity. *Vaccine* 2003, 21:925-931.
29. Saurwein-Teissl M, Zisterer K, Schmitt TL, Gluck R, Cryz S, Grubeck-Loebenstein B: Whole virus influenza vaccine activates dendritic cells (DC) and stimulates cytokine production by peripheral blood mononuclear cells (PBMC) while subunit vaccines support T cell proliferation. *Clin Exp Immunol* 1998, 114:271-276.
30. Jonuleit H, Schmitt E, Schuler G, Knop J, Enk AH: Induction of interleukin 10-producing, nonproliferating CD4(+) T cells with regulatory properties by repetitive stimulation with allogeneic immature human dendritic cells. *J Exp Med* 2000, 192:1213-1222.
31. Dhodapkar MV, Steinman RM, Krasovsky J, Munz C, Bhardwaj N: Antigen-specific inhibition of effector T cell function in humans after injection of immature dendritic cells. *J Exp Med* 2001, 193:233-238.
32. Schumacher R, Adamina M, Zurbriggen R, Bolli M, Padovan E, Zajac P, Heberer M, Spagnoli GC: Influenza virosomes enhance class I restricted CTL induction through CD4+ T cell activation. *Vaccine* 2004, 22:714-723.

33. Schumacher R, Amacker M, Neuhaus D, Rosenthal R, Groeper C, Heberer M, Spagnoli GC, Zurbriggen R, Adamina M: Efficient induction of tumoricidal cytotoxic T lymphocytes by HLA-A0201 restricted, melanoma associated, L(27)Melan-A/MART-1(26-35) peptide encapsulated into virosomes in vitro. *Vaccine* 2005, 23:5572-5582.
34. Hunziker IP, Grabscheid B, Zurbriggen R, Gluck R, Pichler WJ, Cerny A: In vitro studies of core peptide-bearing immunopotentiating reconstituted influenza virosomes as a non-live prototype vaccine against hepatitis C virus. *Int Immunol* 2002, 14:615-626.
35. Amacker M, Engler O, Kammer AR, Vadrucci S, Oberholzer D, Cerny A, Zurbriggen R: Peptide-loaded chimeric influenza virosomes for efficient in vivo induction of cytotoxic T cells. *Int Immunol* 2005, 17:695-704.
36. Ramachandra L, Chu RS, Askew D, Noss EH, Canaday DH, Potter NS, Johnsen A, Krieg AM, Nedrud JG, Boom WH, et al.: Phagocytic antigen processing and effects of microbial products on antigen processing and T-cell responses. *Immunol Rev* 1999, 168:217-239.
37. Straus SE: *Influenza and its virus*, vol Mechanism of Microbial Disease edn 3rd; 1998.
38. Swain SL, Agrewala JN, Brown DM, Jelley-Gibbs DM, Golech S, Huston G, Jones SC, Kamperschroer C, Lee WH, McKinstry KK, et al.: CD4+ T-cell memory: generation and multi-faceted roles for CD4+ T cells in protective immunity to influenza. *Immunol Rev* 2006, 211:8-22.
39. Sallusto F, Lenig D, Forster R, Lipp M, Lanzavecchia A: Two subsets of memory T lymphocytes with distinct homing potentials and effector functions. *Nature* 1999, 401:708-712.
40. Masopust D, Vezys V, Marzo AL, Lefrancois L: Preferential localization of effector memory cells in nonlymphoid tissue. *Science* 2001, 291:2413-2417.
41. Reinhardt RL, Khoruts A, Merica R, Zell T, Jenkins MK: Visualizing the generation of memory CD4 T cells in the whole body. *Nature* 2001, 410:101-105.
42. Rathmell JC, Thompson CB: Pathways of apoptosis in lymphocyte development, homeostasis, and disease. *Cell* 2002, 109 Suppl:S97-107.
43. Schluns KS, Lefrancois L: Cytokine control of memory T-cell development and survival. *Nat Rev Immunol* 2003, 3:269-279.
44. Kang I, Hong MS, Nolasco H, Park SH, Dan JM, Choi JY, Craft J: Age-associated change in the frequency of memory CD4+ T cells impairs long term CD4+ T cell responses to influenza vaccine. *J Immunol* 2004, 173:673-681.
45. Roman E, Miller E, Harmsen A, Wiley J, Von Andrian UH, Huston G, Swain SL: CD4 effector T cell subsets in the response to influenza: heterogeneity, migration, and function. *J Exp Med* 2002, 196:957-968.
46. Brown DM, Roman E, Swain SL: CD4 T cell responses to influenza infection. *Semin Immunol* 2004, 16:171-177.
47. Lucas M, Day CL, Wyer JR, Cunliffe SL, Loughry A, McMichael AJ, Klenerman P: Ex vivo phenotype and frequency of influenza virus-specific CD4 memory T cells. *J Virol* 2004, 78:7284-7287.
48. Danke NA, Kwok WW: HLA class II-restricted CD4+ T cell responses directed against influenza viral antigens postinfluenza vaccination. *J Immunol* 2003, 171:3163-3169.

49. Dercamp C, Sanchez V, Barrier J, Trannoy E, Guy B: Depletion of human NK and CD8 cells prior to in vitro H1N1 flu vaccine stimulation increases the number of gamma interferon-secreting cells compared to the initial undepleted population in an ELISPOT assay. *Clin Diagn Lab Immunol* 2002, 9:230-235.
50. Walker MR, Carson BD, Nepom GT, Ziegler SF, Buckner JH: De novo generation of antigen-specific CD4+CD25+ regulatory T cells from human CD4+CD25- cells. *Proc Natl Acad Sci U S A* 2005, 102:4103-4108.
51. Patke DS, Farber DL: Modulation of memory CD4 T cell function and survival potential by altering the strength of the recall stimulus. *J Immunol* 2005, 174:5433-5443.
52. Jelley-Gibbs DM, Dibble JP, Filipson S, Haynes L, Kemp RA, Swain SL: Repeated stimulation of CD4 effector T cells can limit their protective function. *J Exp Med* 2005, 201:1101-1112.
53. Aberle JH, Formann E, Steindl-Munda P, Weseslindtner L, Gurguta C, Perstinger G, Grilnberger E, Laferl H, Dienes HP, Popow-Kraupp T, et al.: Prospective study of viral clearance and CD4(+) T-cell response in acute hepatitis C primary infection and reinfection. *J Clin Virol* 2006, 36:24-31.
54. Ulsenheimer A, Lucas M, Seth NP, Tilman Gerlach J, Gruener NH, Loughry A, Pape GR, Wucherpfennig KW, Diepolder HM, Klenerman P: Transient immunological control during acute hepatitis C virus infection: ex vivo analysis of helper T-cell responses. *J Viral Hepat* 2006, 13:708-714.
55. Stevenson MM, Riley EM: Innate immunity to malaria. *Nat Rev Immunol* 2004, 4:169-180.
56. Favre N, Daubenberger C, Marfurt J, Moreno A, Patarroyo M, Pluschke G: Sequence and diversity of T-cell receptor alpha V, J, and C genes of the owl monkey Aotus nancymaae. *Immunogenetics* 1998, 48:253-259.
57. Vecino W, Daubenberger C, Rodriguez R, Moreno A, Patarroyo M, Pluschke G: Sequence and diversity of T-cell receptor beta-chain V and J genes of the owl monkey Aotus nancymaae. *Immunogenetics* 1999, 49:792-799.
58. Diaz OL, Daubenberger CA, Rodriguez R, Naegeli M, Moreno A, Patarroyo ME, Pluschke G: Immunoglobulin kappa light-chain V, J, and C gene sequences of the owl monkey Aotus nancymaae. *Immunogenetics* 2000, 51:212-218.
59. Diaz D, Naegeli M, Rodriguez R, Nino-Vasquez JJ, Moreno A, Patarroyo ME, Pluschke G, Daubenberger CA: Sequence and diversity of MHC DQA and DQB genes of the owl monkey Aotus nancymaae. *Immunogenetics* 2000, 51:528-537.
60. Diaz D, Daubenberger CA, Zalac T, Rodriguez R, Patarroyo ME: Sequence and expression of MHC-DPB1 molecules of the New World monkey Aotus nancymaae, a primate model for Plasmodium falciparum. *Immunogenetics* 2002, 54:251-259.
61. Castillo F, Guerrero C, Trujillo E, Delgado G, Martinez P, Salazar LM, Barato P, Patarroyo ME, Parra-Lopez C: Identifying and structurally characterizing CD1b in Aotus nancymaae owl monkeys. *Immunogenetics* 2004, 56:480-489.
62. Daubenberger CA, Salomon M, Vecino W, Hubner B, Troll H, Rodriques R, Patarroyo ME, Pluschke G: Functional and structural similarity of V gamma 9V delta 2 T cells in humans and Aotus monkeys, a primate infection model for Plasmodium falciparum malaria. *J Immunol* 2001, 167:6421-6430.
63. Saalmuller A, Lunney JK, Daubenberger C, Davis W, Fischer U, Gobel TW, Griebel P, Hollemweguer E, Lasco T, Meister R, et al.: Summary of the animal homologue section of HLDA8. *Cell Immunol* 2005, 236:51-58.

64. Herrera S, Perlaza BL, Bonelo A, Arevalo-Herrera M: Aotus monkeys: their great value for anti-malaria vaccines and drug testing. *Int J Parasitol* 2002, 32:1625-1635.
65. Klinman DM, Currie D, Gursel I, Verthelyi D: Use of CpG oligodeoxynucleotides as immune adjuvants. *Immunol Rev* 2004, 199:201-216.
66. Huckriede A, Bungener L, Stegmann T, Daemen T, Medema J, Palache AM, Wilschut J: The virosome concept for influenza vaccines. *Vaccine* 2005, 23 Suppl 1:S26-38.
67. Hemmi H, Takeuchi O, Kawai T, Kaisho T, Sato S, Sanjo H, Matsumoto M, Hoshino K, Wagner H, Takeda K, et al.: A Toll-like receptor recognizes bacterial DNA. *Nature* 2000, 408:740-745.
68. Hartmann G, Weeratna RD, Ballas ZK, Payette P, Blackwell S, Suparto I, Rasmussen WL, Waldschmidt M, Sajuthi D, Purcell RH, et al.: Delineation of a CpG phosphorothioate oligodeoxynucleotide for activating primate immune responses in vitro and in vivo. *J Immunol* 2000, 164:1617-1624.
69. Bauer S, Kirschning CJ, Hacker H, Redecke V, Hausmann S, Akira S, Wagner H, Lipford GB: Human TLR9 confers responsiveness to bacterial DNA via species-specific CpG motif recognition. *Proc Natl Acad Sci U S A* 2001, 98:9237-9242.
70. Coban C, Ishii KJ, Kawai T, Hemmi H, Sato S, Uematsu S, Yamamoto M, Takeuchi O, Itagaki S, Kumar N, et al.: Toll-like receptor 9 mediates innate immune activation by the malaria pigment hemozoin. *J Exp Med* 2005, 201:19-25.
71. Coban C, Ishii KJ, Sullivan DJ, Kumar N: Purified malaria pigment (hemozoin) enhances dendritic cell maturation and modulates the isotype of antibodies induced by a DNA vaccine. *Infect Immun* 2002, 70:3939-3943.
72. Pichyangkul S, Yongvanitchit K, Kum-arb U, Hemmi H, Akira S, Krieg AM, Heppner DG, Stewart VA, Hasegawa H, Looareesuwan S, et al.: Malaria blood stage parasites activate human plasmacytoid dendritic cells and murine dendritic cells through a Toll-like receptor 9-dependent pathway. *J Immunol* 2004, 172:4926-4933.
73. Skorokhod OA, Alessio M, Mordmuller B, Arese P, Schwarzer E: Hemozoin (malarial pigment) inhibits differentiation and maturation of human monocyte-derived dendritic cells: a peroxisome proliferator-activated receptor-gamma-mediated effect. *J Immunol* 2004, 173:4066-4074.
74. Millington OR, Di Lorenzo C, Phillips RS, Garside P, Brewer JM: Suppression of adaptive immunity to heterologous antigens during Plasmodium infection through hemozoin-induced failure of dendritic cell function. *J Biol* 2006, 5:5.
75. Whittle HC, Brown J, Marsh K, Greenwood BM, Seidelin P, Tighe H, Wedderburn L: T-cell control of Epstein-Barr virus-infected B cells is lost during P. falciparum malaria. *Nature* 1984, 312:449-450.
76. Mabey DC, Brown A, Greenwood BM: Plasmodium falciparum malaria and Salmonella infections in Gambian children. *J Infect Dis* 1987, 155:1319-1321.
77. Thursz MR, Kwiatkowski D, Allsopp CE, Greenwood BM, Thomas HC, Hill AV: Association between an MHC class II allele and clearance of hepatitis B virus in the Gambia. *N Engl J Med* 1995, 332:1065-1069.
78. Urban BC, Ferguson DJ, Pain A, Willcox N, Plebanski M, Austyn JM, Roberts DJ: Plasmodium falciparum-infected erythrocytes modulate the maturation of dendritic cells. *Nature* 1999, 400:73-77.

79. Wansbrough-Jones M, Phillips R: Buruli ulcer: emerging from obscurity. *Lancet* 2006, 367:1849-1858.
80. Prevot G, Bourreau E, Pascalis H, Pradinaud R, Tanghe A, Huygen K, Launois P: Differential production of systemic and intralesional gamma interferon and interleukin-10 in nodular and ulcerative forms of Buruli disease. *Infect Immun* 2004, 72:958-965.
81. Phillips R, Horsfield C, Kuijper S, Sarfo SF, Obeng-Baah J, Etuaful S, Nyamekye B, Awuah P, Nyarko KM, Osei-Sarpong F, et al.: Cytokine response to antigen stimulation of whole blood from patients with Mycobacterium ulcerans disease compared to that from patients with tuberculosis. *Clin Vaccine Immunol* 2006, 13:253-257.
82. George KM, Pascopella L, Welty DM, Small PL: A Mycobacterium ulcerans toxin, mycolactone, causes apoptosis in guinea pig ulcers and tissue culture cells. *Infect Immun* 2000, 68:877-883.
83. Pahlevan AA, Wright DJ, Andrews C, George KM, Small PL, Foxwell BM: The inhibitory action of Mycobacterium ulcerans soluble factor on monocyte/T cell cytokine production and NF-kappa B function. *J Immunol* 1999, 163:3928-3935.
84. Rondini S, Horsfield C, Mensah-Quainoo E, Junghanss T, Lucas S, Pluschke G: Contiguous spread of Mycobacterium ulcerans in Buruli ulcer lesions analysed by histopathology and real-time PCR quantification of mycobacterial DNA. *J Pathol* 2006, 208:119-128.
85. Okenu DM, Ofielu LO, Easley KA, Guarner J, Spotts Whitney EA, Raghunathan PL, Stienstra Y, Asamoa K, van der Werf TS, van der Graaf WT, et al.: Immunoglobulin M antibody responses to Mycobacterium ulcerans allow discrimination between cases of active Buruli ulcer disease and matched family controls in areas where the disease is endemic. *Clin Diagn Lab Immunol* 2004, 11:387-391.
86. Diaz D, Dobeli H, Yeboah-Manu D, Mensah-Quainoo DE, Friedlein A, Soder N, Rondini S, Bodmer T, Pluschke PG: Use of the immunodominant 18 kDa small heat shock protein as serological marker for exposure to M. ulcerans. *Clin Vaccine Immunol* 2006.
87. Casanova JL, Abel L: Genetic dissection of immunity to mycobacteria: the human model. *Annu Rev Immunol* 2002, 20:581-620.
88. Gooding TM, Johnson PD, Campbell DE, Hayman JA, Hartland EL, Kemp AS, Robins-Browne RM: Immune response to infection with Mycobacterium ulcerans. *Infect Immun* 2001, 69:1704-1707.
89. Gooding TM, Johnson PD, Smith M, Kemp AS, Robins-Browne RM: Cytokine profiles of patients infected with Mycobacterium ulcerans and unaffected household contacts. *Infect Immun* 2002, 70:5562-5567.
90. Gooding TM, Kemp AS, Robins-Browne RM, Smith M, Johnson PD: Acquired T-helper 1 lymphocyte anergy following infection with Mycobacterium ulcerans. *Clin Infect Dis* 2003, 36:1076-1077.
91. Oliveira MS, Fraga AG, Torrado E, Castro AG, Pereira JP, Filho AL, Milanezi F, Schmitt FC, Meyers WM, Portaels F, et al.: Infection with Mycobacterium ulcerans induces persistent inflammatory responses in mice. *Infect Immun* 2005, 73:6299-6310.
92. Hemmi H, Akira S: TLR signalling and the function of dendritic cells. *Chem Immunol Allergy* 2005, 86:120-135.

93. Jozsef L, Khreiss T, El Kebir D, Filep JG: Activation of TLR-9 induces IL-8 secretion through peroxynitrite signaling in human neutrophils. *J Immunol* 2006, 176:1195-1202.
94. Diehl S, Rincon M: The two faces of IL-6 on Th1/Th2 differentiation. *Mol Immunol* 2002, 39:531-536.
95. Nagabhushanam V, Solache A, Ting LM, Escaron CJ, Zhang JY, Ernst JD: Innate inhibition of adaptive immunity: Mycobacterium tuberculosis-induced IL-6 inhibits macrophage responses to IFN-gamma. *J Immunol* 2003, 171:4750-4757.
96. Klinman DM, Gursel I, Klaschik S, Dong L, Currie D, Shirota H: Therapeutic potential of oligonucleotides expressing immunosuppressive TTAGGG motifs. *Ann N Y Acad Sci* 2005, 1058:87-95.
97. Marshak-Rothstein A: Toll-like receptors in systemic autoimmune disease. *Nat Rev Immunol* 2006, 6:823-835.
98. Etuaful S, Carbonnelle B, Grosset J, Lucas S, Horsfield C, Phillips R, Evans M, Ofori-Adjei D, Klustse E, Owusu-Boateng J, et al.: Efficacy of the combination rifampin-streptomycin in preventing growth of Mycobacterium ulcerans in early lesions of Buruli ulcer in humans. *Antimicrob Agents Chemother* 2005, 49:3182-3186.
99. Phillips R, Adjei O, Lucas S, Benjamin N, Wansbrough-Jones M: Pilot randomized double-blind trial of treatment of Mycobacterium ulcerans disease (Buruli ulcer) with topical nitrogen oxides. *Antimicrob Agents Chemother* 2004, 48:2866-2870.
100. Phillips R, Kuijper S, Benjamin N, Wansbrough-Jones M, Wilks M, Kolk AH: In vitro killing of Mycobacterium ulcerans by acidified nitrite. *Antimicrob Agents Chemother* 2004, 48:3130-3132.
101. Adjei O, Evans MR, Asiedu A: Phenytoin in the treatment of Buruli ulcer. *Trans R Soc Trop Med Hyg* 1998, 92:108-109.
102. Meyers WM, Connor DH, McCullough B, Bourland J, Moris R, Proos L: Distribution of Mycobacterium ulcerans infections in Zaire, including the report of new foci. *Ann Soc Belg Med Trop* 1974, 54:147-157.
103. McNerney R, Traore H: Mycobacteriophage and their application to disease control. *J Appl Microbiol* 2005, 99:223-233.

Chapter 6

Appendix

Chapter 6.1

Raw data, supplementary figures and tables of the Phase Ia clinical trial (Chapter 3.2)

Phase Ia clinical trial (Chapter 3.2)

In this Chapter we report the protocol optimization, the ensemble of raw and processed data of the Phase Ia clinical trial illustrated in Chapter 3.2. Detailed final protocols of *ex vivo* IFNγ ELISpot and lymphoproliferation assays, the vaccine design and formulations are described in Chapter 3.2 (section Material and methods and Table I)

Ex vivo IFNγ-ELISpot, optimization of the pellet pre-incubation step

Fresh isolated PBMC were adjusted to 2 x 10 ^{6} cells/ml and pre-incubated for 24 h in 5 ml polypropylene round-bottom tube (pellet pre-incubation step [1]) at 37 °C, 5 % CO_2 humified atmosphere with 1μg/ml tetanus toxoid (TT). The stimulated cells were transferred on the coated ELISpot plate either directly or by decanting the medium after centrifugation, and incubated at 37 °C for further 20 h. Significantly higher numbers of spots were obtained by changing the medium. A decanting step was therefore adopted for the entire trial with the following antigens: Phytohämagglutinin (PHA), TT, influenza antigens, malaria peptides (UK40, AMA49-C1)

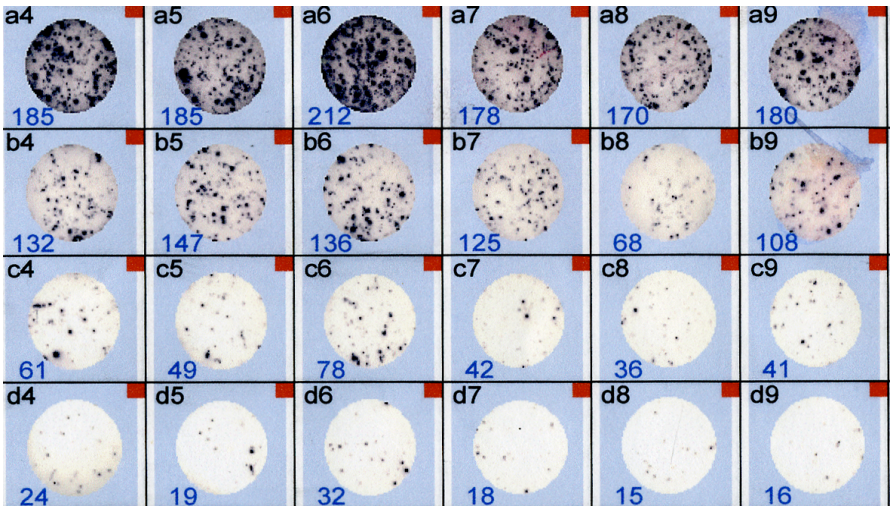

Figure 1 Example of *ex vivo* IFNγ ELISpot results obtained after decanting- or directly-transfer to ELISpot plate of pellet pre-incubated PBMC. Fresh isolated PBMC of Volunteer A were stimulated with 1 μg/ml TT for 24 h, decanted (Columns 4-6) or transferred directly (Columns 7-9) to the IFNγ coated ELISpot plate. Rows: a) 2 x 10^5 cells/well; b) 1 x 10^5 cells/well; c) 0.5 x 10^5 cells/well; d) 0.25 10^5 cells/well

Ex vivo IFNγ ELISpot, plate-layout (Phase Ia clinical trial)

	1-3	4-6	7-9	10-12
A	2x10^5 c/well + **IRIV**	2x10^5 c/well + **w/o S**	2x10^5 c/well + **IRIV**	2x10^5 c/well + **w/o S**
B	1x10^5 c/well + **IRIV**	1x10^5 c/well + **w/o S**	1x10^5 c/well + **IRIV**	1x10^5 c/well + **w/o S**
C	0.5x10^5 c/well + **IRIV**	0.5x10^5 c/well + **w/o S**	0.5x10^5 c/well + **IRIV**	0.5x10^5 c/well + **w/o S**
D	0.25x10^5 c/well+ **IRIV**	0.25x10^5 c/well + **w/o S**	0.25x10^5 c/well+ **IRIV**	0.25x10^5 c/well + **w/o S**
E	2x10^5 c/well + **UK40**	2x10^5 c/well + **AMA49-C1**	2x10^5 c/well + **UK40**	2x10^5 c/well + **AMA49-C1**
F	1x10^5 c/well + **UK 40**	1x10^5 c/well+ **AMA49-C1**	1x10^5 c/well + **UK 40**	1x10^5 c/well+ **AMA49-C1**
G	2x10^5 c/well + **TT**		2x10^5 c/well + **TT**	
H	2x10^5 c/well+ **PHA-P**		2x10^5 c/well+ **PHA-P**	

a)

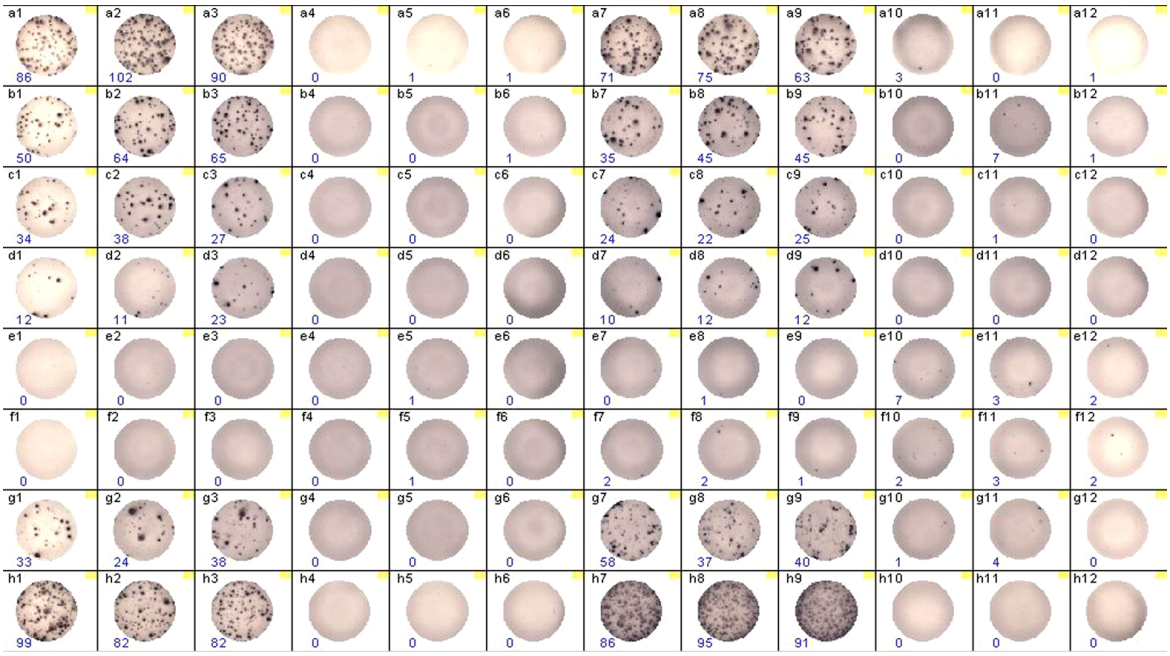

b)

Figure 2 a) *ex vivo* IFNγ ELISpot plate-layout used during the Phase Ia clinical trial (November 2003-November 2004). Volunteer x (Columns 1-6), Volunteer y (Columns 7-12, evidenced in blue). w/o S: PBMC incubated only with cell culture medium, without any Ag-stimulus. b) Example of a developed *ex vivo* IFNγ ELISpot plate. Columns 1-6, fresh isolated PBMC of Volunteer #42 21 days after the 2nd immunization, vaccine formulation: group 6 (IRIV). Columns: 7-12, fresh isolated PBMC of Volunteer #39 21 days after the 2nd immunization, vaccine formulation: group 5 (AMA49-CPE&UK40).

Ex vivo IFNγ ELISpot assessment with inactivated influenza ($H1N1_{Sing/A}$) PBMC stimulation

The measured influenza specific T cell response was an optimal positive control for the validity of the ELISpot assay and the chance to monitor on a large scale the pre-existing inactivated influenza $H1N1_{Sing/A}$ specific effector memory CD4 T cells response in Caucasian healthy volunteers.

Stimulation of inactivated influenza specific CD8 negative T cells

Prior to clinical trial begin the stimulation of total PBMC with TT and inactivated influenza was compared to CD4 and CD8 depleted cells stimulation. Fresh isolated PBMC of Volunteer B were divided in three groups: (i) total PBMC, (ii) CD8 depleted cells (incubation with anti-human CD8 mAb MicroBeads and depletion of labeled cells), (iii) CD4 depleted cells (incubation with anti-human CD4 mAb MicroBeads and depletion of labeled cells). Magnetic-labeling and depletion procedure were performed according to the manifactures instructions using LD columns and MidiMACS separator (Miltenyi Biotec, Germany). By harvesting the flow through with unlabeled cells a pure CD8 negative (CD8 depleted) or CD4 negative (CD4 depleted) population was ready for further Ag-stimulation and *in vitro* cultivation (Figure 3). The cells of the three groups were stimulated with TT and inactivated influenza (1 μg/ml and 40 μg/ml, respectively) for 24 h. CD4 depletion induced a dramatic decrease in spot numbers; on the contrary CD8 depletion induced an increase in spot numbers compared to the whole PBMC (Figure 3c). These results were consistent with published results [2] and were important to evaluate the influenza stimulation of the whole PBMC during the trial.

Optimal concentration of influenza antigens-stimulated cells

To better assess the ELISpot assay validity, the influenza stimulation was performed with four different cell concentrations ($2x10^5$, $1x10^5$, $0.5x10^5$ and $0.25x10^5$, respectively). The obtained curves of each Volunteer are illustrated in Figures 4-7 (ordered per vaccine formulation group and immunization time-point). Missing 2 $x10^5$ cells/well values indicate that the wells were not countable by the AID ELISpot-reader (too many overlapping spots). For further analysis of influenza ELISpot data only the 1 x 10^5 cells/well concentration was considerate because the spot were always distinct and countable by the AID reader and the curve plateau was not reached.

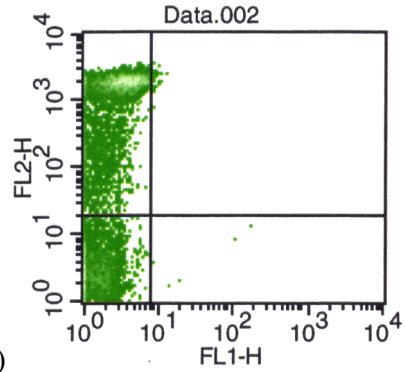

a)

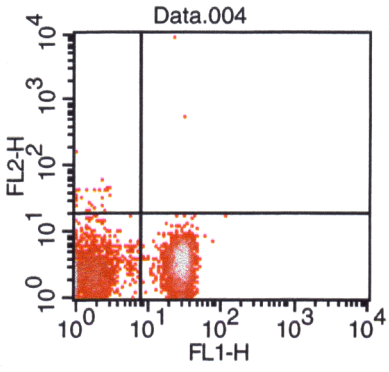

b)

	1-3	4-6	7-9	10-12
A	**2x10^5 c/well + w/o**	**2x10^5 c/well + w/o**	**2x10^5 c/well + w/o**	
B	**1x10^5 c/well + w/o**	**1x10^5 c/well + w/o**	**1x10^5 c/well + w/o**	
C	**2x10^5 c/well + IRIV**	**2x10^5 c/well + IRIV**	**2x10^5 c/well + IRIV**	
D	**1x10^5 c/well+ IRIV**	**1x10^5 c/well+ IRIV**	**1x10^5 c/well+ IRIV**	
E	**2x10^5 c/well + TT**	**2x10^5 c/well + TT**	**2x10^5 c/well + TT**	
F	**1x10^5 c/well+ TT**	**1x10^5 c/well+ TT**	**1x10^5 c/well+ TT**	
G				
H				

c) PBMC CD4 depletion CD8 depletion

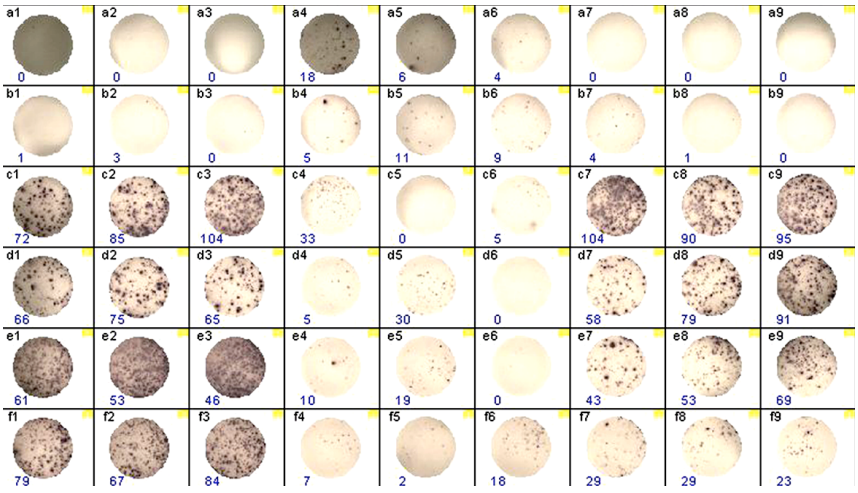

d)

Figure 3 Comparison of inactivated influenza and TT stimulation of total PBMC (black), CD4 depleted (green) and CD8 depleted (red) of Volunteer B. a-b) Double staining FACS control with FITC-labeled anti-CD4 mAb (FL1) and PE-labeled anti-CD8 mAb (FL2) of a) collected CD4 negative cells of CD4 depletion column b) collected CD8 negative of CD8 depletion column. Total PBMC and the collected cells were further stimulated with 40 µg/ml inactivated influenza or 10 µg/ml TT and analysed in *ex vivo* IFNγ ELISpot c) plate-layout d) developed plate.

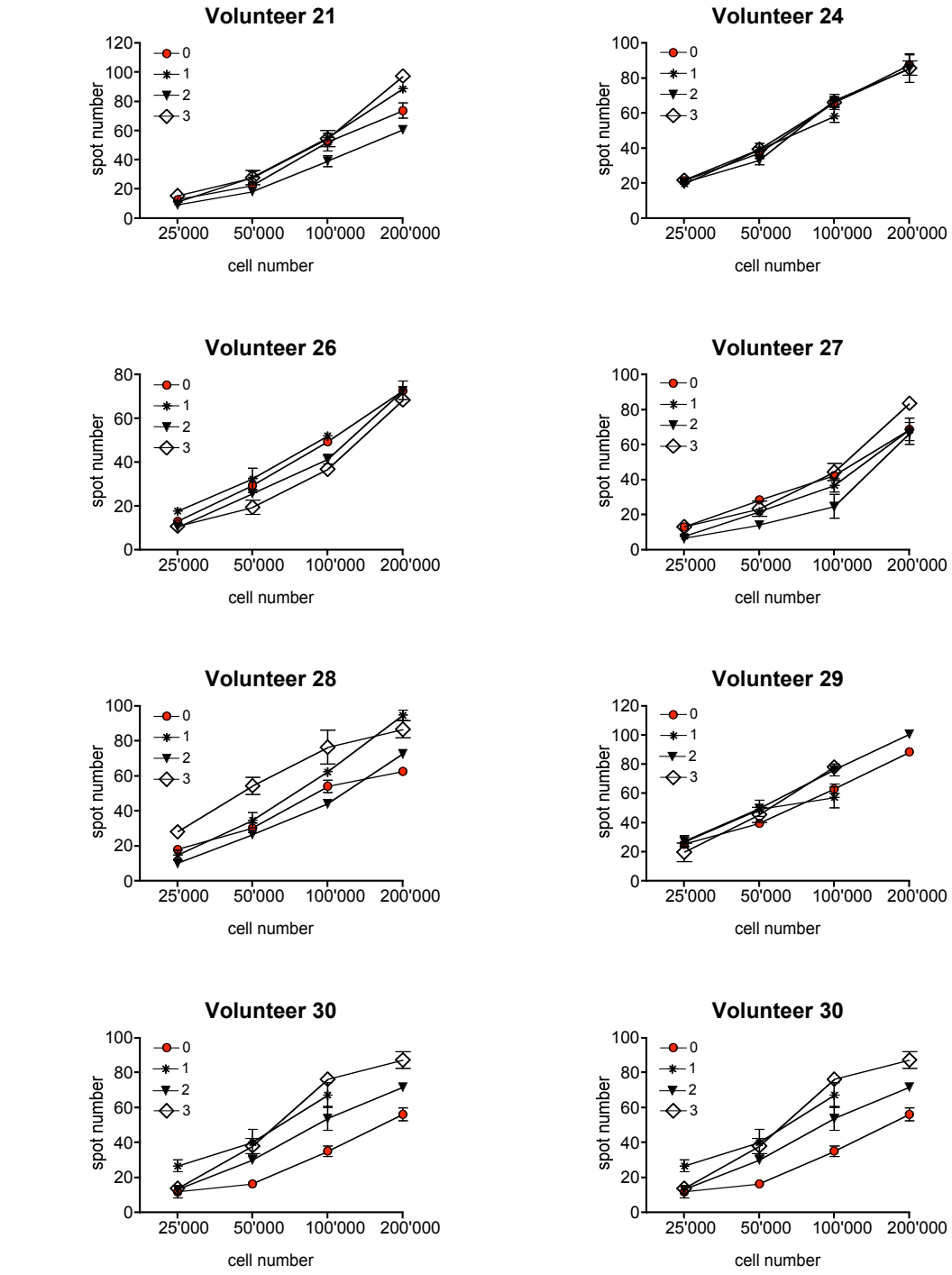

0 21 days post pre-immunization
1 21 days post 1st immunization
2 21 days post 2nd immunization
3 21 days post 3rd immunization

Figure 4. Summary of *ex vivo* IFNγ ELISpot results of fresh isolated PBMC stimulated with inactivated influenza (40 μg/ml); vaccine formulation group 3, 50 μg AMA49-CPE. Each point of the curves represents the triplicate- arithmetic mean of each cell concentra tion with the correspondent standard error mean (SEM).

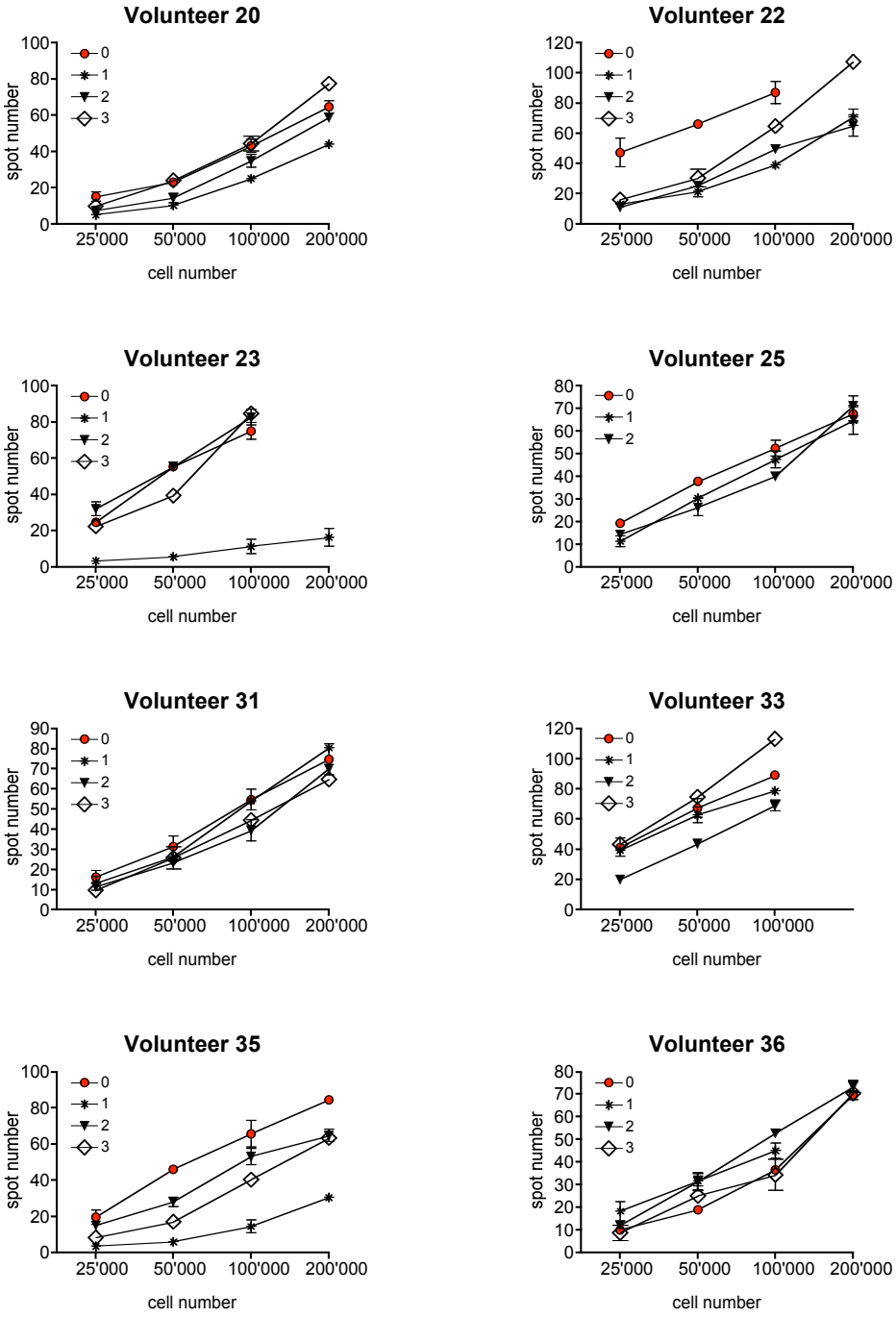

0 21 days post pre-immunization
1 21 days post 1st immunization
2 21 days post 2nd immunization
3 21 days post 3rd immunization

Figure 5 Summary of *ex vivo* IFNγ ELISpot results of fresh isolated PBMC stimulated with inactivated influenza (40 μg/ml); vaccine formulation group 4, 50 μg UK39. Each point of the curves represents the triplicate- arithmetic mean of each cell concentration with the correspondent SEM.

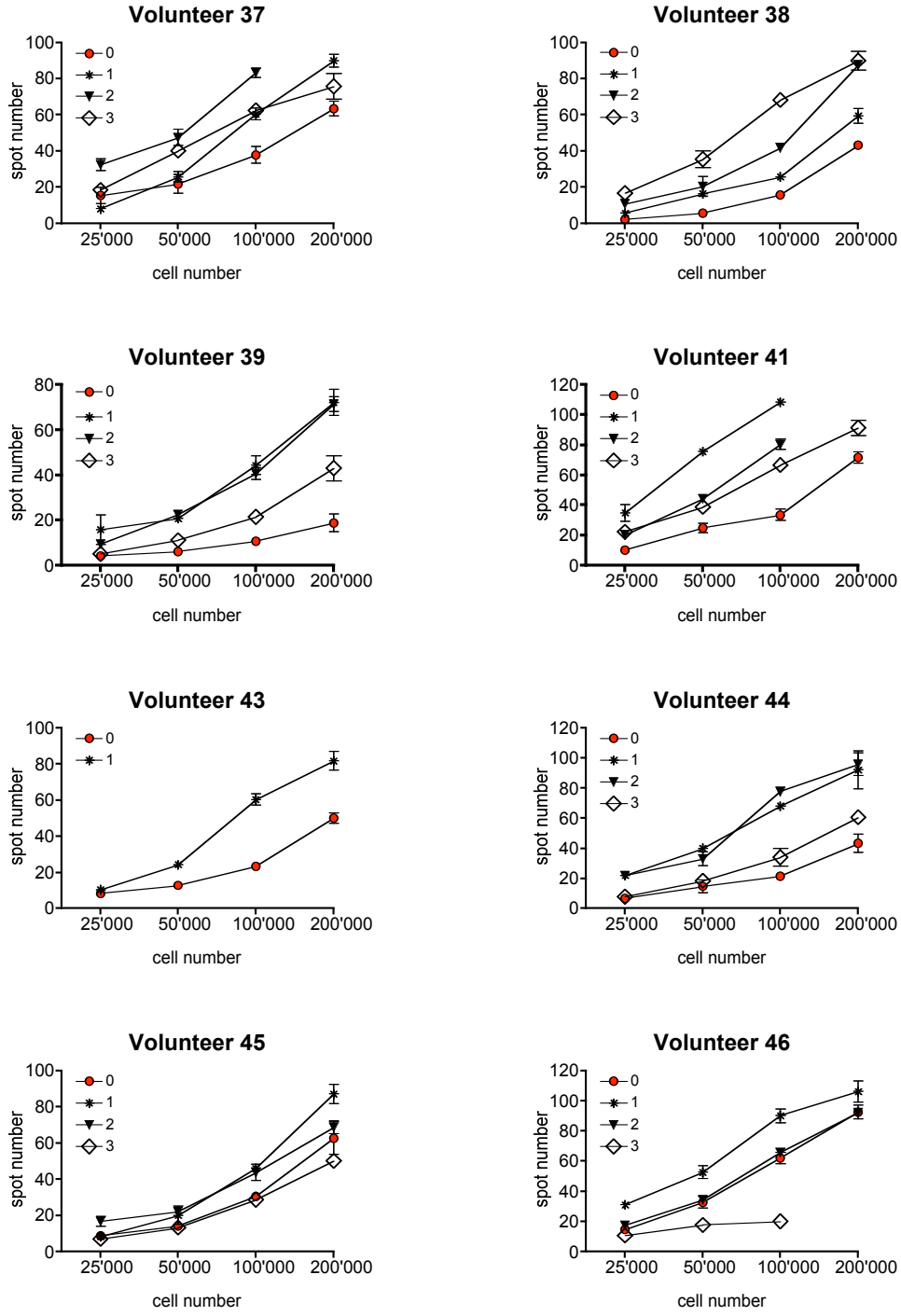

0 21 days post pre-immunization
1 21 days post 1st immunization
2 21 days post 2nd immunization
3 21 days post 3rd immunization

Figure 6 Summary of *ex vivo* IFNγ ELISpot results of fresh isolated PBMC stimulated with inactivated influenza (40 µg/ml); vaccine formulation group 5, 50 µg AMA49-CPE&UK39 immunization. Each point of the curves represents the triplicate- arithmetic mean of each cell concentration with the correspondent SEM.

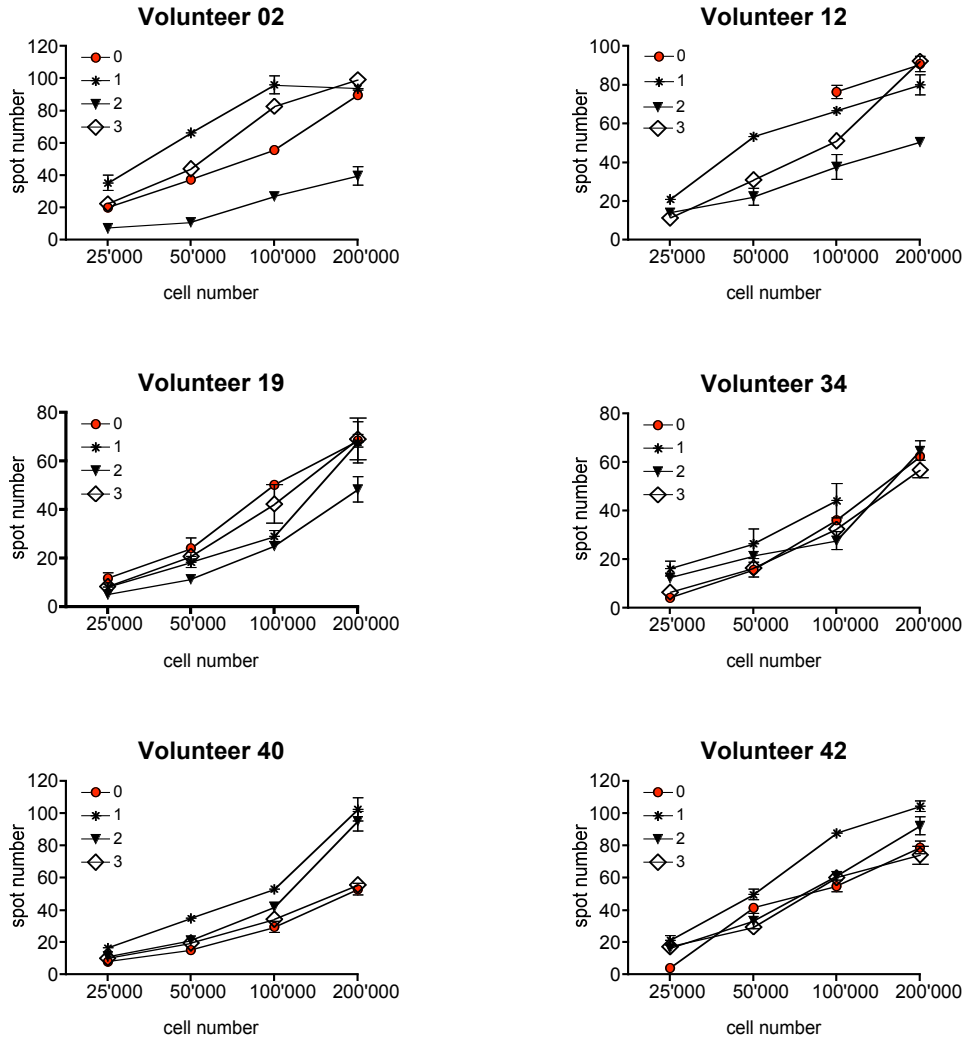

0 21 days post pre-immunization
1 21 days post 1st immunization
2 21 days post 2nd immunization
3 21 days post 3rd immunization

Figure 7 Summary of *ex vivo* IFNγ ELISpot results of fresh isolated PBMC stimulated with inactivated influenza (40 µg/ml); vaccine formulation group group 6, IRIV (placebo). Each point of the curves represents the triplicate- arithmetic mean of each cell concentration with the correspondent SEM.

Raw data Phase Ia clinical trial

Tables I-IV: ex vivo IFNγ ELISpot and lymphoproliferation raw data

Arithmetic means of triplicates with the correspondent standard deviation are reported in the tables I-IV by volunteer, immunization time-point and vaccine formulation and assay.

Lymphoproliferation data are given in counts per minuts (cpm), (LKB-Wallac counter, Sweden)

[Usually, Background counts (not stimulated cells) can range from 160 to 2'000 cpm. Range of counts for immunological recall to complex antigens (for example BCG and TT) are 5'000 to 100'000 counts per minute [3]]

Ex vivo IFNγ ELISpot data are given in spot forming units (SFU) per well (AID-reader system, Germany) using always the same settings. Only raw data of the optimal cell concentration are reported:

100'000 cells/well for inactivated influenza stimulation

200'000 cells/well for malaria peptide stimulation

Figures 8-9: ex vivo IFNγ ELISpot and lymphoproliferation processed data

Lymphoproliferation (Figure 7): Stimulation Index (SI) was calculated by dividing the stimulated vs unstimulated arithmetic mean values.

A response is typically considered positive when a SI > 2 is found [3].

Ex vivo IFNγ ELISpot (Figure 8): The negative control arithmetic mean (not stimulated cells) was subtracted from the positive arithmetic mean (stimulated cells).

References

1. Schmittel A, Keilholz U, Bauer S, Kuhne U, Stevanovic S, Thiel E, Scheibenbogen C: Application of the IFN-gamma ELISPOT assay to quantify T cell responses against proteins. *J Immunol Methods* 2001, 247:17-24.
2. Dercamp C, Sanchez V, Barrier J, Trannoy E, Guy B: Depletion of human NK and CD8 cells prior to in vitro H1N1 flu vaccine stimulation increases the number of gamma interferon-secreting cells compared to the initial undepleted population in an ELISPOT assay. *Clin Diagn Lab Immunol* 2002, 9:230-235.
3. Quakyi IA, Ahlers JD: Assessing CD4+ helper T-lymphocyte responses by lymphoproliferation. *Methods Mol Med* 2002, 72:369-383.

Table 1: Raw data summary of Group 3, PEV 301 (AMA-CPE peptide)

virosome-formulated vaccine incorporating the **AMA-1** derived peptide conjugate **AMA49-CPE,** (n=8), dosis peptide: 50 μg/ml, dosis HA: 10 μg/ml

All assays were run in triplicate with fresh isolated PBMC

Assay:		**Proliferation** (cpm: counts per minute)								**IFN-gamma Elispot** (SFU: spot forming units)									
cell concentration:		*200'000 cells/well*								*100'000 cells/well*				*200'000 cells/well*					
		stimulus:								**stimulus:**									
Volunteer	Immunization	**w/o**	SD	**IRIV**	SD	**AMA-1**	SD	**CSP**	SD	**w/o**	SD	**IRIV**	SD	**w/o**	SD	**AMA-1**	SD	**CSP**	SD
21	0	6'154	1'539	86'183	7'872	4'791	188	3'730	821	2	1	52	11	4	2	3	1	38	0
	1	8'370	1'066	100'847	981	3'625	926	8'739	1'967	0	0	55	1	1	1	1	1	8	3
	2	1'754	590	49'448	2'523	507	150	893	158	1	1	39	7	1	1	1	1	1	1
	3	1'851	767	37'780	1'074	781	193	911	26	1	1	54	10	3	3	7	3	6	2
24	0	1'239	341	56'706	1'728	1'076	104	1'753	629	1	2	66	4	1	1	4	2	3	2
	1	4'438	637	15'278	2'200	1'543	310	1'831	212	0	0	58	6	0	1	6	0	1	1
	2	21'513	31'578	69'724	2'302	1'211	1'496	612	48	1	1	67	7	1	1	0	1	1	1
	3	331	30	32'100	1'988	214	9	244	46	1	1	66	6	1	1	7	3	4	2
26	0	3'746	429	85'242	4'786	1'678	140	1'821	180	0	1	49	3	1	2	1	1	3	2
	1	4'783	1'516	17'097	3'487	2'032	500	2'080	404	0	0	52	3	0	0	1	1	0	1
	2	5'369	4'829	55'107	3'628	2'089	1'897	1'674	683	5	3	41	4	5	1	0	0	1	1
	3	1'267	356	49'182	3'059	819	436	1'224	752	1	1	37	3	2	2	7	3	5	2
27	0	9'083	474	82'675	8'949	1'336	196	2'828	469	1	1	42	4	1	1	0	1	1	1
	1	2'706	669	35'108	1'560	3'219	181	2'433	1'076	0	0	37	7	1	1	1	1	1	1
	2	1'094	121	58'619	4'234	2'576	3'101	685	57	0	0	25	12	1	1	1	1	1	1
	3	1'993	354	49'432	3'370	617	183	504	107	0	0	44	8	0	1	0	1	0	1
28	0	6'390	429	61'555	5'070	2'224	1'101	3'781	1'941	5	1	54	6	9	4	5	1	12	4
	1	7'483	1'108	60'358	7'570	2'720	978	2'333	824	0	1	62	3	1	1	3	1	9	4
	2	1'361	54	37'179	2'861	2'202	322	1'380	396	0	0	44	2	1	1	0	1	0	1
	3	1'595	304	48'873	1'123	2'189	439	1'071	312	2	1	76	17	4	2	10	7	8	1
29	0	7'280	2'391	32'126	2'698	1'929	371	3'604	876	3	2	63	6	6	5	4	2	4	1
	1	6'859	646	19'400	7'421	5'898	1'243	3'796	1'362	1	1	57	13	1	2	3	2	2	0
	2	798	132	49'422	3'679	2860	1624	1'017	357	0	1	76	7	0	0	1	1	0	0
	3	4'796	417	44'915	1'965	674	207	1'444	899	1	1	78	7	2	2	4	2	2	1
30	0	3'169	416	106'880	3'949	1907	360	1'864	215	1	1	35	5	1	1	0	0	23	7
	1	4'840	306	47'712	8'570	9832	11528	2'689	562	0	1	67	12	1	1	2	1	1	1
	2	627	420	55'488	1'608	2538	2383	435	134	0	1	54	12	0	0	4	1	2	1
	3	754	205	52'666	2'177	490	229	1'138	606	1	1	76	5	2	2	6	2	1	1
32	0	4'515	1'045	93'031	4'757	1'572	698	1'925	503	0	0	63	10	0	1	1	0	2	2
	1	8'184	1'037	55'808	4'934	1'938	268	3'101	315	0	0	44	4	0	0	0	1	0	1
	2	5'667	1'728	31'041	7'404	4'127	1'743	3'894	687	2	1	74	15	1	1	1	1	5	2
	3	1'128	499	29'769	2'393	788	437	1'591	1'088	1	1	88	14	2	1	4	2	2	2

0 21 days post pre-immunization
1 21 days post 1st immunization
2 21 days post 2nd immunization
3 21 days post 3rd immunization

w/o: PBMC incubated without any stimulus
IRIV: PBMC incubated with inactivated Influenza A/Sing, 40 μg/ml HA (hemagglutinin)
AMA-1: PBMC incubated with AMA49-C1(AMA49-CPE without lipid anchor, 40 μg/ml
CSP: PBMC incubated with UK40 (UK39 without lipid anchor), 40 μg/ml

n.d.: not done
SD: standard deviation
* single
** duplicate

Table II: Raw data summary of Group 4, PEV 302 (UK39 peptide)

virosome-formulated vaccine incorporating the **CSP** derived peptide conjugate **UK39,** (n=8), dosis peptide: 50 μg/ml, dosis HA: 10 μg/ml

All assays were run in triplicate with fresh isolated PBMC

Assay:		**Proliferation** (cpm: counts per minute)								**IFN-gamma Elispot** (SFU: spot forming units)									
cell concentration:		*200'000 cells/well*								*100'000 cells/well*				*200'000 cells/well*					
		stimulus:								**stimulus:**									
Volunteer	Immunization	**w/o**	SD	**IRIV**	SD	**AMA-1**	SD	**CSP**	SD	**w/o**	SD	**IRIV**	SD	**w/o**	SD	**AMA-1**	SD	**CSP**	SD
20	0	3'667	615	82'531	9'473	848	152	789	46	1	2	43	6	3	2	2	2	42	9
	1	2'256	944	28'167	3'039	1'560	648	1'290	508	0	1	25	2	1	1	2	1	1	1
	2	1'121	458	59'725	3'791	568	425	1'122	345	0	1	35	6	1	0	2	3	2	1
	3	535	197	37'512	4'230	571	143	446	281	2	1	44	7	1	1	9	2	5	3
22	0	n.d		n.d		n.d		n.d		1	1	87	13	1	1	1	0	1	0
	1	1'234	24	16'454	1'560	2'388	1'157	2'390	213	0	1	39	5	1	1	1	1	1	1
	2	1'176	811	83'854	6'430	460	153	782	153	0	0	50	3	1	1	7	5	2	1
	3	395	31	61'281	2'600	374	27	363	25	1	1	65	7	2	2	4	3	1	1
23	0	**5080	1'009	**43097	4'039	**3221	1'157	**2460	176	2	1	75	8	2	2	6	1	4	3
	1	849	43	13'254	1'337	504	26	490	99	0	0	11	7	0	1	0	0	0	0
	2	1'016	667	47'057	4'104	548	78	2'341	1'856	1	1	83	8	1	2	3	2	1	1
	3	444	143	n.d		n.d		1'140	1'352	3	2	85	6	8	1	14	6	15	5
25	0	2'094	165	50'066	2'480	1'217	382	2'225	553	0	1	52	6	0	1	2	1	2	1
	1	1'240	397	14'059	2'750	916	125	1'868	431	1	1	47	6	0	0	2	1	1	1
	2	2'561	1'378	46'313	3'163	461	102	900	32	1	1	40	2	1	1	1	1	0	1
drop out	3																		
31	0	1'385	303	54'713	2'102	1'478	896	1'525	513	1	2	55	9	3	2	2	2	1	1
	1	1'758	214	75'400	1'439	603	84	1'932	362	0	1	54	1	0	1	2	2	1	1
	2	1'017	242	34'017	4'052	732	409	3'661	2'634	0	1	39	9	1	1	1	1	5	2
	3	407	30	29'454	6'806	288	49	465	344	3	2	44	4	6	4	5	2	5	3
33	0	5'043	550	38'088	1'017	7'169	1'552	4'667	537	0	1	89	3	1	1	1	1	0	1
	1	4'564	624	35'140	1'411	2'520	571	7'341	3'055	0	0	79	3	0	1	6	0	1	1
	2	1'754	942	338	313	688	680	499	130	1	1	69	6	1	1	0	1	1	1
	3	1'267	416	27'858	345	858	446	809	120	3	1	113	5	8	1	6	2	7	4
35	0	5'173	503	78'142	10'515	4655	366	4'520	605	8	3	66	13	4	2	3	2	42	11
	1	773	219	5'810	831	485	25	1'383	366	1	1	15	5	0	0	1	1	1	1
	2	3'116	760	59'249	10'190	3970	4703	1'355	103	0	0	53	8	0	1	1	1	0	0
	3	384	19	19'942	4'002	388	103	430	81	3	0	40	5	1	2	6	4	4	2
36	0	**4093	600	**12280	1'018	**1504	23	**2815	387	1	1	37	3	1	1	3	2	1	1
	1	11'203	632	20'886	8'734	4'932	2'172	2'677	57	0	0	45	6	0	1	1	1	0	0
	2	854	302	32'279	4'141	579	72	672	180	0	1	53	3	0	0	0	0	2	1
	3	646	226	16'922	1'651	275	59	240	20	1	1	34	12	3	3	9	6	5	6

0 21 days post pre-immunization
1 21 days post 1st immunization
2 21 days post 2nd immunization
3 21 days post 3rd immunization

w/o: PBMC incubated without any stimulus
IRIV: PBMC incubated with inactivated Influenza A/Sing, 40 μg/ml HA (hemagglutinin)
AMA-1: PBMC incubated with AMA49-C1(AMA49-CPE without lipid anchor, 40 μg/ml
CSP: PBMC incubated with UK40 (UK39 without lipid anchor), 40 μg/ml

n.d.: not done
SD: standard deviation
* single
** duplicate

Table III: Raw data summary of Group 5, PEV 301& PEV 302 (AMA-CPE & UK39- peptides)

virosome-formulated vaccine incorporating **AMA49-CPE & UK39,** (n=8), dosis peptide: 50 μg/ml, dosis HA: 20 μg/ml

All assays were run in triplicate with fresh isolated PBMC

Assay:		**Proliferation** (cpm: counts per minute)								**IFN-gamma Elispot** (SFU: spot forming units)									
cell concentration:		*200'000 cells/well*								*100'000 cells/well*				*200'000 cells/well*					
		stimulus:								**stimulus:**									
Volunteer	Immunization	**w/o**	SD	**IRIV**	SD	**AMA-1**	SD	**CSP**	SD	**w/o**	SD	**IRIV**	SD	**w/o**	SD	**AMA-1**	SD	**CSP**	SD
37	0	605	113	56'125	3'069	241	81	444	104	1	2	38	8	2	2	3	1	3	1
	1	329	59	60'453	4'735	1'325	1'849	303	45	0	1	60	6	0	0	0	1	0	1
	2	648	162	70'543	1'133	598	291	1'223	298	0	1	83	5	0	1	5	5	1	1
	3	371	60	**27603	2,7	339	56	308	27	0	0	62	2	0	0	1	1	1	1
38	0	395	63	16'703	3'780	455	352	389	86	0	1	16	4	1	1	4	18	2	2
	1	297	18	45'847	4'630	206	31	338	126	0	1	26	3	0	1	1	1	0	0
	2	459	11	67'783	2'820	747	456	337	134	0	1	42	1	0	1	1	2	0	1
	3	298	39	**16792	708	277	83	266	38	1	1	68	3	0	0	1	1	0	1
39	0	2'842	2'383	38'083	4'815	3'459	4'318	2'526	967	1	1	11	2	3	1	4	3	2	2
	1	995	311	53'548	1'128	4'369	2'800	5'731	1'813	1	1	44	7	0	1	1	1	16	11
	2	2'262	1'002	42'079	3'676	6'285	3'142	4'324	1'524	1	1	41	5	0	1	5	3	1	1
	3	2'778	641	*22779		**5181	1'648	1'204	577	1	2	21	5	1	2	2	1	0	1
41	0	799	385	51'110	8'860	1'195	1'326	386	2	2	1	33	7	2	1	3	5	6	3
	1	1'258	443	67'894	2'133	5'176	4'479	2'224	1'254	3	0	108	5	6	2	15	2	17	11
	2	1'541	260	70'564	1'211	4'180	1'486	1'574	644	1	1	80	6	1	0	3	2	2	2
	3	1'393	49	33'446	2'649	3'537	597	644	69	1	1	67	4	1	1	0	1	0	1
43	0	728	23	78'167	5'137	694	91	542	75	1	1	23	4	0	1	1	1	48	6
	1	239	18	45'745	2'857	856	1'170	251	9	0	0	60	6	1	1	1	2	1	1
drop out	2																		
	3																		
44	0	483	134	53'318	5'847	447	122	434	47	1	1	22	5	3	2	6	5	5	5
	1	730	76	65'535	4'330	627	253	1'333	1'077	1	1	68	3	4	5	12	4	8	2
	2	1'305	208	61'086	7'129	1'417	682	563	85	2	1	78	4	4	1	7	2	10	5
	3	311	39	4'903		399	111	310	68	2	1	34	10	2	1	0	0	0	1
45	0	498	80	41'777	4'107	525	24	441	62	2	1	31	4	6	1	10	12	18	11
	1	528	98	43'954	742	378	167	727	363	1	1	46	3	2	2	0	0	1	1
	2	560	135	52'611	2'195	940	430	457	50	0	0	44	8	2	3	0	1	1	2
	3	742	12	24'300	1'611	1'195	1'172	369	66	1	1	29	3	1	1	0	0	0	1
46	0	2'012	262	56'883	2'966	1'018	87	834	266	14	2	62	6	11	8	24	7	18	11
	1	575	102	39'865	2'574	1'352	898	404	27	0	1	90	8	1	1	2	1	1	1
	2	1'820	165	52'087	732	4'598	2'835	884	153	2	2	66	3	1	1	2	4	1	0
	3	760	65	n.d.		953	669	457	32	2	1	20	4	2	1	2	0	0	1

0 21 days post pre-immunization
1 21 days post 1st immunization
2 21 days post 2nd immunization
3 21 days post 3rd immunization

w/o: PBMC incubated without any stimulus
IRIV: PBMC incubated with inactivated Influenza A/Sing, 40 μg/ml HA (hemagglutinin)
AMA-1: PBMC incubated with AMA49-C1(AMA49-CPE without lipid anchor, 40 μg/ml
CSP: PBMC incubated with UK40 (UK39 without lipid anchor), 40 μg/ml

n.d.: not done
SD: standard deviation
* single
** duplicate

Table IV: Raw data summary of Group 6, IRIV (virosome)

virosome-formulated vaccine incorporating the **AMA-1** derived peptide conjugate **AMA49-CPE,** (n=8), dosis peptide: 50μg/ml, dosis HA: 10 μg/ml

All assays were run in triplicate with fresh isolated PBMC

Assay:		**Proliferation** (cpm: counts per minute)								**IFN-gamma Elispot** (SFU: spot forming units)							
cell concentration:		*200'000 cells/well*								*100'000 cells/well*				*200'000 cells/well*			
		stimulus:								**stimulus:**							
Volunteer	Immunization	**w/o**	SD	**IRIV**	SD	**AMA-1**	SD	**CSP**	SD	**w/o**	SD	**IRIV**	SD	**w/o**	SD	**AMA-1**	SD	**CSP**	SD
2	0	6'706	1'378	79'212	16'984	3'278	1'340	4'356	831	3	2	56	3	4	3	51	6	0	1
	1	6'045	1'441	73'407	4'291	4'664	236	6'153	899	45	4	96	10	65	13	55	10	82	9
	2	2'965	326	64'563	3'792	1'912	122	2'832	944	0	1	27	4	1	2	0	0	0	0
	3	3'617	786	63'396	7'518	1'328	402	1'078	159	1	0	83	3	1	1	0	1	1	1
12	0	2'667	594	46'466	15'712	4'229	2'389	3'127	802	2	3	76	6	4	4	43	11	35	8
	1	4'284	596	99'329	14'850	2'491	1'162	1'748	489	17	2	67	3	46	17	79	1	50	9
	2	3238	645	80'020	1'740	2'505	189	3'395	625	0	1	38	11	0	0	1	1	1	1
	3	425	63	39'083	5'891	321	32	330	58	0	1	51	4	3	3	8	2	3	2
19	0	5'600	468	62'376	18'077	4'043	3'618	n.d		2	2	50	2	5	3	5	2	3	2
	1	6'248	521	95'683	4'053	1'268	275	1'918	690	1	1	29	4	1	1	1	1	2	2
	2	457	144	44'203	4'471	470	49	1'725	1'564	0	0	25	3	1	0	0	0	1	1
	3	960	683	43'958	986	2'006	2'767	649	95	1	1	42	14	2	1	4	2	2	2
34	0	4'900	1'359	89'587	5'826	9'669	2'963	3'912	234	0	0	36	0	1	1	0	0	1	0
	1	2'519	207	37'800	2'193	1'889	195	4'231	488	1	1	44	12	0	0	0	1	0	1
	2	13'364	1'193	74'570	10'821	10'155	6'100	7'632	877	2	1	28	6	1	1	1	1	1	1
	3	3'840	749	35'990	2'707	2'462	269	3'703	434	3	2	32	5	2	0	6	6	4	3
40	0	982	1'047	47'739	5'779	2'320	551	406	58	1	1	30	6	1	1	13	12	8	3
	1	420	31	54'905	2'428	506	77	440	15	1	0	53	4	0	1	0	0	0	1
	2	1'859	233	50'906	2'422	1'290	787	580	61	1	1	42	2	1	1	3	4	2	2
	3	653	62	19'552	1'524	543	283	456	65	1	1	34	3	1	1	1	1	0	1
42	0	532	90	62'459	1'660	519	195	537	187	1	1	55	6	3	2	6	2	4	1
	1	861	772	50'117	5'437	256	44	305	70	0	0	88	3	0	0	1	2	1	1
	2	449	51	55'808	2'858	529	224	1'640	641	1	1	61	3	0	1	0	1	0	1
	3	296	11	*17190		269	10	363	89	2	1	60	7	2	1	0	0	0	1

0 21 days post pre-immunization
1 21 days post 1st immunization
2 21 days post 2nd immunization
3 21 days post 3rd immunization

w/o: PBMC incubated without any stimulus
IRIV: PBMC incubated with inactivated Influenza A/Sing, 40 μg/ml HA (hemagglutinin)
AMA-1: PBMC incubated with AMA49-C1(AMA49-CPE without lipid anchor, 40 μg/ml
CSP: PBMC incubated with UK40 (UK39 without lipid anchor), 40 μg/ml

n.d.: not done
SD: standard deviation
* single
** duplicate

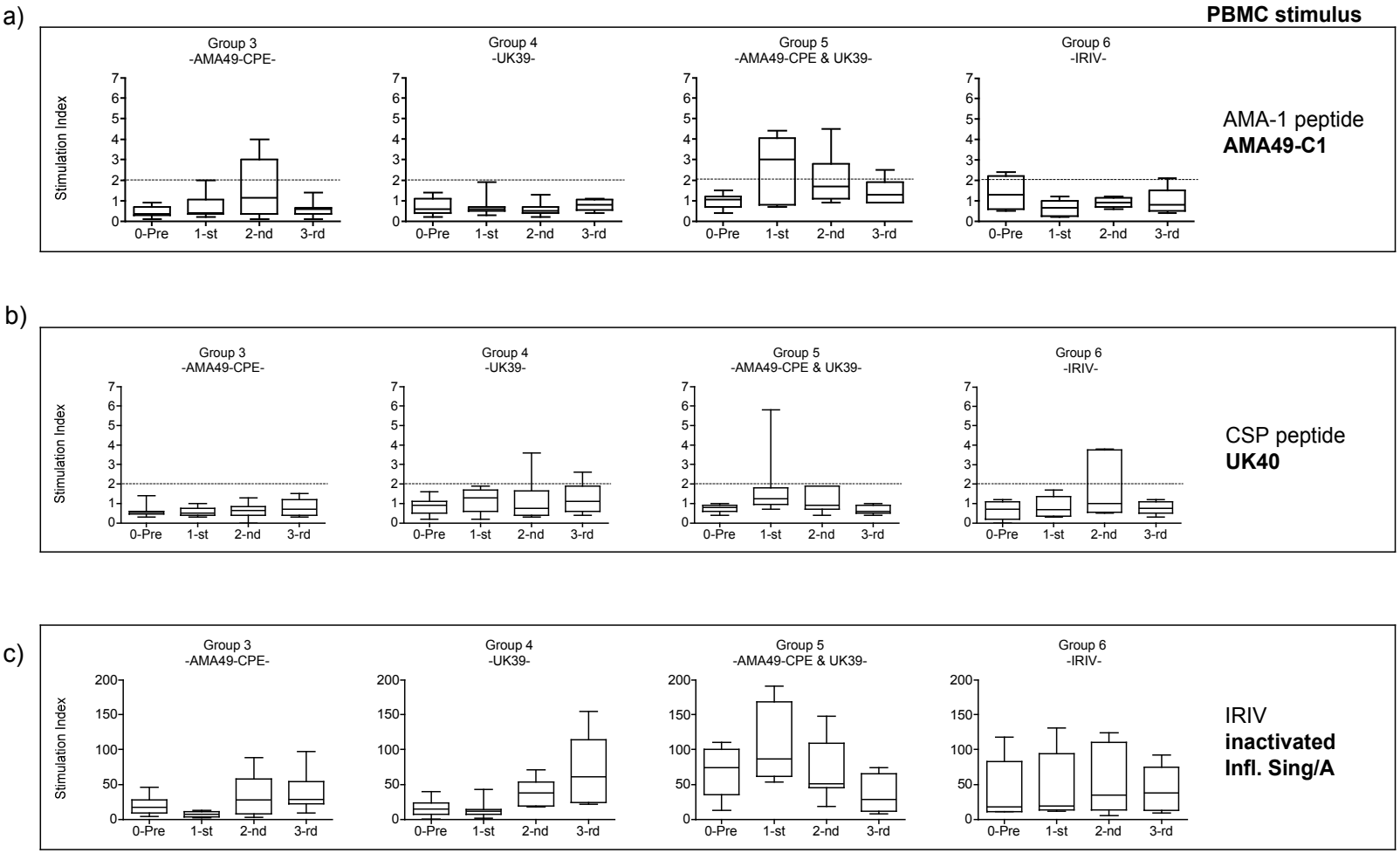

Figure 8 Summary of lymphoproliferation results considering the different immunization groups. Boxes show the distribution of results, the resting line indicating median response, upper and lower box boundaries showing 25th and 75th centiles, and the whiskers show adjacent values

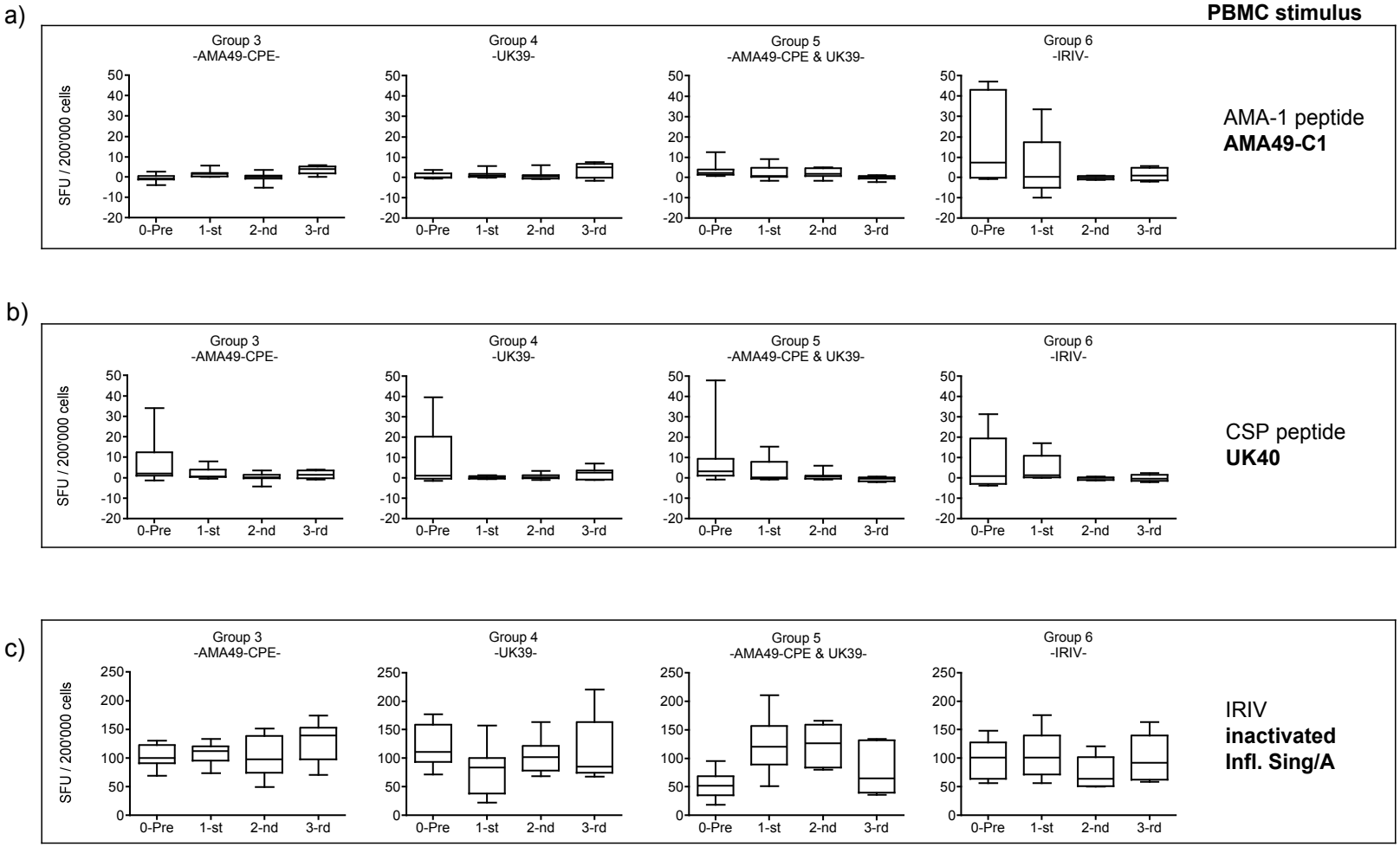

Figure 9 Summary of *ex vivo* IFN-γ ELISpot results considering the different immunization groups. Boxes show the distribution of results, the resting line indicating median response, upper and lower box boundaries showing 25th and 75th centiles, and the whiskers show adjacent values

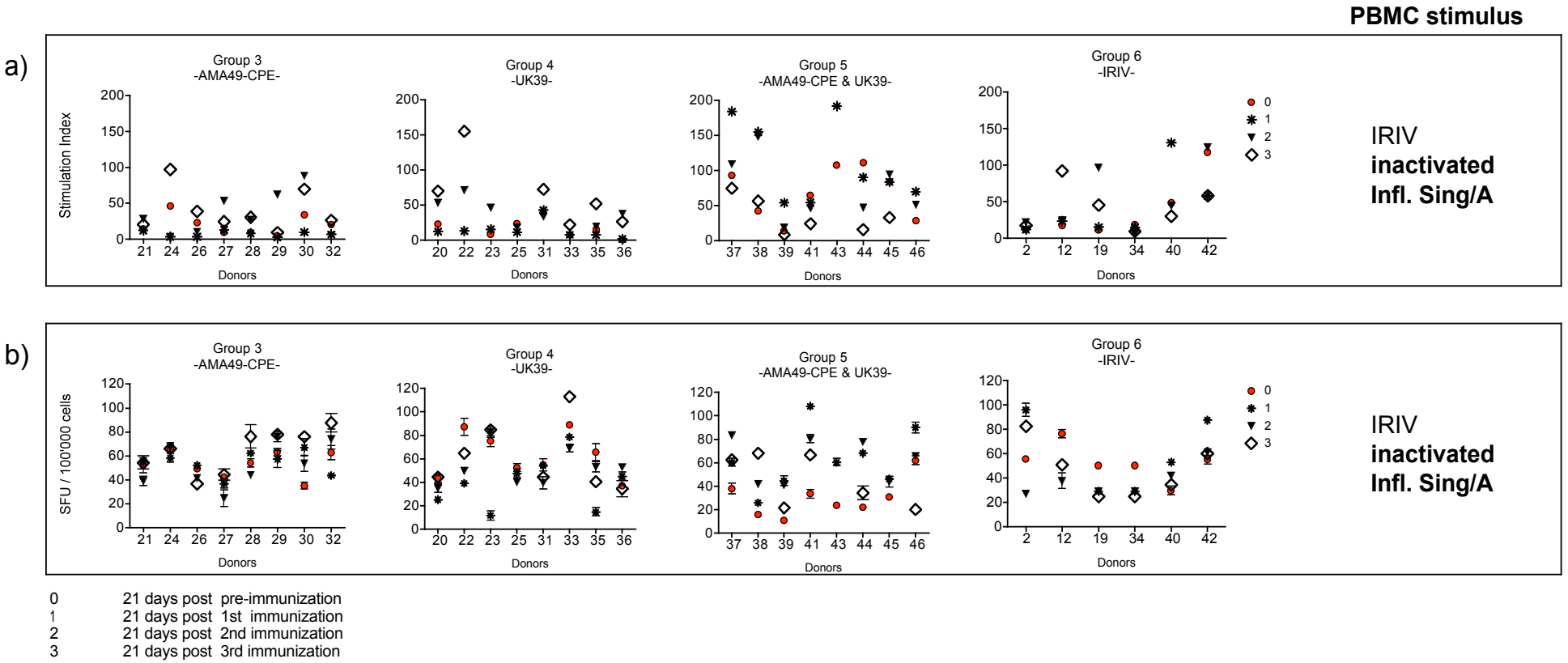

Figure 10 Overview of inactivated influenza lymphoproliferation and *ex vivo* ELISpot results (y-axes) at a single volunteers level (x-axes) by immunization time-point and vaccine formulation group

Chapter 6.2

Preliminary *in vitro* immunological studies with a *M. ulcerans* CpG ODN

Elisabetta Peduzzi [1], Célia Groeper [2], Paul Zajac [2], Giulio C. Spagnoli [2], Claudia A. Daubenberger [1]

[1] Swiss Tropical Institute, Department of Medical Parasitology and Molecular Immunology, Basel, Switzerland

[2] Institut für Chirurgische Forschung und Spitalmanagement, Basel University Hospital, Basel, Switzerland

Background

In Chapter 4.2 we showed a local activation of the innate immune system in Buruli ulcer lesions. The mRNA of plasmacytoid DC (P-DC) and myeloid DC (M-DC) specific surface markers (CD123 and CD11c, respectively) was detected by quantitative real time PCR. Their activation was suggested by a positive correlations with CD83 and TNF-α mRNA expression. Furthermore, mRNA co-expression of P-DC marker was observed with IL-6 but not IFN-α and P-DC expressing TLR9 were evidenced by immunohistochemistry analysis. IFN-γ mRNA was detected in one of the three analysed BU lesions, where it was present in low amount and only in highly focal areas mirroring the systemic IFN-γ down-regulation.

Short term objective

Investigate the mechanisms of P-DC activation by *M. ulcerans*

Long term objective

Study the consequences of intralesionally *M. ulcerans* immunopathogenicity on systemic IFN-γ immunosuppression.

A better understanding of the crosstalk between the host and *M. ulcerans* has the final goal to control the disease in a more effective and rational way.

***M. ulcerans* genome**

Genetic diversity of Mycobacteria is driven by the activity of mobile DNA such as insertion sequences (IS). *M. ulcerans* has at least two high copy number IS elements: IS2404 and IS2606. IS2404 is repeated about 200 times in the entire genome of *M. ulcerans* () and contains large amount of CpG motifs, which are known to activate the innate immune response by binding to TLR9 receptors.

Hypothesis

The *M. ulcerans* IS2404 directly activate the P-DC through TLR9

Material and Methods

Buruli ulcer ODN (selected from the *M. ulcerans* genome IS2404):

- Buruli positive (BU +) **5′-ACG ATC GAG TTG GTT ACT GTT CGT CGT T-3′**
- Buruli negative (BU -) **5′-AGC ATG CAG AAG GAA AGA GAA GCA GCA A-3′**

Optimized ODN from literature:

- positive (2006) **5′-TCG TCG TTT TGT CGT TTT GTC GTT-3′**
- negative (IMT022) **5′-TGC TGC AAA AGA CGA AAA GAG CAA-3′**

(Hartmann and Krieg, *Journal of Immunology* 2000)

Figure 1 ODN used for *in vitro* stimulation assays. Positive and negative Buruli ulcer ODN were selected from the AA IS2404 sequence following the CpG criteria described in the literature. Positive and negative control ODN (2006, IMT022) were included in the analysis.

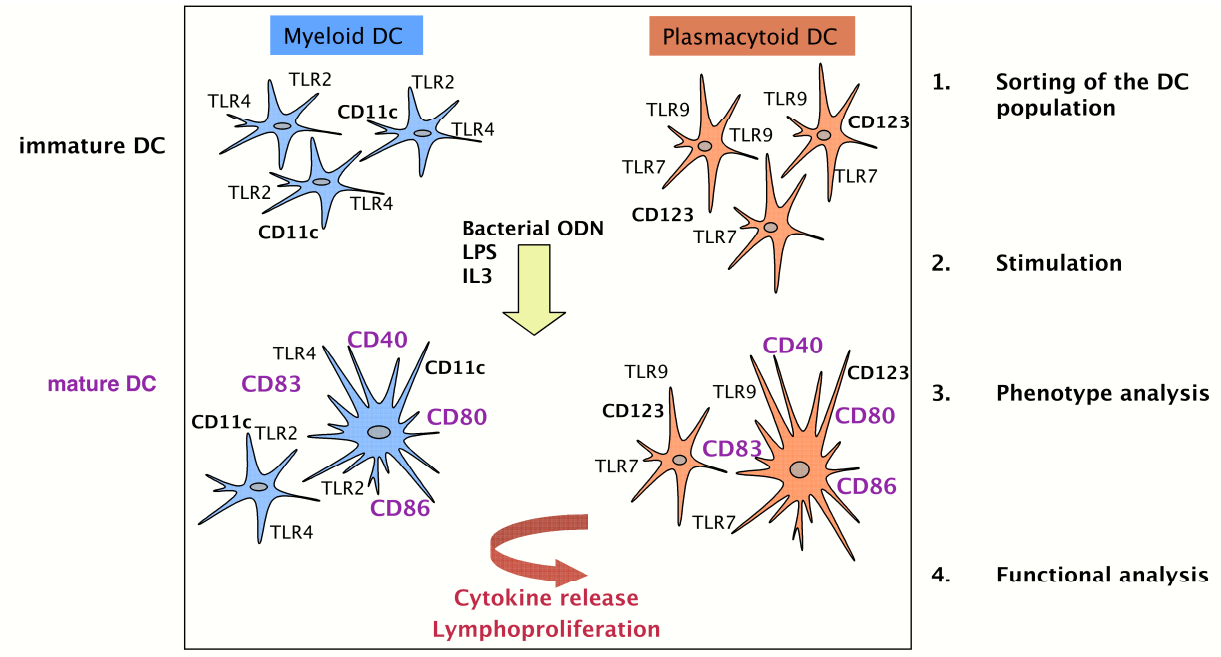

Figure 2 *In vitro* model. First, immature P-DC were positively isolated by magnetic cell sorting (MACS) from PBMC with anti-human BDCA4+ MicroBeads. From the BDCA4- cells, monocytes were positively isolated with CD14+ MicroBeads and cultured with IL-4 and GM-CSF for 6 days to obtain immature M-DC. Both immature DC subsets were stimulated with IL-3, LPS, bacterial- or literature- ODNs, respectively. After 24 h incubation they were characterized for CD80 and CD86 expression by flow cytometry and after 3 days, collected supernatants were tested by ELISA for cytokine release (IFN-γ, IFN-α, TNF-α, IL-4, IL-6, IL-10, IL-12). CD123 (IL-3Rα)

Results

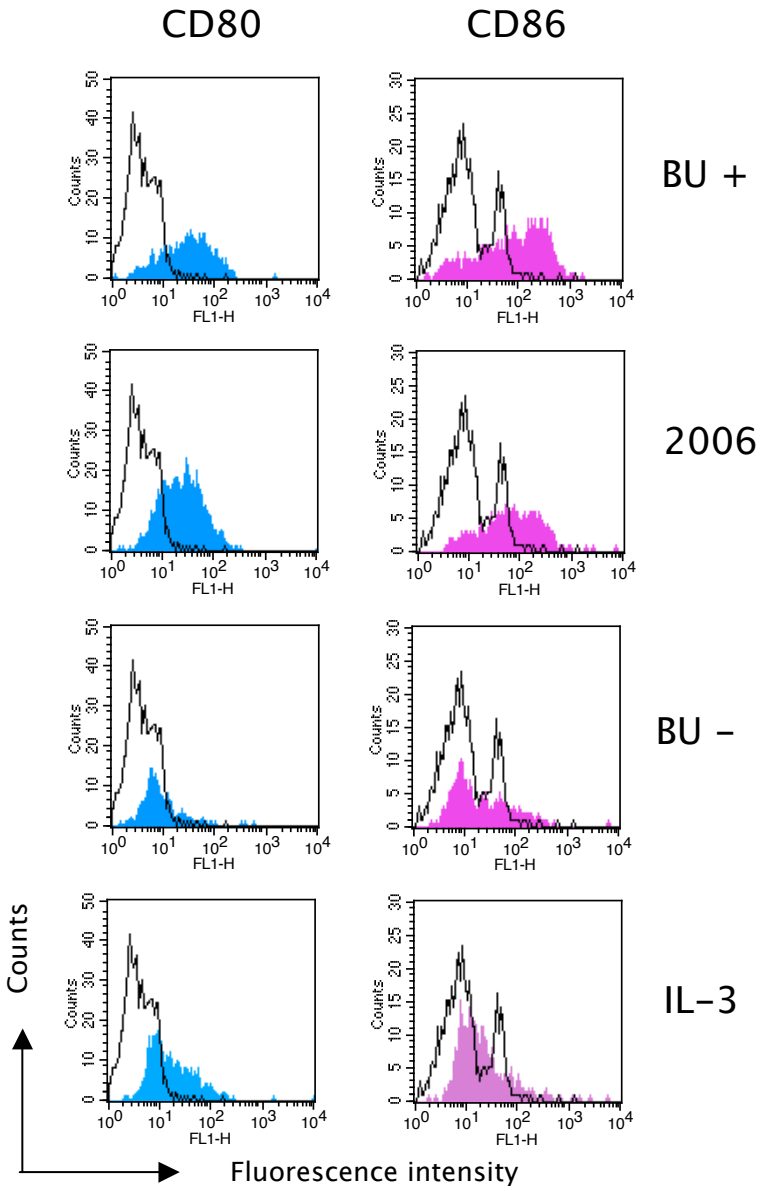

Figure 3 Phenotype FACS profiles. Immature P-DC isolated from PBMC were stimulated for 24 h with BU + (IS2404 CpG ODN), 2006 (literature positive CpG ODN) and IMT022 (literature negative ODN) and IL-3 and characterized for CD80 (blue) and CD86 (pink) expression by flow cytometry. Black lines indicate the CD80 and CD86 expression of not stimulated precursor P-DC. Representative histograms are shown out of four similar experiments.

Results

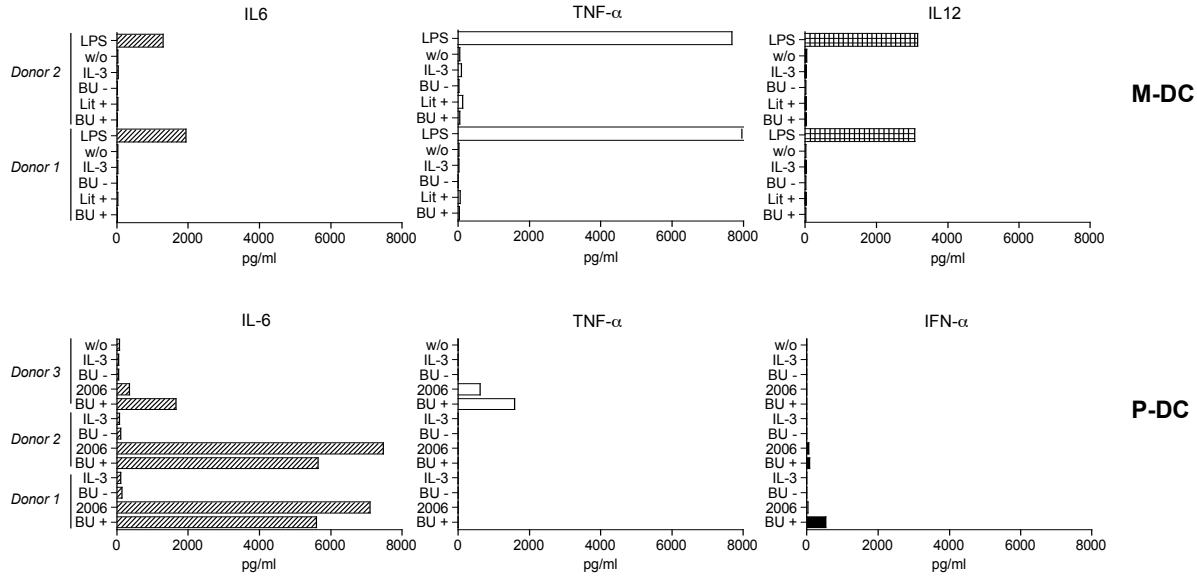

Figure 4 Cytokine profiles. The immature M-DC and P-DC were incubated for 3 days with the stimuli reported on the y-axes (BU +, IS2404 CpG ODN; 2006, literature positive CpG ODN) and BU -, IS2404 negative ODN). The correspondent cytokine release was measured by ELISA. The release of IFN-γ, IL-4, IL-6. IL-10, IL-12, TNF-α was measured for both DC subsets, IFN-α only for P-DC. Only the cytokines giving a detectable optical density are reported.

Summary

An undergoing maturation process of peripheral blood isolated immature P-DC stimulated with BU+ ODN is suggested by the upregulation of the CD80 and CD86 surface markers. Moreover, IL-6 release, but not IFN-γ and IL-12 was detected in all tested donors. In contrast, TNF-α and IFN-α were respectively detected only in one donor. TNF-α in consistent amount (1585 pg/ml) and IFN-α in relative low amount (532 pg/ml). As a negative control, the immature M-DC were stimulated with BU+ ODN which, as expected, did not show any CD40, CD80 and CD86 upregulation and cytokine release indicating a specific interaction of BU + ODN with TLR9. These preliminary results suggest that with the selected *M. ulcerans* CpG ODN is possible, in some extent, to reproduce the local in vivo situation of Buruli ulcer lesions.

Outlook

(i) Further characterize the stimulatory properties of the natural encoded BU+ ODN by evaluating the P-DC priming capacities of the adaptive immune response after undergoing BU+ ODN maturation [1]. Such a well characterized TLR9 ligand could represent a new candidate for a group of immunosuppressive agents [1-3]. (ii) Compare the P-DC activation employing genomic DNA of different Mycobacteria [4]. (iii) Compare the immune system activation in antibiotics treated [5] versus antibiotics untreated Buruli ulcer lesions to better evidence *M. ulcerans* the presence of possible key immunomodulators.

References

1. Diehl S, Rincon M: The two faces of IL-6 on Th1/Th2 differentiation. *Mol Immunol* 2002, 39:531-536.
2. Klinman DM, Gursel I, Klaschik S, Dong L, Currie D, Shirota H: Therapeutic potential of oligonucleotides expressing immunosuppressive TTAGGG motifs. *Ann N Y Acad Sci* 2005, 1058:87-95.
3. Heikenwalder M, Polymenidou M, Junt T, Sigurdson C, Wagner H, Akira S, Zinkernagel R, Aguzzi A: Lymphoid follicle destruction and immunosuppression after repeated CpG oligodeoxynucleotide administration. *Nat Med* 2004, 10:187-192.
4. Nagabhushanam V, Solache A, Ting LM, Escaron CJ, Zhang JY, Ernst JD: Innate inhibition of adaptive immunity: Mycobacterium tuberculosis-induced IL-6 inhibits macrophage responses to IFN-gamma. *J Immunol* 2003, 171:4750-4757.
5. Etuaful S, Carbonnelle B, Grosset J, Lucas S, Horsfield C, Phillips R, Evans M, Ofori-Adjei D, Klustse E, Owusu-Boateng J, et al.: Efficacy of the combination rifampin-streptomycin in preventing growth of Mycobacterium ulcerans in early lesions of Buruli ulcer in humans. *Antimicrob Agents Chemother* 2005, 49:3182-3186.

Acknowledgments

I am very grateful to Gerd Pluschke for giving me the opportunity to do this PhD thesis in his group, for his help, support, confidence and for always having time in the crucial moments of my thesis.

I am very thankful to Claudia Daubenberger for giving me the opportunity to get familiar with the human cellular immunology, for her constant indispensable support during my thesis and for her precious nonstop teamwork in the T cell lab during the vaccine trial.

My sincere thanks go to Giulio Spagnoli, Célia Groeper and Paul Zajac for the 'Buruli-collaboration', the good shared working atmosphere of their lab and their very generous teamwork.

A special thank goes to Penelope Vounatsou and Laura Gosoniu, who patiently helped me in the statistical analysis.

Many thanks to Rinaldo Zurbriggen and Nicole Westerfield of the Pevion Biotech for the vaccine trial collaboration and to all the CRC team of the Kantonspital Basel for their coordinative work to optimize the collection of the blood samples.

I extend my thanks to Markus Müller, Shinji Okitsu, Marjia Curcic and Denise Vogel for sharing and helping with all the blood samples, the numerous tubes and infinite nitrogen tank lists.
My appreciation goes to Daniela Schütte for her very valuable contribution with the Buruli lesions immunohistochemistry results and to Simona Rondini for giving me access to the Buruli ulcer tissue samples.

I would like to thank the diagnostic team of the Swiss Tropical Institute, particularly Elisabeth Escher, Beatrice Cattelan, Angelica Barry for their helpfulness in taking blood samples for my ELISpot analysis.

I am grateful to Georg Holländer for accepting to be Coexaminer of this thesis and for inviting me to join the Immunology PhD student meeting in Wolfsberg.

Very warm thanks are reserved to my friends and colleagues from the Molecular Immunology group for all the wonderful and funny moments shared together and their constant support and help also in more desperate moments ;o) : Simona Rondini, Shinji Okitsu, Max Bastian, Tatjana Zalac, Jean-Pierre Dangy, Marco Tamborrini, Marjia Curcic, Valentino Pflüger, Dani Schüette, Michael Käser, Diana Diaz, Rolf Spirig, Toby Jäggi, Martin Naegeli, Denise Vogel, Sybille Siegrist, Julia Leimkugel, Dorothy Yeboh-Manu, Lucy Ochola, Ernestina Mensah-Quainoo, Anita, Christine Banholzer, Theresa Ruf, Niels Pfeiffer
For all the nice people of the neighbor lab: Selina Bopp, Cornelia Spycher, Anouk Müller, Katrin Widmer, Chrigu Flück, Cornelia Spycher, Francesca Valsangiacomo, Jutta Marfurt, Mirjam Kästli, Sebi Rush, Dania Müller, Matthias Rottmann, Igor Niederwieser, Christian Nsanzadana.
The Parasitology people: Kerstin Gillingwater, Michael Oberle, Christian Scheurer, Moni Fasler, Michael, Sonja, Christian, Sergio,
The GWE people: Monica Daigl, Flavia Pizzagalli, Giovanna Raso, Claudia Sauerborn, Sandra, Abdallah, Sama Wilson, Bianca Plüss.

I extend many thanks to all the people of the STI, which are providing a great working and friendly atmosphere, particularly to Marcel Tanner, Niklaus Weiss, Hans-Peter Beck and Ingrid Felger, Hans-Peter Marti, Werner Rudin, Yvette Endriss, Sergio Wittlin, Amanda Ross, Christian Lengeler, Jakob Zinstag, Axel Hoffmannn, Martin Baumann, Lukas Camenzind, Christine Walliser, Isabelle Bolliger, Agnès Doré, Madleine Buholzer, Beatrice Weckerlin, Heidi Himmler, Martin Raab.

Un grande grazie a tutti i miei amici vicini e lontani in particolare a Célia, Bettina, Lorenza, Christian, Laura, Monica e Chica per le pause pranzo ed i momenti rilassanti e divertenti anche nei periodi più critici della tesi ed a Simone per la sua generosità ed il suo sostegno.

Ed infine, grazie di cuore ai miei genitori, a Rolf, a mio fratello e alle mie amicone ‘basilesi’ Ursula e Simona per il loro indispensabile sostegno, la loro infinita pazienza ed il loro grande affetto durante questi anni.

Curriculum Vitae

Personal details

Name:	Elisabetta Peduzzi
Date of Birth:	11th December 1977
Nationality:	Swiss
Languages:	Italian, French, German and English

Education

2002-2006	Swiss Tropical Institute, Basel PhD in Microbiology
1996-2001	University of Basel Masters Degree of Science, Biological Sciences
1992-1996	Liceo Cantonale di Lugano 1, Matura typus C

Research experience

2002-present	PhD thesis at the Swiss Tropical Institute, Division of Molecular Immunology, Prof. Gerd Pluschke; PD Claudia Daubenberger *"Monitoring of human cellular immune responses in infectious diseases: malaria vaccine associated responses and immune status in Buruli ulcer patients"*
2001	MSc thesis at the Swiss Tropical Institute, Division of Molecular Immunology, Prof. Gerd Pluschke *"Immunological characterization of BP66, a cyclic synthetic peptide that elicits Plasmodium falciparum circumsporozoite protein cross-reactive antibodies*

Work experience

2002	High school (biology and chemistry) and secondary school (mathematics and natural sciences) substitute teacher, Canton Ticino, Switzerland, January-October

Collaborations

2005-2006	Prof. Giulio Spagnoli; Célia Groeper, Msc; Paul Zajac, PhD; University hospital Basel, Division of surgical research *"Local activation of the innate immune system in Buruli ulcer lesions"*
2003-2006	Rinaldo Zurbriggen, PhD; Nicole Westerfeld, PhD; Pevion Biotech, Bern *"Generation of malaria specific CD4 T cell responses with a virosomally formulated synthetic peptide vaccine"*
2003-2006	Prof. Francesco Castelli; Nuccia Saleri, MD; Fabio Buelli, MD; University hospital Brescia, Division Infectious diseases *"Anti-Plasmodium falciparum malaria immunity vanishes with time in migrants to non-endemic areas"*

Courses

2002	Elispot technique and Elispot reader training course, CLB Sanquin, Amsterdam, December
2002	Elispot technique workshop, University of Freiburg, Germany, November

Undergraduate assistance

2003-2005	Bachelor students-assistant for laboratory techniques, Swiss Tropical Institute, February
2003	MSc thesis. "Structural and functional conservation of TLR9 and characterization of cross-reactive mAbs specific for leukocyte surface proteins of *Aotus nancymaae*, a non-human primate model for malaria development"

Thesis committee

Prof. Gerd Pluschke, Prof. Georg Holländer, Prof. Niklaus Weiss, Prof. Giulio Spagnoli, PD Dr. Claudia Daubenberger

PUBLICATIONS

Peduzzi E., Zurbriggen R., Pluschke G., Daubenberger C.A.. Generation of malaria specific CD 4 T cell responses with a virosomally formulated synthetic peptide. this article will be submitted in *Journal of Immunology*

Okitsu S.L., Kienzl U., Mohele K., Silvie O., **Peduzzi E**., Mueller M.S., Sauerwein R.W., Matile H., Zurbriggen R., Mazier O., Robinson J.A., Pluschke G. submitted in *Chemistry & Biology*

Peduzzi E., Groeper C., Schütte D., Zajac P., Rondini S., Mensah-Quainoo E., Spagnoli G.C., Pluschke G., Daubenberger C.A.. Local activation of the innate immune system in Buruli ulcer lesions. Accepted in *Journal of investigative dermatology*, 2006

Yeboah-manu D., **Peduzzi E.**, Mensah-Quainoo E., Asante-Poku A., Ofori-Adjei D., Pluscke G., Daubenberger C.A.. Systemic suppression of IFN-γ responses in Buruli ulcer patients resolves after surgical excision of the lesions caused by the extracellular pathogen *Mycobacterium ulcerans*. *Journal of leukocyte biology*, 2006, 79(6): 1150-6

Spirig R., **Peduzzi E.,** Patarroyo M.E., Pluschke G., Daubenberger C.A., Structural and functional characterization of the Toll like receptor 9 of *Aotus nancymaae*, a non-humnan primate model for malaria vaccine development *Immunogenetics*, 2005, 57: 283-288

Pfeiffer B., **Peduzzi E**., Moehle K., Zurbriggen G., Glück R., Pluschke G., Robinson J.A.. A virosome-mimotope approach to synthetic vaccine design and optimization: synthesis, conformation, and immune recognition of a potential malaria-vaccine candidate, *Angewandte Chemie*, 2003, 42 (21): 2368-71

SEMINARS

Monitoring cellular immune responses during infection Open-seminar at the Swiss Tropical Institute, April 2006

Local Immune response in *Mycobacterium ulcerans* infection, 18th Meeting of the Swiss Immunology PhD Students Wolfsberg, March 2006

Intralesional and *in vitro* immunological studies of Buruli ulcer disease and their implications in the pathogenicity, Institut für Chirurgische Forschung und Spitalmanagement, University of Basel, February 2006

Buruli ulcer disease related reduction of interferon gamma production in peripheral blood.17th Meeting of the Swiss Immunology PhD Students, Wolfsberg, March 2005

Characterisation of T cell profile in Buruli patients, healthy contacts and healthy non-exposed controls; Meeting of PhD students in parasitology and tropical medicine, Münchenwiler, October 2004

Monitoring cellular immune responses, Meeting of PhD students in parasitology and tropical medicine, Münchenwiler, October 2003

Immunological characterisation of BP66: A cyclic synthetic peptide that elicits *Plasmodium falciparum* circumsporozoite protein cross-reactive antibodies, Open-seminar at the Swiss Tropical Institute, May 2002

SYMPOSIUM CONTRIBUTIONS

Yeboah-Manu D., **Peduzzi E**., Mensah-Quainoo E., Pluschke G., Daubenberger C.. Mycobacteria-associated immuno-suppression in Buruli ulcer, Annual Congress of the Swiss Society of Tropical Medicine and Parasitology, Ascona, November 2005, poster

Yeboah-Manu D., **Peduzzi E**., Mensah-Quainoo E., Pluschke G., Daubenberger C.. Mycobacteria-associated immuno-suppression in Buruli ulcer: resemblance to Mycobacterium tuberculosis, International Congress of Medicine and Health in the Tropics, Marseille, France, September 2005, poster

Saleri N., Caligaris S., Matteelli A., **Peduzzi E**., Carvalho A.C., Bienvenu S.S., Nebie I., Pluschke G., Imberti I., Malacarne F., Castelli F.. Decremento dell' immunità anti-*P. falciparum* in migranti da area endemica, Atti del 5° congresso nazionale Brescia, Italia, September 2005, Italian journal of tropical medicine, poster

Peduzzi E., Okitsu S., Pfeiffer B., Silvie O., Moreno R., Moehle K., Mazier D., Zurbriggen R., Robinson J.A. & Pluschke G.. Development of a synthetic peptidomimetic of *Plasmodium falciparum* circumsporozoite protein that elicits invasion inhibitory antibodies, Congress of the Swiss Society of Tropical Medicine and Parasitology Swiss Society, Basel, 2003, poster